University of Nottingham
UK | CHINA | MALAYSIA

ROTHAMSTED RESEARCH

Herbivore-Plant-Soil microbe interaction: Who is helping whom?

Sandra Lucia Cortes Patiño

March 2025

Thesis submitted to the University of Nottingham for the degree of Doctor of Philosophy

School of Biosciences

University of Nottingham

Executive summary

Plant-microbe interactions are key to improving plant defence against herbivory which causes significant losses in food production worldwide. This project aimed to study how aphid herbivory changes the chemical signalling at the plant-soil microbe interface, and to disentangle the complexity of these interactions using a multidisciplinary approach involving microbiology, chemical ecology and bioinformatics.

In an initial experiment where wheat plants were exposed to aphid herbivory for two weeks, rhizosphere bacterial diversity was observed to decrease, with an increased the relative abundance of Actinobacteria class ($p < 0.05$). Furthermore, untargeted metabolomics analyses showed that the profile of volatile organic compounds (VOCs) in the rhizosphere soil was significantly different under herbivory ($p < 0.05$). Based on these findings, a second experiment was design using a semi-hydroponic system to facilitate the analysis of chemical signals released by plants via root exudates and volatile organic compounds. Furthermore, rhizosphere and root tissue collection were performed for DNA extraction and amplicon sequencing analysis (16S rRNA). The metabolomics analysis showed that aphid herbivory induced significant changes in the root exudate profile, with 485 metabolites altered and 39 compounds significantly enriched under herbivory. Chemical classification revealed that some of these compounds belong to the benzoxazinoids, terpenes, coumarins and flavonoid classes of secondary metabolites, with some – like HMBOA – previously identified as key signals in plant-microbe interactions under herbivory. In contrast, herbivory resulted in the depletion of certain oxidised fatty acids and amino acids in root exudates. Amplicon sequencing revealed that, some Actinobacteria genera found in the initial experiment (*Streptacidiphilus, Streptomyces, Catenulispora*), were enriched in the

roots of plants under herbivory. Further investigations demonstrated that four herbivory-regulated compounds influenced the growth of rhizosphere bacteria isolated from wheat rhizosphere, suggesting that these metabolites play a functional role in shaping plant-microbe interactions.

Overall, this work shows that aboveground insect pests can have a significant impact on plant belowground interactions, and further research is needed to investigate how to use this knowledge for the development of sustainable pest management strategies that put the soil microbial communities at the centre of crop production.

Acknowledgements

I would like to thank the ENVISION Doctoral Training Partnership (DTP) for funding my PhD project. Thanks for all the training sessions and opportunities to interact with other students, it was truly a joy to be part of this DTP.

This work could not have been done without the support of all my supervisors, who have provided me with academic and personal guidance at every step of the project. I am especially grateful to John Caulfield for his constant enthusiasm and for encouraging me to explore my ideas with confidence. Thank you, John, for dedicating your time to teach me analytical chemistry, for patiently reading papers with me to navigate the complexities of untargeted metabolomics analysis, and for giving me the freedom to try new approaches.

I want to thank Amanda Rasmussen and Vanessa Nessner-Kavamura, the two incredible women in my supervisory team, who have exemplified academic excellence while leading with kindness and empathy. Since the beginning, Mandy and Vanessa consistently ensured I that I had the support I needed. Mandy, thanks for being a mentor. Thank you for always creating a welcoming and productive environment, even at a distance. Your support and belief in me have truly shaped my experience, and I cannot imagine this PhD journey without your guidance.

Special thanks to Gabriel Castrillo, who has taught me that academic excellence is shown in the smallest details and has always encouraged me to be a better scientist.

Gabriel’s feedback has made my work better, and I am grateful to have had the opportunity to learn from him.

I am also grateful to Tim Mauchline and Mike Birkett for welcoming me into their research groups and providing the resources and encouragement to develop this project. My time with the Chemical Ecology and Molecular Microbial Ecology labs has been an enriching experience. A special thank you to Alex Borg for showing me how to work in the chemistry lab and to maintain the aphid colonies. Thanks to Tessa Reid for her guidance with colony PCR of bacterial isolates. Thanks to Lisa Humbert for being my PhD and desk buddy, it was great to share this PhD experience with you.

A big thank you to Adriana Torres-Ballesteros, who selflessly gave her time to teach me microbiome data analysis. Adriana has also shown me the importance of embracing our identities as Colombian researchers and the value of building networks and seizing opportunities.

Special thanks to George Lund for his generous advice and collaborative spirit. It was a joy to work alongside someone equally passionate about metabolomics. Your positivity and dedication, especially in helping me navigate the challenges of the metabolomics analysis at the beginning, have been greatly appreciated.

On a personal note, I am forever grateful to my friends Izayana Sandoval, Aishwarya Shankhapal, and Anusha Mohan-Kumar. For three and a half years, they have been my support system, and their friendship has been a cornerstone of my PhD experience. I also want to thank Haydn and Carolyn Beaton for their generous support

throughout these years. Their help has made this PhD journey more enjoyable; they have provided me a home and have made me feel like I have a family in the UK.

To my partner, Sam Beaton, thank you for your love, patience, and belief in me. From helping me prepare for interviews to learning about rhizosphere soil and root exudates just to support my work and presentations, you have always been there for me. I am grateful to have you in my life. Together, we make an incredible team.

Finally, I dedicate this thesis to my family. To my mother, Esneda Patiño; my father, Gonzalo Cortés; and my sister, Diana Cortés. You have been my constant source of strength and inspiration. You taught me the values of compassion, resilience, and dedication. Mom and Dad, your sacrifices, love, and support have shaped the person I am today. I am endlessly proud to be your daughter, and I hope this achievement reflects even a fraction of the gratitude I feel for you.

Contents

Executive summary 2
Acknowledgements 4
Table of figures 11
Supplementary figures 16
Table index 17
Supplementary Tables 18
Chapter 1: General Introduction 19
1.1. Moving away from pesticides 19
1.2. Importance of aphid-wheat-microbe interactions in agriculture 21
1.2.1. Aphid herbivory impacts on wheat production 22
1.2.2. Wheat 23
1.2.3. Aphids, plants and their associated microbiomes 24
1.2.3.1. The aphid microbiome 25
1.2.3.2. The plant microbiome 27
1.2.4. Aphid-plant-soil microbe interactions 32
1.2.5. Study system 36
1.3. Chemical signalling in aphid-plant-microbe interactions 37
1.3.1. Chemical cues in host recognition by aphid herbivores 37
1.3.2. Activation of plant response to aphid herbivory 39
1.3.3. Plant defence against aphid herbivory 41
1.3.4. Wheat plant defence against aphid herbivory 43
1.4. Connecting above and below: The role of root exudates in plant-microbe interactions under aphid herbivory 45
1.4.1. The role of root exudates in plant belowground interactions 45
1.4.2. Root exudates mediating plant-microbe interactions under biotic stress 52
1.5. Main techniques used in this study for the analysis of plant-soil microbe interactions 54
1.5.1. Untargeted metabolomics of plant root exudates 55
1.5.2. Microbiome analysis 57
1.6. Thesis objective and research questions 59
1.7. Thesis outline 61
Chapter 2: Exploring changes at the plant-soil microbial interface under aphid herbivory 62
2.1. Introduction 62
2.2. Materials and methods 64
2.2.1. Aphids, plant and soil material 64

2.2.2. Pot experiment under controlled conditions 65
2.2.3. Aboveground measurement of VOCs from wheat plants under aphid herbivory 67
2.2.3.1. Dynamic headspace collection 67
2.2.3.2. Gas chromatography analysis 69
2.2.4. Belowground metabolic profiling at the plant-soil interface of wheat plants under aphid herbivory 69
2.2.4.1. VOCs in the rhizosphere of plants under herbivory 70
2.2.4.2. Non-volatile metabolites in the rhizosphere of plants under aphid herbivory 71
2.2.5. Metabolic activity of microbial communities in the rhizosphere 73
2.2.6. Structure and composition of bacterial communities in the rhizosphere 74
2.2.7. Bioinformatics and statistical analysis 75
2.2.7.1. Volatile Organic Compounds (VOCs) 75
2.2.7.2. Non-volatile metabolites found in the rhizosphere of plants under aphid herbivory 76
2.2.7.3. Metabolic activity of microbial communities in the rhizosphere 78
2.2.7.4. Bacterial community analysis pipeline 79
2.3. Results 81
2.3.1. Belowground metabolic profile changes correlate with changes in aboveground VOCs in response to aphid herbivory 81
2.3.2. Carbon source consumption rate was higher in microbial communities associated with plants under aphid herbivory 87
2.3.3. Aboveground aphid herbivory reduced the diversity of bacterial communities after two weeks of aphid herbivory 90
2.3.4. Actinobacteria were enriched in the rhizosphere of plants subjected to two weeks of aphid herbivory 93
2.4. Discussion 95
2.5. Supplementary material 101
Chapter 3: Interrogating changes in belowground chemical signals from wheat plants during aphid herbivory 111
3.1. Introduction 111
3.2. Methods 114
3.2.1. Root exudates collection 115
3.2.2. Root exudate processing 116
Volatile Organic Compounds (VOCs) sample processing 117
3.2.3. Untargeted metabolomics of wheat root exudates under aphid herbivory 118
3.2.3.1. Data-Dependent Acquisition (DDA) of root exudates 118
3.2.3.2. Chemoinformatic analysis: Data processing and metabolite annotation 120

3.2.3.3. Confirmation of identity of selected metabolites with authentic chemical standards 123
3.2.4. Untargeted metabolomics profiling of root VOCs 124
3.2.5. Statistical analyses 125
3.2.5.1. Root exudates 125
3.2.5.2. Root volatiles (VOCs) 126
3.2.5.3. Plant dry weight 127
3.3. Results 127
3.3.1. Plant biomass production was significantly decreased by aphid herbivory 127
3.3.2. Untargeted metabolomics of non-volatile exudates from wheat plants 128
3.3.2.1. Metabolite annotations 129
3.3.2.2. Significant changes in the chemical profile of non-volatile root exudates from wheat plants occur under aphid herbivory 136
3.3.2.3. Integration of metabolite annotation and statistics 139
3.3.2.4. Confirmation of identity of herbivory-regulated metabolites 143
3.3.3. Untargeted metabolomics of VOCs exudates from wheat plants 146
3.4. Discussion 148
3.4.1. Improving our understanding of plant metabolism and the ecological role of metabolites through untargeted metabolomics 149
3.4.2. Belowground metabolic responses and phytohormone signalling 151
3.4.3. Oxylipins and benzoxazinoids in root exudates were significantly impacted under aphid herbivory 154
3.5. Supplementary files 159
Chapter 4: Response of bacterial communities at the plant-soil interface in wheat plants under aphid herbivory 172
4.1. Introduction 172
4.2. Methods 175
4.2.1. Analysis of bacterial communities 175
4.2.1.1. DNA extractions and amplicon sequencing 176
4.2.1.2. Bioinformatics and statistical analysis 176
4.2.2. Cross association analysis of herbivory-regulated metabolites and bacterial communities 177
4.2.3. Interaction between rhizosphere bacteria and herbivory-regulated metabolites 178
4.2.3.1. Isolation of bacteria from rhizosphere soils 179
4.2.3.2. Identification of bacterial isolates 180
4.2.3.3. Response of bacterial isolates to identified herbivory-regulated metabolites 182
4.3. Results 183

4.3.1. Aphid herbivory impacted root-associated bacterial communities by increasing ASVs from the Actinobacteria class 184
4.3.2. Cross association of microbial taxa and metabolites showing fold changes in the root exudates of wheat plants under aphid herbivory 189
4.3.3. Herbivory-regulated metabolites induced sporulation in Actinobacteria 192
4.3.3.1. Herbivory-regulated metabolites induced aerial hyphae formation and sporulation in Actinobacteria 195
4.4. Discussion 197
4.5. Supplementary information 208
5. General discussion 216
5.1. Capturing plant signals under natural conditions 220
Plant VOCs: Unravelling the Role of Root Volatiles in Plant-Microbe Interactions 222
Hexanal Production and the Complexity of Rhizosphere VOCs 223
5.2. Untargeted Metabolomics: A Key Tool for Understanding Plant-Soil Microbe Interactions 224
5.3. Impact of microbial communities on plant response to aphid herbivory .228
5.4. Impact of timing of aphid herbivory on soil microbial communities 231
5.5. Insect endosymbionts add another layer of complexity to insect-plant-soil microbe interactions 233
5.6. Connecting above and belowground: The need for multidisciplinary studies 234
5.7. Conclusions 236
Key contributions for further research: 239
References 240

Table of figures

Figure 1.1. Plant compartments divided into aboveground and belowground. Overall, in plants, the aboveground part is referred to as the phyllosphere, and the belowground part as the rhizosphere, while divisions can be found in each compartment, as shown in the figure. Taken from Kavamura et al. (2021).....28
Figure 1.2. Aphid-plant-microbe interactions. Modulation of plant hormone signalling by microbial communities can alter the plant defence against insect herbivory. Figure created using Biorender. 34
Figure 1.3. Classes of compounds present in plant rhizodeposits and documented functions. Taken from Rizaludin et al. (2021). 47
Figure 1.4. Fragmentation of precursor ions to obtain product ions used for structural annotation of compounds in complex samples. In this example, the data-dependant acquisition method is used, selection precursor ions based on an intensity threshold. Taken from (Lyu et al., 2024) 56
Figure 2.1. Experimental design to test the effect of aphid herbivory aboveground in belowground plant-microbe communication and microbial responses. 66

Figure 2.2. Placement of aphid in wheat plants. a) Ten pregerminated seedlings after six days of growing under controlled conditions, b) Wheat plants at the third-leaf stage, c) Clip cages containing 10 aphids positioned on the first leaf (counting from the base), d) Wheat plants after a week growing under aphid feeding. 67
Figure 2.3. Schematic figure of aboveground VOC collection and analysis. a) VOCs are collected from the plant headspace for 48 hours using Porapak tubes. b) Porapak tubes are eluted with 750 µL diethyl ether and concentrated to 50 µL. c) Samples are concentrated under nitrogen blowdown to be analysed using gas chromatography (GC).....68
Figure 2.4. *Belowground VOCs collection. a) Placement of Polydimethylsiloxane (PDMS)-coated tubes in pots prior to the experiment. b) Elution of VOCs from PDMS tubes, c) Concentration of eluted samples under nitrogen blowdown before GC analysis.* 71
Figure 2.5. Collection and processing of non-volatile metabolites from wheat rhizosphere. a) 21 grams of rhizosphere soil were placed in a perforated 20 mL tube inside a 50 mL Falcon tube, followed by 10 mL of extraction solvent (95% methanol with 0.05% formic acid). b) After extraction, samples were concentrated by rotary evaporation and nitrogen blowdown to 100 µL. c) Concentrated samples were analysed using LCMS. 72
Figure 2.6. Principal component Analysis (PCA) of aboveground VOC profiles from control plants (NoHerb) and plants under aphid herbivory after two and four weeks of treatment. PCA and PERMANOVA results were obtained by using the MetaboAnalyst platform v.6.0. Ellipses show 95% confidence interval for each condition (n=4).....82
Figure 2.7. Heatmap showing peak intensities of metabolites associated with plants under two weeks of aphid feeding (n=4). Peak areas were normalised using the Z-score. Tentative annotations were obtained by calculating the Kovats index (KI) based on the C7-C22 alkanes standards retention times and matching against an internal data library. In the Function key, metabolites classified as “Unknown” as their identity is not known, and those in the “No” category, have not been commonly observed in response to herbivory. 83

Figure 2. 8. Root dry weight of plants in the two sample points under aphid herbivory. Dry weight was measured after plants were put in an oven at 70 °C for 96 hours (n=5). 84
Figure 2.9. PCA of the metabolic profile of a) VOCs and b) non-volatiles found in the rhizosphere of plants after two weeks of aphid feeding. PCA were generated in MetaboAnalyst. Ellipses show 95% confidence interval for each condition (n=5 except for VOCs of control plants, where n=4). 85
Figure 2.10. Heatmap showing peak intensities of belowground volatile organic compounds associated with plants under two weeks of aphid herbivory (control plants n=4; aphid herbivory n=5). Peak areas were normalised using the Z-score. Tentative annotations were obtained by calculating the Kovats index (KI) based on the C7-C22 alkanes standards retention times and matching against an internal data library. 85
Figure 2.11. Heatmap showing peak intensities of belowground non-volatile metabolites associated with plants under two weeks of aphid feeding (n=3). Peak areas were log-transformed and scaled using the Pareto scaling. Row names correspond to the metabolite ID, followed by accurate mass and retention time separated by underscores. 86
Figure 2.12. Principal Component Analysis (PCA) of microbial carbon-source utilisation based on Biolog™ EcoPlates. Technical replicates were combined into biological replicates (n=3). The data represents the Average Well Colour Development (AWCD) for all 31 carbon sources tested, measured after 72 hours of microbial growth. 88
Figure 2.13. Average Well Colour Development (AWCD) of samples after two weeks of aphid herbivory. a) Line graph of AWCD over 96 hours, with standard error bars (n=3) and statistical significance indicated by letters (SNK test, Bonferroni corrected, padj < 0.05). b) AWCD for each carbon source at 72 hours, with colour intensity representing consumption levels (dark red = high, white = low). Asterisks denote statistical significance (* p = 0.05; *** p = 0.001, paired t-test, Bonferroni corrected, padj < 0.05). 89
Figure 2.14. Taxonomic diversity and richness of bacterial communities during the experiment. a) Observed and b) Shannon diversity index at the ASV level (n=4) Significance is shown by post-hoc Wilcoxon comparison (FDR < 0.05). c) Rank abundance plot (abundance >1%) at the class level. Four biological replicates per sample were used for the analyses. BS= Bulk soil; BEF= Rhizosphere samples before aphid feeding; SH= 2-weeks herbivory; SN = 2-weeks control; FH=4-week herbivory; FN= 4-week control. 91
Figure 2.15. Beta diversity analysis of bacterial communities. a) Non-Multidimensional Scale analysis (NMDS) of Bray-Curtis dissimilarity distance of bacterial communities' composition, b) Partial dbRDA of bacterial diversity showing the explained variance of bacterial communities based on sampling time and insect herbivory (n=4). 92
Figure 2.16. Venn diagram showing the shared ASVs after two and four weeks of aphid feeding. 93
Figure 2.17. ANCOM-BC of the differentially abundant ASVs. LogFoldChange was calculated from the ANCOM-BC log-linear model and shows the significantly (q value < 0.05) enriched (Positive LFC) or decreased (Negative LFC) ASVs in the rhizosphere of plants under herbivory compared to the healthy plants. The genus Burkholderia_Caballeronia_Paraburkholderia was shortened to “Burkholderia” for visualization purposes. 94

Figure 3.1. Plants growing inside mesh cages to prevent aphid transfer from the aphid-herbivory treatment. 114

Figure 3.2. Sampling methodology for root exudates in untargeted metabolomics analysis. Plants were removed from pots, shaken to collect rhizosphere soil, and washed in sterile tap and deionised water. They were then placed in bottles with 100 mL of sterile deionised water and a 10 cm Polydimethylsiloxane (PDMS) tube to capture volatiles. After two hours, 80 mL of exudates were snap-frozen, and PDMS tubes were eluted with 750 µL of diethyl ether for further analysis. 115
Figure 3.3. Sample preparation of non-volatile root exudates for analysis. The frozen root exudates samples were thawed at 4 °C and filtered through a Stericup vacuum filter (0.22 µm). The filtered exudates were then freeze-dried for five days and reconstituted in 2 mL of a 50% methanol solution. Next, the exudates were concentrated under nitrogen, reconstituted in 700 µL of 50% methanol, concentrated a second time under nitrogen and reconstituted in 200 µL of methanol for LCMS analysis. 117
Figure 3.4. Pipeline for untargeted metabolomics analysis of non-volatile root exudates (LC-MS/MS). a) Data processing involved acquisition in Data-Dependent Acquisition mode, file conversion to open-source format, and processing in mzmine v.4.0.3, generating four files for metabolite annotation, molecular networking, and statistical analysis. b) Metabolite annotation strategies included experimental and in silico database matching, chemical classification via CANOPUS (SIRIUS), and integration of all annotations into molecular networks. 121
Figure 3.5. a) Dry weight of shoots and roots of plants after two weeks of aphid herbivory, b) Root to shoot ratio of plant dry weight. The mean comparison was performed using a Wilcoxon test. The error bars represent the standard error (n=5). Herbivory = Plants under aphid herbivory; NoH = Untreated controls. 128
Figure 3.6. Classification of metabolites in each annotation tool based on the natural product classifier (NPC) at the pathway level. 130
Figure 3.7. Spectral matches at the pathway level (Natural Product Classifier-NPC) according to taxonomically informed metabolite annotation (TimaR) software. a) Venn diagram showing the overlap between annotations from LOTUS (taxonomically informed) and ISDB (MS/MS) tools. b) Bar plot showing the count of metabolites annotated at the pathway level using the NPC classifier using only accurate mass in the LOTUS database and the metabolites matched in both LOTUS and ISDB. 131
Figure 3.8. Summary of annotated features using different MS/MS matching strategies. 132
Figure 3.9. Feature-Based Molecular network of metabolites found in the root exudates of wheat plants. Coloured nodes (points) indicate a chemical class was assigned based on an annotation tool: experimental library matching (GNPS: Blue), chemical classification using CANOPUS (Purple), library matching against in silico database (ISDB-DNP: Orange) 134
Figure 3.10. Molecular families detected in plant root exudates. Each node represents a metabolite feature within the molecular network, with edges connecting structurally related features. Arrows indicate metabolites identified through spectral matching against experimental libraries in GNPS. 135
Figure 3.11. Quality assurance of the instrument suitability (LCMS) using pooled samples of all biological replicates (n=10) as quality control (QC). A) PCA showing the clustering of the QC samples compared to the biological replicates from the experiment, b) Example of a randomly selected feature (m/z 149.0107) and the

performance of the three QC technical replicates, c) Complete chromatogram with overlapping signals from the QC samples. 137
Figure 3.12. Statistical analysis of the metabolic profile of root exudates of wheat plants under aphid herbivory. a) PCA showing the metabolic profile of the root exudates from plants under herbivory and healthy plants. Circles represent a confidence interval of 0.95 (n=5), b) Volcano plot showing the results of the differential abundance analysis after false discovery rate correction (FDR = 0.1). Colours represent log_2fold change, with red indicating features that increased in peak area under aphid herbivory, while blue features were decreased. The size of the circles increases according to the p value, as shown in the legend to the right. 139
Figure 3.13. Chemical classification of herbivory-regulated metabolites and their Log2FC based on MS/MS annotation tools (GNPS library matching, CANOPUS, and ISDB in TimaR). 141
Figure 3.14. Molecular network annotated as octadecanoids. a) Pie charts within the octadecanoid network represent the total sum of peak areas, with blue indicating samples from healthy plants and orange representing root exudates from plants under aphid herbivory. The statistical significance is represented by the size of the pies, with the bigger ones being statistically different. b) Mean comparison of normalised peak areas for features in the network, analysed using a t-test ($p< 0.05$). 142
Figure 3.15. Increase in peak area of features putatively annotated as benzoxazinoids based on their MS/MS spectra. Only feature 2269, HMBOA + O-Hex, was close to statistical significance after multiple comparison correction (FDR = 0.057). 143
Figure 3.16. Liquid Chromatography (LC) traces on a C18 column showing the peak for authentic chemical standards and their presence in root exudates, represented by the pooled quality control samples, QC (n=3). The samples and chemical standards were aligned on the software mzmine v.4.0.3. For the compounds HMBOA-O-Hex and salicylic acid, a zoom was applied as the presence of these compounds was several units lower than in the standards. 145
Figure 3.17. Liquid Chromatography (LC) trace on a C18 column showing the peak for authentic chemical standards for 9,10 DiHOME, and its presence in root exudates, represented by the pooled quality control samples, QC (n=3). The samples and chemical standards were aligned on the software mzMine v.4.0. 3.. 146
Figure 3.18. Root VOC analysis under herbivory. a) PCA of root exudate metabolic profiles from herbivory-treated and healthy plants (NoH). Shaded circles indicate a 95% confidence interval (Herbivory: n = 4, NoH: n = 5). b) Key VOC features identified by t-test. Colours represent -log10 of the uncorrected p-value, with red highlighting feature 117 ($p = 0.0033$), annotated as E-β-farnesene based on NIST library matching. 147
Figure 3.19. Matching spectrum for feature 117 with the compound E-β-farnesene according to library matching against NIST library. Cosine score = 0.7359. 148
Figure 4.1. Representation of the sample collection and analysis presented in the previous (Chapter 3) and present chapter. Samples from plant roots and rhizosphere soil samples were collected for amplicon sequencing of the 16S rRNA gene. Glycerol stocks were used for isolation of bacterial strains that were further used for in vitro tests. 175

Figure 4.2. Diagram of work with culturable bacteria. a) Serial dilutions were made from a 1 mL glycerol stock from rhizosphere soil in 9 mL of NaCl (8.5% w/v), b)

Serial dilutions were inoculated in TSA 10% and ISP-3 medium for bacterial isolation, with further purification by picking individual colonies. c) In vitro test with bacteria isolated from ISP-3 medium (Actinobacteria) in media supplemented with salicylic acid, azelaic acid, p-Coumarid acid, and HMBOA-O-Hex at 0.5 mM. Growth presence or absence for each colony was used for further analysis. 179
Figure 4.3. Diversity of microbial communities in the rhizosphere of wheat plants. Alpha diversity analysis using the observed (a) and Shannon index (b). Whiskers show post-hoc Wilcoxon comparison with asterisks showing statistical significance (alpha * < 0.05, ** <0.01, *** < 0.001; c) Rank abundance plot of bacterial communities at the Class taxonomic level; d) non-multidimensional scale analysis (NMDS) of Bray-Curtis dissimilarity distance of bacterial community composition; e) Partial dbRDA of bacterial diversity showing the explained variance of bacterial communities based on compartment and insect herbivory (n=5). RH= Roots of plants under herbivory; RN= Roots of healthy plants; SH= Rhizosphere of plants under herbivory; SN= Rhizosphere of healthy plants; BS= Bulk soil. 186
Figure 4.4. Differential abundance analysis (ANCOM-BC) of amplicon sequence variants (ASVs) in the rhizosphere (a) and plant roots (b). Log-fold change (LFC) indicates enrichment (positive LFC) or reduction (negative LFC) of ASVs in the rhizosphere under herbivory vs. healthy plants. ASVs are labelled by genus (Silva 138 database); unassigned genera are labelled with taxonomy class + NA, or NA if only kingdom was assigned. Bars represent ASVs with a corrected p-value < 0.1 (Holm correction). Error bars indicate standard error (n = 5). 188
Figure 4.5. Spearman correlations between log-transformed pooled ASVs (relative abundance) from rhizosphere and root samples and log-transformed metabolite peak areas. The top bar shows metabolite log-fold changes (blue: decreased, orange: increased under aphid herbivory). Clusters 1 and 3 include bacteria positively correlated with metabolites that increased under herbivory, while Clusters 4 and 5 correlate with metabolites that decreased. Cluster 2 contains bacterial classes where associations were less evident. 190
Figure 4.6. Spearman correlations between log-transformed ASVs (relative abundance) from rhizosphere and root samples and log-transformed metabolite peak areas. The first top bar shows the assigned chemical classification of metabolites. The second top bar shows metabolite log-fold changes (blue: decreased, orange: increased under aphid herbivory). 192
Figure 4.7. Phylogenetic distance tree of 16S amplicon sequencing of bacterial isolates. The identities were determined using the SILVA Alignment, Classification and Tree (ACT) service at https://www.arb-silva.de/aligner/ after the consensus sequences were obtained using Geneious v. 10.2.3 194
Figure 4.8. Growth of bacterial strains after 72 hours of incubation in M9 minimal medium supplemented with 0.5 mM of selected compounds as carbon sources. The left panel shows bacterial growth in M9 medium with the corresponding solvent controls (DMSO), while the right panel shows growth in M9 medium supplemented with the metabolites. The bacterial colonies correspond to the same three isolates in different compounds and their solvent controls. 196
Figure 4.9. Number of bacterial strains that exhibited growth on M9 medium plates supplemented with 0.5 mM of metabolites identified as regulated by aphid herbivory. SA = Salicylic acid, AzA = Azelaic acid, p-Coumaric = p-Coumaric acid, HMBOA = HMBOA-O-Hex. 197

Supplementary figures

Supplementary Figure 2.1. Beta dispersion of absorbance readings from Ecoplates™ after two and four weeks of aphid feeding. 101
Supplementary Figure 2.2. Alpha rarefaction curves a) before and b) after applying rarefaction to the minimum library size. 102
Supplementary Figure 2.3. ANCOM-BC of the differentially abundant ASVs after four weeks of aphid feeding. LogFoldChange was calculated from the ANCOM-BC log-linear model and shows the significantly (q value < 0.05) enriched (Positive LFC) or decreased (Negative LFC) ASVs in the rhizosphere of plants under herbivory compared to the healthy plants. The genus Burkholderia_Caballeronia_Paraburkholderia was shortened to “Burkholderia” for visualization purposes. 103
Supplementary Figure 4. 1. Alpha rarefaction curves a) before and b) after applying rarefaction to the minimum library size 208

Table index

Table 1. 1. Facultative bacteria and their role in aphid defence against biotic and abiotic stress. 26
Table 1.2. Examples of plant root metabolites mediating changes in rhizosphere microbial communities. 49
Table 2.1 Parameters for alignment and deconvolution of chromatograms generated by LC-MS in the mzmine software v.4.0.3 77

Table 3. 1. Description of blanks and quality control samples used for the analysis of root exudates 118

Table 3. 2. Molecular networks where an annotated compound was connected to unknown features 136
Table 3. 3. Metabolites selected for confirmation of identity based on their spectral match and fold change 144

Supplementary Tables

Supplementary Table 2.1. Pairwise PERMANOVA results for profile of aboveground VOCs of plants under aphid herbivory. 104
Supplementary Table 2.2. Tentative annotation of non-volatiles detected with the LC-MS/MS in Data Independent Acquisition (DIA) mode. Annotations were obtained by comparing the fragment ions spectra with publicly available spectra in the GNPS environment. 105
Supplementary Table 2. 3. PERMANOVA results of data absorbance readings from Ecoplates™. 107
Supplementary Table 2.4. Paired t-test comparing the AWCD of individual carbon sources in samples from the rhizosphere of plants under aphid herbivory and control plants. Comparison was performed with the AWCD obtained after 72 hours of incubation. 107
Supplementary Table 2.5. PERMANOVA results of dbRDA for explained variance in microbial communities based in the experiment with sampling and aphid herbivory as factors. 108
Supplementary Table 2. 6. Differential abundance analysis of bacterial communities in plant roots. Analysis of Compositions of Microbiomes with Bias Correction-ANCOM-BC (q value <0.05) 109
Supplementary Table 3.1. Batch order for LCMS injections 159

Supplementary Table 3. 2. Annotations of features based on library matching with public libraries available in the GNPS platform. 160
Supplementary Table 3.3. Annotation of metabolites using the Taxonomically Informed Metabolite Annotation (TimaR) R platform. The platform performs library matching with freely available experimental spectra databases and an in-silico database developed using the MS1 information available in LOTUS (https://lotus.naturalproducts.net/). In the table, matches using only MS/MS (NPC_class) and taxonomy (Triticum aestivum L.) are used to produce a score that combines the biological and chemical matches. 164
Supplementary Table 3.4. Features statistically significant according to the differential abundance analysis of peak areas. These peaks were shown in the volcano plot in figure 3.7. When present, annotation for the pathway was included and the tool used for the annotation. 170
Supplementary Table 4. 1. Quality of merged sequences provided by Novogene for analysis 209

Supplementary Table 4.2. ANOVA result for alpha diversity analysis of bacterial communities 211
Supplementary Table 4. 3. Differential abundance analysis of bacterial communities in plant roots. Analysis of Compositions of Microbiomes with Bias Correction-ANCOM-BC (q value <0.1) 212
Supplementary Table 4. 4. Differential abundance analysis of bacterial communities in the rhizosphere. Analysis of Compositions of Microbiomes with Bias Correction-ANCOM-BC (q value <0.1) 213
Supplementary Table 4.5.. Statistically significant correlations from the Spearman correlation analysis 215

Chapter 1: General Introduction

This chapter provides the foundation for the research presented in this thesis project. It starts with an overview of the importance of ***aphid-wheat interactions*** *in agriculture and the role of microbial communities in shaping these interactions. The second section focuses on the influence of* ***plant metabolites*** *in mediating above and belowground interactions, with an emphasis on the* ***wheat-plant-soil microbe system****. This includes an overview of the methods used throughout this project. Finally, the chapter outlines the research objectives and provides an overview of the thesis structure.*

1.1. Moving away from pesticides

Ensuring food security and sustainability remains a global priority, as highlighted by the United Nations' second Sustainable Development Goal 2: Zero Hunger, which aims at creating a world free of hunger by 2030. The need to sustain food demands led to the green revolution in the 1960s, marked by the widespread use of synthetic nitrogen fertilisers, selective breeding, chemical pesticides and advanced machinery. These innovations contributed to an unprecedented increase in food production worldwide, particularly of staple grains such as wheat, maize and rice (Armanda et al., 2019; John & Babu, 2021). While the green revolution boosted crop yields (production per unit area) it was quickly recognised that these practices are not sustainable over time (Pellegrini & Fernández, 2018). Intensive agricultural practices have made crops more vulnerable to pests and diseases, making crops more reliant on the excessive application of chemical inputs that degrade soil health, contaminate water systems, and pose risks to human health (John & Babu, 2021). These

challenges highlight the need of more sustainable food production systems that balance agricultural productivity with environmental and human well-being.

The use of pesticides – chemical compounds designed to control pest populations – has significantly impacted crops, ecosystems, and human health. While pesticides play a role in increasing food production, they have been linked to health concerns, including respiratory and neurological disorders, reproductive issues, cancer, and diabetes (Rani et al., 2021). In the environment, pesticides pollute soil and water, affecting non-target organisms such as fish and birds. It is estimated that only 0.1% of applied pesticides reach their intended target, with the remainder contaminating soil and disrupting microbial communities critical for nutrient cycling (Rani et al., 2021; Zhou et al., 2025). Furthermore, the continuous use of pesticides tends to inhibit plant growth and induce defence responses in plants (Flors et al., 2024). For instance, in wheat, pesticides have been shown to alter hormone levels and secondary metabolites, while significantly reducing the diversity of soil bacteria associated with the plants (Zhou et al., 2022). Overall, it seems imperative to design better strategies to reduce the application of chemical pesticides, but these strategies need to be developed from knowledge of the agricultural systems and the ecological factors that can influence plant resistance to insect pests, like the intricate interaction between plants and soil microbes.

1.2. Importance of aphid-wheat-microbe interactions in agriculture

Approximately 66% of all known species are insects, contributing to more than three-quarters of our global biodiversity (Jankielsohn, 2018; Kawahara et al., 2021). Although only one million insect species are known, estimates suggest that the number of species could be around eight million (Chung Kim, 1993; Jankielsohn, 2018). As such, insects are a dominant form of life on earth, and their success is attributed to the wide range of ecosystem roles they play, including the most common one, herbivory (Jankielsohn, 2018; Lieutier et al., 2017).

Fossil evidence shows that insect herbivory has existed for over 400 million years (Palaeozoic) (Bruce, 2015; Scott et al., 1992), but the first definitive report of the impact of plant signalling on insect-plant interactions was only published in 1910 (Berenbaum & Zanger, 2008; Fraenkel, 1959). This work was a detailed description of the role of Brassicaceae glucosinolates - a group of secondary plant metabolites - in host plant selection by white cabbage butterflies, and it laid the foundation for the chemical ecology field (Berenbaum & Zanger, 2008). Later, the term 'coevolution' was coined to describe the "*patterns of interaction between two major groups of organisms with a close and evident ecological relationship*" (Ehrlich & Raven, 1964), using butterflies and plants as an example.

In this section, the insect and plant components of the study system will be examined, along with a third critical factor: their microbiome. Studies suggest that microbial communities play a fundamental role in shaping plant-insect interactions and their influence is a key component of this research project.

1.2.1. Aphid herbivory impacts on wheat production

The superfamily *Aphidoidea* is believed to have evolved approximately 280 million years ago (Simon et al., 2021). Of the 4,700 described aphid species, 55% are associated with herbaceous plants (Peccoud et al., 2010). Aphids are predominantly specialists, with more than half of all species restricted to feeding on a single plant species, forming intimate ecological relationships with their hosts. However, some aphids exhibit a broader host range; for instance, *Aphis gossypii* is an extreme generalist, capable of feeding on 912 plant species across 116 families (Peccoud et al., 2010).

Aphids that attack cereal crops are commonly referred to as “cereal aphids.” Some of the most economically significant species in this category include the English grain aphid (*Sitobion avenae*), the bird cherry-oat aphid (*Rhopalosiphum padi* L.), and the greenbug aphid (*Schizaphis graminum* Rondani) (Parry, 2013; Shavit et al., 2018). These insects are among the most damaging pests of cereal crops, with infestations leading to wheat yield losses ranging from 5% to 80% (Aradottir & Crespo-Herrera, 2021; Borg et al., 2024). Their pest status arises from both direct and indirect effects. Direct damage occurs through their feeding behaviour, in which aphids pierce the plant’s phloem and extract sap, diverting essential nutrients away from growth and development (Simon et al., 2021). Indirect damage results from their role as vectors of plant pathogens, particularly viruses and bacteria. Notably, aphids transmit over 40% of known plant viruses (Parry, 2013), including Barley Yellow Dwarf Virus (BYDV), one of the most devastating viral diseases affecting wheat (Nalam et al., 2019; Simon et al., 2021).

Aphids rely on phloem sap mainly for essential amino acids that they cannot synthesize (Nalam et al., 2019; Züst & Agrawal, 2016). However, phloem samp is rich in simple sugars produced by photosynthesis but contains limited essential amino acids, meaning that aphids must consume large quantities of sap to obtain sufficient nutrients (Züst & Agrawal, 2016). To regulate their sugar intake, aphids excrete excess sugars in the form of honeydew, which can serve as a substrate for the growth of sooty moulds. Although these fungi do not invade plant tissues, they form a dense layer on leaves, stems, and other plant surfaces, potentially reducing photosynthetic efficiency and stunting plant growth. In some cases, extensive mould growth has been reported to significantly reduce crop productivity (Thangaraj et al., 2022).

1.2.2. Wheat

Wheat is a major crop for food security, forming a key part of the diet for a significant portion of the world's population (Zhang et al., 2021). It was among the first domesticated crops, with evidence of domestication dating back to 7000–9000 BCE from Neolithic archaeological sites in the western Fertile Crescent (Kavamura et al., 2021; Shan & Osborne, 2024). As a cornerstone of early agricultural economies, wheat has remained essential to global agriculture. Bread wheat (*Triticum aestivum* L.) consistently ranks among the top five most-produced crops worldwide, with over 20,000 known varieties providing a staple food source for approximately 35% of the global population, supplying 20–29% of their dietary calories and protein (Kavamura et al., 2021; Simon et al., 2021). In 2023, global wheat production was estimated at 806 million tonnes (FAO, 2024).

While wheat domestication introduced key agronomic traits such as a non-brittle rachis, larger seeds and leaves, increased above-ground biomass, and faster growth,

these advancements came at the cost of reduced genetic diversity (Shan & Osborne, 2024). The Green Revolution of the 20th century further transformed cereal cultivation by prioritising the selection of above-ground traits to enhance yield and reduce losses by lodging (Waines & Ehdaie, 2007). In wheat, the introduction of dwarfing genes led to the development of shorter, sturdier plants with a greater proportion of assimilates allocated to grain filling, significantly increasing yields (Hedden, 2003). However, evidence suggests that modern wheat varieties, shaped by intensive selection for these traits, may have become more susceptible to environmental stressors, including pests and pathogens (Shan & Osborne, 2024).

1.2.3. Aphids, plants and their associated microbiomes

Besides their intricate association, plants and most animals have also co-evolved with microbial communities, with animals ranging in their degree of dependence of the microbiome from strong reliance to none (Hammer et al., 2019). In 1994, the term *holobiont* was defined as *"a single entity formed by the host and its symbionts"* (Simon et al., 2019). Zilber-Rosenberg and Rosenberg (2008) presented the "hologenome theory of evolution", which proposes the term "hologenome" as the sum of the genetic information contained in the genomes of the eukaryotic host and its microbial symbionts. It also considers that the microbial symbionts are key for the evolution and adaptation of their host. Microbes are, as the authors suggest, a fast way of acquiring new traits that would otherwise be acquired at a slower rate and might not coincide with the rhythm of environmental change. Although this theory has been disputed in recent years (Douglas & Werren, 2016; Moran & Sloan, 2015), there is no doubt that the microbiome can significantly contribute to their host growth, development and interaction with their environment.

The microbiota component of the eukaryote-symbiont interaction includes bacteria, fungi, protists, nematodes, and viruses (Gurung, Wertheim and Falcao Salles, 2019; Trivedi et al., 2020). Microbes can be obligate, co-obligate and facultative endosymbionts, according to the level of dependence on their symbiont partner to survive and reproduce (Nguyen & Van Baalen, 2020). Microbial partners can colonise virtually all parts of the host (plants and animals) and can live on the external surfaces or inside internal tissues. Classical examples of microbial partners key for survival are found in legumes, which form root nodules housing nitrogen-fixing rhizobia, and, on the insect side, aphids, which could not survive without a bacterial endosymbiont that provides them with essential amino acids (Nguyen & Van Baalen, 2020). Although phylogenetically distant, plants and some insects rely on microbes for similar functions, which are mainly related to nutrient acquisition, protection against biotic and abiotic stresses and adaptation to new environments (Stassen et al., 2021).

1.2.3.1. The aphid microbiome

Aphids are a model for studying insect-bacteria interactions due to their reliance on bacterial endosymbionts for survival and their relatively low microbial diversity (Elston et al., 2022; Grigorescu et al., 2018; He et al., 2021). In aphids, the primary endosymbiont *Buchnera* spp. is vertically transmitted via the ovaries (from parents to offspring). This obligate relationship involves specialized cells called bacteriocytes, which form the bacteriome—an organ dedicated to symbiosis (Renoz et al., 2022; Shigenobu & Yorimoto, 2022). In the bacteriome, *Buchnera* spp. supply essential amino acids and vitamins critical for aphid survival. However, their long co-evolution with aphids has led to a reduction in their genome, occasionally compromising their metabolic functions (Chong & Moran, 2018). To compensate for this limitation, aphids have recruited co-obligate endosymbionts, such as *Serratia, Sodalis* and *Erwinia*,

which provide nutrients that *Buchnera* spp. can no longer synthesize (McLean et al., 2019; Renoz et al., 2022).

Beyond obligate symbionts, aphids harbour facultative bacteria, which are horizontally transmitted and found in various tissues, including the haemolymph, salivary glands, and reproductive organs (Luna et al., 2018). These microbes enhance host fitness by increasing stress tolerance, aiding plant colonisation, and providing resistance to natural enemies (Elston et al., 2022; Guo et al., 2017; McLean et al., 2019; Shigenobu & Yorimoto, 2022; Zytynska & Meyer, 2019). However, these benefits come at a cost, often reducing aphid longevity and fecundity (Zytynska & Meyer, 2019). Examples of facultative symbionts and their effects on aphid fitness are summarized in Table 1.1.

Table 1. 1. *Facultative bacteria and their role in aphid defence against biotic and abiotic stress.*

Stress	Facultative symbiont	Host	Outcome for aphid host	Mechanism	Reference
Heat shock	Candidatus *Regiella insecticola* Candidatus *Fukatsuia symbiotica* Candidatus *Hamiltonella defensa*	Pea aphid (*Acyrthosiphon pisum*)	Positive with *Regiella* and *Fukatsuia*	Protection of aphid fecundity after heat shock.	(Heyworth et al., 2020)
Pesticides	*Hamiltonella defensa*	Wheat aphid (*Sitobion miscanthi)*	Positive	Reduced susceptibility to pesticides	(Li et al., 2021)
	Hamiltonella defensa	Pea aphid (*Acyrthosiphon pisum*)	Positive	Reduced the recruitment of natural enemies by the plant	(Frago et al., 2017)

Parasitoid	*Hamiltonella defensa, Regiella insecticola*	Pea aphid (*Acyrthosiphon pisum*)	Positive	Mummification rate after parasitoid attack was zero!	(Sochard et al., 2021)
	Hamiltonella defensa and Arsenophonus sp.	Cotton-melon aphid, (*Aphis gossypii*)	Positive in fitness, neutral in natural enemies	Enhanced performance (fitness), but not effect in parasitoid	(Ayoubi et al., 2020)

1.2.3.2. The plant microbiome

Microorganisms found in plants can be located below and aboveground (Trivedi et al., 2020). Aboveground, microbes colonise the *phyllosphere*, which includes the leaves, stems, buds, and flowers of plants, where they can exist on plant surfaces as epiphytes or within tissues as endophytes (Figure 1.1). Belowground, microorganisms are attracted by root exudates to the *rhizosphere,* a thin layer of soil surrounding the roots that is influenced directly by plant metabolism where microbial activity is significantly higher than in the bulk soil (Oburger & Jones, 2018; Rolfe et al., 2019; Vives-Peris et al., 2020). Some microorganisms are strongly attached to the root surface, in a zone called the *rhizoplane*, and some can penetrate the *root* endosphere (Chaturvedi & Singh, 2016a; Gaiero et al., 2013; Mitter et al., 2017; Reinhold-Hurek & Hurek, 2011). Microbial diversity in the root endosphere is considerably lower than in the rhizosphere and bulk soil, as successful root colonizers must possess specific traits, such as cellulolytic enzyme production to penetrate the root cortex (Mercado-Blanco & Lugtenberg, 2014). Additionally, endophytes can also be transmitted to the next generations of plants by seeds or by vectors (Hardoim et al., 2008; Reinhold-Hurek & Hurek, 2011).

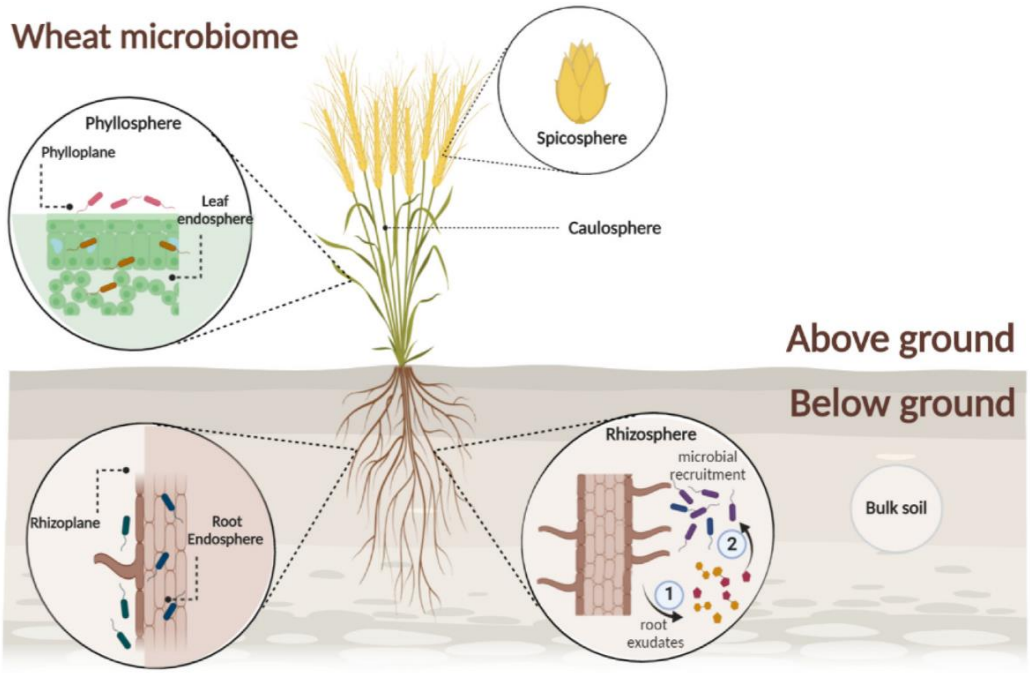

Figure 1.1. *Plant compartments divided into aboveground and belowground. Overall, in plants, the aboveground part is referred to as the phyllosphere, and the belowground part as the rhizosphere, while divisions can be found in each compartment, as shown in the figure. Taken from Kavamura et al. (2021)*

The importance of the rhizosphere microbiome

The interactions occurring in the rhizosphere make it one of the most complex communities on earth and a hotspot for microbial and enzymatic activity (Ma et al., 2018). A diverse group of microbes (e.g., mycorrhizal fungi, plant growth-promoting rhizobacteria (PGPR)) have been observed to be beneficial for plants via direct and indirect mechanisms (Pineda et al., 2010). Direct mechanisms are related to the ability to facilitate nutrient acquisition (e.g., nitrogen fixation, phosphate solubilisation, iron sequestration) and to modulate plant hormone levels (e.g., auxins, cytokines, gibberellins, ethylene). Indirect mechanisms are related to the protection of plants against pests and pathogens (e.g., production of antibiotics, siderophores, induced systemic resistance) (Chaturvedi & Singh, 2016; Nagrale et al., 2023; Oleńska et al., 2020). The effect of beneficial microbes in plants is not restricted to one mechanism at a time: studies have shown that the inoculation of beneficial bacteria like *Bacillus*

subtilis, Pseudomonas fluorescens, and *Azospirillum* spp. improves biomass growth and yield, induces systemic resistance against pathogens and increases plant tolerance to abiotic stresses (Abd-Allah et al., 2018; Pieterse et al., 2021; Rashid et al., 2012).

The rhizosphere microbiome and plant stress response

Under stress, changes in the chemical signals from plant roots have been associated with a "*cry for help*" hypothesis (Bakker et al., 2018; Rolfe et al., 2019), where plants actively influence microbial communities to recruit beneficial microbes, enhancing their health, tolerance and stress resistance. This influence is mostly based on the release of chemical compounds into the soil (i.e., root exudates), and substantial evidence supports this hypothesis in response to both biotic (e.g., herbivory) and abiotic (e.g., drought) stressors (Rolfe et al., 2019; Wang & Song, 2022).

In response to biotic stressors like insect herbivory, one extensively studied benefit of plant-microbe interactions is induced systemic resistance (ISR) (Chen et al., 2022; Friman, Pineda, et al., 2021b; Pieterse et al., 2014; Serteyn et al., 2020). In ISR, the colonisation of plants by beneficial microorganisms induces a state of "defence priming" in which plants respond faster to the attack of pathogens and herbivores. The priming effect of beneficial microbes is mainly regulated by hormones, via the jasmonic acid/ethylene signalling pathway, although in some cases, regulation via salicylic acid has been observed (Pieterse et al., 2014). For example, *Bacillus cereus* has been observed to trigger plant defence against the pathogenic fungus *Botrytis cinerea* by impacting the jasmonic acid/ethylene signalling pathway (Nie et al., 2017), while volatiles from other *Bacillus* spp. have been found to induce systemic resistance

via involvement of the salicylic acid pathway in tobacco plants (Tahir et al., 2017). The most widely studied beneficial bacteria for induced systemic resistance belong to the genera *Bacillus* and *Pseudomonas* (Friman, Pineda, et al., 2021a), which have been proven to improve plant resistance against agriculturally important pathogens like *Fusarium oxysporum* and *Clavibacter michiganensis,* causal agents of Fusarium wilt and bacterial canker, respectively, in tomato (Fatima & Anjum, 2017; Takishita et al., 2018), *Magnaporthe oryzae* in rice (blast disease) (Omoboye et al., 2019), and the Western corn rootworm (*Diabrotica virgifera virgifera)* in maize (Disi et al., 2018).

Although induced systemic resistance is key for plant defence, there are other mechanisms by which microbes can help plants. When plants face nutrient deficiencies, extracellular enzymes of microbes can increase nutrient availability in the soil, which in turn can help plants synthesize proteins and metabolites for their defence (Nagrale et al., 2023). However, this increase in resources does not always result in a positive outcome for plants, as some cases of increased susceptibility to insect herbivory have been observed (Kim et al., 2015; Pineda et al., 2012).

The wheat microbiome

The concept of a *core* microbiome refers to a set of microbial taxa consistently associated with a host across different environments, suggesting potential functional importance for plant health (Kavamura et al., 2021; Simonin et al., 2020). While soil type has been observed as the strongest determinant of rhizosphere microbial communities (Prudence et al., 2021; Worsley et al., 2021), studies have identified a core microbiome for wheat by analysing microbial communities in wheat rhizospheres and roots across diverse soils. For example, Simonin et al. (2020) identified 177 core taxa (2 archaea, 103 bacteria, 41 fungi, and 31 protists) from wheat grown in eight

soils across Europe and Africa. Although these taxa represented only a small fraction of the total soil diversity, they accounted for nearly 50% of microbial abundance in the rhizosphere, suggesting a consistent association with wheat plants regardless of environmental conditions. Similarly, Prudence et al. (2021) found that while soil type was the primary driver of microbial composition in the wheat root endosphere (Paragorn wheat cultivar). The core microbiome included members of the Streptomycetaceae (25.1%) and Burkholderiaceae (12%) bacterial families. These bacterial taxa declined as plants reached senescence, suggesting a strong dependence on a living host.

There is growing evidence that domestication has shaped wheat-microbe interactions. Modern wheat cultivars may have lost the ability to recruit beneficial microbes compared to their wild ancestors (Kavamura et al., 2020; Reid et al., 2021). Recent studies are starting to show that root exudate composition differs significantly between ancient and modern wheat cultivars, which may drive changes in microbial community structure. For example, Yue et al. (2023) observed the presence of unique specialised metabolites (e.g., oleamide, apiin, xanthine) in the root exudates of wild emmer wheat, and a different assemblage of microbial communities from wild and modern wheat. Their findings indicated that fungi play a more prominent role in shaping microbial communities in wild wheat, whereas bacterial communities dominated in modern cultivars. Their work suggested that fungi respond more strongly to the diverse range of metabolites present in wild wheat root exudates, while bacteria are more adapted to the less diverse exudates of modern wheat cultivars. These findings highlight the critical role of plant root exudates in mediating belowground interactions. Since root exudates serve as a primary means of communication between plants and soil microbes, more research is needed to

understand the contribution of these chemicals to the potentially beneficial functions of soil microbes.

Despite efforts to define a core microbiome, methodological inconsistencies remain. Different methodologies for collection of rhizosphere and rhizoplane soil make the comparison of studies difficult, while the methodology and pipeline for analysis, and applied thresholds for relative abundance can have a significant impact on the results. Furthermore, some studies focus on the rhizosphere microbiome, while others argue that root endosphere bacteria are more strongly correlated with wheat yield and quality (Zheng et al., 2023). The root endosphere, however, seems to be significantly influenced by the seed microbiome (Abdullaeva et al., 2022), which points at more research needed to disentangle the contribution of environmental and genetic factors to the wheat microbiome, which will be essential for developing strategies to harness beneficial microbes for sustainable wheat production.

1.2.4. Aphid-plant-soil microbe interactions

Most of our current understanding of insect-plant-microbe interactions comes from studies on the effects of beneficial rhizobacteria inoculation, which largely demonstrate a negative impact on insect performance (Friman et al., 2021b). In the context of aphid herbivory, bacterial strains from the genera *Bacillus, Pseudomonas, Azospirillum*, and *Acidovorax* have been shown to significantly reduce populations of aphids such as *Rhopalosiphum padi* and *Sitobion avenae* in bread wheat and barley (Mbaluto & Zytynska, 2024; Naeem et al., 2018; Santos et al., 2025). The primary mechanism through which these bacteria enhance plant defence appears to involve the modulation of hormonal signalling in the host plant (Figure 1.2). For instance,

Santos et al. (2025) found that inoculation of wheat plants with *Azospirillum brasilense* reduced the salicylic acid response to aphid herbivory, which correlated with a significant decrease in *R. padi* populations and, importantly, a reduction in Barley Yellow Dwarf Virus (BYDV) particles transmitted by this aphid.

Similarly, transcriptomic analysis by Mbaluto & Zytynska (2024) revealed that inoculation with *Acidovorax radicis* (N35) and *Bacillus subtilis* (B171) modulated the phenylpropanoid pathway—responsible for the synthesis of flavonoids, lignans, and other specialised metabolites—leading to a reduced *S. avenae* population in barley. Interestingly, their study observed that rhizobacteria initially suppressed plant defences at early time points when aphid densities were low. However, by 21 days post-infestation, when aphid numbers increased, bacterial suppression of plant defence was no longer evident.

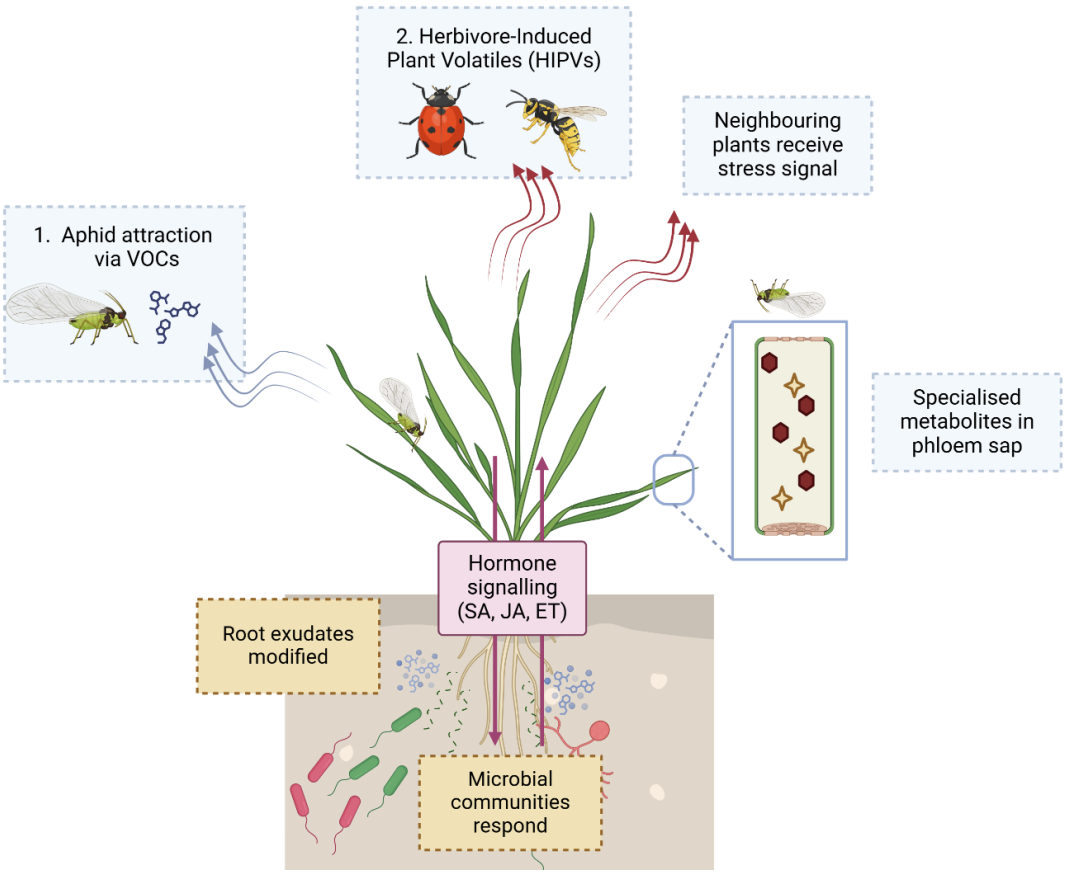

Figure 1.2. *Aphid-plant-microbe interactions. Modulation of plant hormone signalling by microbial communities can alter the plant defence against insect herbivory. Figure created using Biorender.*

While microbial modulation of plant hormones often enhances resistance, it can also result in induced susceptibility. Pineda et al. (2013) demonstrated that inoculation with *Pseudomonas fluorescens* strain WCS417r altered plant volatile emissions, reducing the attraction of natural enemies of *Myzus persicae*. Using *Arabidopsis thaliana* mutant lines impaired in jasmonic acid production, it was shown that these volatile changes were dependent on jasmonic acid signalling. Additionally, increased susceptibility to aphids has been correlated with an increased abundance of *Paenibacillus, Bacillus*, and *Pseudomonas* in the rhizosphere, though the underlying mechanisms remain unexplored (Blubaugh et al., 2018; Kim et al., 2015). Similar

cases of increased susceptibility have been observed with strains of arbuscular mycorrhiza and *Cladosporium oxysporum* (Razak & Gange, 2023).

The impact of aphid herbivory on plant-associated microbiomes has been less extensively studied, though recent research is beginning to unravel these complex interactions. Beyond the use of individual inoculation of bacterial strains, Hubbard et al. (2019) investigated the role of microbial community composition in aphid resistance by comparing plants grown in soils inoculated with intact soil solutions versus disrupted (filtered through a 0.2 µm mesh to remove all microbes) soil solutions. Their findings showed that plants with a disrupted microbiome were more susceptible to aphid infestation, with microbial disruption having a greater impact than plant genotype.

A top-down approach to aphid-plant-microbe interactions suggests that aphid herbivory can reduce rhizosphere bacterial diversity, with effects dependent on infestation severity (French et al. 2021). For example, aphid herbivory has been linked to a reduction of the abundance of bacterial amplicon sequence variants (ASVs) from genera such *as Rhodanobacter, Flavobacterium, Azospirillum, Hyphomicrobium, Alkanibacter, Cytophaga* in the rhizosphere of cabbage plants (Friman et al., 2021a). Interestingly, bacteria from the *Rhodanobacter* genus were also found to be less abundant in the soil of Pedunculate oak (*Quercus robur*) plants under aphid herbivory (Wolfgang et al., 2023). However, these effects appear to be soil-dependent, as two of the three soil types used in the latter study did not show significant microbial changes. Other studies have similarly reported no detectable effect of aphid herbivory on rhizosphere bacterial communities (O'Brien et al., 2018). Collectively, these studies demonstrate that plant-microbe-aphid interactions are species- and soil-specific, emphasizing the need for further research to unravel the complexities of these interactions.

Aphid-killing microbes

Culturable bacteria from soil and plant tissues (e.g., roots, leaves) have proven effective as foliar sprays to mitigate aphid damage. Most research on aphid-killing bacteria has focused on the genera *Bacillus* and *Pseudomonas*, which are widely used in biocontrol (Dimkić et al., 2022; Maksimov et al., 2020). Although most work with these bacteria has been performed with chewing insects in larval stages, recent work has shown their insecticidal activity against sap-sucking insects, including aphids (Álvarez-Lagazzi et al., 2021; López-Isasmendi et al., 2019; Paliwal et al., 2022). Other microbes that have been shown to be effective "*aphicidals*" are the enthomopathogenic fungi *Beauveria bassiana, Metarhizium brunneum* and *M. robertsii* (Rasool et al., 2021). However, most of these tests have been performed under *in vitro* conditions and more research is needed to simulate the complexity of what aphids and bacteria would encounter under natural conditions. Smee & Hendry (2022) showed that bacterial infection rates on aphids were lower in plants compared to what was observed by inoculating the bacteria in artificial diets (*in vitro)*. Additionally, they found that more time was needed to observe similar results as those with artificial diets. Overall, although there is potential for these microbes, more research is needed to establish effective methods for the use of these microbes in agriculture.

1.2.5. Study system

To investigate aphid-wheat-soil microbiome interactions, this study focused on the bird cherry-oat aphid (*Rhopalosiphum padi* L.), one of the most destructive insect pests worldwide (Li et al., 2017; Weibull, 1990). *R. padi* primarily damages wheat and barley crops (Peng et al., 2020) and has been extensively used in studies on aphid

resistance within the Chemical Ecology group at Rothamsted Research (Borg et al., 2024; Simon et al., 2021; Singh et al., 2020).

The wheat cultivar selected for this study, *Triticum aestivum* (L.) var. Solstice, has also been widely used in previous research by the Chemical Ecology group. This cultivar is highly susceptible to *Rhopalosiphum padi* and *Sitobion avenae*, attracting significantly higher aphid densities than other wheat varieties (Simon et al., 2021). In olfactometer assays using synthetic volatile blends, *S. avenae* aphids spent more time in the area containing volatiles from Solstice than in the area with volatiles from resistant wheat lines, further confirming its susceptibility (Borg et al., 2024). Additionally, *R. padi* exhibits prolonged phloem feeding on Solstice compared to resistant wheat lines, which may be linked to the cultivar's higher concentrations of total carbohydrates and organic acids (Greenslade et al., 2016).

1.3. Chemical signalling in aphid-plant-microbe interactions

1.3.1. Chemical cues in host recognition by aphid herbivores

Aphids recognise their hosts using both visual and olfactory cues (Webster, 2012). Olfactory cues primarily consist of volatile organic compounds (VOCs), which aphids use to distinguish host plants from non-hosts (Borg et al., 2024). These VOCs are low molecular weight compounds that plants constitutively produce and release into the environment, where they can be detected by other organisms. VOCs play a crucial role in mediating ecological interactions, including attracting pollinators and seed dispersers, recruiting beneficial microbes, signalling neighbouring plants, and deterring herbivorous insects and pathogens. While plants produce a vast array of

volatiles, certain classes of compounds exhibit near-universal distribution across species (Zhou & Jander, 2022). Neighbouring plants can also perceive these chemical cues, triggering responses related to competition, defence, and resistance.

Like many other insects, aphids detect VOCs through a complex molecular system involving odorant-binding proteins (OBPs). These proteins transport VOCs to olfactory receptors, which then activate sensory neurons, converting chemical signals into electrical impulses that guide insect behaviour (Loreto & D'Auria, 2022). The unique blend of VOCs emitted by a plant, in terms of both composition and concentration, acts as a chemical fingerprint that aphids use to assess host suitability (Loreto & D'Auria, 2022; Ninkovic et al., 2021).

After host location by aphids, the next steps also involve plant chemistry and are key for aphid success. After landing, aphids move their antennae to enable detection of odours and detect gustatory cues, including cuticular wax, trichome exudates, topology and colour (Shih et al., 2022). The next phase involves probing the plant tissue by ingesting small quantities of sap to evaluate host quality. During this process, aphids assess the chemical composition of the plant, with nitrogen and sugar concentrations serving as key indicators of nutritional suitability (Shih et al., 2022). Additionally, the presence of antifeedant or toxic compounds influences host acceptance. Prolonged phloem feeding—often lasting several hours—indicates successful host selection (Powell et al., 2006).

Penetration of the plant tissue is performed by the aphid's stylet, a specialised piercing-sucking mouthpart adapted to navigate plant tissues while minimising host defence activation. The stylet allows aphids to access phloem sap with minimal

mechanical damage, reducing plant-induced resistance responses. During penetration, aphids secrete a gelling saliva sheath that stabilises the stylet within the apoplast, enabling efficient probing and feeding. Additionally, they release watery saliva into parenchyma cells and sieve elements before ingestion. This secretion contains effector proteins that modulate plant defence responses, facilitating prolonged feeding and host exploitation (Silva-Sanzana et al., 2023).

1.3.2. Activation of plant response to aphid herbivory

When feeding on plants, aphids release salivary factors that serve multiple functions, including pre-digestion, enhancing aphid performance, and modulating plant defences (Kaloshian & Walling, 2016). Plants can perceive these factors, along with other damage-associated molecular patterns (DAMPs) caused by disruption of cells by herbivores (Arimura, 2021). Some of these factors are conserved across insect species, allowing plants to recognize them as Herbivore-Associated Molecular Patterns (HAMPs) and trigger Pattern-Triggered Immunity (PTI) (Kloth & Dicke, 2022).

In response to PTI, aphids can secrete effectors that suppress this plant immunity strategy. As an evolutionary response, plants have developed Resistance (R) proteins, which recognise these effectors and initiate a stronger Effector-Triggered Immunity (ETI) (Kaloshian & Walling, 2016; Nalam et al., 2019). Among these R proteins, those encoded by Nucleotide-Binding Site-Leucine-Rich Repeat (NBS-LRR) genes constitute the largest group of plant resistance genes, playing a crucial role in pathogen and herbivore defence (Mou et al., 2023).

Herbivore attack rapidly alters plasma membrane potential (*Vm*), leading to the production of secondary messengers such as calcium ions (Ca^{2+}), reactive oxygen species (ROS), mitogen-activated protein kinases (MAPKs), and transcription factors (TFs), which act as signal transducers (Kloth & Dicke, 2022). These changes are among the earliest plant defence responses, occurring within seconds to minutes after the attack (Kloth & Dicke, 2022; Pachú et al., 2023). Once the signalling is activated at the wounding site, long distance signals are released as an important defence strategy for plant survival. This systemic signalling involves movement of ions across plasma membranes, facilitating long-distance communication between cells (Mostafa et al., 2022).

The principal hormones involved in plant-insect interactions are jasmonic acid, salicylic acid, and ethylene (Eichmann et al., 2021). Other hormones that might influence plant response include abscisic acid, auxin, cytokinins, brassinosteroids, and gibberellic acid (Thaler et al., 2012). Jasmonic acid is considered a conserved core signal responsible for the transcriptional activation of the defence response in plants to insects. However, plants fine-tune their hormonal responses based on the feeding mode of the herbivore. (e.g., chewing, biting, sap-sucking) (Felton et al., 2014; Friman, Pineda, et al., 2021b). This is the case for aphids and other phloem feeders, where salicylic acid signalling seems to be the key regulator of plant defence response (Erb et al., 2012; Nalam et al., 2019; Züst & Agrawal, 2016). Interestingly, aphids show susceptibility to jasmonic acid-mediated defences (Züst & Agrawal, 2016). As jasmonic acid and salicylic acid signalling pathways are often antagonistic, some aphid species appear to manipulate this crosstalk to their advantage (Züst & Agrawal, 2016). However, this interaction is highly species-specific; and while some studies report no effect of salicylic acid on aphid performance (Zhang et al., 2019), others have observed an increase in plant defence under exogenous application of

salicylic acid (Xiao et al., 2022). This variability highlights the complexity of hormonal interactions and the co-evolutionary arms race between plants and aphids.

1.3.3. Plant defence against aphid herbivory

Plant defence against aphids can be categorised into two primary strategies: antixenosis and antibiosis. Antixenosis refers to the influence of plants on aphid behaviour, such as plant choice and feeding behaviour (Friman et al., 2021b; Simon et al., 2021; Zhou & Jander, 2022). This strategy typically involves physical or chemical traits that deter aphids from feeding. Antibiosis, on the other hand, refers to direct effects on aphid physiology, leading to reduced growth, survival and reproduction of aphids. This includes the production of toxic secondary metabolites, defence proteins, enzymes, and proteinase inhibitors (Howe & Jander, 2008; War et al., 2018).

The formation of a waxy cuticle, trichomes, spines, and hardening of leaves constitute an example of antixenosis, as these traits make it more difficult for aphids to feed. These structural defences constitute the first line of defence against any time of pest attack (Zhang et al., 2024). Another key antixenosis mechanism is the release of Herbivore-Induced Plant Volatiles (HIPVs), which can repel aphids, attract natural aphid predators, and signal neighbouring plants about herbivore presence (Turlings & Erb, 2017). As discussed in Section 1.3.1, plants constitutively produce volatile organic compounds (VOCs) to interact with their environment. However, VOC release following herbivore damage (HIPV) appears to be a general plant response, with biosynthesis occurring *de novo* and the volatiles released in the damaged tissues (Dudareva et al., 2004).

While plant volatiles are associated with the antixenosis strategy, non-volatile specialized metabolites are often linked to antibiosis. These metabolites are typically encountered by herbivores when they feed on plant tissues. In the case of sap-sucking aphids, the lack of significant cell disruption means they are exposed only to low concentrations of these metabolites, which are primarily found in the phloem sap (Züst & Agrawal, 2016). Nevertheless, these secondary metabolites are crucial to plant defence, playing roles in antibiosis strategies.

Most Herbivore-Induced Plant Volatiles (HIPV) and non-volatile metabolites involved in plant defence are considered plant specialised metabolites. These metabolites are at the core of plant response to aphids and other stressors. In addition to primary metabolites –required for plant growth- and hormones –necessary for regulation of plant growth and development, secondary metabolites help plants survive in a competitive environment (Al-Khayri et al., 2023). Currently, more than 2,140,000 secondary metabolites have been reported in the plant kingdom, with a diverse set of structures and functions, and it is believed that, out of these, a single plant species can contain around 5,000 metabolites (Al-Khayri et al., 2023; Wang et al., 2019). At least five classes of secondary metabolites are confirmed to play a role in the regulation of plant defence: glucosinolates, benzoxazinoids, aromatics, terpenes and green leaf volatiles (Erb & Kliebenstein, 2020; Mostafa et al., 2022).

Glucosinolates and benzoxazinoids are particularly associated with *Brassicaceae* (cabbage family) and *Poaceae* plants (grasses), respectively (Erb & Kliebenstein, 2020). These metabolites have been shown to induce callose deposition, a key defence response to aphid herbivory. Callose forms “plugs” in sieve tubes, preventing aphids from feeding and acting as both a chemical and physical barrier against

phloem-feeding insects and pathogens (Hao et al., 2008; Mbiza et al., 2022; Wang et al., 2021). However, the mechanism underlying the induction of callose formation by these secondary metabolites remains to be elucidated (Erb & Kliebenstein, 2020). Moreover, these metabolites are also directly involved in antifeedant effect against aphid herbivory and are thought to be involved in the regulation of other metabolic pathways (Erb & Kliebenstein, 2020; Florean et al., 2023; J. H. Kim et al., 2008). Volatile secondary metabolites, including terpenoids, green leaf volatiles (GLVs), and aromatic compounds, also play a role in plant defence. Many of these volatiles can prime or induce hormonal signalling pathways that enhance plant resistance (Turlings & Erb, 2017). Notably, parasitoid insects are highly sensitive to GLVs, which are often produced in response to herbivore attack (Turlings & Erb, 2017).

1.3.4. Wheat plant defence against aphid herbivory

Salicylic acid plays a central role in wheat's defence against aphid herbivory and is recognized as a key phytohormone mediating wheat plant-aphid interactions. While this hormone is often thought to be exploited by aphids to suppress jasmonic acid - mediated plant defences (Züst & Agrawal, 2016), recent studies have revealed diverse mechanisms by which salicylic acid contributes to plant resistance.

Exogenous application of salicylic acid has resulted in changes in the phenolic compounds coumaric acid, ferulic acid, caffeic acid and chlorogenic acid in leaves of wheat plants that resulted in a decreased reproduction rate of the aphid *Sitobion avenae* (Feng et al., 2021). The application of methyl salicylate (MeSA), a volatile compound resulting from the methylation of salicylic acid, and a common herbivore-induced plant volatile, resulted in the release of a unique blend of VOCs that increased the attraction of the aphid parasitic wasp *Aphidius difuensis,* a natural

enemy of the grain aphid *Sitobion miscanthi* (Xiao et al., 2022). Three volatiles were identified as attractants of the parasitoid: p-Cymene, m-Diethyl benzene and Carveol (Xiao et al., 2022). Furthermore, exposure of wheat seedlings for 6 h to 10 µL of methyl salicylate resulted in an increase in the content of two flavonoids (xanthohumol and isobavachalcone) and one benzoxazinoid, DIMBOA, on wheat leaves (Li et al., 2025). In the latter, transcriptomic analysis revealed that priming plants with methyl salicylate resulted on the differential expression of genes involved in diverse metabolic pathways, including flavonoids, monoterpenoids and alpha-linolenic acid metabolism. Furthermore, hormone analysis revealed increases in salicylic acid and jasmonoyl-L-isoleucine.

Flavonoids, and overall total concentration of phenolic compounds, has been positively associated with aphid-resistant wheat cultivars (Wang et al., 2024; Zhang et al., 2022). Moreover, research with ancestral resistant-wheat lines has shown that antixenosis (the reduced attractiveness) of ancestral wheat resistance cultivars could partially be explained by the presence of 21 confirmed metabolites to which aphid antennae responded (EAG-active) belonging mostly to green leaf volatiles and benzenoids (e.g., heptanal, nonanal, decanal, hexanoic acid as green leaf volatile and ethylbenzene, benzaldehyde, 3-ethylbenzaldehayde as benzenoids) (Borg et al., 2024). A comprehensive study by Wang et al. (2024) demonstrated how integrating transcriptomic and metabolomic approaches can unravel resistance mechanisms in wheat. Their work identified four key metabolites—crotonoside, guanine, 2′-O-methyladenosine, and ferulic acid—associated with high resistance against *Sitobion miscanthi* in the highly resistant wheat cultivar ZM9. Notably, their findings highlighted the importance of belowground factors in aphid-plant interactions. Increased nitrogen (N) availability in the soil benefited aphids, even in the highly resistant wheat cultivar ZM9, reducing resistance at higher N fertilization levels.

The identification of these metabolites is key for the development of pest management strategies. External application of nano-Selenium and melatonin enhanced the concentration of DIMBOA (a benzoxazinoid), melatonin and jasmonic acid by 34.8, 70.8 and 51.3%, respectively, reducing aphid population in wheat plants to 52.2% (Zhou et al., 2021). The authors show that this application resulted in a different profile of VOCs released by wheat plants, including an increase in 1-propanol, isopentyl alcohol, and acetoin, among others. This points at a systemic response that is not dependant on the ability of one compound to increase wheat resistance to aphid herbivory. An interesting result from this work is the use of melatonin, which has recently gained attention as a key regulator of phytohormonal signalling in biotic and abiotic stresses (Di et al., 2019; C. Sun et al., 2021).

1.4. Connecting above and below: The role of root exudates in plant-microbe interactions under aphid herbivory

1.4.1. The role of root exudates in plant belowground interactions

Plants move around 50% of the fixed carbon to belowground tissues (Ma et al., 2022), of which approximately 40% is released into the rhizosphere in rhizodeposits (Seitz et al., 2022). Plants release rhizodeposits into the soil that include cell debris, mucilage, sloughed root cap cells, and metabolites broadly classified as root exudates (Oburger & Jones, 2018; Tian et al., 2020). These rhizodeposits have diverse functions, e.g., alter soil biochemical properties, increase nutrient acquisition, detoxify metals, and communicate and maintain positive relationships with other organisms while avoiding or repelling pathogens (Ma et al., 2022; Warren, 2016) (Figure 1.3).

The diverse metabolites present in rhizodeposits can be broadly classified into high molecular weight (>1000 Da), such as polysaccharides and enzymes, and low molecular weight (<1000 Da), including sugars, organic acids, phenolics, lipids, and other specialised metabolites (Warren, 2016). While definitions vary, root exudates typically refer to the low molecular weight fraction, which can be further categorized into primary and secondary metabolites, as discussed in Section 1.3.3. Briefly, primary metabolites are essential for plant growth and cellular function, whereas secondary (or specialised) metabolites play ecological roles, mediating plant interactions with their environment (Delory et al., 2016). However, this distinction is not absolute, as primary metabolites, mainly comprising carbohydrates, organic acids, amino acids (Canarini et al., 2019) have important roles in attracting of microbial communities in the soil (Broeckling et al., 2008; Chaturvedi & Singh, 2016a).

The majority of root exudation is thought to occur in the root tips (Canarini et al., 2019; Kranawetter & Sumner, 2025). However, there is evidence of compounds such as flavonoids, which can be released from more mature root cells near root hairs (Kranawetter & Sumner, 2025). The root tip produces a root cap to protect the meristem (undifferentiated cells undergoing continuous cellular division) that contains loosely attached cells programmed to be released into the rhizosphere. Once released, these loose cells, or *border cells*, secrete DNA, protein, mucilage and specialised metabolites (Kranawetter & Sumner, 2025; Ropitaux et al., 2020; Sasse et al., 2018). These border cells have roles including lubrication for the movement of roots through the soil, binding cations of heavy metals to prevent toxicity, and are the first line of defence against microbial pathogens. Among their diverse functions, border cells have been suggested to act as a decoy, releasing signals to attract pathogens, and then inhibit their growth or prevent root colonisation (Hawes et al., 2016; Hawes et al., 1998).

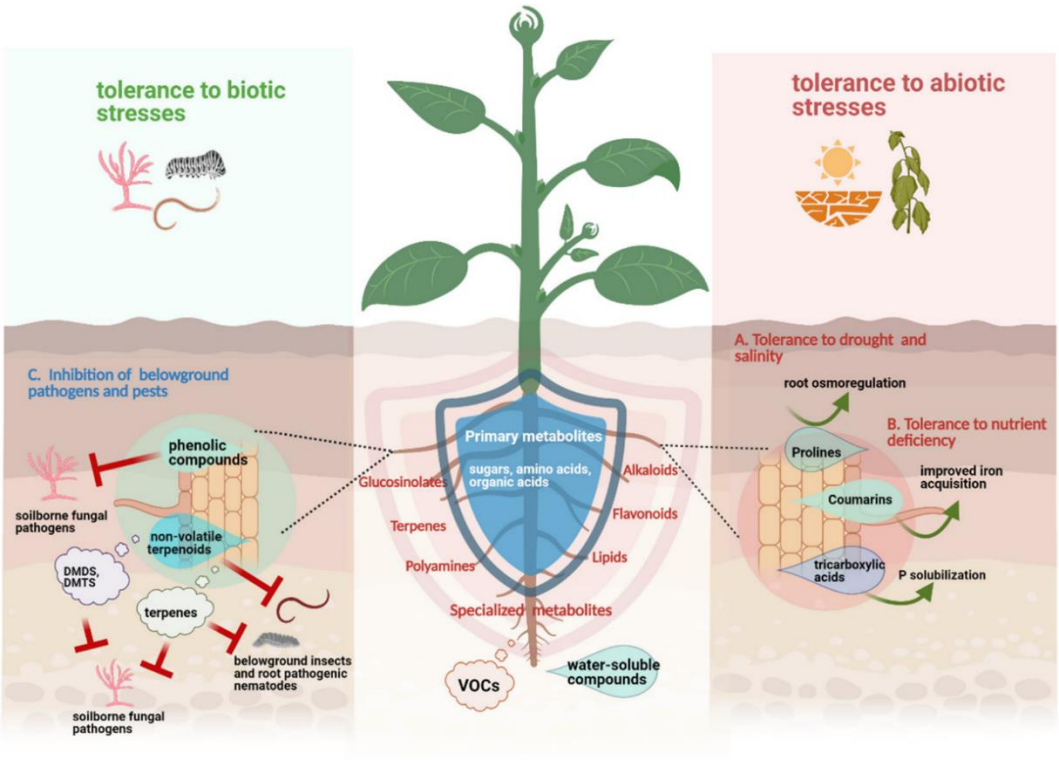

Figure 1.3. *Classes of compounds present in plant rhizodeposits and documented functions. Taken from Rizaludin et al. (2021).*

Root exudates are affected by different factors including the plant host, plant developmental stage and environmental conditions such as salinity, temperature, pH, soil chemical properties and presence of microbes and other plants (Ma et al., 2022; Sasse et al., 2018). Mirroring this, microbial communities have also been observed to change according to plant species and developmental stage, diurnal timepoints, and environmental factors, which is why these exudates are thought to play a key role shaping microbial communities (Bending et al., 2024; McLaughlin et al., 2023). While primary metabolites are mainly direct carbon and nitrogen sources for microbial communities, specialised metabolites are believed to help plants regulate and control the composition of microbial communities in the rhizosphere.

As described for insect herbivores (Section 1.3.3), different specialised metabolites released by plant roots have been observed to play a key role in regulating beneficial and pathogenic plant-microbe interactions. These metabolites are often inducible by plant exposure to stress, are not metabolised by all microbes, and typically have antimicrobial and/or signalling activities (Rolfe et al., 2019). Some of the most well-known regulators belong to the same classes involved in plant-insect interactions, including glucosinolates, flavonoids, coumarins, benzoxazinoids, terpenes, and phytohormones like salicylic acid and jasmonic acid (Koprivova & Kopriva, 2022). For instance, in the legume-rhizobia interaction, flavonoids induce the expression of the *nod* gene in rhizobia, and further function as chemoattractants enhancing the concentration of the bacteria on root surfaces. Strigolactones, a class of phytohormones, stimulate germination and branching of arbuscular mycorrhizal fungi (AMF) (Al-Khayri et al., 2023; Koprivova & Kopriva, 2022). Table 1.2 shows some examples of primary and specialised metabolites regulating plant-microbe interactions.

Table 1.2. *Examples of plant root metabolites mediating changes in rhizosphere microbial communities.*

Compound*	Condition	Plant	Microorganism	Effect	Reference
Oxylipins	Root pathogen, salt, aboveground mechanic wounding	Tomato and cucumber	*Trichoderma harzianum* T22	Increased chemotaxis	(Lombardi et al., 2018)
Glucosinolates	Plant cultivars with different levels of metabolite secretion	Field mustard (*Brassica rapa*)	Rhizosphere bacterial communities	Negative and positive associations with bacterial taxa	(DeWolf et al., 2023)
Jasmonic acid	Plant cultivars with different levels of metabolite secretion	Maize (*Zea mays*)	Rhizosphere bacterial communities	Significantly different assembly at different growth stages	(Lopes et al., 2022)
Total sugars	Plant cultivars with different levels of metabolite secretion	Maize (*Zea mays*)	Rhizosphere bacterial communities	Significantly different assembly at different growth stages	(Lopes et al., 2022)
γ-Aminobutyric acid (GABA)	Plant cultivars with different levels of metabolite secretion	Maize (*Zea mays*)	Rhizosphere bacterial and fungal communities	Changes in community assembly	(Wang et al., 2022)
2,4-dihydroxy7-methoxy-2H-1,4-	Plant cultivars with different levels of metabolite secretion	Maize *(Zea mays*)	Rhizosphere bacterial and fungal communities	Changes in community assembly and upregulation of metabolic pathways	(Wang et al., 2022)

Compound*	Condition	Plant	Microorganism	Effect	Reference
benzoxazin-3(4H)-one (DIMBOA)				related to biofilm formation in bacteria (among others) and sugars metabolism in fungi.	
6-methoxy-benzoxazolin-2-one (MBOA)	Wild type (WT) and mutant (*bx1*) plants. Mutants exuded 90% less than WT plants	Maize (*Zea mays*)	Rhizosphere bacterial and fungal communities	Changes in community assembly and legacy effect	(Hu et al., 2018)
Quercetin	Native and introduced plant populations with different levels of metabolite secretion in root exudates	Chinese tallow tree (*Triadica sebifera*)	Arbuscular Mycorrhiza Fungi (AMF)	Increased colonisation by the fungi with higher levels of quercetin	(Tian et al., 2021)
Flavonoids	Plants exposed to different types of foliar herbivory (*Spodoptera litura, Spodoptera frugiperda, Cnidocampa flavescens, Bikasha collaris*)	Chinese tallow tree (*Triadica sebifera*)	Arbuscular Mycorrhiza Fungi (AMF)	Increased colonisation correlated with increased flavonoids content in roots	(Xing et al., 2024)
Dolabralexins (diterpenoids)	Wild type (WT) and mutant *(Zman2*) deficient in dolabralexins.	Maize (*Zea mays*)	Rhizosphere bacterial communities	Changes in community structure	(Murphy et al., 2021)

Compound*	Condition	Plant	Microorganism	Effect	Reference
Salicylic acid	Wild type and mutant	*Arabidopsis thaliana*	Root endospheric bacterial communities	Changes in abundance and composition of communities	(Lebeis et al., 2015)

*Compounds with the same colour belong to the same chemical class.

Diterpenoids Phenylpropanoids Benzoxazinoids Amino acids Sugars Glucosinolates Oxylipins

1.4.2. Root exudates mediating plant-microbe interactions under biotic stress

Changes in root exudation profiles, triggered by biotic or abiotic stressors, can significantly influence microbial recruitment, which, in turn, may have positive, negative, or neutral effects on plant resistance. According to the "cry for help" hypothesis, plants can modulate microbial community composition by releasing chemical signals (i.e., root exudates) that attract beneficial microbes, which enhance the plant's defence against pests and pathogens (Rolfe et al., 2019). Supporting this hypothesis, studies comparing microbial communities from healthy and stressed plants have highlighted differences in microbial composition, correlating with varying plant responses to stress. However, only a limited number of compounds in root exudates have been identified as key players in these microbial shifts. Most of the identified compounds are linked to the changes in root exudates of plants to enhance the recruitment of beneficial microbes that can aid supress root colonization by microbial pathogens like *Fusarium oxysporum* (Huang et al., 2020; Tong et al., 2024) and *Ralstonia solanacearum* (Gu et al., 2016). Nevertheless, changes in root exudate profiles in response to aboveground pests or pathogens remain largely unexplored.

Currently, the best documented compounds observed to drive changes in microbial communities associated with plants under aboveground biotic stress are the coumarin scopoletin and the benzoxazinoid 6-methoxy-benzoxazolin-2-one (MBOA). Scopoletin has been studied related to their ability to increase plant resistance against different soil-borne pathogens (Stringlis et al., 2019; Sun et al., 2014; Yang et al., 2016), however, using *Arabidopsis thaliana* mutants deficient in scopoletin production showed that this compound is needed to create the legacy effect (long-lasting changes in soil microbiome composition) that enhances plant response to the foliar

biotrophic downy mildew pathogen *Hyaloperonospora arabidopsidis* (*Hpa*) (Vismans et al., 2022). Furthermore, the authors showed that the modified bacterial communities were able to enhance plant resistant to the pathogen via salicylic acid signalling. Interestingly, scopoletin has been observed to directly correlate with jasmonic acid levels in leaves of wild tobacco, *Nicotiana attenuata,* against the necrotrophic fungus *Alternaria alternata*, pointing at possible plant-specific and pest-specific (biotroph vs. necrotroph) defence responses modulation by scopoletin (Sun et al., 2014).

The second compound, *6-methoxy-benzoxazolin-2-one (MBOA)*, belongs to the benzoxazinoids (BXs) class, which has been suggested to be key in modulating the maize root microbiome, with positive correlations between the ability of bacteria to tolerate BXs presence and their relative abundance in the rhizosphere (Thoenen et al., 2023). Moreover, in an interesting study, Hu et al. (2018) showed that accumulation of MBOA is necessary to trigger changes in soil microbial communities that will in turn modulate plant response to *Spodoptera frugiperda*. Notably, the changes in rhizosphere microbial communities increased jasmonic acid signalling, further highlighting the specificity of plant-microbe interactions.

Finally, some classes of primary metabolites including long chain fatty acids, short and long-chain amino acids, present in root exudates, have been observed to modulate recruitment of microbial communities in plants under pathogen attack. Wen et al. (2021) reported that a mix of five long chain fatty acids (pentadecanoic acid, hexadecanoic acid, palmitoleic acid, octadecanoic acid, and arachidic acid) and six aminoacids (isoleucine, leucine, methionine, proline, tryptophan, and ornithine) were responsible for the attraction of beneficial bacteria from the *Pseudomonas* genus that

induced plant resistance against aboveground pathogen. Foliar infection of *Panax notoginseng* by *Alternaria panaxe* enhanced the exudation of short- and long-chain organic acids, sugars, and amino acids from roots (Huang et al., 2020). In response, an increase in abundance of *Trichoderma*, *Bacillus*, and *Streptomyces* genera were observed in the rhizosphere of plants. The authors also observed a suppressive effect of the root exudates against the root pathogen *Ilyonectria destructans* showing that the changes in root exudates can have impacts in both positive and negative interactions.

Given the diversity of plant metabolites and their ability to modulate their release according to environmental conditions, more research is needed to increase our understanding of how different primary and specialised metabolites can mediate the recruitment of beneficial microbes that can result in an enhancement of plant resistance to aboveground pests and pathogens.

1.5. Main techniques used in this study for the analysis of plant-soil microbe interactions

At the core of this thesis, two main techniques were used to characterise changes in plant-soil microbial communities: untargeted metabolomics of plant root exudates and amplicon sequencing analysis of bacterial communities. Here, a short overview of these techniques is presented.

1.5.1. Untargeted metabolomics of plant root exudates

Root exudate samples contain a wide diversity of metabolites, including sugars, amino acids, organic acids, fatty acids, specialised metabolites and plant hormones (Feng et al., 2024). This diversity has traditionally made it difficult to capture all signals present in the root exudates using one single method.

Advances in instrumentation and analysis platforms have allowed the rapid growth of the metabolomics field, which aims at capturing the small molecules (metabolites) present in complex samples. Within the field, targeted (based on known information) and untargeted (exploratory methods) have helped unravelled the complexity of biological samples. The latter, often yields metabolites in the range of hundreds to low thousands, helping to detect small molecules and signatures of the organismal response to biotic and abiotic stresses in plants, animals and microbes (Evans et al., 2020).

Four major technologies have been key for the development of the metabolomics field: gas chromatography mass spectrometry (GC-MS), liquid chromatography mass spectrometry (LC-MS), capillary electrophoresis mass spectrometry (CE-MS), and nuclear magnetic resonance spectroscopy (NMR) (Perez de Souza et al., 2021). However, LC-MS is one of the most widely employed techniques for untargeted metabolomics due to its high sensitivity, specificity, and broad coverage capabilities (Broeckling et al., 2023; Perez de Souza et al., 2021). More specifically, liquid chromatography coupled to tandem mass spectrometry (LC-MS/MS) has been widely used in metabolomics as it allows the simultaneous detection and qualitative annotation of many metabolites (Pakkir Shah et al., 2024).

In LC-MS/MS for metabolomics studies, a first step is performed by separating the molecules based on their physical or chemical properties (according to the column and mobile phases in the liquid chromatograph). Then, these molecules are introduced into the mass spectrometer, where they are converted to ions that are then detected by the mass analyser to obtain their molecular mass. In a further step, these ions, also known as “precursor ions”, continue to the collision cell, where they are further fragmented to obtain product ions (Figure 1.4), which are detected and analysed to obtain their molecular mass (Thomas et al., 2022). These fragments are then used to construct the structure of the compounds and further obtain their chemical classes or tentative identities (annotations).

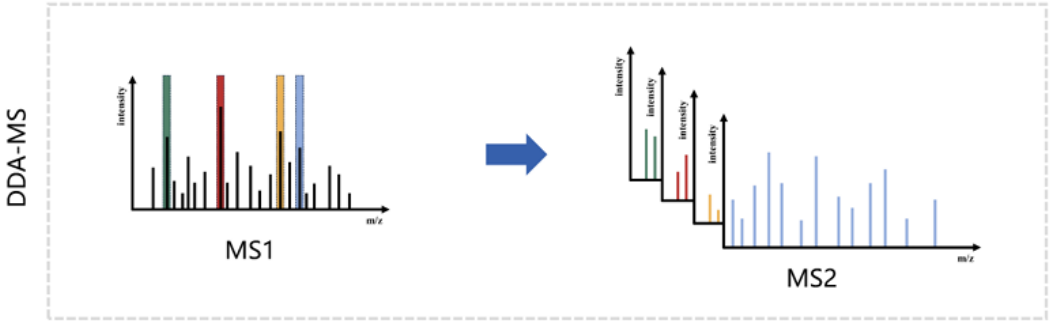

Figure 1.4. *Fragmentation of precursor ions to obtain product ions used for structural annotation of compounds in complex samples. In this example, the data-dependant acquisition method is used, selection precursor ions based on an intensity threshold. Taken from (Lyu et al., 2024)*

During data acquisition in the mass spectrometer, the selection of precursor ions can be performed mainly using two approaches: data-dependent and data-independent acquisition methods. The main difference between the two is that, in data-dependent methods, a selection of precursor ions based on user-guided criteria, while in the data-independent method all precursor ions are fragmented. The data-dependent acquisition method is preferred in the untargeted metabolomics field as, since not all

ions are fragmented, the complexity of the data is reduced, allowing for higher quality of fragmentation data (Guo & Huan, 2020).

The steps that follow the LC-MS/MS analysis involves the use of specialised software aimed at the analysis of the big datasets produced. They involve the removal of potential unwanted signals, aligning of precursor ions, and obtaining the fragment ions data. These fragments are used as *fingerprints* to compare against available experimental and *in silico* structural databases (Pakkir Shah et al., 2024). The current rate of annotation using untargeted metabolomics is low due to reasons that include the lack of mass spectral libraries, potentially undescribed metabolites and complexity of the datasets. However, the tools currently being developed for the analysis of these datasets, including clustering techniques and machine learning algorithms to predict structural classes, will continue to increase annotation rates from untargeted metabolomics and allow the discovery of so-far unknown metabolites (El Abiead et al., 2025).

1.5.2. Microbiome analysis

The study of the *microbiome* –-the assembly of all living organisms in a defined environment, including their genomes, structural elements and metabolites (Berg et al., 2020; Hou et al., 2022)- has been key to unravel how different environmental and biotic conditions can impact host-microbe interactions. Three main strategies to study these communities have been used, including the marker gene analysis (also known as metabarcoding, or amplicon sequencing analysis), whole metagenome analysis, and metatranscriptomics (Knight et al., 2018).

Marker gene, or amplicon sequencing analysis, is the most common technique used to study the composition of microbial communities (Knight et al., 2018; Liu et al., 2021). Amplicon sequencing uses primers that target a specific region of a gene of interest to determine the phylogeny of microbial communities in a sample (Knight et al., 2018). This region usually contains a highly variable region used for detailed identification, flanked by highly conserved regions that serve as reliable binding sites for PCR primers (Knight et al., 2018).

Amplicon sequencing offers several advantages, including its well-established protocols, speed, cost-effectiveness, and suitability for samples with host DNA contamination (Callahan et al., 2019; Knight et al., 2018). However, it has limitations. The technique generally provides genus-level resolution, and primer bias can occur if primers do not bind equally to all DNA sequences, potentially leading to amplification bias (Knight et al., 2018; Liu et al., 2021).

The major marker genes for bacterial and fungal communities are the 16S rRNA gene, and the internal transcribed spacers (ITS), respectively (Liu et al., 2021). In bacteria and archaea, the 16S rRNA gene is approximately 1,500 bp long and contains nine different hypervariable regions (V1-V9) (Kameoka et al., 2021) Sequencing these regions generates short reads that can be used to infer microbial diversity. Taxonomic identification is often based on operational taxonomic units (OTUs), which group sequences with ≥97% similarity, or amplicon sequence variants (ASVs), which differentiate sequences with single-nucleotide precision (Callahan et al., 2017). The resulting OTU or ASV tables, containing DNA sequences and their corresponding counts, are used for downstream analysis (Knight et al., 2018).

Amplicon sequencing analysis can answer questions related to the microbes present in the samples, typically through three main approaches: alpha diversity, beta diversity, and differential abundance analysis (Liu et al., 2021). The alpha diversity refers to the diversity within a sample considering both richness (the number of species) and evenness (the distribution of species) (Hugerth & Andersson, 2017; Liu et al., 2021). For instance, the Shannon diversity index investigates the richness and evenness by calculating the uncertainty of predicting the identity of randomly selected individual. Other diversity index can focus on richness (e.g., counts of observed reads), or evenness of the distribution (e.g., Simpson index) (Hugerth & Andersson, 2017). Beta diversity analyses, on the other hand, evaluates the dissimilarity in the microbiome composition of different samples, and is frequently visualised using dimensional reduction methods such as non-multidimensional scaling (NMDS) and principal coordinates analysis (PCoA) (Liu et al., 2021). Differential abundance analysis identifies potential key taxa involved in structural changes in microbial composition in response to a given condition. Different tools have been developed to investigate these differences, or borrowed from other fields like transcriptomics (e.g., DeSEQ2). Since no single method is universally superior, it is recommended to apply multiple approaches to determine which yields the most biologically meaningful insights for a given dataset (Nearing et al., 2022).

1.6. Thesis objective and research questions

This research investigates wheat-soil microbe interactions under aphid herbivory. The objectives and hypotheses are:

1. **Investigate changes in the plant-soil microbe system in wheat in response to aphid herbivory.**

Hypothesis: Aphid herbivory induces changes in the composition of both belowground volatile and non-volatile exudates. Since plants use these chemicals to communicate with microbes, it is expected that these changes will influence microbial community composition and activity in the rhizosphere.

2. **Identify potential key metabolites in root exudates that act as signals for recruiting specific bacterial communities under aphid herbivory.**

   Hypothesis: Aphid herbivory triggers the release of different compounds in wheat root exudates, serving as chemical signals for the recruitment of distinct bacterial communities.

3. **Investigate the structure and composition of bacterial communities at the root-soil interface in wheat plants under aphid herbivory.**

   Hypothesis: Root exudates influence the selection of bacterial communities from the soil to the rhizosphere. However, not all recruited bacteria will successfully colonise plant roots. If aphid-induced changes in root exudates specifically recruit bacteria capable of root colonisation, the bacteria taxa enriched in the rhizosphere should also show an increase in root colonisation.

4. **Investigate changes in culturable bacterial isolates exposed to identified key metabolites in root exudates of plants under aphid herbivory.**

   Hypothesis: Bacterial isolates of interest will exhibit distinct responses to metabolites tentatively identified as stress signals under aphid herbivory.

1.7. Thesis outline

Based on the aims presented above, the structure of this doctoral thesis is detailed below:

Chapter 1: General introduction and a comprehensive literature review of current research on insect-plant-soil microbe interactions.

Chapter 2: Results from the first experiment, which explored plant-soil microbe interactions in the rhizosphere of wheat plants under aphid herbivory over four weeks. This chapter includes untargeted metabolite analysis, carbon metabolism profiling of microbial communities, and 16S rRNA amplicon sequencing to examine bacterial community structure and diversity.

Chapter 3: Results from a second experiment, focusing on untargeted metabolomics to characterize root exudates under aphid herbivory. Cheminformatics approaches were used to annotate key metabolites differentially abundant between herbivory and control treatments.

Chapter 4: Microbiome analysis from the second experiment, including 16S rRNA amplicon sequencing of rhizosphere and root bacterial communities. This chapter also includes *in vitro* testing of bacterial isolates with selected metabolites to assess their responses.

Chapter 5: General discussion and conclusions, synthesizing results within the context of existing literature. This chapter also highlights study limitations and proposes future directions for research on insect-plant-soil microbe interactions.

Chapter 2: Exploring changes at the plant-soil microbial interface under aphid herbivory

Plants communicate with their environment by emitting chemical signals that other organisms can perceive. This chapter addresses the ***first*** *aim of this project:* ***to investigate changes in the plant-soil microbe system in wheat in response to aphid feeding****. By using a combination of volatile and non-volatile metabolic profiling of the rhizosphere of wheat plants, it was determined that* ***aphid herbivory impacted the belowground signals in the rhizosphere****. Furthermore, metabolic profiling of microbial communities showed a much* ***more active community in plants under aphid herbivory****, while amplicon sequencing of the 16S rRNA gene showed bacterial communities with lower diversity in the rhizosphere compared to those associated with healthy plants,* ***with an increase in bacteria from the Actinobacteria class****. Overall, these results show that aphid herbivory correlates with chemical and biological changes at the root-soil interface.*

2.1. Introduction

Aphid herbivory can significantly impact plant growth, both directly and indirectly. Directly, aphids remove resources from plants by feeding on phloem sap, a process that can severely affect plant health. Indirectly, aphids induce plant defence responses that alter the balance between plant growth and defence (Mou et al., 2023; Silva-Sanzana et al., 2023; Züst & Agrawal, 2016). By creating a resource sink, aphids can prompt defensive mechanisms that are costly in terms of plant energy and nutrient allocation, affecting overall growth and productivity (Nalam et al., 2019).

While the aboveground effects of aphid herbivory on plant responses have been extensively studied, its impact on belowground processes remains less explored. However, given the reliance of plants in soils, it is expected that aphid herbivory will impact plant-soil interactions. For instance, when feeding, aphids seek amino acids and fatty acids from their host plants (Powell et al., 2006), as they have limited ability to synthesise these compounds. To synthesize amino acids and other metabolites, plants obtain nitrogen primarily from the soil, where microbes play a key role in nitrogen availability and overall nutrient acquisition (Haribal & Jander, 2015, Finkel et al., 2017; Mitter et al., 2013; Nagrale et al., 2023; Pineda et al., 2010).

Beyond nutrient availability, the soil also hosts complex biotic interactions that play a pivotal role in plant responses to aphid herbivory. Research has demonstrated that inoculation with beneficial microbial strains can alter plant chemical defence pathways, resulting in changes in plant response to aphids and other pests and pathogens (Deb & Tatung, 2024; Dimkić et al., 2022; Saikia & Bora, 2021). However, the study of individual microbial strains can potentially oversimplify the complex plant-soil microbe interactions occurring in natural environments. To gain a more comprehensive understanding, it is essential to adopt ecological approaches that capture the dynamic interactions within the rhizosphere.

This chapter focuses on wheat (Triticum aestivum var. Solstice), one of the world's most important staple crops (Balcerowicz, 2024; Kavamura et al., 2020, 2021) and investigates how aphid herbivory influences plant-soil microbe interactions. The bird cherry-oat aphid (*Rhopalosiphum padi*) was used in this study, it is one of the most damaging pests on wheat. To evaluate the impact of aphid herbivory on plant-soil microbe interaction, three approaches were employed. First, changes in the

rhizosphere metabolic profile were analysed in both volatile and non-volatile metabolites, as shifts in metabolite composition are anticipated in response to herbivory. Second, the metabolic activity of microbial communities was assessed, with the hypothesis that aphid-induced plant metabolites would influence microbial metabolic responses. Lastly, the taxonomic composition of bacterial communities was examined, as the release of specific metabolites is expected to recruit distinct microbial populations. These parameters were monitored for four weeks to observe how aphid herbivory might influence plant-soil microbe dynamics.

Through this analysis, this study aims to provide ecological insights into the interactions between aphids, plants, and soil microbes. Understanding these relationships is essential for developing sustainable agricultural practices that harness soil microbiomes to enhance plant resilience against herbivory.

2.2. Materials and methods

2.2.1. Aphids, plant and soil material

Bird cherry-oat aphids (*Rhopalosiphum padi* L.) were obtained from non-viruliferous insect colonies maintained by the Chemical Ecology Group at Rothamsted Research. Seeds of the wheat cultivar *Solstice* were also obtained from Rothamsted Research and maintained at 4°C until the start of the experiment.

The soil used in this experiment was collected from the bare fallow soil mine at Woburn, Bedfordshire (UK) (latitude: 52°00′04.3"N, 0°36′49.0"W). This is a well-draining sandy loam soil part of the long-term bare fallow experiments from the Rothamsted Research experimental farm. This soil was collected from the field,

sieved (5 mm) to remove big particles and stored at 4°C until the start of the experiment.

2.2.2. Pot experiment under controlled conditions

Wheat seeds were surface sterilised with 70% ethanol and 1.5% sodium hypochlorite for 7 and 10 minutes, respectively, followed by three washes with sterile distilled water. The seeds were placed in sterile Petri dishes with germination paper and incubated in the dark for four days at 20°C. After that, ten pregerminated seedlings were planted in pots containing 1.7 kg of unsterile soil mixed with sterile perlite substrate (70:30 v/v) supplemented with 6.5 g granules of NPK (Osmocote, 15% N, 9% P_2O_5, 11% K_2O, 2% MgO) mixed with the soil before potting. A total of 25 pots were put in a controlled environmental chamber for three weeks (21ºC, 16h light/8h darkness photoperiod). Five additional pots containing only soil were used as negative control.

Once the seedlings reached the third-leaf stage, 20 pots were randomly assigned to one of the two groups (10 each): aphid herbivory (treatment) and no herbivory (control). The extra five pots were used for DNA extractions to characterise microbial communities in the soil before aphid herbivory, with the aim to assess the starting point of the microbial communities before imposing the stress. Clip cages containing 10 non-winged bird cherry-oat aphids (*Rhopalosiphum padi* L.) were put on the first leaf (counting from the base) of each plant. Following treatment allocation, sampling was conducted two and four weeks after the start of aphid herbivory and included the collection of five (5) pots per condition (herbivory and control plants) for aboveground VOCs collections, belowground metabolic profiling, and analysis of microbial

communities (see below sections for more details). Sampling times are shown in Figure 2.1, while photos of the experiment can be found in Figure 2.2.

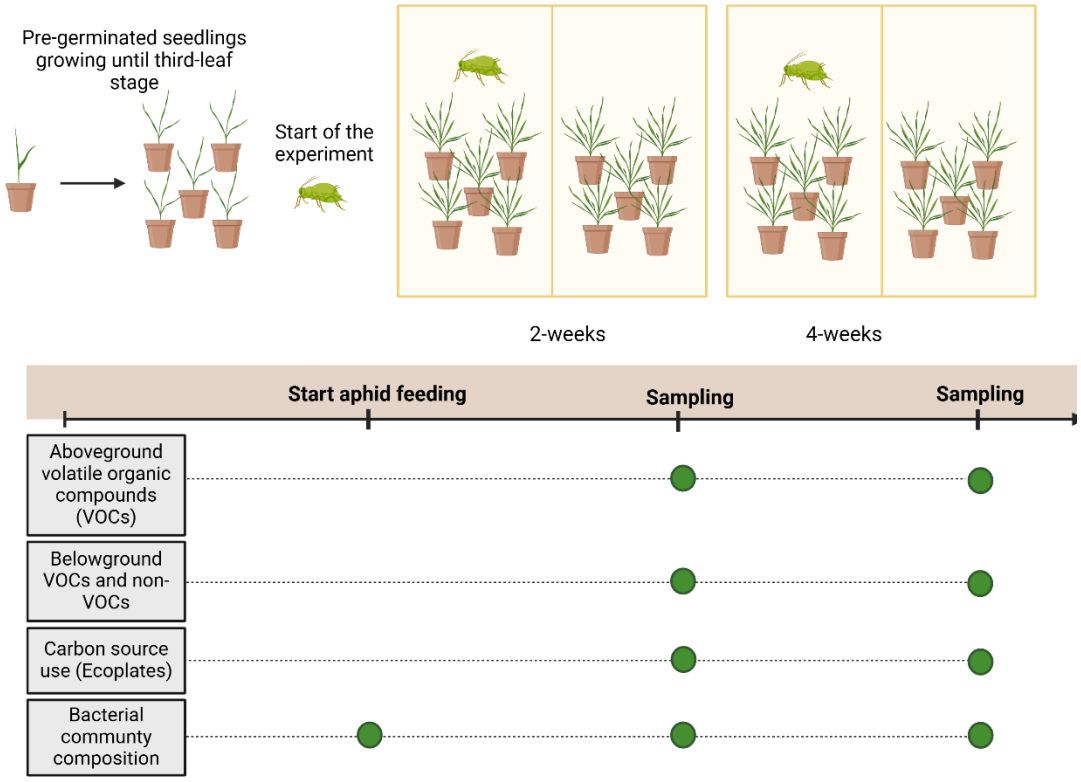

Figure 2.1. *Experimental design to test the effect of aphid herbivory aboveground in belowground plant-microbe communication and microbial responses.*

Collection of rhizosphere soil in each sampling time consisted of gently removing plant roots from the soil and shaking to remove loosely attached soil. A second, more vigorous shaking was performed to obtain rhizosphere soil samples. The samples for metabolic profiling of non-volatile metabolites were placed into sterile 50 mL falcon tubes, while samples for DNA extraction and microbial metabolic activity were first passed through sterile stainless-steel sieves (2 mm) to remove perlite and potential remaining roots. Further, these samples were divided into two 2 mL Eppendorf tubes per sample: one was snap-frozen in liquid nitrogen and stored at -80 °C for microbial DNA extractions and one was immediately used for testing microbial metabolic activity, which will be described below. After each sampling, the plant root dry weight

was measured by removing the soil from plant roots and drying them in the oven at 70°C for 96 hours, before weighing.

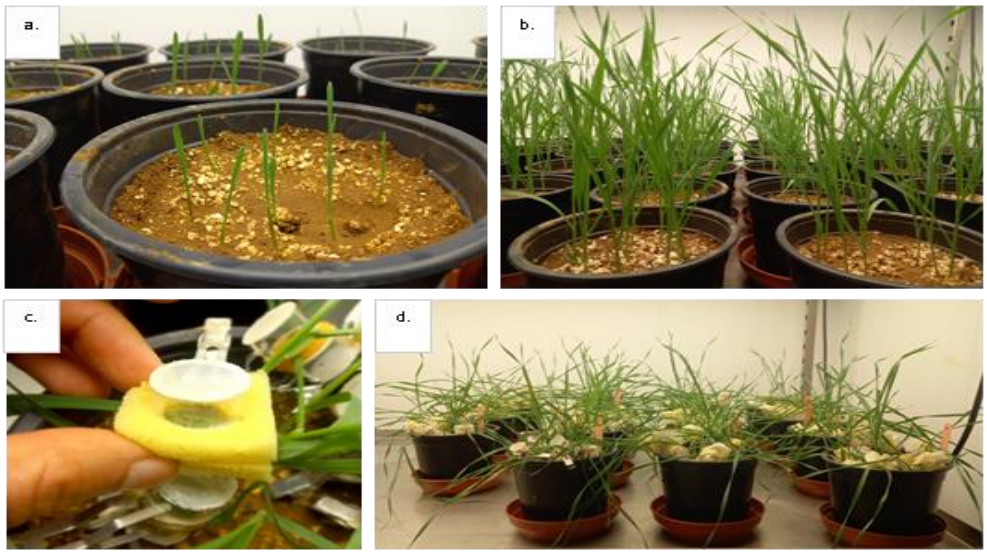

***Figure 2.2**. Placement of aphid in wheat plants. a) Ten pregerminated seedlings after six days of growing under controlled conditions, b) Wheat plants at the third-leaf stage, c) Clip cages containing 10 aphids positioned on the first leaf (counting from the base), d) Wheat plants after a week growing under aphid feeding.*

2.2.3. Aboveground measurement of VOCs from wheat plants under aphid herbivory

2.2.3.1. Dynamic headspace collection

To monitor changes in the aboveground VOCs emitted by wheat plants in response to aphid herbivory, a dynamic headspace collection was performed using air entrainment kits (BJ Pye, Kings Walden, UK), according to the methodology described by Simon et al. (2021) and described in detail below.

Before each sampling, all materials for VOCs collection were conditioned to remove particles or contaminants from the system. Charcoal filters, used to purify the air entering the system, were heated in an oven at 140°C for 2 hours under continuous nitrogen flow. Porapak *tubes,* used for VOCs collection, were prepared by filling borosilicate tubes with 50 mg of Porapak Q (60/80 mesh; Supelco, Bellefonte, PA,

USA), a porous polymer designed for VOCs capture. These tubes were washed with 1 mL of diethyl ether and heated at 140°C for two hours. This cleaning process was performed twice before setting up the system. Polyethylene terephthalate (PET) bags were used to entrain the plants during VOCs collection and were also put in the oven for two hours at 140°C to remove contaminants.

For VOCs collection, plant pots were sealed inside the PET bags. Purified air was pumped into the bag at a flow rate of 600 mL min^{-1}, while VOCs were collected by extracting air at a flow rate of 400 mL min^{-1} through a Porapak tube placed at the top of the bag (Figure 2.3). The headspace collection duration was 48 hours. To recover VOCs for analysis, the Porapak tubes were eluted with 750 µL of diethyl ether and further concentrated under a gentle nitrogen stream to a final volume of 50 µL before injection into a gas chromatograph (GC).

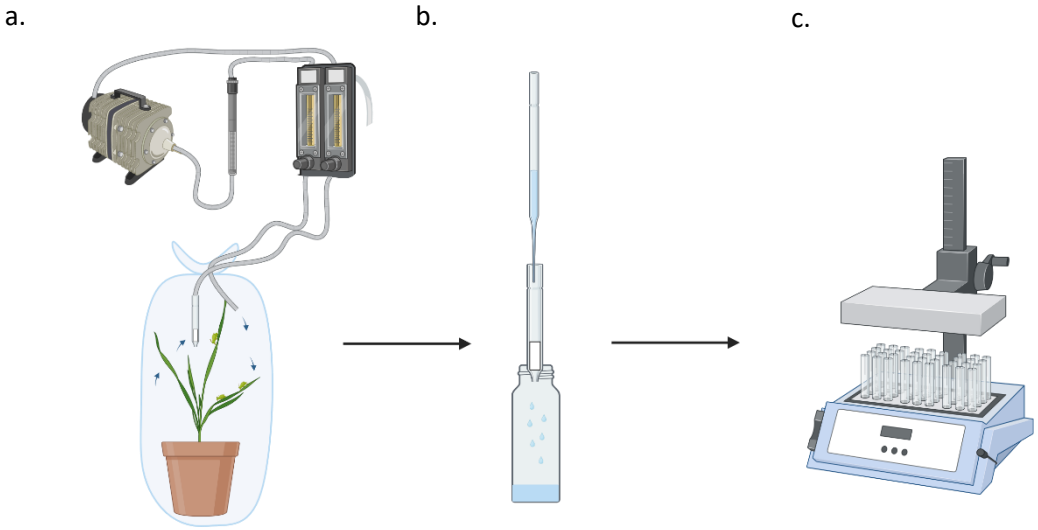

Figure 2.3. *Schematic figure of aboveground VOC collection and analysis. a) VOCs are collected from the plant headspace for 48 hours using Porapak tubes. b) Porapak tubes are eluted with 750 µL diethyl ether and concentrated to 50 µL. c) Samples are concentrated under nitrogen blowdown to be analysed using gas chromatography (GC).*

2.2.3.2. Gas chromatography analysis

Chemical analyses were performed using gas chromatography (GC). Concentrated VOCs samples were injected into an Agilent 6890A GC equipped with a non-polar HP-1 column of 50 m length, 0.32 mm inner diameter and 0.52 µm film thickness (J&W Scientific). The oven temperature was maintained at 30°C for 5 min and temperature increased 5°C per minute to 150°C, followed by a 10°C per minute increase to 230°C, with a total runtime of 60 minutes per sample. Helium served as the carrier gas.

Samples were analysed in two randomised batches, each including a solvent blank and a series of C7-C22 alkane standards to ensure system suitability. Peak selection from the chromatograms was based on the following criteria: peak width = 0.04, area reject = 0.10, height reject = 0.10 and slope sensitivity = 10.0. Chromatograms, or traces, from the alkane standards were used to calculate the Kováts retention index, a dimensionless value determined by interpolating the retention time of peaks between those from the n-alkanes. The calculated indices were compared against an internal database for tentative annotation of metabolites.

2.2.4. Belowground metabolic profiling at the plant-soil interface of wheat plants under aphid herbivory

Belowground chemical responses to aboveground aphid herbivory were measured by changes in the metabolic profile of low molecular weight compounds (VOCs and non-volatiles) present in the rhizosphere soil. In the following sections, each method is described in detail.

2.2.4.1. VOCs in the rhizosphere of plants under herbivory

Polydimethylsiloxane (PDMS) coated tubes (internal diameter 1,00 mm, external diameter 1,80 mm, wall thickness 0,40 mm, VWR INTERNATIONAL LTD) were used to capture volatiles from the rhizosphere. These hollow tubes have an inner surface coated with the sorbent material (PDMS), which adsorbs VOCs as air flows through them. A 70 cm-long tube was used per plant pot. Prior to use, tubes were submerged in methanol for 24 hours and placed in an oven at 140ºC under nitrogen flow to remove contaminants.

The PDMS tubes were positioned in a spiral pattern within the soil when pots were filled with the soil mix (Figure 2.4), prior to placing the pre-germinated wheat seeds. This was performed to increase the area of contact of the tubes with the plant roots as plants developed. For sampling, the tubes were carefully removed from the soil, placed on a stand to facilitate handling, and eluted with 2 mL of diethyl ether. To remove soil particles that might have reached the glass vial during elution, samples were passed through glass syringes containing cotton wool. Samples were then concentrated under a gentle nitrogen stream to 50 µL prior to GC analysis. After sample preparation, GC analysis followed the same method described above (Section 2.3) for aboveground VOCs.

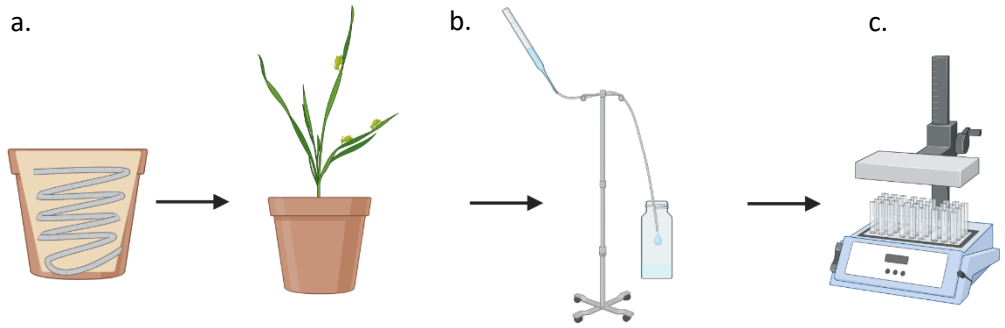

Figure 2.4. *Belowground VOCs collection. a) Placement of Polydimethylsiloxane (PDMS)-coated tubes in pots prior to the experiment. b) Elution of VOCs from PDMS tubes, c) Concentration of eluted samples under nitrogen blowdown before GC analysis.*

2.2.4.2. Non-volatile metabolites in the rhizosphere of plants under aphid herbivory

Non-volatile collection was performed following the methodology of Pétriacq et al. (2017) with major modifications. A total of 21 grams of rhizosphere soil from each pot were placed in 20 mL tubes with perforated bottoms, which were nested inside 50 mL falcon tubes (Figure 2.5). Then, 10 mL of a cold extraction solution (95% methanol with 0.05% formic acid) was slowly added to each 20 mL tube and centrifuged for 5 min at 4000 rpm to facilitate solvent infiltration and extraction of metabolites, which were collected in the 50 mL falcon tubes. Approximately 7 mL of extracts were recovered from each of the samples. The extracts were then concentrated via rotary evaporation until methanol was completely removed. The metabolites were resuspended in 1 mL of the same solvent, further concentrated under nitrogen, and resuspended in 100 µL of methanol. The samples were vortexed and centrifuged at 8000 g and 4ºC for 5 min to prevent UPLC column blockages. Finally, 50 µL of the solution were transferred to glass vials with inserts to accommodate the low volume samples for UPLC-QTOF analysis.

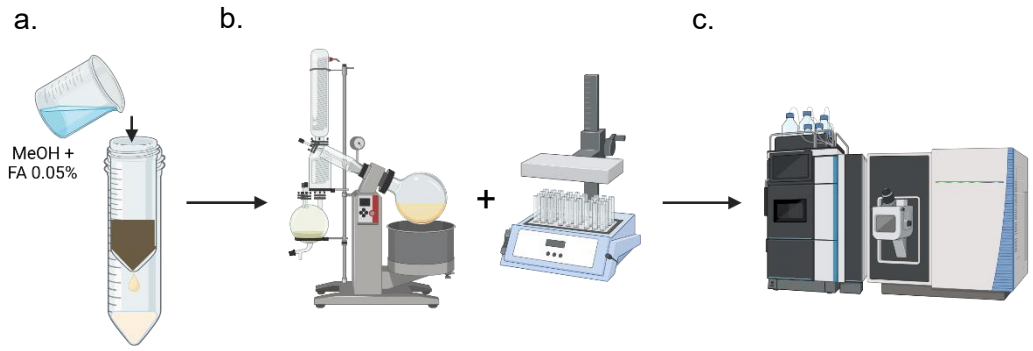

Figure 2.5. *Collection and processing of non-volatile metabolites from wheat rhizosphere. a) 21 grams of rhizosphere soil were placed in a perforated 20 mL tube inside a 50 mL Falcon tube, followed by 10 mL of extraction solvent (95% methanol with 0.05% formic acid). b) After extraction, samples were concentrated by rotary evaporation and nitrogen blowdown to 100 µL. c) Concentrated samples were analysed using LCMS.*

Liquid chromatography coupled with tandem mass spectrometry (LC-MS/MS) analysis

Data acquisition was carried out using an ACQUITY ultra-high-pressure liquid chromatography (UPLC I-class) system coupled to a SYNAPT G2Si Q-TOF mass spectrometer with an electrospray (ESI) ionization source (Waters, Manchester, UK). For this, a 2 µL aliquot of each sample was chromatographically separated using a C18 reverse-phase column (BEH C18 1.7 µm, 2.1 mm X 50 mm; Waters, Manchester, UK). The mobile phase consisted of solvent A (0.01% formic acid v/v in water and solvent B (0.01% formic acid v/v in methanol), which were used at a flow rate of 0.21 mL/min. The gradient was set as follows: 0–3 min, 95% A; 3–7 min, 95% A; 7–11 min, 85% A; 11–13 min 75% A; 13–18, 70% A; 18–25 min, 50% A; 25–30 min, 25% A; 30–39.1 min, 0% A; 39.1–43 min, 95% A, for a total time of 43 min. The column was maintained at 50ºC.

To capture the broad spectrum of metabolites in the samples, mass spectrometric (MS) analysis was initially performed in full scan mode (50-1100 Da, scan time = 0.2

s), using sensitivity mode with negative ionization (ESI^-). In full scan mode, the mass-to-charge ratio (m/z) of all ions is detected, and their intensities are measured; however, metabolite annotation is not possible in this mode. To further investigate metabolites identities, a data-independent acquisition (DIA) approach was applied to a subset of samples (three per condition). In DIA, a full MS scan was conducted using the MS^E function, which fragments all detected precursor ions across the 50-1100 m/z range, independent of their intensity. A collision energy ramp in the transfer cell from 20 to 40 eV was applied to generate the fragmentation spectra. The resulting fragment ions were further analysed for metabolite annotation (see details in Section 2.2.7). Accurate mass detection was performed on sensitivity mode with negative ionisation. The Q-TOF was calibrated with a sodium formate solution and lockmass correction applied to maintain high mass accuracy throughout the LCMS runs, performed with leucine-enkephalin during each run.

2.2.5. Metabolic activity of microbial communities in the rhizosphere

Biolog EcoPlates™ (Biolog, Inc., Hayward, CA, United States) were used to test differences in the metabolic activity of microbial communities in the rhizosphere of plants under aphid herbivory, following the protocol by Mendes et al. (2019). These Ecoplates are commonly used as “fingerprints” of the metabolic potential of microbial communities and consist of 96-well plates containing three replicates of 31 carbon sources (amino acids, carbohydrates, carboxylic acids, phenolic compounds, polymers, amides, and amides). A redox tetrazolium dye is present in each well, and changes in colour intensity indicate microbial respiration in the presence of each carbon substrate.

To assess microbial metabolic activity, one gram of rhizosphere soil (1 g) was suspended in 9 mL of NaCl 0.85% (w/v) and shaken for 20 min at room temperature. The suspension was allowed to settle for 10 min, and a 100-fold dilution was prepared from the supernatant. A volume of 125 µL of the latter dilution was inoculated in each well of the Ecoplates™. Initial absorbance readings (OD_{590nm}) were recorded in a spectrophotometer (Varioskan, Thermo Fisher Scientific, Wilmington, DE, United States) immediately after inoculation. The plates were incubated at 25°C in the dark, with absorbance readings taken every 24 h for four days (96 h). These readings were measured to follow changes in colour development, indicating microbial activity on each carbon source. At each time point measured, an Average Well Colour Development (AWCD) was calculated as follows:

$$AWCD = \sum \frac{Ci - R}{31}$$

Where *Ci* is the absorbance of each of the 31 carbon wells and R represents the absorbance in the control well. The AWCD is used as a normalisation step to reduce background noise and to control for variability between plates. For this test, three replicates (n=3) per condition were used in each sampling time.

2.2.6. Structure and composition of bacterial communities in the rhizosphere

Metabarcoding of the 16S rRNA gene was conducted to assess changes in the structure and composition of bacterial communities in the rhizosphere of wheat plants under aphid herbivory. DNA was extracted from 250 mg of rhizosphere soil using the DNeasy PowerSoil Pro Kit (Qiagen, Hilden, Germany) following the manufacturer's protocol. DNA concentration was quantified using a Qubit 2.0 fluorimeter with a dsDNA HS assay kit (Thermo Fisher Scientific, Wilmington, DE, United States) and

DNA quality was measured with a NanoDrop spectrophotometer (Thermo Fisher Scientific, Wilmington, DE, United States). Bacterial community composition was assessed by sequencing the V4-V5 hypervariable region of the *16S rRNA* gene using the primers 515F (GTGCCAGCMGCCGCGGTAA) and 907R (CCGTCAATTCCTTTGAGTTT). The 16S rRNA PCR, library preparation and pair-end sequencing (PE250) were performed by Novogene (HK) on the NovaSeq 6000 platform for high-throughput microbial community analysis (Caporaso et al., 2011).

2.2.7. Bioinformatics and statistical analysis

2.2.7.1. Volatile Organic Compounds (VOCs)

All statistical analyses were performed using R Studio v.4.2.3 (RStudio Team, 2020). The GCAlignR package v.1.0.5 (Ottensmann et al., 2018) was used to align the chromatograms before statistical analyses of plant-released volatiles. Above and belowground VOCs were analysed using the same pipeline described here; however, the analysis was carried out separately.

First, all the chromatograms (from plants under aphid herbivory and control plants) were aligned to a randomly chosen chromatogram within the samples. Then, single peaks, those present in the solvent blanks and in the negative controls (pots containing soil) were removed. The alignment conditions were as follows: cut-off before 5 min and after 35 min, maximum and minimum distance from the chosen peak for alignment 0.03 min, maximum linear shift = 0.05. After alignment, a data frame containing the retention time and peak areas of the aligned peaks was exported as a .csv file for statistical analysis and calculation of the Kovats retention index, a numerical value that allows the comparison of peaks against an internal data library for tentative metabolite annotation.

Statistical analyses were performed in the MetaboAnalyst platform v.6.0 (Pang et al., 2024). Peaks with near-constant values across all conditions were removed using the interquartile range (IQR), and the remaining peaks were normalised and scaled using log10 transformation and Pareto scaling to improve the data distribution and adjust variances for statistical analysis. After this, Permutational Multivariate Analysis (PERMANOVA) and principal component analysis (PCA) were performed to find statistical differences according to the treatment, while heatmaps were generated to identify unique metabolites present or absent in the samples of plants under aphid herbivory. For visualisation of unique peaks with tentative annotations for aboveground VOCs, the package ComplexHeatmap v.2.20.0 (Gu et al., 2016) was used in R Studio v.4.2.3.

2.2.7.2. Non-volatile metabolites found in the rhizosphere of plants under aphid herbivory

The raw files from the LC-MS full scan mode analysis were first converted to open-format files (.mzML) using the Waters Data Connect software v.2.1.0 (Waters, Manchester, UK) for further processing in open-source software. These files were processed using the Processing Wizard utility of the mzmine software v.4.0.3 (Schmid et al., 2023). The data processing steps included deconvolution, alignment, and removal of peaks present in blanks according to the parameters shown in Table 2.1. After alignment, the data was exported as a .csv file for further analysis in MetaboAnalyst v.6.0. As with VOCs analysis, statistical analysis was performed using PERMANOVA, followed by Principal Component Analysis (PCA) after normalisation using log10 transformation and Pareto scaling.

Table 2.1 *Parameters for alignment and deconvolution of chromatograms generated by LC-MS in the mzmine software v.4.0.3*

Parameter	Value
Crop retention time	0.30 - 30 min
Minimum consecutive scans	4
FWHM (Full Width at Half Maximum)	0.05 s
RT tolerance intrasample	0.04 min
RT tolerance sample-to-sample	0.10 min
Noise threshold MS1	5.00E+02
Minimum feature height	3.00E+03
m/z tolerance (scan-to-scan)	0.005
m/z tolerance (intrasample)	0.0015
m/z tolerance (sample-to-sample)	0.004

As explained in Section 2.2.4.2, three replicates per group (aphid herbivory and control) were selected for fragmentation analysis (LC-MS/MS). File conversion and processing were carried out as for the full scan mode, with minor adjustments to minimise background noise. The noise threshold for MS1 scans was increased to 1.0E3, the threshold for fragment ions (MS2) was set to 5.0E2, and the minimum peak height was set to 1.0E4. These parameter values were optimised based on testing different thresholds on individual chromatograms. Following processing, the resulting files, including peak alignment and area data (.csv), edges annotation (.csv), and fragment spectra (.MGF), were uploaded to the Global Natural Product Social Molecular Networking (GNPS2) platform (Aron et al., 2020). There, data was searched against publicly available experimental libraries for tentative metabolite annotation. The following parameters were used for the annotation: Precursor ion tolerance: 0.02 ppm, fragment ion tolerance: 0.02 ppm, minimum cosine score: 0.7, and a minimum of 4 matched peaks. The cosine score is a measure that quantifies how similar two spectra are by evaluating the cosine of the angle between two vectors

representing the spectra (Bittremieux et al., 2022). The similarity is represented on a scale from 0 to 1, with 1 indicating identical spectra.

2.2.7.3. Metabolic activity of microbial communities in the rhizosphere

The data obtained from the Biolog EcoPlates™ (Biolog, Inc., Hayward, CA, United States) was analysed in RStudio v.4.2.3 using the *vegan* package v. 2.6.8 (Oksanen et al. 2024). Each plate contained three replicates of each carbon source, thus the Average Well Colour Development (AWCD) was calculated from these replicates, as explained in Section 2.2.5. After this, the data was tested for normality with a Shapiro-Wilk test. PERMANOVA and principal Component Analysis (PCA) were performed to compare samples from plants subjected to two and four weeks of aphid herbivory, using the absorbance readings taken 72 hours after incubation. PCA visualization was performed using the *FactoMineR* v.2.11 (Lê et al., 2008) and *factoextra* v.1.0.7 (Kassambara & Mundt, 2020) packages.

To calculate statistical differences in AWCD, measured every 24 hours for each plate, a repeated measures Two-way ANOVA was used to account for the use of the same biological replicates in each absorbance reading. Following this, a Student-Newman-Keuls (SNK) test was used for multiple comparisons. Finally, statistical differences between the treatment (aphid herbivory) and control conditions for each of the 31 compounds were assessed using the AWCD measured at 72 hours of incubation using Wilcoxon tests, with p-values adjusted with Bonferroni corrections ($p_{adj} < 0.05$), in the *rstatix* package v. 0.7.2 (Kassambara, 2023). Data visualisation was performed using the packages *dplyr* v.1.1.2 (Wickham et al. 2023), *ggpubr* v.0.6.0 (Kassambara, 2023), and *ggplot2* v.3.4.2 (Wickham, 2016).

2.2.7.4. Bacterial community analysis pipeline

Once the amplicon sequences were obtained from the sequencing service, data processing was performed using Quantitative Insights Into Microbial Ecology (QIIME2, 2019.7) (Bolyen et al., 2019). First, raw sequence data were demultiplexed using the q2-demux plugin and denoised with DADA2 (Callahan et al., 2016). The resulting amplicon sequence variants (ASVs) were aligned using mafft (Katoh et al., 2002), and taxonomy was assigned using the q2-feature-classifier (Bokulich et al., 2018) with the Vsearch consensus taxonomy classifier against the Silva132 99% OTUs reference sequences (Quast et al., 2013).

After processing the raw sequences in QIIME2, the obtained data files containing the ASVs table, their taxonomical classification and abundance were uploaded in R Studio to be processed. First, the data was converted to a *phyloseq* object using the *Phyloseq* package v.1.48.0 (McMurdie & Holmes, 2013) and ASVs from mitochondria and chloroplasts were filtered out of the dataset. Using the *vegan* package v.2.6.8 (Oksanen et al. 2024), bacterial alpha diversity was calculated. First, the data was rarefied to the minimum library size confirming that this sequencing depth was enough to cover the diversity present in the samples. Further, the alpha diversity indexes were calculated, and visualization was performed using the ggplot2 package v.3.5.1. Venn diagrams were created to observe the similarity in the composition of bacterial communities using the *VennDiagram* package v.1.7.3 (Chen, 2022).

Beta diversity and differential abundance analysis were performed in the *mia* package v.1.13.46 (Ernst et al. 2024). For these analyses, the data was not rarefied, but a filter was applied to retain only ASVs present in at least 50% of the samples in each condition. This filter was applied to increase the chance of working with sequences

that are more likely representative of the true microbial community. Beta diversity analyses were conducted to compare the bacterial community composition between all rhizosphere and bulk soil samples. The data was transformed using the Total-Sum Scaling (TSS), and the Bray-Curtis dissimilarity metric was calculated to generate a Non-Multidimensional Scaling (NMDS) plot with the *miaViz* package v.1.13.14 (Borman et al. 2024b). PERMANOVA was used to assess community differences across all sample groups, including bulk soil, samples before and after two and four weeks of aphid herbivory. Additionally, a distance-based redundance analysis (dbRDA) was performed to investigate the impact of aphid herbivory on the composition of bacterial communities. For the dbRDA, only samples from weeks two and four after aphid herbivory were included, with sampling time included as a covariate. The dbRDA model was specified as:

Partial_dbRDA = assay ~ Insect + Condition (Sampling time)

Following this, a differential abundance analysis was conducted to identify ASVs that were significantly affected by aphid herbivory using the Analysis of Compositions of Microbiomes with Bias Correction (ANCOM-BC) method, implemented in the ANCOM-BC package v.2.6.0 (Lin & Peddada, 2020). Rhizosphere samples from control plants were used as a reference to assess changes observed in communities under aphid herbivory. A significance threshold of $\alpha = 0.05$ was applied, with p-values adjusted for multiple comparisons using the Holm method. To enhance the detection of differentially abundant taxa, conservative estimation was applied to reduce the risk of false positives. Finally, the results were visualised with *ggplot2* v.3.4.2.

2.3. Results

2.3.1. Belowground metabolic profile changes correlate with changes in aboveground VOCs in response to aphid herbivory

Plant aboveground VOCs were measured to investigate wheat response to aphid herbivory, as some herbivore-induced plant volatiles are expected to be released only in response to this stress. The analysis of leaf VOC profiles showed that aphid herbivory triggered changes in plant chemistry (Figure 2.6).

After processing the chromatogram files (see methods Section 2.2.7.1 for details), a total of 193 peaks, hereby referred to as VOCs or metabolites, were retained for statistical analysis. The PCA (Figure 2.6) shows separation between the aboveground VOC profiles of control plants and those under aphid herbivory, but only after two weeks of herbivory. This separation contributed the most to the explained variance in principal component 1 (18.2%). Interestingly, after four weeks the aboveground VOCs from plants under aphid herbivory clustered closer with those of the control samples. A pairwise PERMANOVA analysis (Supplementary Table 2.1) showed that the metabolite profile of plants under two weeks of herbivory was significantly different from that of control samples at week four of herbivory ($p_{adjust} < 0.05$), and a similar trend was observed when compared to other samples ($p_{adjust} < 0.08$). These results indicate that, in this experiment, most pronounced changes in the aboveground VOC metabolic profiles occurred after two weeks of aphid herbivory, showing temporal dynamics in the response of wheat plants to herbivory.

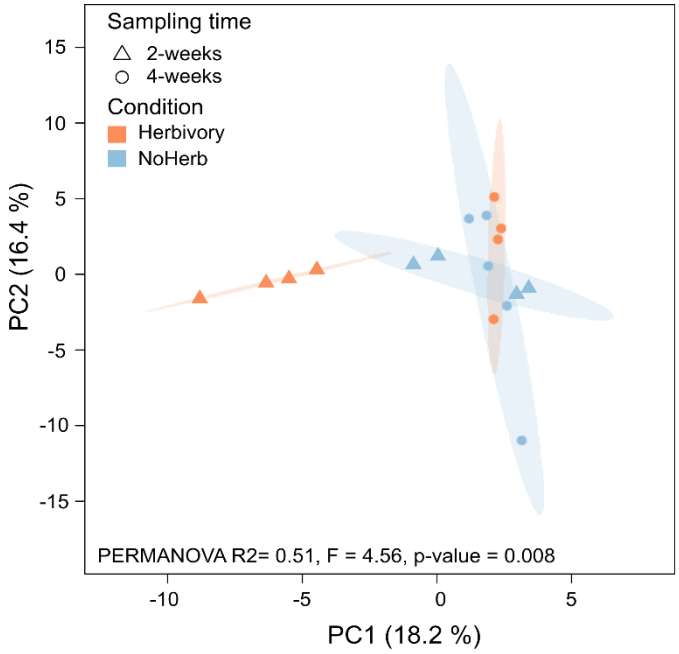

Figure 2.6. *Principal component Analysis (PCA) of aboveground VOC profiles from control plants (NoHerb) and plants under aphid herbivory after two and four weeks of treatment. PCA and PERMANOVA results were obtained by using the MetaboAnalyst platform v.6.0. Ellipses show 95% confidence interval for each condition (n=4).*

A detailed look at the individual metabolites after two weeks of herbivory revealed a cluster found almost exclusively in plants under aphid herbivory (Figure 2.7). Tentative annotations, based on matching their calculated Kovats Index against an internal data library, suggest the presence of herbivore-induced VOCs. These include green leaf volatiles and jasmonates from the lipoxygenase (LOX) pathway, terpenoids from the mevalonate (MEV) and methylerylthritol (MEP) pathways, as well as phenolics and indole compounds derived from the shikimate and phenylpropanoid pathways (Figure 2.7). In addition to being involved in known pathways, they have a range of functions such as involvement in direct or indirect defence, or antimicrobial functions. Overall, the presence of these metabolites suggests a distinct biochemical response to aphid herbivory.

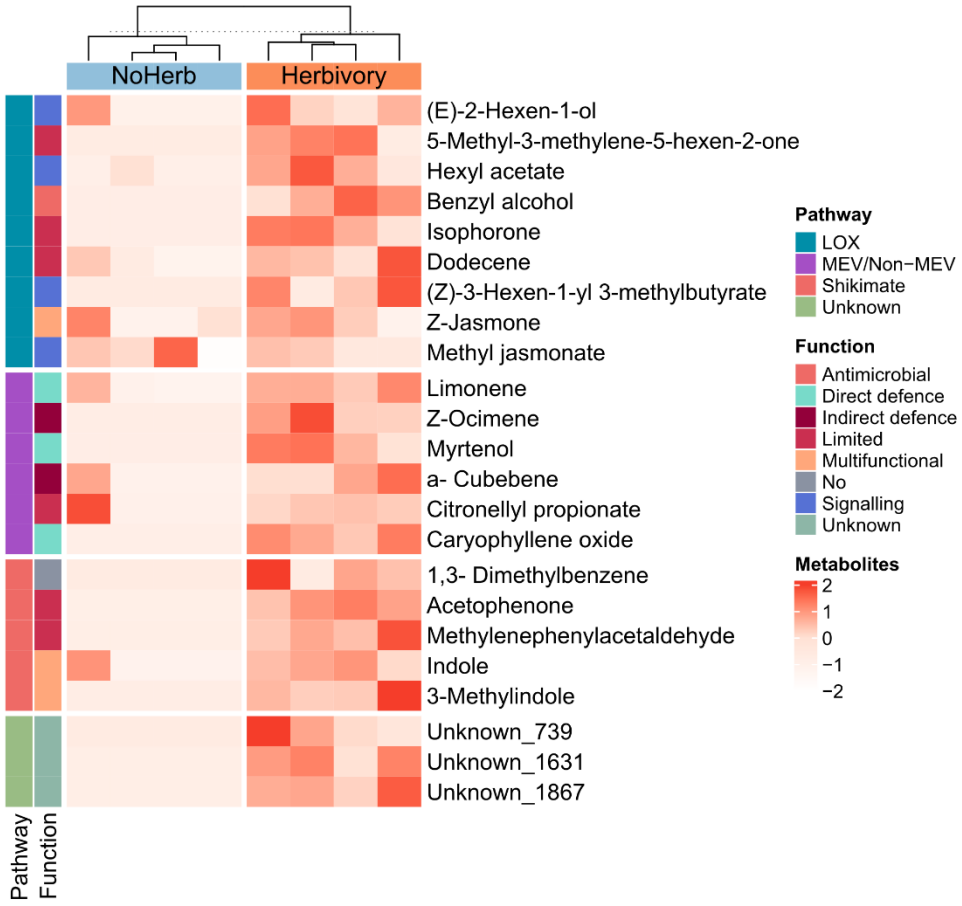

Figure 2.7. *Heatmap showing peak intensities of metabolites associated with plants under two weeks of aphid feeding (n=4). Peak areas were normalised using the Z-score. Tentative annotations were obtained by calculating the Kovats index (KI) based on the C7-C22 alkanes standards retention times and matching against an internal data library. In the Function key, metabolites classified as "Unknown" as their identity is not known, and those in the "No" category, have not been commonly observed in response to herbivory.*

Changes in plant aboveground VOCs after two weeks of aphid herbivory led to question whether aphid feeding exerted enough pressure to disrupt the sink/source allocation of resources, affecting belowground processes like root growth and release of root exudates. Regarding root biomass production, Figure 2.8 shows a decrease in root dry weight of plants under aphid herbivory that was more pronounced after four weeks of herbivory ($p = 0.056$), which confirmed that aphid feeding progressively reduced biomass production in the roots.

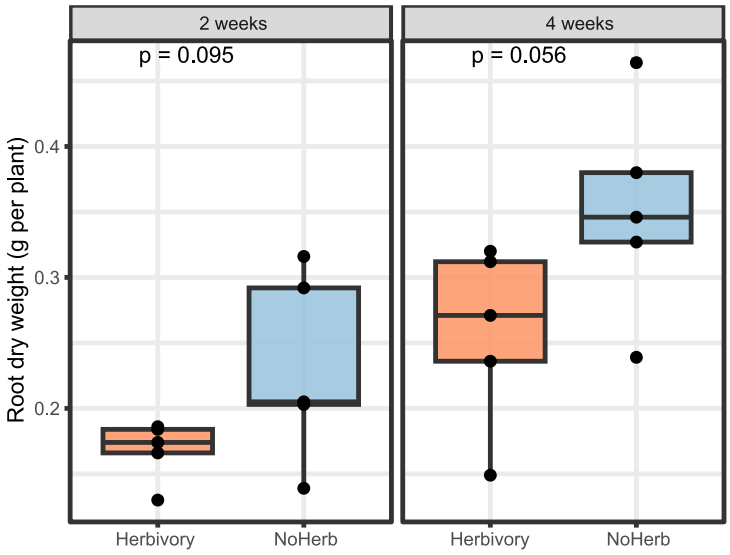

Figure 2. 8. *Root dry weight of plants in the two sample points under aphid herbivory. Dry weight was measured after plants were put in an oven at 70 °C for 96 hours (n=5).*

To detect changes in the release of root exudates in the rhizosphere, samples of both belowground volatile organic compounds (VOCs) and non-volatile metabolites were analysed. Since aboveground differences were only observed after two weeks of aphid herbivory, only belowground metabolites from this time point were selected for analysis. After processing belowground VOCs, a total of 117 peaks (metabolites) were detected, of which 111 were retained for statistical analysis after removal of near-constant peaks. As observed in Figure 2.9a, VOCs samples were clustered based on condition (aphid herbivory and control plants), which was confirmed by the PERMANOVA test ($F= 6.48$, $p < 0.05$). The VOCs were inspected to identify metabolites uniquely present in samples under aphid herbivory, as performed for aboveground VOCs. This time, the analysis revealed a subset of 18 metabolites associated to aphid herbivory, of which tentative annotation was possible for 7 metabolites. Some of the tentatively annotated metabolites belong to green leaf volatiles, like hexanal, (Z)-3-hexenal and (E)-2-pentenal, but notably, these metabolites were different from VOCs released aboveground (Figure 2.10).

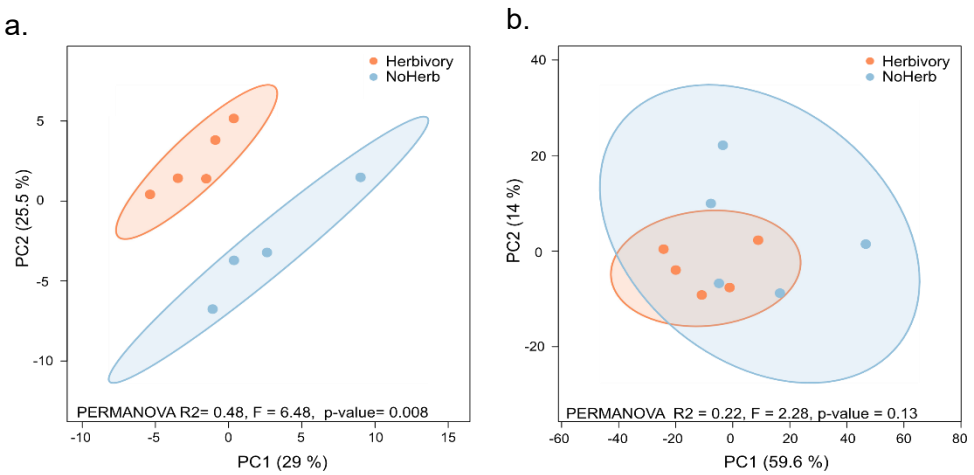

Figure 2.9. *PCA of the metabolic profile of a) VOCs and b) non-volatiles found in the rhizosphere of plants after two weeks of aphid feeding. PCA were generated in MetaboAnalyst. Ellipses show 95% confidence interval for each condition (n=5 except for VOCs of control plants, where n=4).*

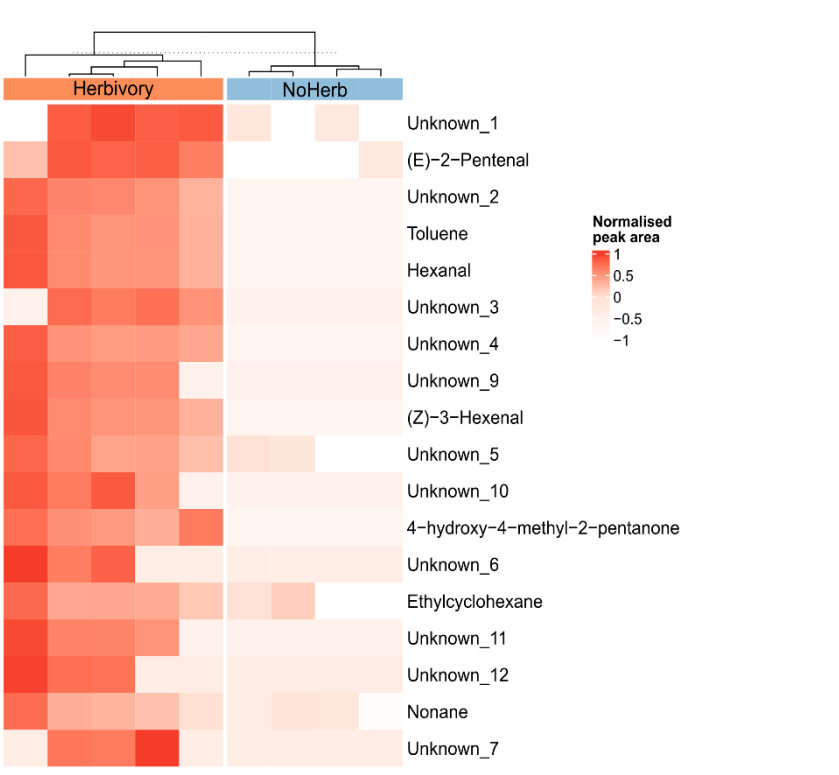

Figure 2.10. *Heatmap showing peak intensities of belowground volatile organic compounds associated with plants under two weeks of aphid* herbivory *(control plants n=4; aphid* herbivory *n=5). Peak areas were normalised using the Z-score. Tentative annotations were obtained by calculating the Kovats index (KI) based on the C7-C22 alkanes standards retention times and matching against an internal data library.*

In contrast to VOCs, the separation of samples from plants under aphid herbivory was less evident for non-volatile metabolites (Figure 2.9b). After processing the chromatograms from non-volatile samples run in LC-MS, a total of 1,775 peaks were obtained. Filtering for peaks with near-constant values across both conditions, based on the interquartile range (IQR), the number of peaks was reduced to 1,065. Samples from control plants showed higher variability, which is evident in the PCA and was confirmed by the lack of statistical significance in the PERMANOVA test (F=2.28, p=0.13). As mentioned before, a subset of these samples was selected for tentative annotation of metabolites by reanalysing them using LC-MS/MS in Data-Independent Acquisition mode. Similarly to the approach used for belowground VOCs, a subset of metabolites exclusively present in samples from plants under aphid herbivory was identified and is shown in Figure 2.11.

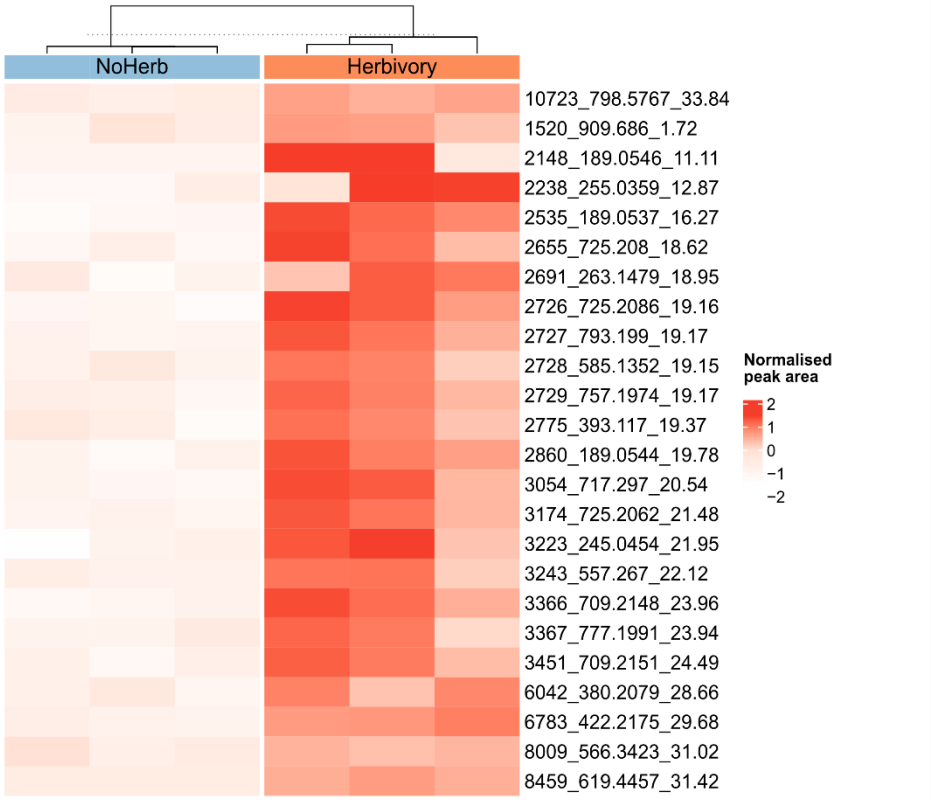

Figure 2.11. *Heatmap showing peak intensities of belowground non-volatile metabolites associated with plants under two weeks of aphid feeding (n=3). Peak areas were log-transformed and scaled using the Pareto scaling. Row names correspond to the metabolite ID, followed by accurate mass and retention time separated by underscores.*

Subsequently, spectral matching of these metabolites was performed using the public databases available in the Global Natural Product Social Molecular Networking (GNPS) environment. This analysis resulted in 24 tentatively annotated metabolites; however, none belonged to the cluster of metabolites that was shown to increase under herbivory. These tentative annotations are summarised in Supplementary Table 2.2. Overall, the profiles of low-molecular weight VOCs and non-volatiles in the rhizosphere reveal changes in chemistry in the rhizosphere of plants after two weeks of aphid herbivory.

2.3.2. Carbon source consumption rate was higher in microbial communities associated with plants under aphid herbivory

The ability of rhizosphere microbial communities to metabolise carbon sources was tested using Biolog EcoPlates™, which include different carboxylic acids, carbohydrates, amino acids, phenolic acids, and polymers – many of which are commonly found in root exudates. Microbial capacity to use these carbon sources was indicated by the absorbance readings (OD_{590nm}) which were used to calculate the Average Well Colour Development (AWCD). Readings at 72 hours of growth were used for exploratory and multivariate analysis. PCA analysis (Figure 2.12) revealed that the largest difference in carbon substrate utilisation occurred at the sampling point after two weeks of aphid herbivory although the variability in the samples from aphid herbivory was higher than that of control plants. Differences were also observed at four weeks, although the samples were more closely clustered in the PCA plot. PERMANOVA tests confirmed that the sampling time ($F= 6.715$, $p < 0.001$), aphid herbivory ($F= 5.703$, $p < 0.001$), and their interaction ($F= 2.937$, $p = 0.026$) were statistically significant (Supplementary Table 2.3). Beta dispersion analysis indicated

homogeneity of variance across groups (F = 0.2506, p = 0.866), supporting the validity of the analysis (Supplementary Figure 2.1).

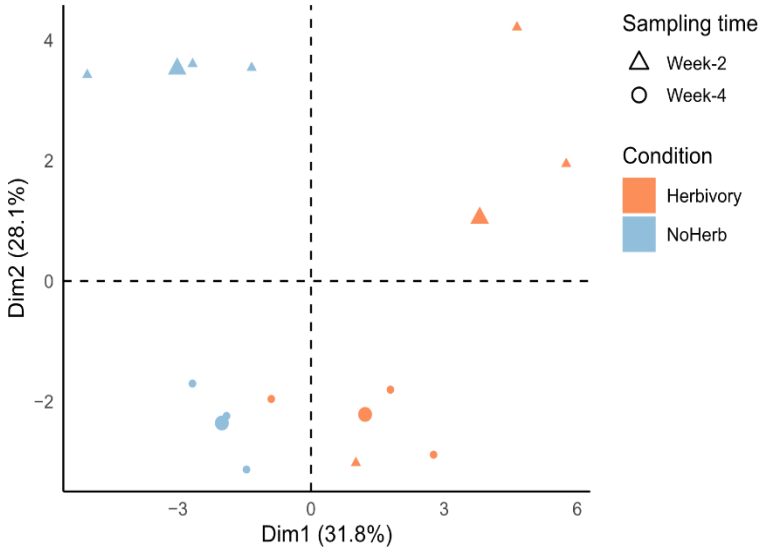

Figure 2.12. *Principal Component Analysis (PCA) of microbial carbon-source utilisation based on Biolog™ EcoPlates. Technical replicates were combined into biological replicates (n=3). The data represents the Average Well Colour Development (AWCD) for all 31 carbon sources tested, measured after 72 hours of microbial growth.*

Samples collected two weeks after aphid herbivory were selected for further analysis, as the largest differences were observed at this sampling time. Microbial activity, as indicated by colour development in the Ecoplates™, was observed in 26 out of the 31 carbon sources tested. No differences were found in carbon substrate preference between rhizosphere samples from plants under aphid herbivory and control plants; however, differences in the rate of colour development were observed based on the AWCD measured every 24 hours. The two-way ANOVA test showed significant effects of aphid herbivory, hour of absorbance reading, and their interaction (Aphid herbivory: $F= 12.304$, $p <0.001$; Hour: $F=60.160$, $p <0.001$, Interaction: $F = 8.561$, $p < 0.01$). As shown in Figure 2.13a, after 48 hours, AWCD of samples from plants under aphid

herbivory was significantly higher than that of control plants, and this difference continued in subsequent incubation sampling times.

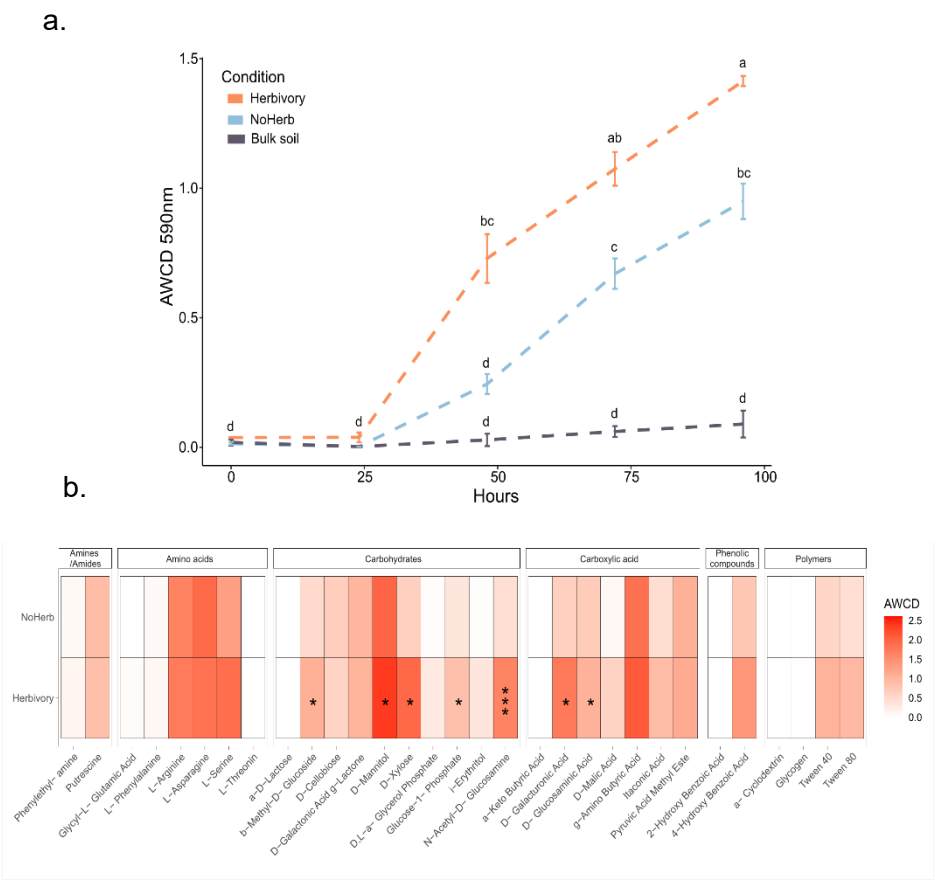

Figure 2.13. *Average Well Colour Development (AWCD) of samples after two weeks of aphid herbivory. a) Line graph of AWCD over 96 hours, with standard error bars (n=3) and statistical significance indicated by letters (SNK test, Bonferroni corrected, padj < 0.05). b) AWCD for each carbon source at 72 hours, with colour intensity representing consumption levels (dark red = high, white = low). Asterisks denote statistical significance (* p = 0.05; *** p = 0.001, paired t-test, Bonferroni corrected, padj < 0.05).*

A detailed analysis of individual carbon source use (Figure 2.13b) shows that the AWCD was statistically significant in seven carbon sources (p_{adj} < 0.05). These sources encompassed five carbohydrate and two carboxylic acid compounds, with N-acetyl D-Glucosamine displaying the highest statistical significance (p < 0.001). Differences in L-Asparagine, 4-Hydroxy Benzoic Acid, and Tween 80 were also

observed (p=0.08). Detail of statistical analyses can be found in Supplementary Table 2.4. These results show that the Ecoplates™ were able to capture differences in metabolic rate of consumption of carbon sources after two weeks of aphid herbivory.

2.3.3. Aboveground aphid herbivory reduced the diversity of bacterial communities after two weeks of aphid herbivory

The impact of aboveground herbivory on bacterial communities in the rhizosphere of wheat plants was assessed using amplicon sequencing. A total of 1,516,620 sequences corresponding to 4,914 ASVs were obtained. After filtering out mitochondrial and chloroplast sequences, 1,506,648 sequences and 4,863 ASVs remained. To account for differences in sequencing depth, all samples were rarefied to the minimum library size (25,058) for alpha diversity analysis. Rarefaction curves (Supplementary Figure 2.2) show that subsampling captured the ASV diversity of the samples. Bacterial alpha diversity, measured by richness (number of observed amplicon sequence variants –ASVs) and the Shannon index (Figure 2.14a, b), in the rhizosphere of wheat plants decreased after two weeks of aphid herbivory when compared to samples from the control plants. However, this reduction was statistically significant only when compared with samples from four weeks ($p_{adj} < 0.05$). Boxplots show a progressive increase in bacterial diversity over time, starting from the initial sampling point (plants at third-leaf stage), followed by two and four weeks after aphid herbivory. By the final time point, diversity index was similar to that of the bulk soil, suggesting an increase in bacterial diversity as the plants aged.

For further analysis, a filter by prevalence was applied to select only bacteria with a presence equal or higher to 50% in each treatment, which reduced the number of

ASVs to 1,965. A phylogenetic classification of bacteria with abundances higher than 1% (Figure 2.14c) revealed that all rhizosphere samples were characterised by a higher relative abundance of the Actinobacteria class (>29%) and a lower relative abundance of Bacilli (<9%) when compared to the bulk soil (24% and 14%, respectively). Furthermore, bacterial communities from plants at the initial sampling point and after two weeks under aphid herbivory shared a remarkable similarity in the relative abundance of the Actinobacteria class (40%), which was higher than in any other condition. Relative abundance of Alphaproteobacteria seemed to increase over time, with the highest abundance displayed in samples from soil of control plants at four weeks (from 8% to 13%).

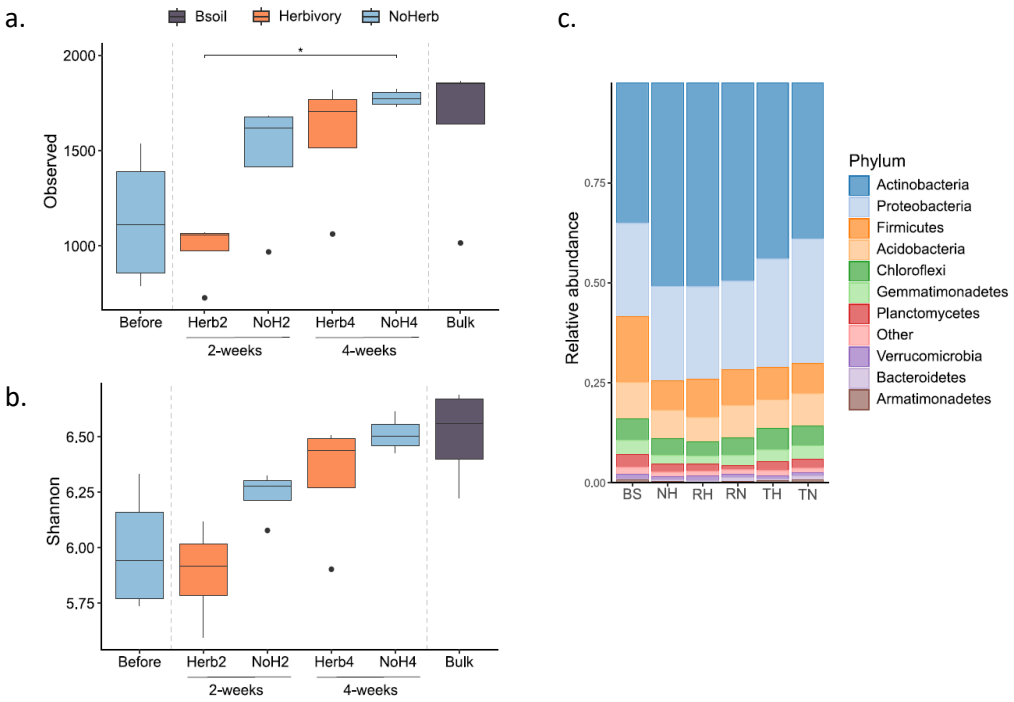

Figure 2.14. *Taxonomic diversity and richness of bacterial communities during the experiment. a) Observed and b) Shannon diversity index at the ASV level (n=4) Significance is shown by post-hoc Wilcoxon comparison (FDR < 0.05). c) Rank abundance plot (abundance >1%) at the class level. Four biological replicates per sample were used for the analyses. BS= Bulk soil; BEF= Rhizosphere samples before aphid feeding; SH= 2-weeks herbivory; SN = 2-weeks control; FH=4-week herbivory; FN= 4-week control.*

The NMDS analysis, which reflects the Bray-Curtis distance of bacterial communities among samples (Figure 2.15a) revealed significant differences in bacterial community

structure among samples (PERMANOVA F = 3.4405, p = 0.001). Samples from the rhizosphere at the initial sampling point clustered closer to those collected after two weeks of aphid herbivory. To isolate the effect of aphid herbivory, a dbRDA was constructed using only the samples from weeks two and four of aphid herbivory (Figure 2.15b). This analysis showed that sampling time explained 24.9% of the observed variability (p = 0.001) while aphid herbivory explained 10.2% (p = 0.026). When sampling time was included as a covariate and aphid herbivory was treated as the main factor, the explained variance attributed to aphid herbivory increased to 13.5% (p = 0.004) (Supplementary Table 2.5).

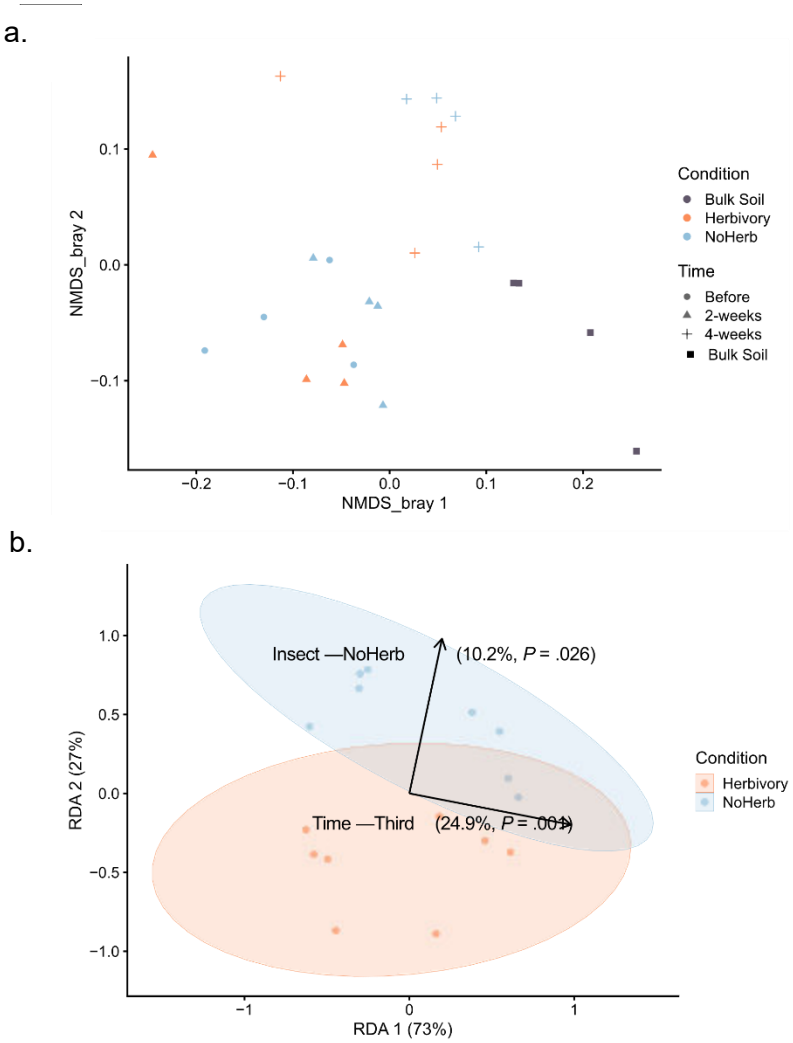

Figure 2.15. *Beta diversity analysis of bacterial communities. a) Non-Multidimensional Scale analysis (NMDS) of Bray-Curtis dissimilarity distance of bacterial communities' composition, b) Partial dbRDA of bacterial diversity showing the explained variance of bacterial communities based on sampling time and insect herbivory (n=4).*

Venn diagrams comparing the bacterial communities at the ASVs level (Figure 2.16) show that, after two weeks of aphid herbivory, rhizosphere bacterial communities of plants under aphid herbivory shared most of their ASVs with the control plants, but the number of ASVs was smaller (1,355) than that of control samples (1,661), and only 87 ASVs were unique to plants under aphid herbivory. At the four weeks sampling point, the number of ASVs in samples from plants under aphid herbivory increased, becoming more similar to the control plants. This pattern further supports the observation that bacterial diversity in the wheat rhizosphere increased with plant age.

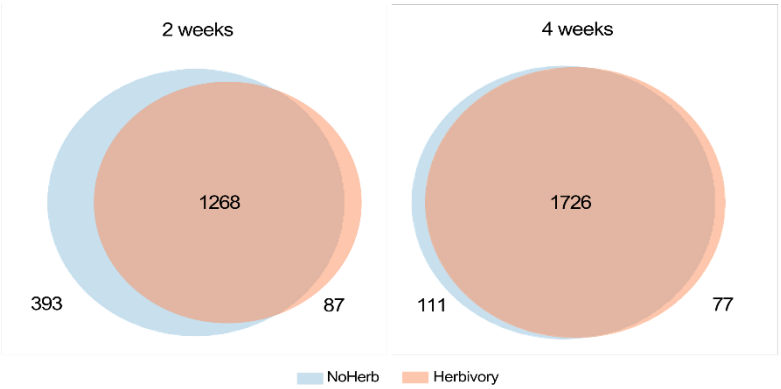

Figure 2.16. *Venn diagram showing the shared ASVs after two and four weeks of aphid feeding.*

2.3.4. Actinobacteria were enriched in the rhizosphere of plants subjected to two weeks of aphid herbivory

Samples from the second week of aphid herbivory showed the biggest difference in diversity and composition when compared with the control plants. A differential abundance analysis (ANCOM-BC) was performed to investigate the ASVs that were enriched under aphid herbivory (Figure 2.17). A total of 17 ASVs were significantly increased under herbivory (q value < 0.05), of which 9 belong to the Actinobacteria

phylum (53%). Among them, 8 belong to the Actinobacteria class and one to Acidimicrobiia. The second most enriched phylum is Proteobacteria, with 6 ASVs enriched (35.3%). The complete results from the analysis can be found in Supplementary Table 2.6. Three genera showed different ASVs that increased and decreased under herbivory (*Burkholderia, Aquisphaera, Luedemannella*). Among them, bacteria from the *Burkholderia_Caballeronia_Paraburkholderia* genus showed the highest log fold changes (4.928, -4.404).

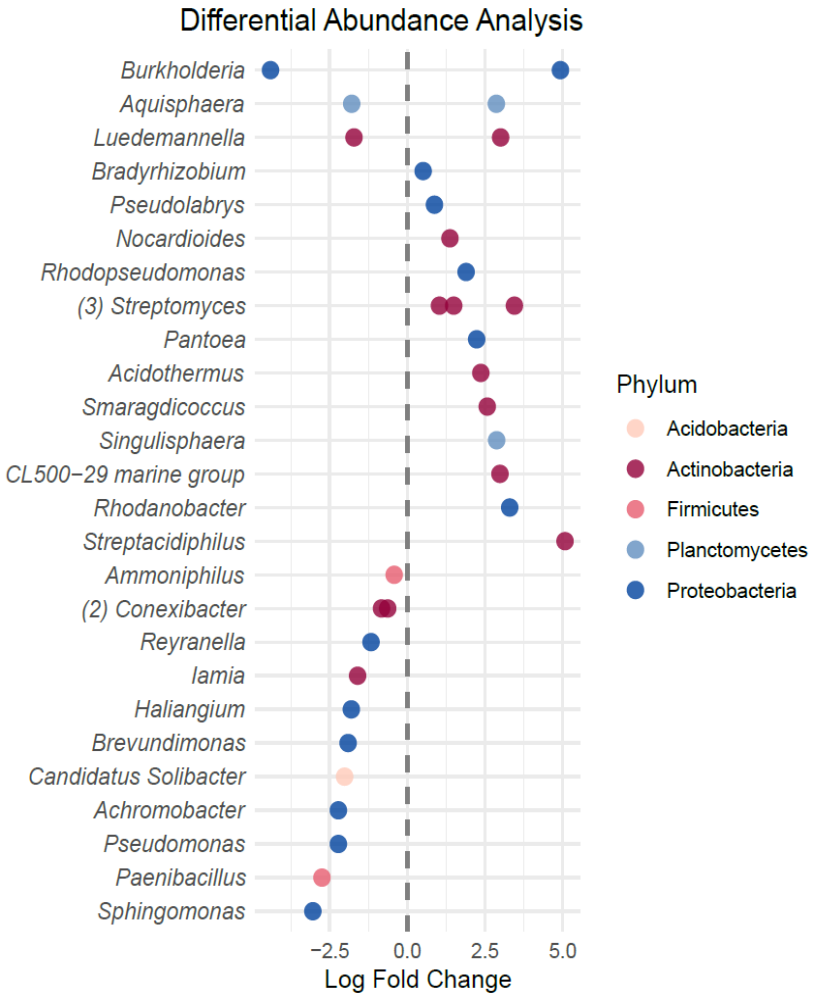

Figure 2.17. *ANCOM-BC of the differentially abundant ASVs. LogFoldChange was calculated from the ANCOM-BC log-linear model and shows the significantly (q value < 0.05) enriched (Positive LFC) or decreased (Negative LFC) ASVs in the rhizosphere of plants under herbivory compared to the healthy plants. The genus Burkholderia_Caballeronia_Paraburkholderia was shortened to "Burkholderia" for visualization purposes.*

ANCOM-BC was also performed for the bacterial communities of plants under four weeks of aphid herbivory, but the number of differentially abundant bacteria was reduced, at this timepoint, with only 5 ASVs increased from a total of 23 differentially abundant ASVs (Supplementary Figure 2.3). Overall, bacterial communities showed significant changes and differentially abundant taxa, but differences between control plants and those under aphid herbivory were more evident after two weeks of herbivory.

2.4. Discussion

This study aimed to investigate how aboveground aphid herbivory can impact belowground wheat plant-soil microbe interactions. Timing of the plant response to aphid herbivory was tested (aboveground VOCs), as well as changes in belowground chemistry, microbial metabolic response and composition of bacterial communities. Overall, it was possible to observe that aphid herbivory had an impact in the plant system and belowground plant-soil microbe interactions; however, the impact seemed to decrease over time.

After two weeks of herbivory, plants emitted a cluster of aboveground VOCs that were absent, or nearly absent, from the control plants (Figure 2.7). This cluster included commonly herbivory-induced green leaf VOCs and terpenoids like (E)-2-Hexen-1-ol, dodecane, limonene and caryophyllene oxide, which have diverse roles in plant response including defence at wound sites, attraction of natural predators, and plant-plant communication (Matsui & Engelberth, 2022; Qiu et al., 2024; Rosenkranz et al., 2021; Hassan et al., 2015), and in some cases, increase pest preference for their host

(Chen et al., 2022). However, the similarity of aboveground VOCs from plants under aphid herbivory and control plants after four weeks may indicate different scenarios that would require further investigation, which will be explored below.

If the stress imposed by aphid herbivory was mild or insufficient to significantly impact plant fitness, plants might have adopted a “tolerance” strategy, allocating more resources to sustaining growth rather than sustained defence (Baldwin & Preston, 1999). As younger plants are more susceptible to pests and diseases (Huang et al., 2014), the initial stress from 10 aphids per leaf during the first two weeks may have triggered a defensive response in juvenile plants. However, as the plants matured, they might have become less vulnerable, potentially reducing the production of energetically costly defensive metabolites. Visual observations supported this hypothesis, as both control and aphid-fed plants continued growing, though plants subjected to four weeks of herbivory appeared less turgid than controls. Aphid herbivory reduced root dry biomass, indicating an impact on plant growth. To investigate this, further experiments focusing on the tolerance vs. defence trade-off are needed.

Belowground, aphid herbivory was associated with changes in the rhizosphere metabolite profile, assessed using untargeted metabolomics. This approach aims to measure all possibly detected metabolites to create a “metabolic fingerprint” of organismal responses to specific conditions –e.g., abiotic stress, pests, and diseases (Dudzik et al., 2018). Investigating these profiles, and the significant changes in individual metabolites can further lead to the discovery of potential biomarkers. Using this approach, distinct metabolite profiles have been observed in different plant species in response to herbivory, including maize (Marti et al., 2013), tomato (Rivero

et al., 2021) and legumes like *Medicago sativa, Pisum sativum, Trifolium pratense,* and *Vicia faba* (Sanchez-Arcos et al., 2019). Moreover, by using this approach, these studies have identified clusters of secondary metabolites, including coumarins, benzoxazinoids, and alkaloids, highlighting their potential roles in plant defence.

Although this experiment aimed to capture the belowground “metabolic fingerprint” rather than identify specific metabolites, tentative annotations were generated when possible. For rhizosphere VOCs, 7 metabolites unique to aphid herbivory were tentatively identified; however no non-volatile metabolites of interest could be annotated. The annotation of metabolites using untargeted metabolomics remains challenging due to the complexity of the generated data and the limited spectral data available in public repositories (Caesar et al., 2019; Dudzik et al., 2018; Nothias et al., 2024). Despite these challenges, the accurate mass of several non-volatile metabolites that were exclusively present under herbivory were obtained, which could guide more targeted approaches for their fragmentation and tentative annotation of these potential biomarkers.

LC-MS/MS analysis involves two steps, 1) the mass-to-charge (m/z) ratio of a molecule is determined using low collision energy; and 2) a higher collision energy is applied to generate fragments that serve as fingerprints for compound annotation. In this study, the use of Data-Independent Acquisition (DIA) mode may have produced low-quality fragment spectra, as in this mode all detected peaks are fragmented resulting in highly complex datasets where precursor ions and their fragments can be poorly matched (Guo & Huan, 2020). To address this limitation, further experiments could consider using Data-Dependent Acquisition mode (DDA), which selects precursor ions by applying thresholds to reduce the number of fragmented peaks

(Defossez et al., 2023). This mode simplifies the complexity of the data, increases the quality of the spectra, and could potentially enhance the number of annotated metabolites.

The distinct metabolic profiles found in the plant rhizosphere suggests that plant-microbe communication was affected by aphid herbivory. However, due to the complexity of the rhizosphere environment, the direction of these changes is difficult to establish. In the rhizosphere, the metabolites detected could be a result of various processes, such as plant root exudation, microbial interactions with these exudates, microbe-microbe interactions, or microbial responses to soil nutrients (Huang et al., 2014; Oburger & Jones, 2018; van Dam & Bouwmeester, 2016; Williams et al., 2021). Nevertheless, the changes in overall profile of metabolites indicated changes in plant-microbe interactions, which were further tested by assessing the metabolic capacity of the microbial communities and the structure of bacterial communities in the rhizosphere.

To investigate the impact of aboveground aphid herbivory in the rhizosphere microbial communities, Ecoplates™ were used to assess their metabolic activity in response to a diverse set of carbon sources. Under herbivory, microbial communities displayed a faster growth rate, particularly in the presence of carbohydrates and carboxylic acids. This rapid response suggests that rhizosphere bacterial communities under herbivory could be efficiently incorporating root-derived carbon into microbial biomass (Fan et al., 2022; Malik et al., 2020), implying that plants could be increasing carbon release to recruit bacteria that help enhance nutrient availability. This response may be driven by the high demand of aphids for phloem sap resources, as well as by the plant need

for nutrients to sustain its defence. However, further work is needed to determine how changes in rhizosphere microbial metabolic activity influences aphid populations.

In contrast to the above hypothesis, evidence suggests that under aphid herbivory plants can reduce the content of sugars like glucose and fructose in root exudates (Hoysted et al., 2018) and decrease their investment in microbial symbiotic relationships (Charters et al., 2020). The variation in plant responses could depend on the degree of resistance or susceptibility to aphid herbivory, and further research is needed to better understand carbon allocation and microbial uptake in this wheat variety.

Finally, in this chapter, the structure of bacterial communities was studied to investigate if plants under herbivory would recruit different bacterial communities. Bacterial diversity was lower in the rhizosphere of plants under herbivory, a finding consistent with other studies. For instance, aphid colonisation reduced the diversity and altered bacterial networks in the rhizosphere of potato and European beech plants (Malacrinò et al., 2021; Potthast et al., 2022) and increased the abundance of specific bacterial genera like *Bacillus, Paenibacillus* and *Pseudomonas* in tomato and pepper rhizospheres (French et al., 2021; Kim et al., 2015; Kong et al., 2016). In contrast, we observed a significantly decreased abundance of *Paenibacillus* spp. under herbivory, while *Pseudomonas* spp. were enriched in the rhizospheres of control plants.

Bacteria from the Actinobacteria class were significantly increased under herbivory. These bacteria have been widely known for their beneficial role in plant nutrient acquisition and production of secondary metabolites involved in plant defence (Anwar

et al., 2016; Chukwuneme et al., 2020). They have also been observed to be recruited by plants when they are more susceptible to disease (Huang et al., 2014), which would align with the results of our work. However, the data collected in our experiment is not sufficient to determine if these Actinobacteria have any role in plant defence or susceptibility to the aphids. Potential defence mechanisms mediated by Actinobacteria may include enhancing nitrogen availability, which plants could use to synthesize primary and secondary metabolites that negatively affect herbivore performance (Hubbard et al., 2019), production of antimicrobial compounds to enhance belowground plant defence, and induced systemic resistance (Matsumoto & Takahashi, 2017; Narsing Rao et al., 2022; Singh & Dubey, 2018), but further research is needed to fully understand the role of these bacteria in the aphid-wheat system.

This chapter demonstrates that aboveground aphid herbivory induced wheat plant responses that became weaker over time. Moreover, it highlights the impact of aphid herbivory on plant-soil microbial interactions, observed as increased microbial metabolic activity and a reduction in bacterial diversity. Interestingly, the reduced diversity was accompanied by the enrichment of members of the Actinobacteria class, emphasizing their potential importance in the rhizosphere under herbivory.

2.5. Supplementary material

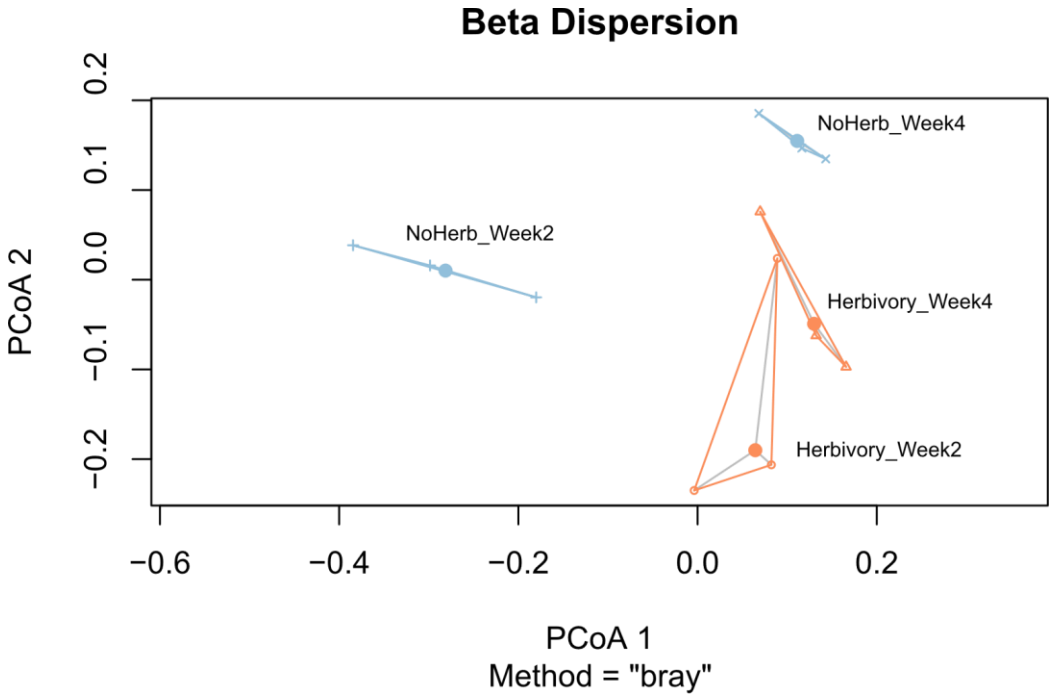

Supplementary Figure 2.1. *Beta dispersion of absorbance readings from Ecoplates™ after two and four weeks of aphid feeding.*

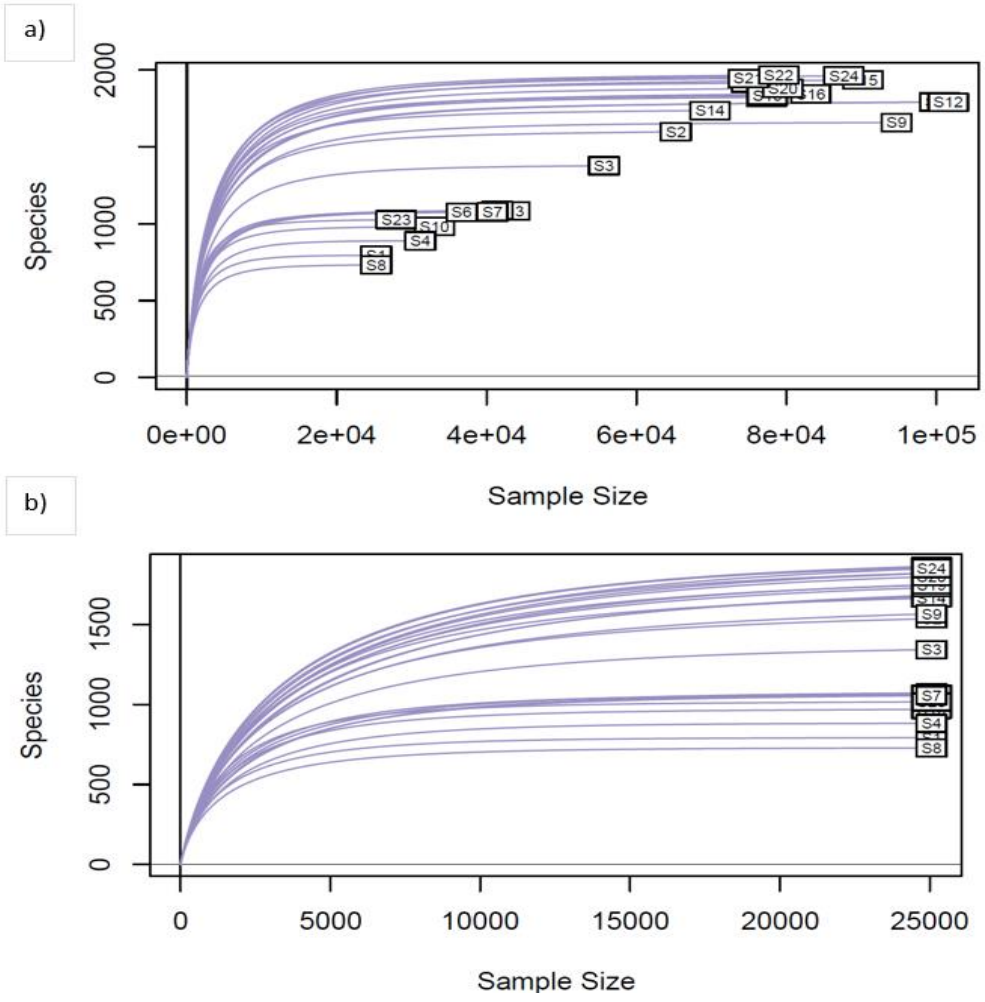

Supplementary Figure 2.2. *Alpha rarefaction curves a) before and b) after applying rarefaction to the minimum library size.*

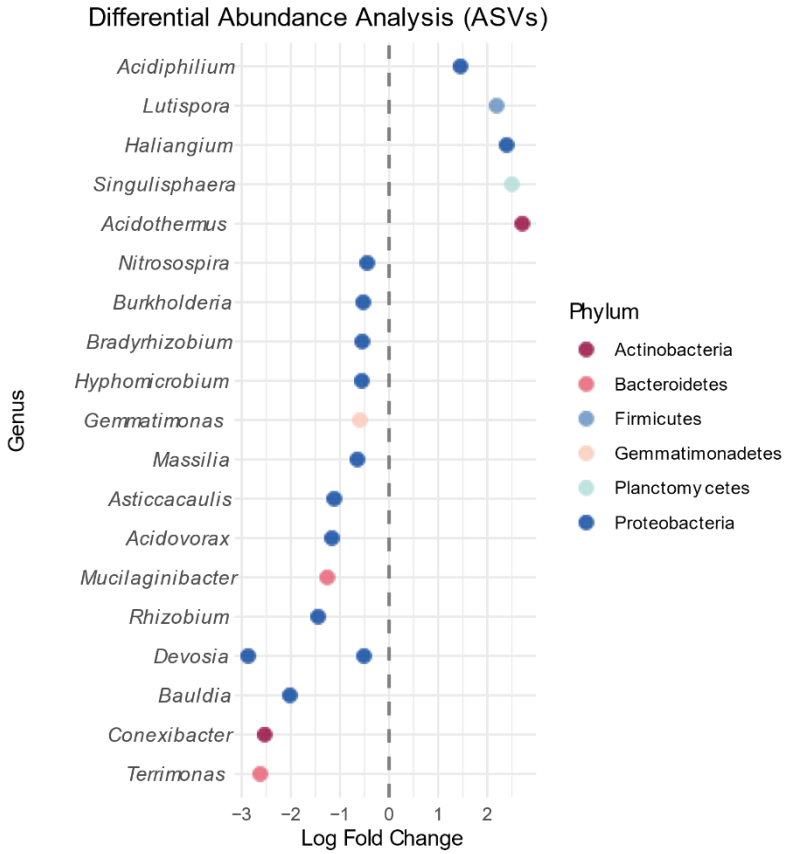

Supplementary Figure 2.3. *ANCOM-BC of the differentially abundant ASVs after four weeks of aphid feeding. LogFoldChange was calculated from the ANCOM-BC log-linear model and shows the significantly (q value < 0.05) enriched (Positive LFC) or decreased (Negative LFC) ASVs in the rhizosphere of plants under herbivory compared to the healthy plants. The genus Burkholderia_Caballeronia_Paraburkholderia was shortened to "Burkholderia" for visualization purposes.*

Supplementary Table 2.1. *Pairwise PERMANOVA results for profile of aboveground VOCs of plants under aphid herbivory.*

pairs	Df	SumsOfSqs	F.Model	R2	p.value	p.adjusted	sig
A2 vs C2	1.000	0.022	5.198	0.464	0.025	0.075	
A2 vs A4	1.000	0.052	11.795	0.663	0.039	0.078	
A2 vs C4	1.000	0.047	8.434	0.546	0.005	0.030	.
C2 vs A4	1.000	0.019	2.795	0.318	0.092	0.138	
C2 vs C4	1.000	0.010	1.268	0.153	0.298	0.358	
A4 vs C4	1.000	0.005	0.710	0.092	0.562	0.562	

A2 and A4 refer to aphid herbivory in weeks 2 and 4, respectively, while C2 and C4 refers to the control plants from the same sample times.

Supplementary Table 2.2. *Tentative annotation of non-volatiles detected with the LC-MS/MS in Data Independent Acquisition (DIA) mode. Annotations were obtained by comparing the fragment ions spectra with publicly available spectra in the GNPS environment.*

FeatureID	SharedPeaks	MassDiff	SpecMZ	Compound_Name	Adduct	Precursor_MZ	IonMode
6666	7	0.975	828.520	Massbank:PR308678 Ginsenoside Rg3(S-FORM)	M+HCOO	829.495	Negative
5883	7	1.708	339.395	(8,8-dimethyl-2,10-dioxo-9H-pyrano[2,3-f]chromen-9-yl) (Z)-2-methylbut-2-enoate	[M-H]-	341.103	Negative
5919	7	0.098	341.201	(8,8-dimethyl-2,10-dioxo-9H-pyrano[2,3-f]chromen-9-yl) (Z)-2-methylbut-2-enoate	[M-H]-	341.103	Negative
4493	6	0.000	293.176	EMBELIN	[M-H]-	293.176	Positive
2286	6	0.000	356.098	Massbank:PR309386 HMBOA + O-Hex	M-H	356.098	Negative
4516	6	2.011	295.187	EMBELIN	[M-H]-	293.176	Positive
5905	6	1.097	342.200	(8,8-dimethyl-2,10-dioxo-9H-pyrano[2,3-f]chromen-9-yl) (Z)-2-methylbut-2-enoate	[M-H]-	341.103	Negative
9839	6	1.677	591.511	Massbank:PR305683 2',6'-Dihydroxy-4-methoxychalcone-4'-O-neohesperid	M-H	593.188	Negative
2275	6	0.096	356.194	Massbank:PR309386 HMBOA + O-Hex	M-H	356.098	Negative
2276	6	0.200	356.298	Massbank:PR309386 HMBOA + O-Hex	M-H	356.098	Negative
11018	6	2.015	802.559	(2-{[3-(hexadecanoyloxy)-2-[octadec-9-enoyloxy]propyl phosphono]oxy}ethyl)trimethylazanium	M+Formate	804.574	Negative
5475	6	1.964	529.311	Bisu-13	M+H	527.347	Positive
9052	7	1.114	453.392	PE(16:0/0:0); [M-H]- C21H43N1O7P1	M-H	452.278	Negative
9050	6	0.023	452.255	PE(16:0/0:0); [M-H]- C21H43N1O7P1	M-H	452.278	Negative
1275	7	2.693	305.926	(4S,4aR,8aS)-4-[(3R)-3-hydroxy-3-methylpent-4-enyl]-3,4a,8,8-tetramethyl-5,6,7,8a-tetrahydro-4H-naphthalen-1-one	[M-H]-	303.233	Negative

9149	6	0.216	503.334	Massbank:PR310870 Isoflavone base + 2O, O-MalonylHex	M+H	503.118	Positive
9112	6	2.290	549.436	Massbank:PR309398 Anthraquinone base + 1O, MeOH, O-Hex-Pen	M-H	547.146	Negative
5803	6	1.854	413.288	CHEMBL1513915	[M+H]+	415.142	Positive
9777	8	1.644	605.498	5-methoxy-3-methyl-4-[(2S,3R,4S,5S,6R)-3,4,5-trihydroxy-6-[[(2R,3R,4S,5S,6R)-3,4,5-trihydroxy-6-(hydroxymethyl)oxan-2-yl]oxymethyl]oxan-2-yl]oxy-3H-benzo[f][2]benzofuran-1-one	[M+K]+	607.142	Positive
9057	6	1.924	663.405	PA(16:0/17:0); [M-H]- C36H70O8P1	M-H	661.481	Negative
9618	6	2.903	297.049	1-(5,10-dioxo-2,3,5a,6,7,8-hexahydro-1H-dipyrrolo[1,2-d:1',2'-f]pyrazin-10a-yl)propan-2-yl carbamate	[M-H]-	294.146	Negative
919	6	1.670	250.819	NCGC00180818-02_C15H20O3_Azuleno[6,5-b]furan-2,5-dione, decahydro-4a,8-dimethyl-3-methylene-, (3aR,4aS,7aS,8R,9aS)-	M+H	249.149	Positive
10516	6	2.071	585.395	NCGC00385693-01_C32H48O8_Propanedioic acid, mono[12-(acetyloxy)-4,4,8,10,14-pentamethyl-17-(tetrahydro-2-methyl-5-oxo-2-furanyl)gonan-3-yl] ester	M+Na	583.324	Positive
9086	6	1.894	489.274	"2,8-Dimethyl-5,7-dimethoxychromone"	[2M+Na]	491.168	Positive

Supplementary Table 2. 3. *PERMANOVA results of data absorbance readings from Ecoplates™.*

	Df	SumOfSqs	R2	F	Pr(>F)
Week	1	0.219	0.288	6.715	0.001
Treatment	1	0.186	0.244	5.703	0.001
Week:Treatment	1	0.096	0.126	2.937	0.026
Residual	8	0.261	0.343		
Total	11	0.761	1.000		

Supplementary Table 2.4. *Paired t-test comparing the AWCD of individual carbon sources in samples from the rhizosphere of plants under aphid herbivory and control plants. Comparison was performed with the AWCD obtained after 72 hours of incubation.*

Name	.y.	statistic	df	p	p.adj	p.adj.signif
2-Hydroxy Benzoic Acid	AWCD	NA	NA	NA	NA	
4-Hydroxy Benzoic Acid	AWCD	1.822	13.938	0.090	0.169	ns
D,L-a- Glycerol Phosphate	AWCD	2.448	12.534	0.030	0.084	ns
D- Galacturonic Acid	AWCD	3.227	11.262	0.008	0.034	*
D- Glucosaminic Acid	AWCD	3.400	11.892	0.005	0.027	*
D-Cellobiose	AWCD	-0.346	13.979	0.734	0.759	ns
D-Galactonic Acid g-Lactone	AWCD	1.877	10.131	0.090	0.169	ns
D-Malic Acid	AWCD	3.122	7.711	0.015	0.056	ns
D-Mannitol	AWCD	4.103	8.256	0.003	0.024	*
D-Xylose	AWCD	4.210	13.710	0.001	0.014	*
Glucose-1- Phosphate	AWCD	3.683	8.943	0.005	0.027	*
Glycogen	AWCD	2.109	7.168	0.072	0.154	ns
Glycyl-L- Glutamic Acid	AWCD	2.638	7.038	0.033	0.084	ns
Itaconic Acid	AWCD	1.463	7.956	0.182	0.260	ns
L- Phenylalanine	AWCD	-0.478	12.606	0.641	0.687	ns
L-Arginine	AWCD	1.178	13.790	0.259	0.324	ns
L-Asparagine	AWCD	2.551	9.169	0.031	0.084	ns
L-Serine	AWCD	1.591	13.995	0.134	0.201	ns
L-Threonin	AWCD	-1.105	9.800	0.295	0.354	ns
N-Acetyl-D- Glucosamine	AWCD	8.212	13.977	0.000	0.000	****
Phenylethyl- amine	AWCD	-1.648	9.210	0.133	0.201	ns
Putrescine	AWCD	1.782	13.784	0.097	0.171	ns
Pyruvic Acid Methyl Este	AWCD	1.236	13.414	0.238	0.310	ns
Tween 40	AWCD	0.747	9.970	0.472	0.524	ns
Tween 80	AWCD	2.428	9.686	0.036	0.084	ns
a- Cyclodextrin	AWCD	1.419	7.302	0.197	0.269	ns
a-D-Lactose	AWCD	-0.890	7.602	0.401	0.463	ns
a-Keto Butyric Acid	AWCD	0.243	13.823	0.812	0.812	ns
b-Methyl-D- Glucoside	AWCD	4.289	8.960	0.002	0.020	*

g-Amino Butyric Acid	AWCD	2.578	9.147	0.029	0.084	ns
i-Erythritol	AWCD	1.676	7.747	0.134	0.201	ns

Supplementary Table 2.5. *PERMANOVA results of dbRDA for explained variance in microbial communities based in the experiment with sampling and aphid herbivory as factors.*

	Df	SumOfSqs	F	Pr(>F)	Total variance	Explained variance
Model	1	0.078	2.032	0.004	0.575	0.135
Aphid	1	0.078	2.032	0.003	0.575	0.135
Residual	13	0.497			0.575	0.865

Supplementary Table 2. 6. *Differential abundance analysis of bacterial communities in plant roots. Analysis of Compositions of Microbiomes with Bias Correction-ANCOM-BC (q value <0.05)*

taxon_id	Phylum	Genus	LFC	W	p-val	q-val
5c75e45b7ed1d2a6f0d83da881c19e88	p_Proteobacteria	*g_Sphingomonas*	-3.040	-21.398	0.000	0.000
e6fe291048daee402e6a14f0a809c9d2	p_Firmicutes	*g_Paenibacillus*	-2.747	-9.649	0.000	0.000
7f27c463c123c31a66ab8b1159e0f305	p_Proteobacteria	*g_Pseudomonas*	-2.219	-4.443	0.000	0.015
3a8da6b2caa6a4af12e1a6191c638285	p_Proteobacteria	*g_Achromobacter*	-2.219	-5.440	0.000	0.000
c7a48726e2f6ca86fd0b046d5edf31e8	p_Acidobacteria	*g_Candidatus Solibacter*	-2.019	-7.113	0.000	0.000
82f59b6ac24edd88c4a2f8388871c63a	p_Proteobacteria	*g_Brevundimonas*	-1.906	-4.850	0.000	0.002
d0ef28ce164116ab436cde247533bd21	p_Proteobacteria	*g_Haliangium*	-1.803	-9.733	0.000	0.000
3ad66ca8ed35cfa86f542a97a960a5fa	p_Actinobacteria	*g_Iamia*	-1.600	-4.981	0.000	0.001
8624cc78759c1d01fbc987b6ef50823a	p_Proteobacteria	*g_Reyranella*	-1.168	-7.392	0.000	0.000
18dc584ed9b3f31a7fc6529f3d00ef25	p_Actinobacteria	*g_Conexibacter*	-0.631	-4.929	0.000	0.001
7f3982dfaafd2c5bc889c50c5c23a573	p_Actinobacteria	*g_Conexibacter*	-0.831	-7.217	0.000	0.000
86ec590bc5216a031f548651939ccdc0	p_Firmicutes	*g_Ammoniphilus*	-0.423	-4.839	0.000	0.002
f47be1e444de7e20e9dbc45c7b2424c3	p_Actinobacteria	*g_Streptacidiphilus*	5.077	12.158	0.000	0.000
12f890e95c4db01952a0b98ec94a0d0e	p_Proteobacteria	*g_Rhodanobacter*	3.296	4.774	0.000	0.003
643e9b9539936644669a5913fb230b62	p_Actinobacteria	*g_CL500-29 marine group*	2.982	4.997	0.000	0.001
688513cbe9b7a45063622375fee9e742	p_Planctomycetes	*g_Singulisphaera*	2.876	4.895	0.000	0.002
c88f433e7fb724aa97f075fcbd3b7b3f	p_Actinobacteria	*g_Smaragdicoccus*	2.573	5.041	0.000	0.001
03e53aa8bbbec1c754dfe7874dbc84c3	p_Actinobacteria	*g_Acidothermus*	2.365	5.967	0.000	0.000
3da9789d812b366b23f07b4565621404	p_Proteobacteria	*g_Pantoea*	2.232	5.196	0.000	0.000

taxon_id	Phylum	Genus	LFC	W	p-val	q-val
1931ff69d6539ab76f63f4f38bf4f45d	p_Actinobacteria	*g_Streptomyces*	3.447	5.512	0.000	0.000
fe152f052d61329f69f35978cbe387ee	p_Actinobacteria	*g_Streptomyces*	1.493	5.300	0.000	0.000
de1b7d4b13be4049f61f3a4af40d521c	p_Actinobacteria	*g_Streptomyces*	1.034	5.902	0.000	0.000
363554a6ab57095ae390a5d862704968	p_Proteobacteria	*g_Rhodopseudomonas*	1.892	5.215	0.000	0.000
e906dacf4ad9961bd9f3cd1857d0d4d2	p_Actinobacteria	*g_Nocardioides*	1.372	5.324	0.000	0.000
dd3b89cecb3d1db087c193a430cee2d9	p_Proteobacteria	*g_Pseudolabrys*	0.873	7.269	0.000	0.000
d903338d829c8c63825342ed3280bd2b	p_Proteobacteria	*g_Bradyrhizobium*	0.509	4.309	0.000	0.028
9e6d3839fd6ed558c7e67d491c0c17de	p_Actinobacteria	*g_Luedemannella*	3.003	4.583	0.000	0.008
5f083980228e2b7296dfb6687352b6b0	p_Actinobacteria	*g_Luedemannella*	-1.716	-7.655	0.000	0.000
498e52d9c7dbf7ea60c2200bfb9f0fbc	p_Planctomycetes	*g_Aquisphaera*	2.866	5.588	0.000	0.000
e6f87ae780d2f4047b601cf218e4f2e8	p_Planctomycetes	*g_Aquisphaera*	-1.790	-5.311	0.000	0.000
ce77271d1f9b686e489b358febeb0676	p_Proteobacteria	*g_Burkholderia*	4.928	4.822	0.000	0.002
91096c5afda672fe78390db90141f215	p_Proteobacteria	*g_Burkholderia*	-4.404	-8.405	0.000	0.000

Chapter 3: Interrogating changes in belowground chemical signals from wheat plants during aphid herbivory

Plants communicate with their environment through chemical signals that, belowground, play a crucial role in shaping and selecting microbial communities that can influence plant health. This chapter addresses the ***second aim*** *of this project:* ***to identify potential key metabolites that mediate the recruitment of distinct bacterial communities in response to aphid herbivory****. Using an* ***untargeted metabolomics*** *approach, both volatile organic compounds (VOCs) and non-volatile metabolites exuded from plant roots were analysed, revealing the impact of aphid herbivory on most secondary metabolic pathways. Among these different chemical classes,* ***benzoxazinoids*** *and* ***oxylipins*** *emerged as key chemical signals, potentially orchestrating belowground microbial recruitment in response to aboveground herbivore attack.*

3.1. Introduction

Plants produce a myriad of chemically and functionally diverse metabolites, with estimates ranging from 200,000 to over a million across the plant kingdom (Walker et al., 2022; Wang et al., 2019). For comparison, whilst it has been estimated that the bacterium *Escherichia coli* contains around 750 metabolites (Nobeli et al., 2003), a single plant may produce more than 5,000 (Fernie et al., 2004; Hall et al., 2002). Primary metabolites, essential for plant growth, are largely conserved across prokaryotes and eukaryotes (Wang et al., 2019). However, plants (and other eukaryotes, like fungi) have additional capacity to produce specialised (secondary) metabolites, which contain most of the plant *metabolome* – the complete set of

metabolites within an organism (Shen et al., 2023). These secondary metabolites provide plants with a vast set of mechanisms for defence against adverse biotic and abiotic stresses, increasing their chance for survival (Walker et al., 2022; Wang et al., 2019).

A metabolome is the reflection of the combined regulation of genes, transcripts, and proteins, and can be used to measure the full spectrum of metabolic responses of organisms to their surroundings (Luque de Castro & Priego-Capote, 2018; Rattray et al., 2018). For this reason, the study of *metabolomics* plays a central role in understanding ecological interactions (Kuhlisch & Pohnert, 2015). Since the term was first coined in 1998, *metabolomic* approaches have been increasingly applied to diverse fields including natural product discovery, medicine, microbiology, and agriculture (Broeckling et al., 2023).

This field can be divided into two main approaches: targeted and untargeted. The targeted metabolomics approach focuses on specific metabolites with prior knowledge about their identities, biological role, or pathways. In contrast, untargeted metabolomics aims to investigate the full spectrum of detectable metabolites within a system (Caesar et al., 2019; Dudzik et al., 2018). The latter offers a unique possibility of exploring the chemical diversity and complexity of biological systems under different conditions.

A common method employed in untargeted metabolomics is metabolic profiling, in which a “fingerprint” of the metabolome can be observed across different biological systems, conditions, or treatments (Fernie et al., 2004; Quiros-Guerrero et al., 2024). Using this technique, global changes can be measured, and multiple metabolic

pathways can be studied. Based on these observed changes, along with existing knowledge of the organisms and metabolite classes involved (e.g., plants, animals, microorganisms), hypotheses can be formulated and tested through bioassays (Caesar et al., 2019; Guo & Huan, 2020). Thus, untargeted metabolomics serves as a critical tool for generating hypotheses that can later be rigorously tested using targeted approaches.

In Chapter 2, the results suggested that aphid herbivory had a significant impact on the selection of bacterial communities in wheat rhizosphere, with the strongest impact observed after two weeks of aphid herbivory. Based on these findings, a new experiment was designed to investigate the interaction between wheat plants, root exudates and soil bacterial communities. The results from this new experiment are presented in two chapters: Chapter 3 (present chapter: root exudate analysis) and Chapter 4 (next chapter: microbiome analysis). The current chapter presents the results of an untargeted metabolomics approach to examine the chemical changes in wheat root exudates following two weeks of aphid herbivory. Comparative metabolomics was employed to detect global changes in the metabolome of root exudates, with the goal to identify metabolites that could act as signals influencing bacterial community assembly in the rhizosphere.

The central objective of this chapter was to use cutting-edge metabolomics tools to uncover how aphid herbivory alters the chemical signals released by plant roots into the soil environment. To achieve this, root exudates were analysed using a combination of liquid chromatography (LC) and gas chromatography (GC) coupled with mass spectrometry (MS). Chemoinformatic analyses were performed using both vendor software (GC-MS) and freely available tools (LC-MS/MS), alongside

experimental and *in silico* databases for compound annotation. Furthermore, for the LC-MS/MS data, feature-based molecular networking (FBMN) within the Global Natural Products Social Molecular Networking (GNPS) environment was employed to explore the relationships among detected metabolites. These annotation strategies, along with multivariate statistical analysis, were used to reveal potential metabolites with a critical role in modulating wheat-associated bacterial community assembly in response to aphid herbivory.

3.2. Methods

In this chapter, a new experiment was performed following the methods described in Chapter 2, Sections 2.2.1 and 2.2.2. However, in this experiment, samples were collected only after two weeks of aphid herbivory, as this timepoint showed the most pronounced differences in plant and microbial responses in Chapter 2. As an additional step in this experiment, individual pots were kept in mesh cages to prevent any aphid from going to the untreated control plants (Figure 3.1).

Figure 3.1. *Plants growing inside mesh cages to prevent aphid transfer from the aphid-herbivory treatment.*

3.2.1. Root exudates collection

Root exudates were collected using a soil-hydroponic hybrid approach (Figure 3.2) based on the methodologies developed by Lohse et al. (2023) and Williams et al. (2021). This was achieved by carefully removing the plants from the pots and gently shaking the roots to remove the soil. The roots of all plants (n=10) from each pot were washed twice in sterile tap water, followed by a wash with sterile deionised water. After washing, the roots were submerged in 100 mL of sterile deionised water in beakers while the remaining roots were processed, ensuring the entire washing procedure lasted less than one hour from the first to the last pot to reduce the possibility of changes in root exudation patterns. Following the washing step, all plants were allowed an additional 30 minutes to adapt to the deionised water before exudate collection.

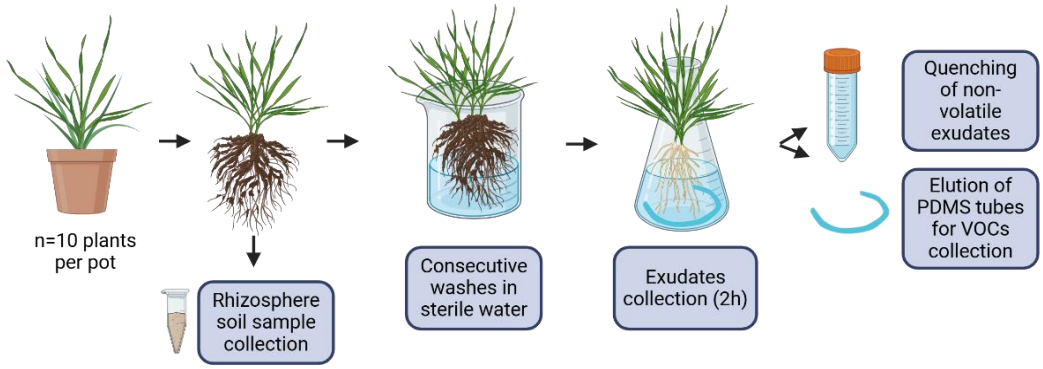

Figure 3.2. *Sampling methodology for root exudates in untargeted metabolomics analysis. Plants were removed from pots, shaken to collect rhizosphere soil, and washed in sterile tap and deionised water. They were then placed in bottles with 100 mL of sterile deionised water and a 10 cm Polydimethylsiloxane (PDMS) tube to capture volatiles. After two hours, 80 mL of exudates were snap-frozen, and PDMS tubes were eluted with 750 µL of diethyl ether for further analysis.*

To avoid aphid transfer between plants, healthy plants were processed first and returned to their individual cages while awaiting the completion of the procedure. Once all plants were prepared for exudate collection, they were transferred to new

flasks containing 100 mL of sterile deionised water. These flasks also contained a 10 cm sterile Polydimethylsiloxane (PDMS) tube (internal diameter 1,00 mm, external diameter 1,80 mm, wall thickness 0,40 mm, VWR INTERNATIONAL LTD), placed at the bottom, to capture root exudate volatile organic compounds (VOCs). The collection process took place between the hours of 14.30h and 16.30h, with all plants kept in the same mesh cages they had been growing in throughout the experiment.

After collection, the plants were removed from the flasks, and 80 mL of the exudates were transferred to two 50 mL Falcon tubes. The tubes were immediately snap-frozen in liquid nitrogen. The exudates were later thawed at 4°C, filtered through 0.2 µm membranes, and stored at -20°C. The PDMS tubes were left in the flasks and transported back to the laboratory for elution. During exudate collection, three process blanks were also collected using deionised water (without plants), and an extra blank was set up with only aphids (>10) in the deionised water to evaluate potential VOCs released by aphids.

After collecting the root exudates, the plants from each replicate were divided in two groups: Three plants were taken for measurements of dry weight and the others were kept for DNA extraction. Dry weight measurements were taken after drying the plants at 70°C for 96 hours.

3.2.2. Root exudate processing

The filtered root exudates were freeze-dried for five days until all water was evaporated. After freeze-drying, the exudates were resuspended in 2 mL of a 50:50 water:methanol solution and thoroughly vortexed. The solution was then concentrated under a gentle stream of nitrogen and resuspended in 700 µL of 50:50

water:methanol solution. Following this, the exudates were vortexed and placed in a 2 mL Eppendorf tube to be concentrated again under nitrogen. Finally, the concentrated exudates were resuspended in 200 µL of methanol (>99%), vortexed, and centrifuged at 4°C for 8 minutes. The resulting exudates were stored at -20°C until further use. A schematic representation is shown in Figure 3.3.

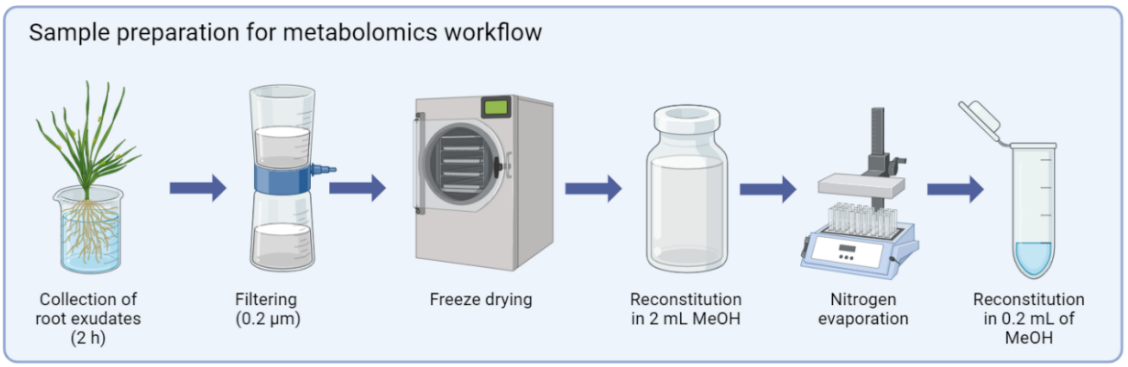

Figure 3.3. *Sample preparation of non-volatile root exudates for analysis. The frozen root exudates samples were thawed at 4 °C and filtered through a Stericup vacuum filter (0.22 µm). The filtered exudates were then freeze-dried for five days and reconstituted in 2 mL of a 50% methanol solution. Next, the exudates were concentrated under nitrogen, reconstituted in 700 µL of 50% methanol, concentrated a second time under nitrogen and reconstituted in 200 µL of methanol for LCMS analysis.*

Volatile Organic Compounds (VOCs) sample processing

The PDMS tubes were eluted with 1 mL of diethyl ether and further concentrated under a gentle stream of nitrogen to a final volume of 50 µL. After this, the samples were kept at -20 °C until analysis by GC-MS.

3.2.3. Untargeted metabolomics of wheat root exudates under aphid herbivory

3.2.3.1. Data-Dependent Acquisition (DDA) of root exudates

Following sample preparation, a 50 µL aliquot of each root exudate sample was transferred into HPLC vial inserts for analysis. Following the guidelines from the Metabolomics Quality Assurance and Quality Control Consortium (mQACC) (Broeckling et al., 2023; Evans et al., 2020), additional blanks and quality control samples were added to ensure system suitability and quality control. A table describing these samples is shown (Table 3.1):

Table 3. 1. *Description of blanks and quality control samples used for the analysis of root exudates*

Name	Description
Process blank	Blank sample passed through the analytical process including sample processing and analysis. These were freeze-dried, concentrated, and resuspended alongside the root exudate samples (n=3).
Solvent blank	A methanol (>99%) solvent that has not passed through the sample preparation process applied to the root exudates samples (n =1).
Standards solution	A solution containing a mix of flavonoids (isovitexin, schasftoside, galangin, and fisetin) at a concentration of 100 ng/µL (n=1)
Quality Control (QC) samples	Intra-study QC samples created by pooling an aliquot (10 µL) of all the root exudates samples. This sample was divided in three vials that were spread throughout the LCMS run (n=3)

The biological samples, blanks, standards, and quality control (QC) samples were organised into a single batch for analysis via liquid chromatography- tandem mass

spectrometry (LC-MS/MS). The sequence of the batch was carefully designed to minimize potential instrument drift and contamination, and the specific order, including sample replicates and QC distribution, are detailed in Supplementary Table 3.1.

Data acquisition was carried out by using an I-class ACQUITY ultra-high-pressure liquid chromatography (UPLC) system coupled to a SYNAPT G2SiG2 Q-TOF mass spectrometer with an electrospray (ESI) ionization source (Waters, Manchester, UK). Liquid chromatography conditions were maintained as those described in Chapter 2, Section 2.2.4.2.

Mass spectrometric analysis was conducted using negative ionisation mode (ESI-) with a data-dependent acquisition (DDA) approach. In this approach, an intensity threshold is applied to peaks detected in full scan mode to select precursor ions for further fragmentation in the collision cell. The FastDDA method provided in the instrument software (MassLynx, Waters) was employed for this process. The switching criteria from MS to MS/MS included a maximum of 20 precursors per cycle and an intensity threshold of 5000. A mass range of 50 to 1100 Da was used, with a collision energy ramp in the transfer cell set from 10 to 30 eV for low mass ions and from 30 to 90 eV for high mass ions. Accurate mass detection was performed in sensitivity mode. The Q-TOF was calibrated using a sodium formate solution, and lock mass correction was applied with leucine-enkephalin during each run. An exclusion list, based on previous full scan mode runs of certain samples and blanks, was created to prevent the fragmentation of background noise signals.

3.2.3.2. Chemoinformatic analysis: Data processing and metabolite annotation

Following sample acquisition in FastDDA mode, raw data files were converted to an open-source format (.mzML) using the vendor software Waters DataConnect v.2.1.0. This was performed to enable compatibility with open-source analytical tools. After conversion to .mzML format, data processing and spectral alignment were performed using the processing wizard mode on the mzmine software v.4.0.3. Two representative samples per condition were initially evaluated to determine appropriate noise thresholds and minimum feature intensities, to optimize the processing parameters. Noise levels were set at an intensity of 500 for MS and 100 for MS/MS spectra, with a minimum feature height intensity of 1000. Chromatograms were cropped to 30 min to remove late-eluting peaks associated with background noise. As observed in Figure 3.4, the processing pipeline generated output files required for further analysis, including: 1) an .mgf file containing MS/MS spectral data for annotation; 2) an .mgf file formatted for chemical classification using the software Sirius v.6.0.0; 3) a .csv file listing precursor ion masses, retention times, and peak areas; and 4) a .csv file containing edges information for molecular network analysis and visualization.

a.

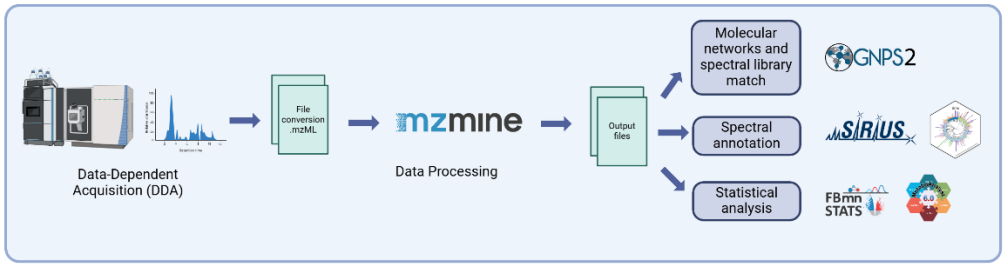

b.

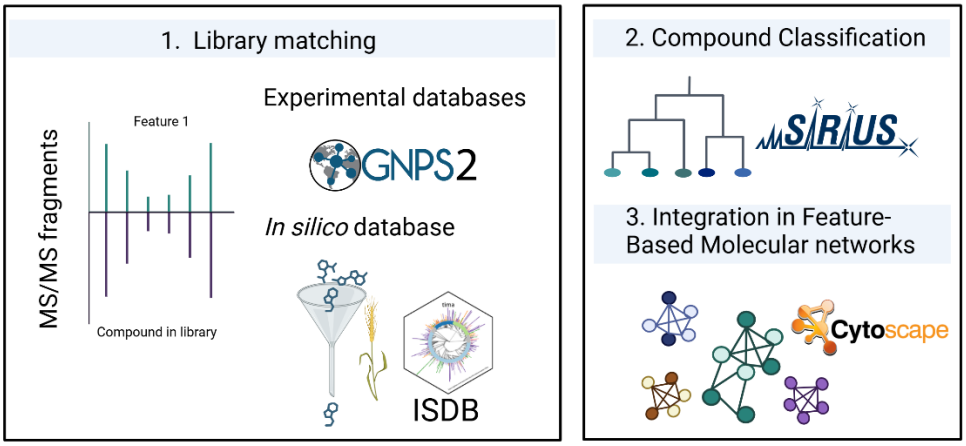

Figure 3.4. *Pipeline for untargeted metabolomics analysis of non-volatile root exudates (LC-MS/MS). a) Data processing involved acquisition in Data-Dependent Acquisition mode, file conversion to open-source format, and processing in mzmine v.4.0.3, generating four files for metabolite annotation, molecular networking, and statistical analysis. b) Metabolite annotation strategies included experimental and in silico database matching, chemical classification via CANOPUS (SIRIUS), and integration of all annotations into molecular networks.*

Metabolite annotation and Feature-Based Molecular Networking (FBMN) on the Global Natural Product Social Molecular Networking (GNPS) platform

All data files exported from mzmine v.4.0.3 were uploaded in the Global Natural Product Social Molecular Networking (GNPS) environment for metabolite annotation against experimental libraries and Feature-Based Molecular Networking (FBMN). A metadata file specifying sample identities and conditions (herbivory, control, QC, blanks) was included for FBMN visualization.

Metabolite annotation was performed using a precursor ion and MS/MS fragment mass tolerances set to 0.02 Da. Matches between experimental data and experimental spectral libraries using the cosine score. A cosine similarity score threshold of 0.6 was selected for library matching (from 0 to 1, one being identical or 100% match), with a minimum of four matched peaks. Library matching was performed against all spectral libraries available in GNPS. Molecular networks, constructed in GNPS based on MS/MS similarity between unique peaks, or *features*, were constructed using a minimum cosine similarity score of 0.7 and at least five matched peaks, with clustering requiring a minimum of two spectra per node.

Metabolite annotation using other open-source tools

For chemical classification of the identified features (unique peaks in the root exudate samples), the precursor and fragment data contained in the .mgf file was analysed using the software SIRIUS v.6.0.0 (Dührkop et al., 2019), applying the Compound Class Prediction module CANOPUS. Chemical classes were assigned based on the Natural Product Classifier (Kim et al., 2021), in which pathway, super classes and classes of compounds were predicted for the detected features. Annotation quality was filtered based on a confidence score > 0.8 (from 0 to 1, where 1 is a confidence level of 100%).

In addition, a taxonomically informed approach was applied using the software TimaR v.2.11.0 (Rutz et al., 2019). This software matched spectral data against an *In Silico* Spectral Database (ISDB) of natural products and, when possible, re-ranked candidate metabolites based on their reported presence in wheat (*Triticum aestivum)* in the LOTUS database of natural products (Rutz et al., 2022). Annotation quality was

filtered based on a confidence score > 0.45 (from 0 to 1, where 1 is a confidence level of 100%).

Integration of annotation tools on FBMN

The resulting molecular networks were visualized in Cytoscape software v. 3.10.2, where nodes represented individual metabolite features, and edges indicated the cosine similarity scores between the MS/MS fragmentation patterns. Multiple layers of metadata were incorporated into network visualisations to integrate all the annotation tools. First, nodes were colour-coded based on the chemical classifications derived from the different annotation tools (e.g., GNPS spectral library match, chemical classification, or taxonomically informed annotation), to visualise the coverage of annotated metabolites. Pie charts representing the total sum of peak areas between treatments (herbivory vs. no herbivory) were added to nodes. Finally, node size was scaled according to statistical significance (p_{adj}-values), highlighting metabolites that showed significant differences between treatments.

3.2.3.3. Confirmation of identity of selected metabolites with authentic chemical standards

Following the statistical analysis (detailed below in Section 3.2.4), five features were selected for identity confirmation, as aphid herbivory was observed to influence their concentration in plant root exudates. Authentic chemical standards were obtained and prepared to a final concentration of 100 ng/µL. These standards were analysed using LC-MS/MS under the same conditions as root exudate samples (Section 3.2.3.1). After data conversion, standard files were aligned with pooled quality control (QC) samples (n = 3) from root exudates in the mzmine software (v.4.0.3), applying the

same parameters as in Section 3.2.3.1. The alignments were then examined to verify whether the retention times of standard peaks matched those of the selected features.

The following standards were used: 7-methoxy-2-[3,4,5-trihydroxy-6-(hydroxymethyl)oxan-2-yl]oxy-4H-1,4-benzoxazin-3-one (HMBOA-O-Hex) (BenchChem, USA; Cat# B095448); azelaic acid (Merck, Germany; Cat# 46379-2); p-Coumaric acid (Merck, Germany; Cat# 90088); Salicylic acid (Merck, Germany; Cat# 247588); (12Z)-9,10-Dihydroxyoctadec-12-enoic acid (9,10 DiHOME) (Cayman Chemical, USA; Cat# CAY53400).

3.2.4. Untargeted metabolomics profiling of root VOCs

After root volatile extract collection and concentration under a flow of nitrogen, chemical analysis of the extracts was carried out using an Agilent Gas Chromatography Quadrupole Time of Flight Mass Spectrometer (Agilent 7250 GC/QToF) with a 8890 Gas Chromatography system fitted with an Agilent HP-5 30 m column (15 m length X 0.25 mm inner diameter X 0.2552 µm film thickness). GC oven conditions were: Initial Temp 30°C hold time 0.1 min, followed by a 5°C/min ramp to 150°C with a hold time of 0.1 mins, final ramp was 10°C/min to 250°C with a hold time of 25 min (total run time 59.2 min). The extracts (4 µL) were injected into a split-splitless injector programmed with a heater temperature of 250°C, pressure 7.5 psi and set to a 20:1 split ratio. The QToF-MS was run with the following specifications: electron energy 70 eV, source temperature 220°C. GC alkanes standards C7-C22 were run on the system to establish retention index values for the volatile extracts, and mass spectra produced were tentatively identified using the NIST mass spectral library (2020).

Chemoinformatic analysis: Data processing

To process VOC datasets, the data files were converted to the open-source format .mzML using the software MSConvert v.3.0.24197. The files were then analysed in the mzmine software v.4.0.3 to determine parameters for alignment and noise levels. Using the processing wizard mode, a noise threshold of 500 intensity and a minimum feature height of 1000 were applied. After alignment, a .csv file containing retention times and peak areas was generated for downstream statistical analysis in MetaboAnalyst v.6.0 (Pang et al., 2024).

3.2.5. Statistical analyses

3.2.5.1. Root exudates

The feature table, containing all detected features (i.e., metabolites) and their respective peak areas, was uploaded into the FBMNStats website (Pakkir Shah et al., 2024). A blank removal step was applied based on a cut-off intensity of 0.30, to remove low-intensity features that were likely noise or artifacts. The resulting data frame was saved as a .csv file and uploaded into the MetaboAnalyst platform v.6.0 for further statistical analysis.

In the MetaboAnalyst platform v.6.0, the data was normalised based on root dry weight to ensure that metabolite concentrations were adjusted to relative biomass. A log10 transformation was applied to reduce skewness, and Pareto scaling was used to minimize the influence of large peak areas, allowing the detection of medium and smaller peaks that could also be biologically relevant. To remove features with high variance and those that remained stable across the evaluated conditions, a filtering step was used following standard guidelines for the analysis of untargeted metabolomics datasets based on the variance of pooled QC samples using the

relative standard deviation and the interquartile range (IQR). A Principal Component Analysis (PCA) was performed to assess the structure of the dataset. The distribution of QC samples in the PCA was manually reviewed to confirm data quality. Afterwards, the QC samples were removed from the dataset, and the statistical analysis was conducted with the samples from wheat plants subjected to aphid herbivory and untreated controls.

The statistical analysis included a new PCA without the QC samples, followed by a PERMOVA test to evaluate differences between the groups. Differential abundance analysis was performed using a combination of log2 fold change (log2FC) and a t-test, with p-values adjusted using a false discovery rate (FDR) correction set at $p < 0.1$. A higher p-value threshold was chosen to increase the coverage of potentially important metabolites that might be otherwise ignored due to the low statistical power due to small sample size.

Additional statistical analyses were conducted in R studio v.4.2.3 (RStudio Team, 2020). For the molecular networks, t-tests were performed for the total sum of peak areas from networks of interest. The analyses were performed using the packages *tidyverse* v.2.0.0 (Wickham et al. 2019), *vegan* v. 2.6-8 (Oksanen et al. 2018) and *ggplot2* v.3.5.1 (Wickham H. 2016). For visualization of the results, the packages *ggpubr* v.0.6.0 (Kassambara A. 2023), *gridExtra* v.2.3 (Auguie B. 2017) and *VennDetail* v.1.20.0 (Guo et al. 2024) were used.

3.2.5.2. Root volatiles (VOCs)

The VOC analysis pipeline followed the same steps to the non-volatile exudate analysis, although filtering was based solely on IQR to remove near-constant peaks.

The same PCA, PERMANOVA, and heatmap analyses were applied to identify significant VOCs influenced by aphid herbivory.

3.2.5.3. Plant dry weight

The data from plant dry weight (root and shoot) was analysed in R Studio v.4.2.3 (RStudio Team, 2020) using the Wilcoxon non-parametric test. The analyses were performed using the packages *tidyverse* v.2.0.0, *vegan* v. 2.6-8, and *ggplot2* v.3.5.1.

3.3. Results

3.3.1. Plant biomass production was significantly decreased by aphid herbivory

Aphid herbivory significantly affected plant growth (Figure 3.5). The main effect was observed in the aboveground plant parts, with dry weight reduced by 38% in the plants under herbivory compared to the healthy control plants (no herbivory). Although the dry weight of roots was not significantly reduced ($p = 0.095$), root biomass tended to be higher in control plants than in plants under aphid herbivory. The root-to-shoot ratio did not differ significantly among treatments ($p = 0.42$), though there was a nonsignificant trend toward a lower ratio in herbivory-treated plants. These results suggest that aphid herbivory created a sink for plant resources altering plant resource distribution that affected the production of biomass above and belowground.

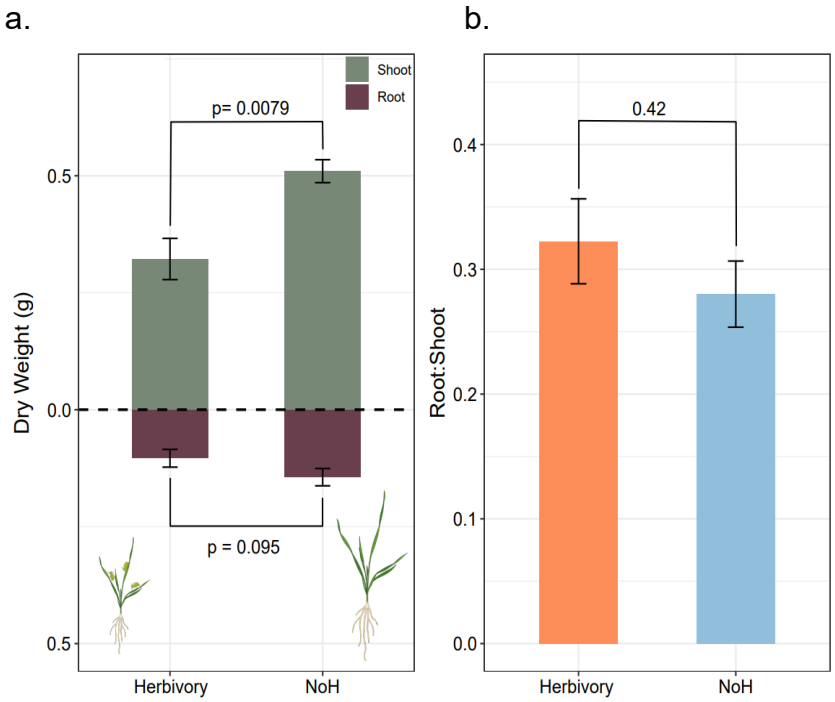

Figure 3.5. *a) Dry weight of shoots and roots of plants after two weeks of aphid herbivory, b) Root to shoot ratio of plant dry weight. The mean comparison was performed using a Wilcoxon test. The error bars represent the standard error (n=5). Herbivory = Plants under aphid herbivory; NoH = Untreated controls.*

3.3.2. Untargeted metabolomics of non-volatile exudates from wheat plants

This results section is divided into two main parts. The first part focuses on the annotation of metabolites to identify compounds present in wheat root exudates, with the goal of identifying metabolites that could be relevant in the context of aphid herbivory. The second section presents the statistical analysis of root exudates from wheat plants under aphid herbivory and control conditions, integrating metabolite annotations to characterise shifts in exudate composition under herbivory more effectively. These findings will provide a foundation for linking metabolite shifts to microbial community dynamics in Chapter 4.

3.3.2.1. Metabolite annotations

Metabolite annotation was performed following the analysis of wheat root exudate samples and processing of LC-MS/MS data, as described in Section 3.2.3. A total of 2,211 features (i.e., unique peaks) were identified in the samples. As described in the methods Section 3.2.3.2, multiple annotation strategies were employed to classify metabolites present in the root exudates. These included matching against both experimental (GNPS) and *in silico* (ISDB) databases. Additionally, the taxonomically informed tool TimaR was used to refine *in silico* annotations by prioritising metabolites previously reported in wheat plants. Finally, the CANOPUS classification tool was applied to predict the chemical classes of unannotated features.

Metabolite annotation against public experimental and in silico data bases in the Global Natural Product Social Molecular Networking (GNPS) platform

Spectral matching against experimental databases within the GNPS environment allowed the annotation of 93 features across all samples. Subsequent manual curation based on ppm accuracy error and adduct type refined the dataset to 59 metabolites, corresponding to an annotation coverage of 2.67% (Supplementary Table 3.2). These putative annotations included diverse metabolic pathways, such as the shikimate pathway, amino acid metabolism, and fatty acid biosynthesis, among others. A summary of the chemical classification of these metabolites is presented in Figure 3.6, along with the metabolite classification from other MS/MS strategies.

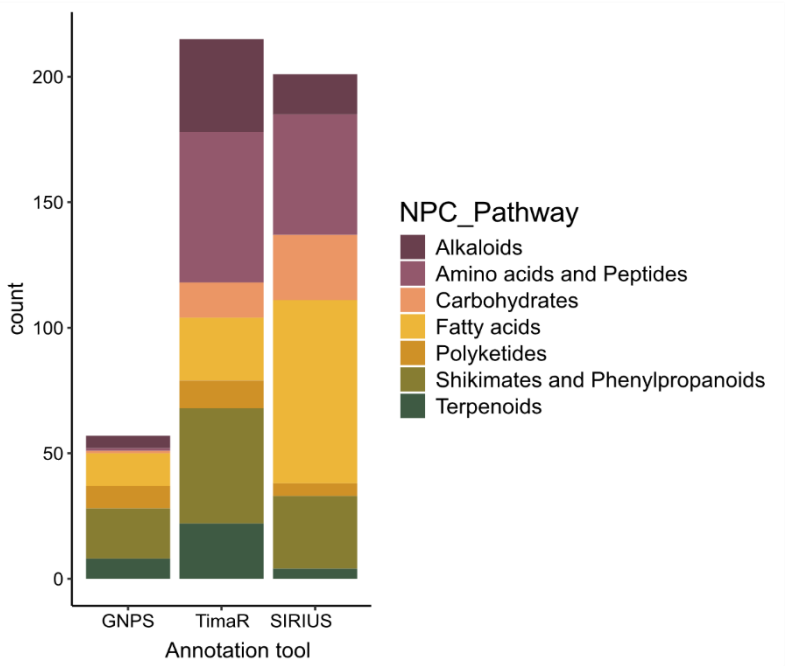

Figure 3.6. *Classification of metabolites in each annotation tool based on the natural product classifier (NPC) at the pathway level.*

Metabolite annotation using in silico libraries and prediction of chemical classes

The second annotation tool employed in this study was TimaR, which conducts spectral matching in two stages. Initially, library matches are identified against an *in silico* spectral database (ISDB), followed by a re-ranking of the potential candidates based on exact precursor ion mass searches within host-specific databases, in this case, *Triticum aestivum* (wheat). The ISDB matching resulted in the annotation of 237 metabolites, accounting for 10.7% of the detected features, which were classified into chemical classes based on MS/MS fragmentation patterns. As shown in Figure 3.6, nearly 50% of the putatively annotated metabolites were assigned to the alkaloids and amino acids classes.

In the second stage, the accurate mass of the features was cross-referenced with the LOTUS database – a curated database for experimental data - focusing solely on metabolites reported in wheat, leading to the identification of 99 metabolites previously described in this plant species. Of these, 28 metabolite identifications overlapped with those from ISDB matching. These metabolites were classified into the same pathways, class, and superclass by both MS/MS spectral matching against ISDB and accurate mass matching against LOTUS, demonstrating congruence between the two annotation approaches (Figure 3.7). The remaining 71 metabolites were annotated based solely on matching of the accurate mass against metabolites present in wheat plants. A comprehensive list of the metabolites annotated using this methodology is provided in Supplementary Table 3.3.

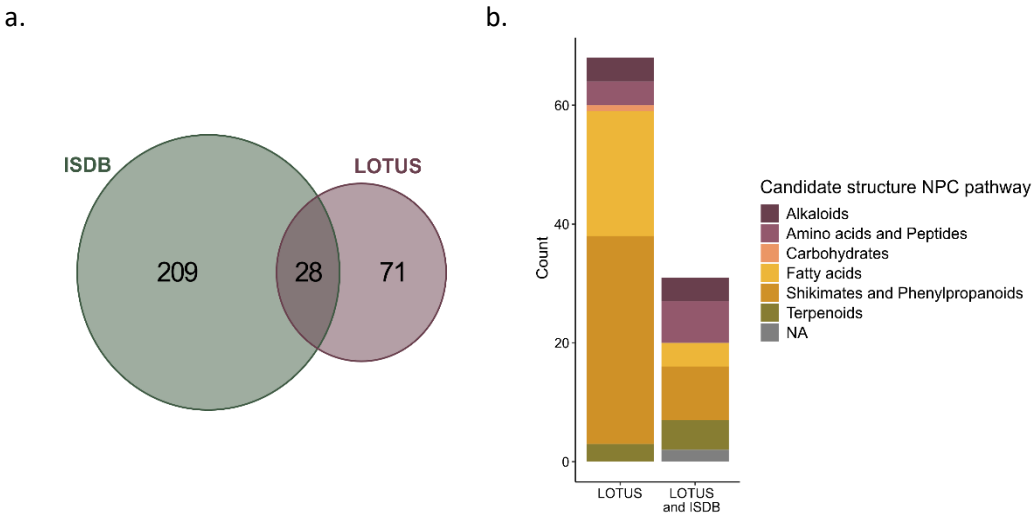

Figure 3.7. *Spectral matches at the pathway level (Natural Product Classifier-NPC) according to taxonomically informed metabolite annotation (TimaR) software. a) Venn diagram showing the overlap between annotations from LOTUS (taxonomically informed) and ISDB (MS/MS) tools. b) Bar plot showing the count of metabolites annotated at the pathway level using the NPC classifier using only accurate mass in the LOTUS database and the metabolites matched in both LOTUS and ISDB.*

The chemical classification of metabolites present in the sample was further investigated using Compound Class Prediction module –CANOPUS, a machine learning prediction module from the SIRIUS software v.6.0.0. This analysis resulted

in the classification of 1,294 features. Following quality filtering based on a confidence score greater than 0.8 on the confidence of annotations (on a scale of 0 to 1, where 1 represents 100% confidence), against the Natural Product Classifier Pathways, Superclass, and Class levels, a total of 201 features were identified with a high level of confidence (Figure 3.6). These 201 features represent 9.09% of all metabolites detected in the root exudates.

A low overlap was observed among the three MS/MS annotation strategies used (Figure 3.8), with only two features shared by the three strategies. Furthermore, different strategies for annotation were shown to target different chemical classes (Figure 3.6). For instance, the chemical classification in CANOPUS allowed for more fatty acids to be annotated, while the *in silico* matching in ISDB, allowed the annotation of mainly amino acids and peptides, shikimates and phenylpropanoids, and alkaloids. Overall, the three strategies allowed the chemical classification of 446 features, which represent 20.17% of all features present in the wheat root exudates.

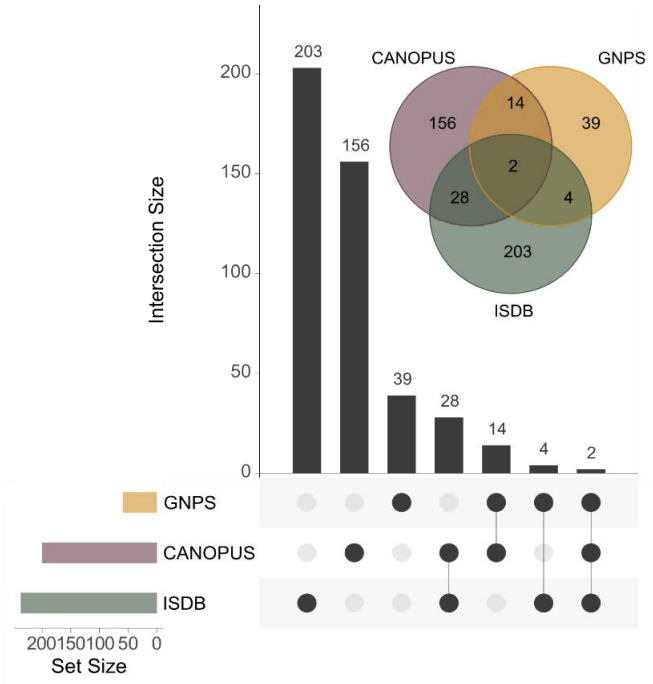

Figure 3.8. *Summary of annotated features using different MS/MS matching strategies.*

Increasing annotation power with Feature-Based Molecular Networking (FBMN)

To gain more information about the metabolites present in the samples, a tool from the GNPS environment, Feature-Based Molecular Networking (FBMN), was used to propagate the annotations described above. FBMN allows the alignment of experimental spectra based on the similarity of their fragments (MS/MS), as it is expected that metabolites with similar spectra will belong to the same chemical class (Nothias et al., 2020). Based on the MS/MS similarity, the features were clustered in "molecular families" or "networks", where features differ only in simple modifications. The resulted FBMN from wheat root exudates can be observed in Figure 3.9, where some clusters of spectral families can be observed as groups of nodes (points) which are connected to features of similar MS/MS. In the figure, each node indicates a feature, and the colouring represents the features that were annotated using any of the three strategies for chemical classification.

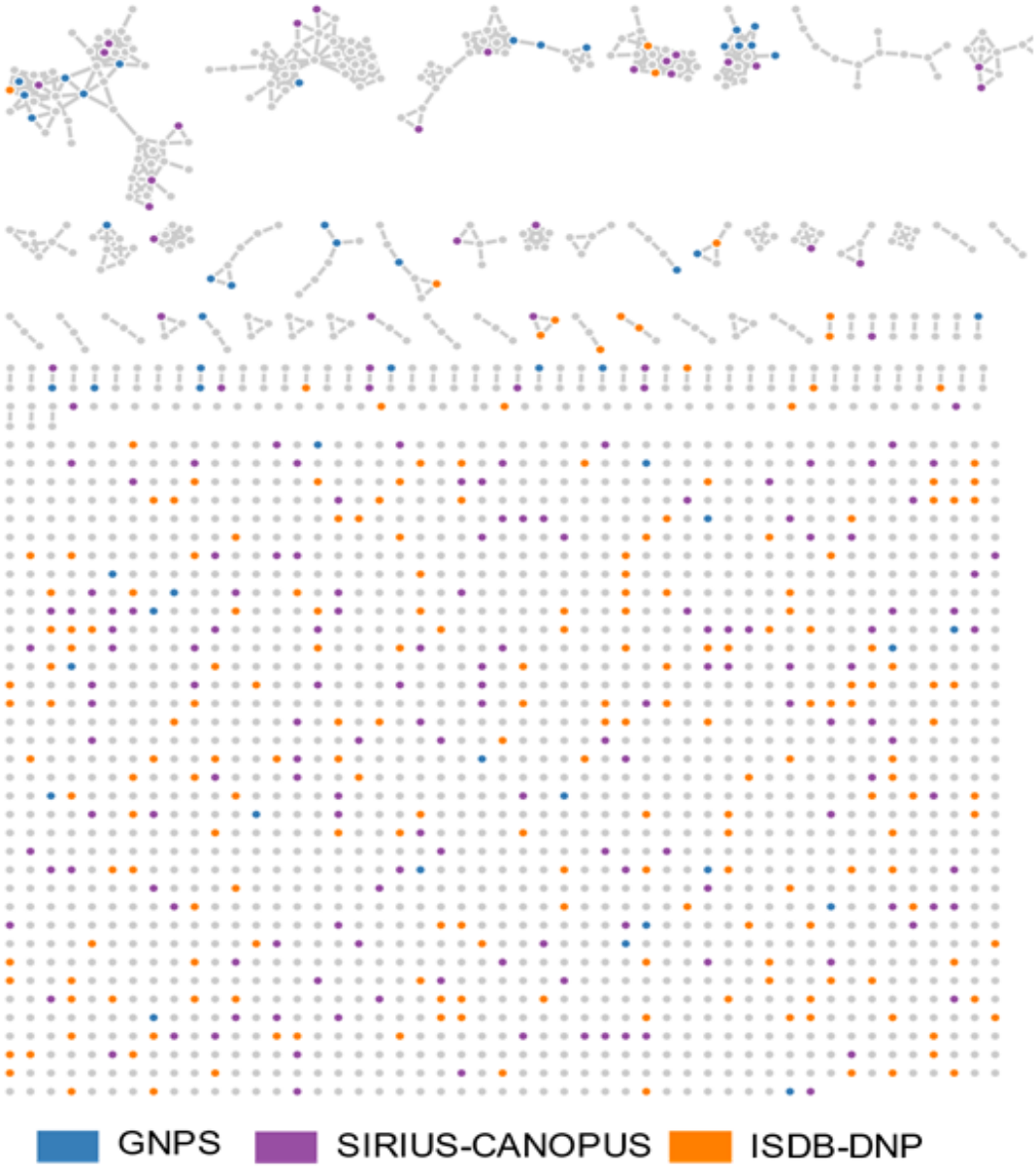

Figure 3.9. *Feature-Based Molecular network of metabolites found in the root exudates of wheat plants. Coloured nodes (points) indicate a chemical class was assigned based on an annotation tool: experimental library matching (GNPS: Blue), chemical classification using CANOPUS (Purple), library matching against in silico database (ISDB-DNP: Orange)*

To illustrate how Feature-Based Molecular Networking (FBMN) facilitates annotation propagation, Figure 3.10 presents three molecular networks integrating metabolite annotations from all three approaches used in this study. The arrows highlight features that were tentatively identified through spectral matching against experimental libraries. By incorporating the annotations to the networks, previously

unannotated features were grouped with annotated metabolites, suggesting they share a similar chemical structure or belong to the same molecular family. This enabled the putative classification of molecular families, including octadecanoids and flavones, within the root exudates, providing a more comprehensive view of the metabolite composition.

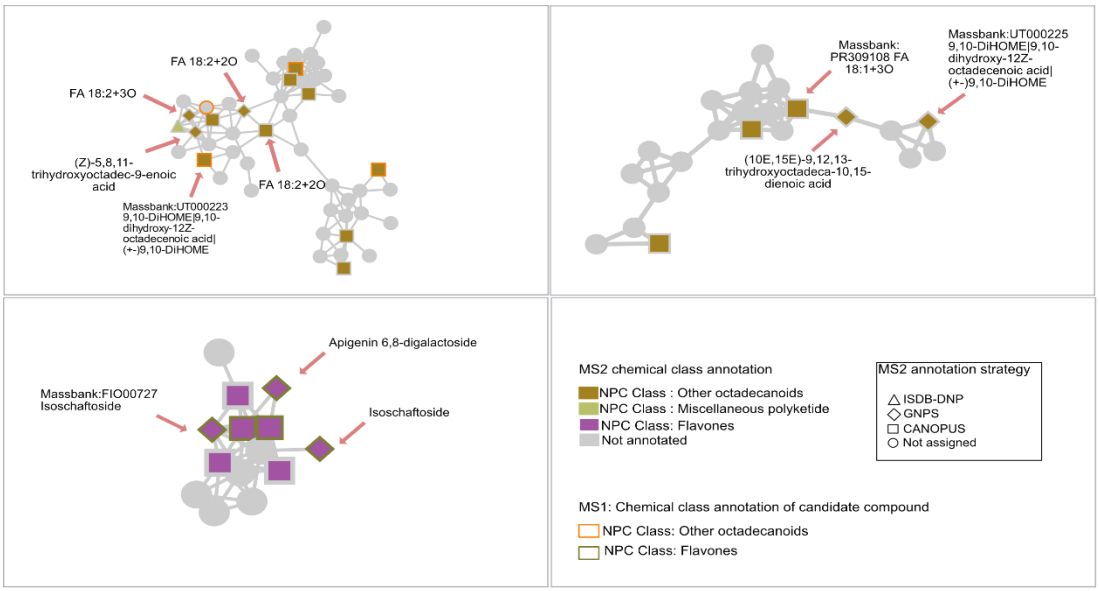

Figure 3.10. *Molecular families detected in plant root exudates. Each node represents a metabolite feature within the molecular network, with edges connecting structurally related features. Arrows indicate metabolites identified through spectral matching against experimental libraries in GNPS.*

A total of 41 molecular families were identified, defined as networks containing more than three connected nodes. Among these, six molecular families contained at least one feature that could be putatively annotated through spectral library matching against experimental databases (GNPS). Table 3.2 summarizes the number of features within each of these networks, where their association with putatively annotated compounds – and in some cases other annotation tools - enabled a tentative chemical classification. This approach facilitated the classification of an additional 91 features, expanding the proportion of chemically classified metabolites by 4.1%. Consequently, a total of 24.27% of the metabolites detected in plant root

exudates were assigned to a chemical class, enhancing the overall coverage of metabolite annotation.

Table 3. 2. *Molecular networks where an annotated compound was connected to unknown features*

Network	Reference annotation	Molecular family	Number of nodes
1	9,10-dihydroxy-12Z-octadecenoic acid	Other Octadecanoids	49
2	(10E,15E)-9,12,13-trihydroxyoctadeca-10,15-dienoic acid	Other Octadecanoids	22
3	Isoschaftoside	Flavones	14
4	3-Dehydroxyshikimate	Shikimic acids	7
5	Azelaic acid	Fatty Acids	6
6	Cryptotanshinone	Diterpenoids	4

3.3.2.2. Significant changes in the chemical profile of non-volatile root exudates from wheat plants occur under aphid herbivory

After metabolite annotation, statistical analyses were performed to assess whether aphid herbivory on aboveground plant tissues significantly influenced the chemical signals released into the soil via root exudates. To achieve this, the feature list obtained after peak alignment using *mzmine* v.4.0.3 was processed in the FBMNStats website, an extended tool for analysis of metabolomics data (Pakkir Shah et al., 2024). Features detected in blank samples were removed using an intensity cut-off of 0.30, retaining only those above this threshold as potentially biologically relevant, resulting in the removal of 105 features and the retention of 2,106 peaks. From this, most features were shared between treatments, with 54 features unique to the herbivory treatment and 20 unique to the control plants. After this, statistical analyses were performed in MetaboAnalyst v.6.0.0.

System suitability and potential instrumental drifts were assessed using pooled quality control (QC) samples. Principal component analysis (PCA) and chromatogram alignment (Figure 3.11) illustrate the performance of three QC samples, which were distributed across the analytical run—at the beginning, middle, and end. The chromatograms demonstrate consistency in peak detection across QC samples, enabling the identification of minor variations in retention time and peak intensity. Overall, the strong alignment of QC samples throughout the run indicates the robustness and reliability of the analytical workflow.

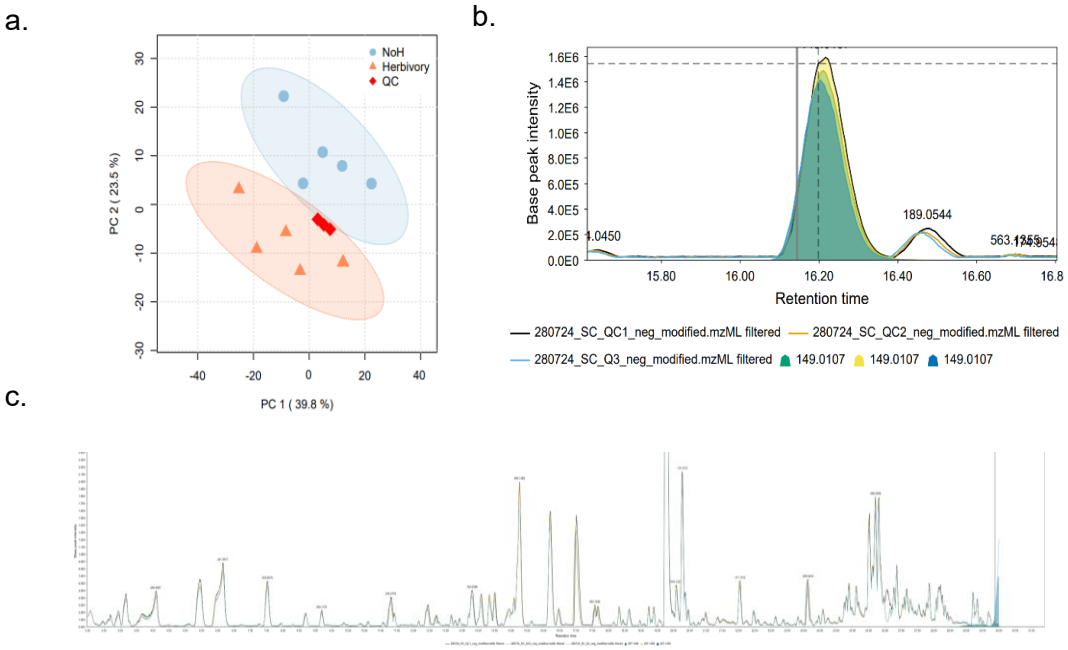

Figure 3.11. *Quality assurance of the instrument suitability (LCMS) using pooled samples of all biological replicates (n=10) as quality control (QC). A) PCA showing the clustering of the QC samples compared to the biological replicates from the experiment, b) Example of a randomly selected feature (m/z 149.0107) and the performance of the three QC technical replicates, c) Complete chromatogram with overlapping signals from the QC samples.*

To identify differences in root exudates between plants subjected to aphid herbivory and control plants (no herbivory), first, filtering was performed to remove features with high intravariance within the quality control (QC) samples, and those with near-constant values across experimental conditions using the interquantile range (IQR) filter (Pang et al., 2024). The intravariance and IQR filters removed 356 and 700

features, respectively, reducing noise and improving the robustness of downstream analyses. Following these preprocessing steps, a total of 1,050 features were retained for further statistical analysis. Data normalisation, as described in the methods Section 3.2.5, was applied to improve the distribution of the data before investigating features that were significantly altered in the non-volatile fraction of root exudates of plants under aphid herbivory.

The profile of metabolites found in the root exudates was significantly different when plants were experiencing stress under aphid herbivory, as shown in the PCA (Figure 3.12a) and the PERMANOVA results ($F= 5.46$, $p = 0.035$). A differential analysis, visualised using a volcano plot, showed a total of 75 features that were significantly different in wheat plants under herbivory ($p = 0.1$) (Figure 3.12b). Of these, 39 (52%) were increased under herbivory, while 36 (48%) were significantly decreased, suggesting both up and down-regulation of specific compounds in the root exudates of plants under herbivory. The list of metabolites that were significantly different in plants under aphid herbivory is shown in the Supplementary Table 3.4.

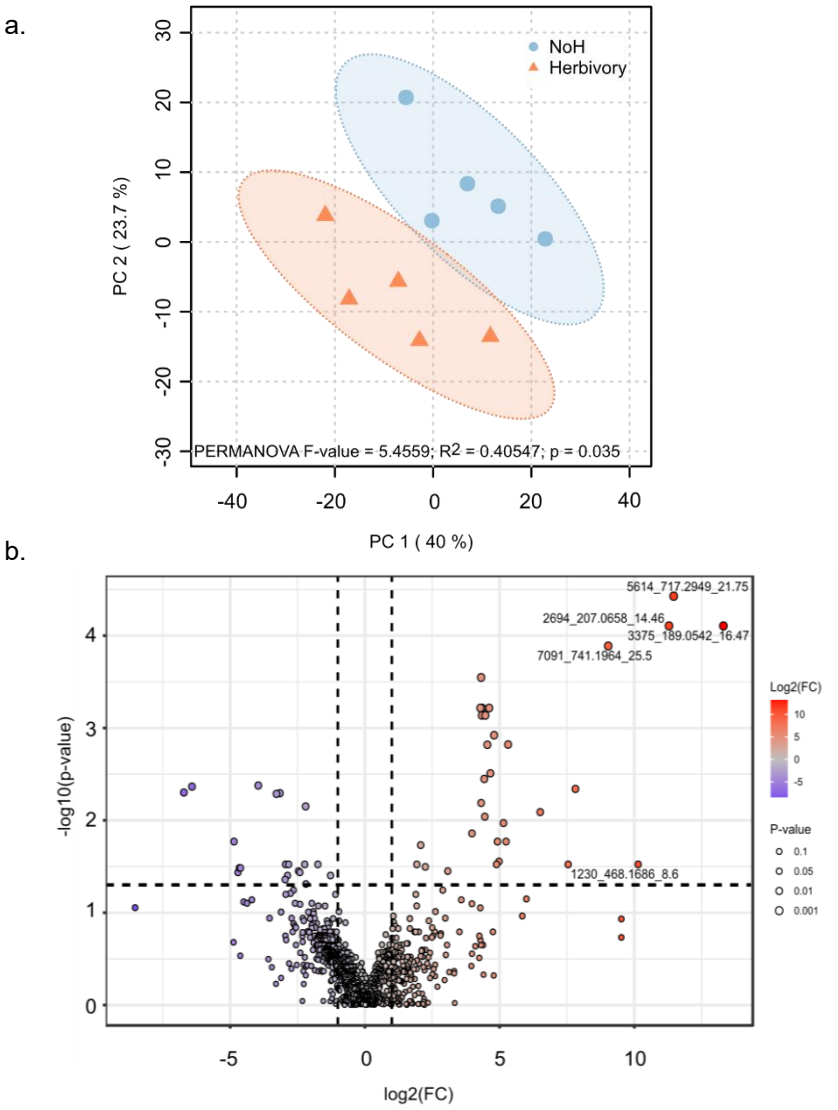

Figure 3.12. *Statistical analysis of the metabolic profile of root exudates of wheat plants under aphid herbivory. a) PCA showing the metabolic profile of the root exudates from plants under herbivory and healthy plants. Circles represent a confidence interval of 0.95 (n=5), b) Volcano plot showing the results of the differential abundance analysis after false discovery rate correction (FDR = 0.1). Colours represent log_2fold change, with red indicating features that increased in peak area under aphid herbivory, while blue features were decreased. The size of the circles increases according to the p value, as shown in the legend to the right.*

3.3.2.3. Integration of metabolite annotation and statistics

Integration of the statistical dataset with metabolite annotations (Section 3.3.2.1) revealed that of the 75 significant features identified in the differential analysis, three had compound matches when searched against experimental libraries in GNPS. Among these, the feature annotated as Massbank:PR309386 HMBOA + O-Hex,

increased under herbivory, while the other two, classified as octadecanoids, decreased.

Given the limited number of annotated metabolites, the search was expanded to include metabolites that, while not statistically significant, showed fold changes in the fold change analysis (Figure 3.12b). This approach aimed to capture potentially relevant metabolites that might have been overlooked due to limited statistical power from the small sample size. A total of 485 features displayed fold changes, with 202 increasing and 283 decreasing under herbivory. Among these, 54 metabolites were chemically classified (Figure 3.13) based on their MS/MS spectra. Notably, 53% (29 metabolites) of the classified compounds were downregulated by aphid herbivory, with 24 belonging to the fatty acid and amino acid pathways. In contrast, the upregulated metabolites exhibited greater chemical diversity, including terpenoids, shikimates and phenylpropanoids, amino acids, polyketides, and alkaloids. Of these, 36% were classified within the shikimate and phenylpropanoid pathways. Additionally, three metabolites, grouped as "other alkaloids" in Figure 3.13, belong to the benzoxazinoid class but were categorized as “alkaloid-like” due to the absence of a specific benzoxazinoid category in the Natural Product Classifier.

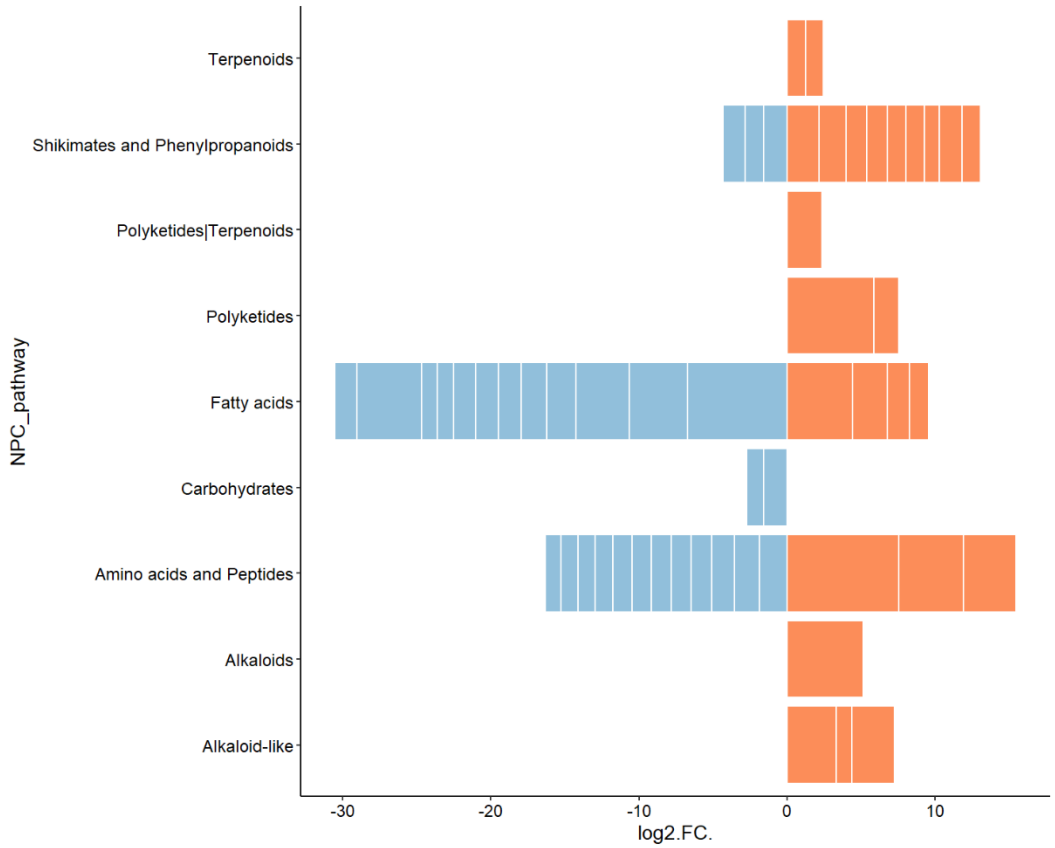

Figure 3.13. *Chemical classification of herbivory-regulated metabolites and their Log2FC based on MS/MS annotation tools (GNPS library matching, CANOPUS, and ISDB in TimaR).*

When analysing herbivory-regulated metabolites, fatty acids were the most downregulated group under herbivory, as indicated by fold-change analysis. Several of these metabolites clustered within the same molecular family (Table 3.2) and were putatively annotated under the "Other octadecanoids" superclass in the NPC classification. Feature-Based Molecular Networking (FBMN) analysis revealed a distinct cluster containing the majority of annotated octadecanoids (Figure 3.14). This network comprised five metabolites confidently identified using GNPS experimental data libraries, along with ten additional compounds classified as "Other octadecanoids" by CANOPUS or TimaR. Statistical analysis of this network confirmed a significant reduction in these metabolites under herbivory (Figure 3.14b), highlighting the robustness of these findings across multiple annotation platforms.

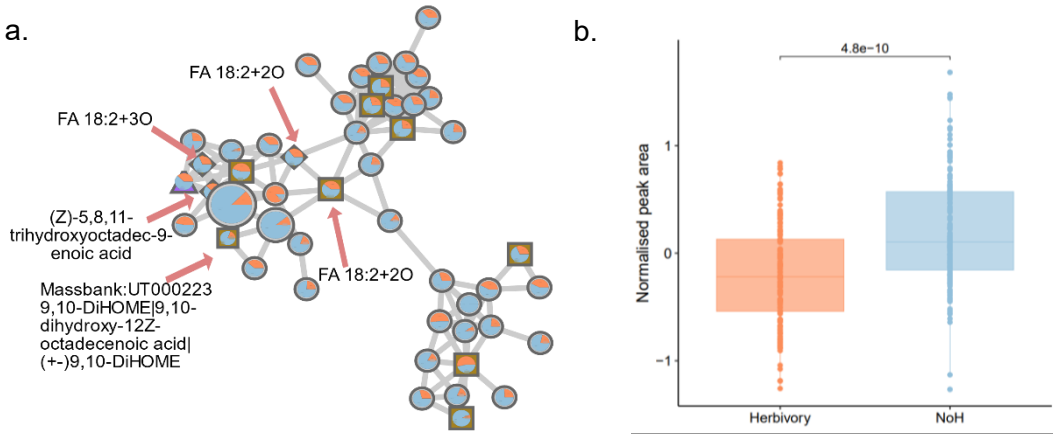

Figure 3.14. *Molecular network annotated as octadecanoids. a) Pie charts within the octadecanoid network represent the total sum of peak areas, with blue indicating samples from healthy plants and orange representing root exudates from plants under aphid herbivory. The statistical significance is represented by the size of the pies, with the bigger ones being statistically different. b) Mean comparison of normalised peak areas for features in the network, analysed using a t-test ($p < 0.05$).*

Another group of metabolites significantly regulated by aphid herbivory, for which all compounds were tentatively annotated, was the benzoxazinoids. Three benzoxazinoid features increased in the exudates of wheat plants under herbivory. Among them, HMBOA + O-Hex showed a statistically significant increase (FDR = 0.057), while the other two also exhibited notable log fold changes, with HMBOA increasing by 2.37 and DIBOA β-D-glucoside by 1.066. A comparison of mean values for these features is presented in Figure 3.15.

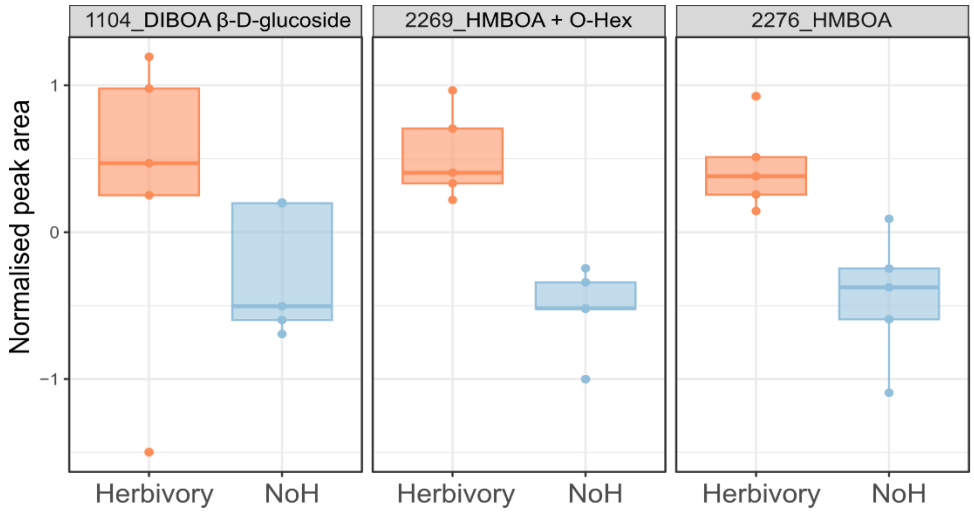

Figure 3.15. *Increase in peak area of features putatively annotated as benzoxazinoids based on their MS/MS spectra. Only feature 2269, HMBOA + O-Hex, was close to statistical significance after multiple comparison correction (FDR = 0.057).*

3.3.2.4. Confirmation of identity of herbivory-regulated metabolites

Among the 54 chemically classified features, five were selected for further identity confirmation against chemical standards, as it was possible to get compound annotations based on MS/MS spectral matches with experimental and *in silico* libraries (Table 3.3). As shown in Figures 3.16 and 3.17, these include one benzoxazinoid (HMBOA-O-Hex), which increased under herbivory, and four metabolites that decreased: 9,10-DiHOME, salicylic acid, azelaic acid, and p-coumaric acid. To validate their identities, chemical standards were analysed via LC-MS and compared to pooled QC samples (n=3) using the same pipeline described in the methods Sections 3.2.3.1 and 3.2.3.2. Four features had retention times matching the chemical standards (Figure 3.16), supporting confident annotation through retention time and MS/MS fragment alignment. However, 9,10-DiHOME (Figure 3.17) aligned with peaks in the QC samples but exhibited two distinct retention time peaks in the standard. This discrepancy may result from residual solvent traces following evaporation and resuspension of the standard in methanol, the solvent used for exudate samples.

Table 3. 3. *Metabolites selected for confirmation of identity based on their spectral match and fold change*

Feature_ID	Compound	MS/MS match	Fold_change
8,923	(+-)9,10-DiHOME	Experimental	-1.749
2,490	4-Hydroxycinnamic acid	*In silico*	-1.561
3,174	Salicylic acid	*In silico*	-1.204
4,630	Azelaic acid	Experimental	-0.880
2,269	HMBOA-O-Hex	Experimental	2.760

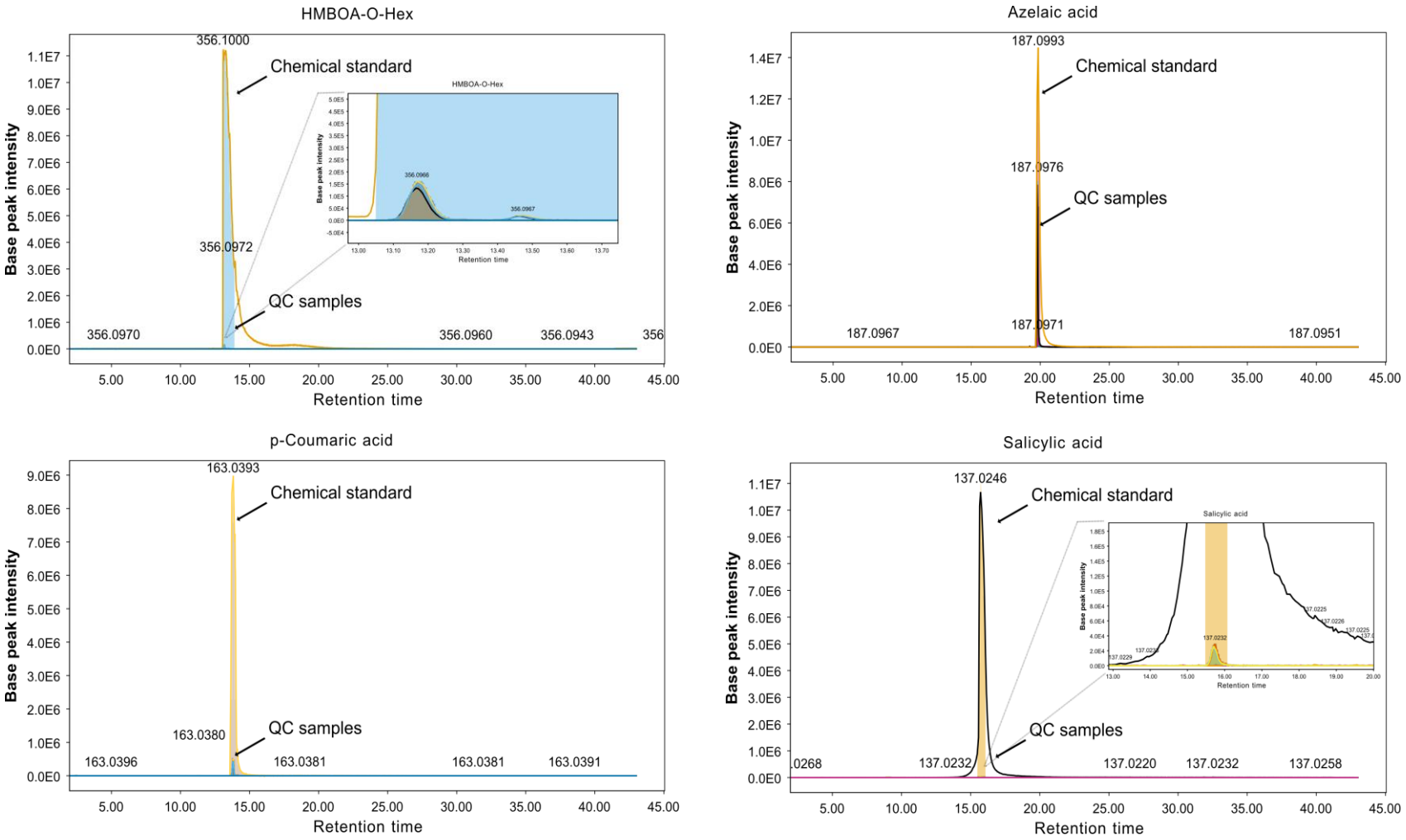

Figure 3.16. *Liquid Chromatography (LC) traces on a C18 column showing the peak for authentic chemical standards and their presence in root exudates, represented by the pooled quality control samples, QC (n=3). The samples and chemical standards were aligned on the software mzmine v.4.0.3. For the compounds HMBOA-O-Hex and salicylic acid, a zoom was applied as the presence of these compounds was several units lower than in the standards.*

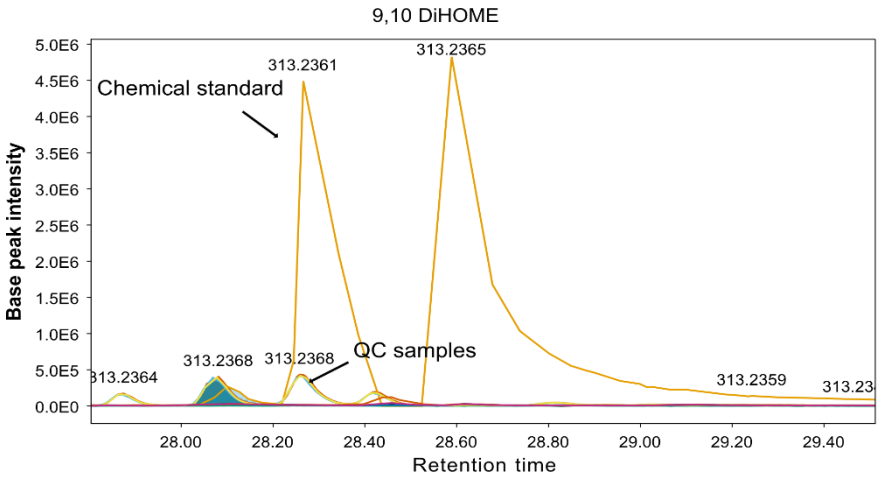

Figure 3.17. *Liquid Chromatography (LC) trace on a C18 column showing the peak for authentic chemical standards for 9,10 DiHOME, and its presence in root exudates, represented by the pooled quality control samples, QC (n=3). The samples and chemical standards were aligned on the software mzMine v.4.0. 3.*

3.3.3. Untargeted metabolomics of VOCs exudates from wheat plants

Volatile organic compounds (VOCs) from wheat roots were collected by placing a polydimethylsiloxane (PDMS) tube inside the flasks used for non-volatile exudate collection. GC-MS analysis identified 229 metabolic features across all samples. As described in Methods Section 3.2.4, a blank removal step was applied using an intensity cut-off of 0.30, reducing the dataset to 114 features for downstream analysis. To improve data distribution, the dataset was normalised by root dry weight, log-transformed, and Pareto-scaled, following the same pipeline used for non-volatile metabolites (Methods Section 3.2.5). PERMANOVA analysis did not reveal significant differences between conditions ($F = 0.99$, $R^2 = 0.125$, $p = 0.416$), consistent with the principal component analysis (PCA) results (Figure 3.18a).

While t-tests identified no statistically significant features after false discovery rate (FDR) correction (Figure 3.18b), one compound with the lowest uncorrected p-value ($p = 0.003$) was of particular interest. Annotation using the National Institute of

Standards and Technology (NIST) spectral library identified this feature as (E)-β-farnesene (Figure 3.19), an aphid alarm pheromone typically described in aboveground plant tissues. Manual inspection of all samples confirmed that this compound was exclusively detected in samples exposed to aphid herbivory, suggesting a potential root-derived response to aphid attack.

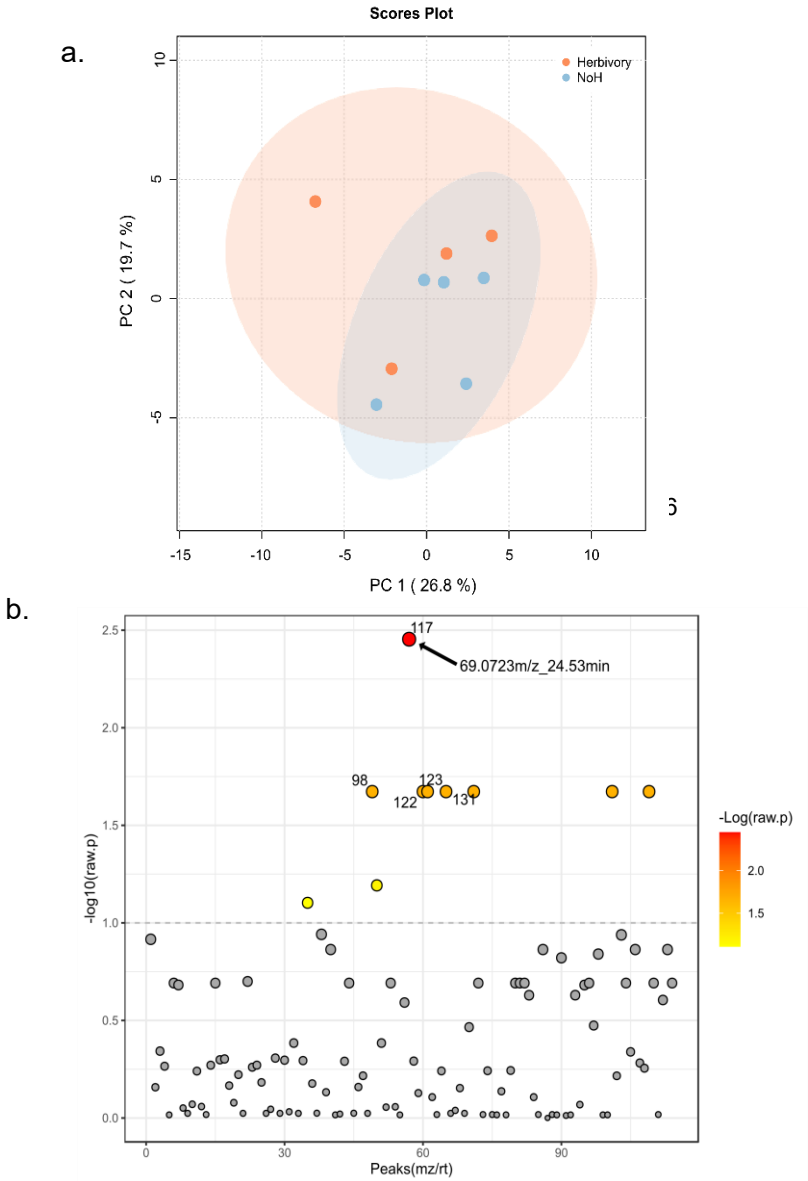

Figure 3.18. *Root VOC analysis under herbivory. a) PCA of root exudate metabolic profiles from herbivory-treated and healthy plants (NoH). Shaded circles indicate a 95% confidence interval (Herbivory: n = 4, NoH: n = 5). b) Key VOC features identified by t-test. Colours represent -log10 of the uncorrected p-value, with red highlighting feature 117 (p = 0.0033), annotated as E-β-farnesene based on NIST library matching.*

The analysis of MS spectra revealed a Cosine similarity score of 0.7359 (Figure 3.19), but further co-injection with chemical standards is needed for confirmation of identity of this compound.

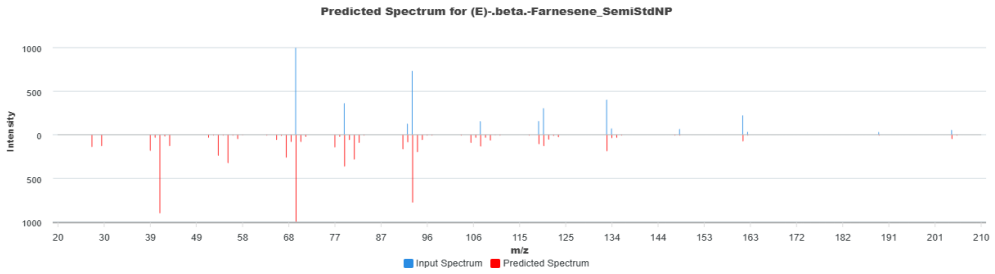

Figure 3.19. *Matching spectrum for feature 117 with the compound E-β-farnesene according to library matching against NIST library. Cosine score = 0.7359.*

3.4. Discussion

This study aimed to determine whether aphid herbivory on aboveground plant tissues alters belowground chemical signalling in ways that could influence microbial communities near the roots. Using untargeted metabolomics, it was possible to characterise shifts in the overall metabolic profile of non-volatile root exudates and identify potentially key metabolites affected by herbivory, increasing the knowledge on how aboveground stressors can shape belowground plant interactions. To our knowledge, this is the first study to integrate non-volatile metabolite profiling with VOCs analysis to investigate aphid-induced changes in root exudation. These findings reveal that aboveground aphid herbivory significantly alters the release of not only primary metabolites, but mostly all metabolic pathways for specialised metabolites, including oxidized fatty acids, phenylpropanoids, terpenoids, and benzoxazinoids in root exudates. These results highlight how plant responses to stress can reshape interactions within their environment, raising important questions about the role of these chemical signals in recruiting beneficial or pathogenic

microbes, particularly when plants prioritise aboveground defences at the potential expense of belowground susceptibility.

3.4.1. Improving our understanding of plant metabolism and the ecological role of metabolites through untargeted metabolomics

Studying root exudates presents various challenges at different stages, including the selection of plant growth conditions, sample collection and processing, and the choice of analytical tools (Oburger & Jones, 2018; van Dam & Bouwmeester, 2016; Vives-Peris et al., 2020). Even after collection and processing, one of the major obstacles remains the annotation of metabolites, particularly for non-volatile compounds analysed using LC-MS/MS. In our study, library matching in the GNPS platform allowed the annotation of 2.8% of the metabolites detected in the samples. While this percentage seems low, it is consistent with findings from other untargeted metabolomics studies, which report annotation coverage rates of 1.5% and 2-4% when using a C18 column for characterisation of specialised plant metabolites (Nothias et al., 2024; Quiros-Guerrero et al., 2024).

In this study, different annotation tools were explored to address the low availability of experimental data in public databases. These tools included library matching, *in silico annotation,* MS annotation based on taxonomy, and the use of Feature-Based Molecular Networks (FBMN) to cluster features based on their similarity. By integrating these approaches, it was possible to assign a chemical class to 24.27% of all the features found in the root exudates. This highlights how different strategies can complement each other to gain information about the systemic changes in plant metabolism. However, despite advances in annotation, a significant portion of

features that were significantly increased under herbivory could not be assigned to any chemical class using the described tools. Some of these metabolites might potentially represent unknown chemical signals emitted by plant roots in response to aphid herbivory. It will be interesting to explore their structure and function, as part of future work.

The annotation against public experimental databases remains the most reliable of the annotation tools when compared, for example, with *in silico* predictions of MS/MS fragments. In this study, most of the annotated compounds using experimental libraries belonged or corresponded to reported plant metabolites, but some of these features have not been previously reported or annotated as plant metabolites. An example is feature 8724, classified as a meroterpenoid —a class of metabolites characterized by a partial terpenoid structure (Fuloria et al., 2022). The closest library match, *Andrastin A*, corresponds to a metabolite reported in fungi from the genus *Penicillium*. A search for this metabolite in publicly available plant datasets (https://masst.gnps2.org/plantmasst/) did not show a match for this compound. Nevertheless, most compounds of this class have shown important biological activities like antimicrobial, cytotoxic, antioxidant, among others (Nazir et al., 2021), which could potentially have a role in the recruitment of microbial communities. This example highlights the complexity of the signals in root exudates and the challenge of determining the precise source of these metabolites, as plant-associated metabolites may not always align with known compounds in existing databases.

Study of plant root VOCs

Although the majority of the results in this study are derived from the non-volatile fraction of root exudates, the VOCs fraction revealed a potentially key metabolite, putatively identified as (E)-β-Farnesene. While the analysis of VOCs has been well-established, with widely available and expansive databases such as the National Institute of Standards and Technology (NIST) GC-MS library, the main challenge lies in the sample collection process as the concentration of VOCs in the soil is low, and these metabolites quickly interact with soil organic matter and other living organisms present in the soil (Eilers et al., 2015; Tholl et al., 2021). In this study, no significant metabolic profile differences were observed, and most VOC signals showed high variability, making them difficult to interpret. Furthermore, over 50% of the features identified were also present in the blank samples, suggesting that the concentration of plant root VOCs was low. This likely indicates that the two-hour collection period was insufficient for capturing detectable VOC levels for downstream analysis. However, in this effort to isolate plant root volatiles from other sources of VOCs in the soil, it was possible to identify a metabolite that increased in root VOCs under aphid herbivory, which validates the method, although the protocol needs further improvement to enhance VOCs signal capture. This will be critical for future studies as increasing attention is placed on the plant volatilome as a key factor in mediating plant-microbe communication (Bouwmeester et al., 2019; Honeker et al., 2021).

3.4.2. Belowground metabolic responses and phytohormone signalling

Aphids are well known for their ability to manipulate the immune response to increase the transport of plant resources to their feeding site, reducing the allocation of nutrients to other sink organs, including roots (Morkunas et al., 2011). While feeding, aphids release effectors —such as enzymes, proteins, and metabolites—that

modulate plant hormone signalling and stress response (Giordanengo et al., 2010; Goggin, 2007; Morkunas et al., 2011; Mou et al., 2023). In plants, recognition of cues from aphid herbivory is followed by changes in plant signalling pathways coordinated by plant growth hormones including jasmonic acid, salicylic acid, auxins, ethylene, and abscisic acid (Giordanengo et al., 2010; Jaouannet et al., 2014; Morkunas et al., 2011; Züst & Agrawal, 2016).

In this study, a metabolite annotated as salicylic acid in plant root exudates was shown to decrease under aphid herbivory. Moreover, although jasmonic acid was not directly observed in the reported metabolomics analysis, other metabolites belonging to the same class, oxylipins, were found to decrease in the exudates of plants under herbivory. These results point at a disruption of hormonal signalling in plant roots due to aphid herbivory, which could suggest that aphid effectors were successful at manipulating or supressing plant defence responses after two weeks. However, understanding the meaning of these changes is challenging as most studies measure plant hormone responses at earlier stages of aphid herbivory, and mostly in aboveground tissues. For instance, upregulation of indole acetic acid (auxin), salicylic acid and jasmonic acid was shown to occur after two hours of aphid herbivory and was maintained after 96 hours in leaves of maize plants (Tzin et al., 2015). In sorghum, the difference between resistant and susceptible genotypes was consistent with an increased level of salicylic acid and jasmonic acid in the leaves of the resistant sorghum genotype Tx2783, while the susceptible cultivar (BTx623) showed a higher concentration of jasmonic acid before infestation that was significantly lower during six days of aphid herbivory (Huang et al., 2022). The results for salicylic acid and oxylipins shown in this thesis chapter align with the susceptibility of the *Solstice* wheat cultivar used in this study. However, increases in specialised metabolites were

observed – like those belonging to the benzoxazinoids class - pointing at a plant defence response.

These results are part of only a few studies investigating the belowground effect of aboveground herbivory, and more studies measuring belowground responses are needed to elucidate the impact of aphid herbivory in plant belowground chemistry. For instance, one study showed that 72 hours of aboveground herbivory by the aphid *Brevicoryne brassicae* on cabbage plants did not affect jasmonic acid concentration on plant primary roots, nor had any impact in the performance of a root herbivore (Karssemeijer et al., 2020). Nevertheless, other types of oxylipins could have been impacted under aphid herbivory, as has been shown previously in maize leaves (Tzin et al., 2015) and is suggested by the results in this chapter.

Beyond plant hormones, a diverse set of specialised metabolites have been shown to impact plant responses to aphid herbivory. For instance, triterpenoids were observed to increase in leaves of resistant peach plants against the Green Peach Aphid, but not in susceptible plants (Pan et al., 2024). A blend of metabolites from the green leaf volatiles class –derived from the fatty acid pathway- and benzenoids were shown to negatively affect aphid preference to an aphid-resistant ancestral wheat line (Borg et al., 2024). Moreover, in cereals, one of the most reported metabolite classes shown to be regulated in plant leaves by aphid herbivory are benzoxazinoids (BXs) (Meihls et al., 2013; Shavit et al., 2018), although their concentration in plant leaves does not always correlate with resistance against herbivory (Zhang et al., 2021). In this results chapter, it was possible to determine that aphid herbivory impacted primary and specialised metabolites, pointing at the necessity of studying species-specific relationships between plants and aphids, and to investigate and try to capture

the diversity of specialised metabolites produced by plants, which will help uncover less-known metabolites that could play key roles in plant-aphid interactions.

The impact of aphid herbivory on belowground plant chemistry needs further investigation, as shifts in plant hormones, primary metabolites, and specialized metabolites can directly influence soil microbial communities. For example, salicylic acid plays a key role in plant defence by activating systemic acquired resistance (SAR), a mechanism that primes both local and distant tissues against microbial pathogens (Zeier, 2021). Beyond pathogen defence, salicylic acid levels have been shown to affect beneficial plant-microbe interactions; for instance, elevated salicylic acid reduces nodule formation by the nitrogen-fixing bacterium *Sinorhizobium meliloti*, and salicylic acid increases have been observed during the early stages of arbuscular mycorrhizal root colonisation (Benjamin et al., 2022). Understanding how aphid herbivory alters root exudate composition will provide critical insights into plant-microbe interactions and may reveal the role of microbial communities in mediating plant defence responses.

3.4.3. Oxylipins and benzoxazinoids in root exudates were significantly impacted under aphid herbivory

In this study, the untargeted metabolomic analysis showed great complexity of changes in the root exudates of plants under aphid herbivory. Compounds putatively annotated as unsaturated fatty acids, belonging to the oxylipin class, were significantly decreased under aphid herbivory, while compounds annotated as benzoxazinoids (HMBOA, HMBOA +O-Hex, DIBOA- β-d-glucoside) were shown to increase.

The oxylipins class has been identified as a key signalling molecules in inter-kingdom communication and plant defence (Mosblech et al., 2009). These metabolites, derived from the oxidation of unsaturated fatty acids such as oleic (18:1), linoleic (18:2), and linolenic (18:3) acid derivatives (He & Ding, 2020), are precursors of green leaf volatiles in plants, a group of VOCs that are rapidly synthesised and released in response to stresses, such as insect herbivory (Sugimoto et al., 2022; Hassan et al., 2015). Under herbivory, green leaf volatiles act as chemical signals that alert neighbouring plants and attract natural enemies of the pest (Matsui & Engelberth, 2022). In this study, a decrease in the detected oxylipins derived from linoleic acid (FA 18:2) in root exudates of plants under aphid herbivory poses great questions about the role of these fatty acid derivatives. These results could suggest that, as aphids take up nutrients from the phloem sap, the transport of plant resources to the aphid feeding site will increase, reducing the allocation of resources to the roots (Shih et al., 2022). Furthermore, plants will need to relocate resources to produce secondary metabolites to defend from aphid herbivory. In this context, our data could suggest that observed decreases in fatty acids may be due to their conversion into important signalling molecules such as methyl jasmonate or green leaf volatiles by the plant in response to biotic stress.

The role of these oxylipins should be further investigated as they can directly interact with microbial communities in both beneficial and pathogenic interactions. These metabolites have previously been shown to mediate plant-fungi communication through a mechanism that resembles bacterial quorum sensing (Affeldt et al., 2012; Pohl & Kock, 2014). Plant oxylipins can also exert direct antimicrobial activity, and it has been demonstrated that oxylipins like 9,10-dihydroxy-12z-octadecenoic acid –a metabolite observed to significantly decrease in the exudates of plants under

herbivory in this study- showed antimicrobial activity against the fungi *Alternaria brassicae* and *Sclerotinia sclerotiorum (Deboever et al., 2020; Granér et al., 2003).* This could suggest that in the rhizosphere of wheat plants under aphid herbivory, the decrease in these compounds could act as a modulator of the microbial community structure.

The second class of chemical compounds of interest in the root exudates analysis, were benzoxazinoids. These are a group of molecules released by gramineous plants, well-known by their toxicity and allelopathic properties (Hickman et al., 2021). These compounds are typically stored in plants as glycosylated conjugates to prevent autotoxicity and are released in response to biotic stresses, such as herbivory or pathogen attack (S. Zhou et al., 2018a). Genetic studies in maize have shown that benzoxazinoid levels peak within the first 2 weeks after germination and decline as plants age (Batyrshina et al., 2020; Neal et al., 2012; Zhou et al., 2018). Although benzoxazinoids have been primarily considered as plant defence compounds, some studies suggest they can also act as iron-chelating agents and even attract beneficial bacteria such as *Pseudomonas putida* (Batyrshina et al., 2020; Neal et al., 2012).

Regarding plant-microbe interactions mediated by benzoxazinoids, Neal et al. (2012) showed that the *Pseudomonas* strain can tolerate high concentrations of DIMBOA, a member of this class, and show the preference of bacteria to move towards the metabolite. Moreover, these compounds have also been shown to mediate the interaction of plants with root herbivores. Previous studies have shown that benzoxazinoids that form stable complexes with iron are preferred by the western corn rootworm, as these herbivores can use the iron from these complexes and the benzoxazinoid breakdown product for self-defence against entomopathogens (Hu et

al., 2018). The authors suggest that the response to different types of benzoxazinoids is species dependent. In this thesis chapter, it was observed that the plants increased the release of three classes of benzoxazinoids: HMBOA, HMBOA +O-Hex and DIBOA- β-d-glucoside. Two of these were found to be conjugated with glycosides in our dataset, which is the “inactive” form. Previous work has shown that microbes can convert these compounds to their active form by using different enzymes, like β-glucosidases, to release the glycoside, which can be a readily available carbon source, and the benzoxazinoid, which some microbes can metabolise to also use as carbon and energy sources (Neal et al., 2012).

Given that not all microbes can degrade these aromatic compounds, it is reasonable to suggest that when wheat plants are attacked by aboveground aphid herbivores, they may use benzoxazinoids as chemical cues to shape the microbial communities, as shown for other crops like maize (Cotton et al., 2019; Kudjordjie et al., 2019). Moreover, bacterial isolates from maize were observed to have different degrees of tolerance to these compounds, correlated with their abundance in benzoxazinoid-exuding roots (Thoenen et al., 2023). This finding aligns with the bacterial amplicon sequencing results from Chapter 2, which indicated that the structure of the bacterial communities in the rhizosphere from plants under two weeks of aphid herbivory was similar to that of younger plants. After four weeks, the impact of herbivory on the rhizosphere microbiome community was less pronounced, with the bacterial community structure more closely resembling that of healthy plants. This change could potentially be explained by the decline in plant production of benzoxazinoids during plant development, but further research is needed to test this hypothesis.

Overall, this chapter shows that untargeted metabolomics can be used to elucidate how aboveground aphid herbivory impacts plant belowground communication via root exudates. In the following chapter, the implication for root-associated microbial communities will be explored in detail.

3.5. Supplementary files

Supplementary Table 3.1. *Batch order for LCMS injections*

ID	*Sample*
1	Solvent Blank
2	Solvent Blank
3	Process blank
4	Standard
5	QC1
5	Sample 10 NoH
6	Sample 3 Herbivory
7	Sample 4 NoH
8	Sample 8 Herbivory
9	Sample 15 NoH
10	QC2
11	Sample 9 Herbivory
12	Sample 13 Herbivory
13	Sample 5 NoH
14	Sample 1 NoH
15	Sample 12 Herbivory
16	QC3
17	Solvent blank

Supplementary Table 3. 2. *Annotations of features based on library matching with public libraries available in the GNPS platform.*

Feature_ID	Library Name	Shared Peaks	Mass Difference	Spec m/z	Spec Charge	Compound Name	Adduct	Precursor m/z	Ion Mode
15	BERKELEY-LAB.mgf	4	0.0762024	405.025	-1	quinic acid CollisionEnergy:205060	2M-2H+Na	405.101	Negative
183	GNPS-LIBRARY.mgf	4	0.0016022	191.018	-1	Citric acid	M-H	191.02	Negative
570	MSNLIB-NEGATIVE.mgf	5	0.0011902	266.088	-1	312693-72-4	[M-H]-	266.089	Negative
573	MSNLIB-NEGATIVE.mgf	4	0.0501099	533.182	-1	BI-1935	[M+Cl]-	533.132	Negative
1042	BERKELEY-LAB.mgf	4	0.0036926	429.15	-1	tryptophan CollisionEnergy:102040	2M-2H+Na	429.154	Negative
2269	MASSBANK.mgf	4	0.0022888	356.096	-1	Massbank:PR309386 HMBOA + O-Hex	M-H	356.098	Negative
2465	MONA.mgf	7	0.0040283	593.147	-1	apigenin 6,8-digalactoside	[M-H]-	593.151	negative
2552	MONA.mgf	7	0.0050659	563.136	-1	5,7-dihydroxy-2-(4-hydroxyphenyl)-8-[3,4,5-trihydroxy-6-(hydroxymethyl)oxan-2-yl]-6-(3,4,5-trihydroxyoxan-2-yl)chromen-4-one	[M-H]-	563.141	negative
2555	LDB_NEGATIVE.mgf	5	0.0772705	725.241	-1	Leprapinic acid	[2M-2H+Na]	725.164	Negative
2640	MSNLIB-NEGATIVE.mgf	5	0.005188	563.136	-1	Isoschaftoside	[M-H]-	563.141	Negative
2759	SUMNER.mgf	5	0.0011597	593.148	-1	Saponarin - 50eV	M-H	593.149	Negative
2935	MASSBANK.mgf	11	0.0053101	563.136	-1	Massbank:PR307031 NP-000062(6)	M-H	563.141	Negative
3033	MASSBANK.mgf	12	0.0048828	563.136	-1	Massbank:FIO00727 Isoschaftoside	M-H	563.141	Negative
3433	MASSBANK.mgf	10	0.0056152	563.135	-1	Massbank:PR307037 NP-000062(6)	M-H	563.141	Negative
3544	MONA.mgf	5	0.0039063	577.152	-1	5,7-dihydroxy-2-(4-hydroxyphenyl)-6-[(2S,3R,4R,5S,6R)-3,4,5-trihydroxy-6-(hydroxymethyl)oxan-2-yl]-8-	[M-H]-	577.156	negative

						[(2S,3R,4R,5R,6S)-3,4,5-trihydroxy-6-methyloxan-2-yl]chromen-4-one			
3655	MSNLIB-NEGATIVE.mgf	15	0.0048218	533.125	-1	SCHEMBL12907661	[M-H]-	533.13	Negative
4508	MSNLIB-POSITIVE.mgf	4	0.0155945	317.159	-1	NCGC00380965-01	[M+H]+	317.175	Positive
4525	GNPS-NIH-NATURALPRODUCTSLIBRARY_ROUND2_POSITIVE.mgf	4	0.0613098	327.061	-1	NCGC00385045-01_C19H20O6_(3R,5S)-5-(3-Furyl)-8a'-hydroxy-7'-methyl-3',4,5,5',5a',7',8',8a'-octahydrospiro[furan-3,6'-naphtho[1,8-bc]furan]-2,2'(4'H)-dione	M-H2O+H	327.122	positive
4625	MONA.mgf	4	0.0713959	169.085	-1	Gallic acid	[M-H]-	169.014	negative
4630	MONA.mgf	7	0.0015106	187.096	-1	Azelaic acid	[M-H]-	187.098	negative
4794	MONA.mgf	4	0.001709	187.096	-1	Azelaic acid	[M-H]-	187.098	negative
4853	BMDMS-NP.mgf	4	0.0018921	255.067	-1	1,8-dihydroxy-3-methylanthra-9,10-quinone	[M+H]+	255.065	Positive
5301	LDB_POSITIVE.mgf	4	0.077301	459.125	-1	Cryptochlorophaeic acid	[M-H]	459.202	Negative
5684	GNPS-MSMLS.mgf	5	0.141602	365.191	-1	3-DEHYDROSHIKIMATE	2M-2H+Na	365.049	Negative
5830	NEO-MSMS.mgf	4	0.0035095	343.21	-1	ent-16(RS)-9-epi-ST-D14-10-PhytoF	M-H	343.213	Negative
6007	NEO-MSMS.mgf	4	0.0037231	343.209	-1	ent-16(RS)-13-epi-ST-D14-9-PhytoF	M-H	343.213	Negative
6328	GNPS-LIBRARY.mgf	4	0.0330963	239.033	-1	alizarin	M-H	239	Negative
6524	MONA.mgf	4	0.0020142	267.064	-1	FORMONONETIN	[M-H]-	267.066	negative
6599	GNPS-LIBRARY.mgf	4	0.0883179	625.338	-1	Rubranoside D	M-H	625.25	Negative
6924	MASSBANK.mgf	4	0.038208	313.2	-1	Massbank:UT000225 9,10-DiHOME|9,10-dihydroxy-12Z-octadecenoic acid|(+-)9,10-DiHOME	M-H	313.238	Negative
7013	GNPS-LIBRARY.mgf	9	0.0072022	677.418	-1	(10E,15E)-9,12,13-trihydroxyoctadeca-10,15-dienoic acid	2M-2H+Na	677.425	Negative

7232	GNPS-LIBRARY.mgf	9	0.0036926	327.214	-1	(10E,15E)-9,12,13-trihydroxyoctadeca-10,15-dienoic acid	M-H	327.218	Negative
7458	MASSBANK.mgf	9	0.000885	329.23	-1	Massbank:PR309108 FA 18:1+3O	M-H	329.231	Negative
7621	GNPS-NIH-NATURALPRODUCTSLIBRARY_ROUND2_POSITIVE.mgf	4	0.101013	635.406	-1	NCGC00170014-03!(E)-N-(4-acetamidobutyl)-3-(4-hydroxy-3-methoxyphenyl)prop-2-enamide [IIN-based on: CCMSLIB00000848670]	[2M+Na]+	635.305	Positive
7733	MONA.mgf	5	0.0578003	329.23	-1	(Z)-5,8,11-trihydroxyoctadec-9-enoic acid	M-H	329.288	negative
8051	MASSBANK.mgf	8	0.0023193	327.215	-1	Massbank:PR309101 FA 18:2+3O	M-H	327.217	Negative
8103	MASSBANK.mgf	8	0.0029907	311.22	-1	Massbank:PR309094 FA 18:2+2O	M-H	311.223	Negative
8169	MONA.mgf	4	0.0926971	239.128	-1	1,4-dihydroxyanthraquinone	[M-H]-	239.035	negative
8224	MONA.mgf	4	0.0170898	287.219	-1	Epitestosterone	[M-H]-	287.202	negative
8454	BERKELEY-LAB.mgf	4	0.0404968	353.228	-1	Rauwolscine CollisionEnergy:102040	M-H	353.187	Negative
8724	MONA.mgf	14	0.0039063	485.25	-1	andrastin A	[M-H]-	485.254	negative
8815	BMDMS-NP.mgf	4	0.170319	311.22	-1	(2S)-2-(3,4-dihydroxyphenyl)-5,7-dihydroxy-2,3-dihydro-4H-chromen-4-one	[M+Na]+	311.05	Positive
8923	MASSBANK.mgf	9	0.0025024	313.236	-1	Massbank:UT000223 9,10-DiHOME|9,10-dihydroxy-12Z-octadecenoic acid|(+-)9,10-DiHOME	M-H	313.238	Negative
9000	MASSBANK.mgf	10	0.002594	311.22	-1	Massbank:PR309094 FA 18:2+2O	M-H	311.223	Negative
9099	CMMC-REFRAME-NEGATIVE-LIBRARY.mgf	4	0.0032044	388.152	-1	DMP-695 free base	[M-H]-	388.155	Positive
9373	MONA.mgf	5	0.0707092	327.231	-1	(3E,12E)-3,12-dimethyl-8-methylidene-6,18-dioxatricyclo[14.2.1.0?,?]nonad	[M-H]-	327.16	negative

						eca-3,12,16(19)-triene-7,17-dione			
9386	MONA.mgf	5	0.127502	315.251	-1	Epiafzelechin Trimethyl Ether	[M-H]-	315.124	negative
9416	GNPS-NIST14-MATCHES.mgf	5	0.0997009	297.241	-1	Spectral Match to Decylbenzenesulfonic acid from NIST14	M-H	297.141	Negative
9424	MONA.mgf	6	0.14502	329.067	-1	Hydroxyprogesterone	[M-H]-	329.212	negative
9446	MONA.mgf	6	0.127899	311.22	-1	5,6,2'-Trimethoxyflavone	[M-H]-	311.092	negative
9487	MONA.mgf	5	0.0744019	311.166	-1	5,6,2'-Trimethoxyflavone	[M-H]-	311.092	negative
9492	MONA.mgf	6	0.0327148	287.235	-1	Epitestosterone	[M-H]-	287.202	negative
9540	MONA.mgf	5	0.142609	317.21	-1	(2R,3R)-2-(3,4-dihydroxyphenyl)-3,5-dihydroxy-7-methoxy-2,3-dihydrochromen-4-one	[M-H]-	317.067	negative
9554	GNPS-NIST14-MATCHES.mgf	6	0.0100098	297.151	-1	Spectral Match to Decylbenzenesulfonic acid from NIST14	M-H	297.141	Negative
9579	MONA.mgf	4	0.091095	327.251	-1	(3E,12E)-3,12-dimethyl-8-methylidene-6,18-dioxatricyclo[14.2.1.0?,?]nonadeca-3,12,16(19)-triene-7,17-dione	[M-H]-	327.16	negative
9660	MONA.mgf	7	0.0915833	295.226	-1	Cryptotanshinone	[M-H]-	295.134	negative
9667	MONA.mgf	4	0.084198	311.198	-1	1-[2-methyl-6-[(2S,3R,4S,5S,6R)-3,4,5-trihydroxy-6-(hydroxymethyl)oxan-2-yl]oxyphenyl]ethanone	[M-H]-	311.114	negative
9672	MONA.mgf	6	0.0387878	323.22	-1	(3S)-5-[(1R,2R,8aS)-2-hydroxy-2,5,5,8a-tetramethyl-3,4,4a,6,7,8-hexahydro-1H-naphthalen-1-yl]-3-methylpentanoic acid	[M-H]-	323.259	negative
9699	GNPS-NIST14-MATCHES.mgf	4	0.0898132	297.241	-1	Spectral Match to Decylbenzenesulfonic acid from NIST14	M-H	297.151	Negative

Supplementary Table 3.3. *Annotation of metabolites using the Taxonomically Informed Metabolite Annotation (TimaR) R platform. The platform performs library matching with freely available experimental spectra databases and an in-silico database developed using the MS1 information available in LOTUS (https://lotus.naturalproducts.net/). In the table, matches using only MS/MS (NPC_class) and taxonomy (Triticum aestivum L.) are used to produce a score that combines the biological and chemical matches.*

Feature_ID	Feature m/z	Feature RT	NPC_Class	Class score	Candidate Structure molecular formula	Candidate adduct	Candidate structure name	Score biological	Score chemical	Score final
19	191.0182907	2.09	Hydroxy fatty acids	0.540	C6H8O7	[M-H]-	2-(Carboxymethyl)-2-hydroxybutanedioate;hydron $ Hydron;2-hydroxypropane-1,2,3-tricarboxylate $ Citric Acid	0.9	1	0.616616617
46	115.002922	2.13	Dicarboxylic acids	0.540	C4H4O4	[M-H]-	2-Butenedioic acid	0.9	1	0.616616617
175	180.0653491	2.47	Aminoacids	0.540	C9H11NO3	[M-H]-	(2S)-2-ammonio-3-(4-hydroxyphenyl)propanoate $ Tyrosine	0.9	1	0.616616617
183	191.0183643	2.48	Hydroxy fatty acids	0.540	C6H8O7	[M-H]-	2-(Carboxymethyl)-2-hydroxybutanedioate;hydron $ Hydron;2-hydroxypropane-1,2,3-tricarboxylate $ Citric Acid	0.9	1	0.616616617
316	130.0861395	2.95	Aminoacids	0.540	C6H13NO2	[M-H]-	(2S,3S)-2-ammonio-3-methylpentanoate $ l-Isoleucine	0.9	1	0.616616617
316	130.0861395	2.95	Aminoacids	0.540	C6H13NO2	[M-H]-	(2S)-2-azaniumyl-4-methylpentanoate $ Leucine	0.9	1	0.616616617
396	130.0862397	3.17	Aminoacids	0.540	C6H13NO2	[M-H]-	(2S,3S)-2-ammonio-3-methylpentanoate $ l-Isoleucine	0.9	1	0.616616617
396	130.0862397	3.17	Aminoacids	0.540	C6H13NO2	[M-H]-	(2S)-2-azaniumyl-4-methylpentanoate $ Leucine	0.9	1	0.616616617
413	345.1321265	3.18	Gibberellins	0.540	C19H22O6	[M-H]-	Gibberellic acid	0.9	1	0.616616617
690	194.0447167	4.98	Aminoacids	0.240	C9H9NO4	[M-H]-	(2R)-7-Methoxy-2-hydroxy-2H-1,4-benzoxazine-3(4H)-one	0.9	1	0.616616617
768	164.0701965	5.45	Aminoacids	0.540	C9H11NO2	[M-H]-	(2S)-2-azaniumyl-3-phenylpropanoate $ Phenylalanine	0.9	1	0.616616617
1015	194.0447456	7.35	Aminoacids	0.240	C9H9NO4	[M-H]-	(2R)-7-Methoxy-2-hydroxy-2H-1,4-benzoxazine-3(4H)-one	0.9	1	0.616616617
1043	159.0914781	7.52	Aminoacids	0.540	C11H12N2O2	[M-CO2-H]-	2-azaniumyl-3-(1H-indol-3-yl)propanoate $ DL-Tryptophan	0.9	1	0.616616617
1046	203.0810415	7.52	Aminoacids	0.540	C11H12N2O2	[M-H]-	2-azaniumyl-3-(1H-indol-3-yl)propanoate $ DL-Tryptophan	0.9	1	0.616616617
1104	342.081063	7.86	dummy	0.540	C14H17NO9	[M-H]-	DIBOA beta-D-glucoside	0.9	1	0.616616617
1213	342.0840047	8.46	dummy	0.540	C14H17NO9	[M-H]-	DIBOA beta-D-glucoside	0.9	1	0.616616617
1271	137.0237783	8.82	Simple phenolic acids	0.540	C7H6O3	[M-H]-	4-Oxoniobenzoate $ 4-Hydroxybenzoic acid	0.9	1	0.616616617

1271	137.0237783	8.82	Simple phenolic acids	0.540	C7H6O3	[M-H]-	2-Carboxyphenolate;hydron $ Salicylic Acid	0.9	0.75	0.575075075
1278	197.0439711	8.77	Simple phenolic acids	0.540	C9H10O5	[M-H]-	Syringic acid	0.9	1	0.616616617
1319	137.0232922	8.96	Simple phenolic acids	0.540	C7H6O3	[M-H]-	4-Oxoniobenzoate $ 4-Hydroxybenzoic acid	0.9	1	0.616616617
1319	137.0232922	8.96	Simple phenolic acids	0.540	C7H6O3	[M-H]-	2-Carboxyphenolate;hydron $ Salicylic Acid	0.9	0.75	0.575075075
1701	121.0283471	11.07	Shikimic acids and derivatives $ Simple phenolic acids	0.540	C7H6O2	[M-H]-	4-Hydroxybenzaldehyde	0.9	0.5	0.533533534
1703	167.0341078	11.14	Cinnamic acids and derivatives $ Simple phenolic acids	0.540	C8H8O4	[M-H]-	Vanillic acid	0.9	0.25	0.491991992
1746	167.0336437	11.22	Cinnamic acids and derivatives $ Simple phenolic acids	0.540	C8H8O4	[M-H]-	Vanillic acid	0.9	0.25	0.491991992
1863	194.0440316	11.68	Aminoacids	0.240	C9H9NO4	[M-H]-	(2R)-7-Methoxy-2-hydroxy-2H-1,4-benzoxazine-3(4H)-one	0.9	1	0.616616617
1864	164.0344132	11.68	notClassified	0.540	C8H7NO3	[M-H]-	Coixol	0.9	1	0.616616617
1896	167.0338309	11.77	Cinnamic acids and derivatives $ Simple phenolic acids	0.270	C8H8O4	[M-H]-	Vanillic acid	0.9	0.5	0.533533534
2054	197.0439098	12.48	Simple phenolic acids	0.540	C9H10O5	[M-H]-	Syringic acid	0.9	1	0.616616617
2058	180.0652378	12.48	Aminoacids	0.540	C9H11NO3	[M-H]-	(2S)-2-ammonio-3-(4-hydroxyphenyl)propanoate $ Tyrosine	0.9	1	0.616616617
2083	197.0440579	12.53	dummy	0.000	C9H10O5	[M-H]-	Syringic acid	0.9	0	0.45045045
2139	197.0439439	12.67	dummy	0.000	C9H10O5	[M-H]-	Syringic acid	0.9	0	0.45045045
2145	153.0182498	12.75	dummy	0.000	C7H6O4	[M-H]-	2,5-Dihydroxybenzoic acid	0.9	0	0.45045045
2145	153.0182498	12.75	dummy	0.000	C7H6O4	[M-H]-	3,4-Dihydroxybenzoic acid	0.9	0	0.45045045
2158	197.0440056	12.84	dummy	0.000	C9H10O5	[M-H]-	Syringic acid	0.9	0	0.45045045
2212	151.0388772	13.00	dummy	0.000	C8H8O3	[M-H]-	4-Hydroxyphenylacetic acid	0.9	0	0.45045045
2212	151.0388772	13.00	dummy	0.000	C8H8O3	[M-H]-	Vanillin	0.9	0	0.45045045
2214	197.0440229	12.98	dummy	0.000	C8H8O3	[M+CH2O2-H]-	4-Hydroxyphenylacetic acid	0.9	0	0.45045045

2214	197.0440229	12.98	dummy	0.000	C8H8O3	[M+CH2O2-H]-	Vanillin	0.9	0	0.45045045
2214	197.0440229	12.98	dummy	0.000	C9H10O5	[M-H]-	Syringic acid	0.9	0	0.45045045
2246	193.0493533	13.17	dummy	0.000	C10H10O4	[M-H]-	Ferulic acid	0.9	0	0.45045045
2276	194.0445381	13.17	dummy	0.000	C9H9NO4	[M-H]-	(2R)-7-Methoxy-2-hydroxy-2H-1,4-benzoxazine-3(4H)-one	0.9	0	0.45045045
2322	166.0500013	13.29	Simple oxindole alkaloids	0.240	C9H9NO4	[M-CO-H]-	(2R)-7-Methoxy-2-hydroxy-2H-1,4-benzoxazine-3(4H)-one	0.9	1	0.616616617
2323	194.0445821	13.29	dummy	0.000	C9H9NO4	[M-H]-	(2R)-7-Methoxy-2-hydroxy-2H-1,4-benzoxazine-3(4H)-one	0.9	0	0.45045045
2408	193.0490648	13.52	dummy	0.000	C10H10O4	[M-H]-	Ferulic acid	0.9	0	0.45045045
2465	593.1469647	13.74	dummy	0.000	C27H30O15	[M-H]-	Vicenin-2	0.9	0	0.45045045
2465	593.1469647	13.74	dummy	0.000	C27H30O15	[M-H]-		0.9	0	0.45045045
2480	119.0488165	13.80	dummy	0.000	C9H8O3	[M-CO2-H]-	4-Hydroxycinnamic acid	0.9	0	0.45045045
2480	119.0488165	13.80	dummy	0.000	C9H8O3	[M-CO2-H]-	Coumarinic acid	0.9	0	0.45045045
2480	119.0488165	13.80	dummy	0.000	C8H8O	[M-H]-	4-Vinylphenol	0.9	0	0.45045045
2490	163.0389333	13.80	dummy	0.000	C9H8O3	[M-H]-	4-Hydroxycinnamic acid	0.9	0	0.45045045
2490	163.0389333	13.80	dummy	0.000	C9H8O3	[M-H]-	Coumarinic acid	0.9	0	0.45045045
2528	305.0682081	14.00	dummy	0.000	C15H14O7	[M-H]-	(+)-Gallocatechin	0.9	0	0.45045045
2552	563.1358853	14.06	dummy	0.000	C26H28O14	[M-H]-	Neoschaftoside	0.9	0	0.45045045
2552	563.1358853	14.06	dummy	0.000	C26H28O14	[M-H]-	5,7-dihydroxy-2-(4-hydroxyphenyl)-8-[(2S,3R,4R,5R,6S)-3,4,5-trihydroxy-6-(hydroxymethyl)oxan-2-yl]-6-[(2R,3R,4R,5S)-3,4,5-trihydroxyoxan-2-yl]chromen-4-one	0.9	0	0.45045045
2640	563.1358184	14.34	dummy	0.000	C26H28O14	[M-H]-	Neoschaftoside	0.9	0	0.45045045
2640	563.1358184	14.34	dummy	0.000	C26H28O14	[M-H]-	5,7-dihydroxy-2-(4-hydroxyphenyl)-8-[(2S,3R,4R,5R,6S)-3,4,5-trihydroxy-6-(hydroxymethyl)oxan-2-yl]-6-[(2R,3R,4R,5S)-3,4,5-trihydroxyoxan-2-yl]chromen-4-one	0.9	0	0.45045045
2695	165.0547381	14.46	dummy	0.000	C9H10O3	[M-H]-	Acetovanillone	0.9	0	0.45045045
2747	165.0547482	14.63	dummy	0.000	C9H10O3	[M-H]-	Acetovanillone	0.9	0	0.45045045
2759	593.1477584	14.65	dummy	0.000	C27H30O15	[M-H]-	Vicenin-2	0.9	0	0.45045045
2759	593.1477584	14.65	dummy	0.000	C27H30O15	[M-H]-		0.9	0	0.45045045
2798	210.040126	14.76	dummy	0.000	C9H9NO5	[M-H]-	(2s)-2,4-Dihydroxy-7-Methoxy-2h-1,4-Benzoxazin-3(4h)-One	0.9	0	0.45045045
2873	203.0812841	14.93	dummy	0.000	C11H12N2O2	[M-H]-	2-azaniumyl-3-(1H-indol-3-yl)propanoate $ DL-Tryptophan	0.9	0	0.45045045
2935	563.1357474	15.10	dummy	0.000	C26H28O14	[M-H]-	Neoschaftoside	0.9	0	0.45045045
2935	563.1357474	15.10	dummy	0.000	C26H28O14	[M-H]-	5,7-dihydroxy-2-(4-hydroxyphenyl)-8-[(2S,3R,4R,5R,6S)-3,4,5-trihydroxy-6-	0.9	0	0.45045045

							(hydroxymethyl)oxan-2-yl]-6-[(2R,3R,4R,5S)-3,4,5-trihydroxyoxan-2-yl]chromen-4-one			
3033	563.1361167	15.27	dummy	0.000	C26H28O14	[M-H]-	Neoschaftoside	0.9	0	0.45045045
3033	563.1361167	15.27	dummy	0.000	C26H28O14	[M-H]-	5,7-dihydroxy-2-(4-hydroxyphenyl)-8-[(2S,3R,4R,5R,6S)-3,4,5-trihydroxy-6-(hydroxymethyl)oxan-2-yl]-6-[(2R,3R,4R,5S)-3,4,5-trihydroxyoxan-2-yl]chromen-4-one	0.9	0	0.45045045
3063	121.0288962	15.38	dummy	0.000	C7H6O2	[M-H]-	4-Hydroxybenzaldehyde	0.9	0	0.45045045
3173	93.03391412	15.71	dummy	0.000	C7H6O3	[M-CO2-H]-	4-Oxoniobenzoate $ 4-Hydroxybenzoic acid	0.9	0	0.45045045
3173	93.03391412	15.71	dummy	0.000	C7H6O3	[M-CO2-H]-	2-Carboxyphenolate;hydron $ Salicylic Acid	0.9	0	0.45045045
3174	137.023113	15.71	dummy	0.000	C7H6O3	[M-H]-	4-Oxoniobenzoate $ 4-Hydroxybenzoic acid	0.9	0	0.45045045
3174	137.023113	15.71	dummy	0.000	C7H6O3	[M-H]-	2-Carboxyphenolate;hydron $ Salicylic Acid	0.9	0	0.45045045
3223	563.1359387	15.92	dummy	0.000	C26H28O14	[M-H]-	Neoschaftoside	0.9	0	0.45045045
3223	563.1359387	15.92	dummy	0.000	C26H28O14	[M-H]-	5,7-dihydroxy-2-(4-hydroxyphenyl)-8-[(2S,3R,4R,5R,6S)-3,4,5-trihydroxy-6-(hydroxymethyl)oxan-2-yl]-6-[(2R,3R,4R,5S)-3,4,5-trihydroxyoxan-2-yl]chromen-4-one	0.9	0	0.45045045
3287	593.1472687	16.16	dummy	0.000	C27H30O15	[M-H]-	Vicenin-2	0.9	0	0.45045045
3287	593.1472687	16.16	dummy	0.000	C27H30O15	[M-H]-		0.9	0	0.45045045
3295	164.0340766	16.21	dummy	0.000	C8H7NO3	[M-H]-	Coixol	0.9	0	0.45045045
3342	563.1361569	16.40	dummy	0.000	C26H28O14	[M-H]-	Neoschaftoside	0.9	0	0.45045045
3342	563.1361569	16.40	dummy	0.000	C26H28O14	[M-H]-	5,7-dihydroxy-2-(4-hydroxyphenyl)-8-[(2S,3R,4R,5R,6S)-3,4,5-trihydroxy-6-(hydroxymethyl)oxan-2-yl]-6-[(2R,3R,4R,5S)-3,4,5-trihydroxyoxan-2-yl]chromen-4-one	0.9	0	0.45045045
3426	179.033884	16.68	dummy	0.000	C9H8O4	[M-H]-	Caffeic Acid	0.9	0	0.45045045
3433	563.1353941	16.69	dummy	0.000	C26H28O14	[M-H]-	Neoschaftoside	0.9	0	0.45045045
3433	563.1353941	16.69	dummy	0.000	C26H28O14	[M-H]-	5,7-dihydroxy-2-(4-hydroxyphenyl)-8-[(2S,3R,4R,5R,6S)-3,4,5-trihydroxy-6-(hydroxymethyl)oxan-2-yl]-6-[(2R,3R,4R,5S)-3,4,5-trihydroxyoxan-2-yl]chromen-4-one	0.9	0	0.45045045
3636	151.0389911	17.63	dummy	0.000	C8H8O3	[M-H]-	4-Hydroxyphenylacetic acid	0.9	0	0.45045045
3636	151.0389911	17.63	dummy	0.000	C8H8O3	[M-H]-	Vanillin	0.9	0	0.45045045
3809	194.0443029	18.16	dummy	0.000	C9H9NO4	[M-H]-	(2R)-7-Methoxy-2-hydroxy-2H-1,4-benzoxazine-3(4H)-one	0.9	0	0.45045045
3841	607.16145	18.23	dummy	0.000	C28H32O15	[M-H]-	4'-O-Glucosylisoswertisin	0.9	0	0.45045045
3872	341.1109343	18.33	dummy	0.000	C12H22O11	[M-H]-	Î±,Î±-trehalose $ alpha-D-Glucopyranoside, alpha-D-glucopyranosyl	0.9	0	0.45045045
3872	341.1109343	18.33	dummy	0.000	C12H22O11	[M-H]-		0.9	0	0.45045045
3884	193.0496073	18.34	dummy	0.000	C10H10O4	[M-H]-	Ferulic acid	0.9	0	0.45045045

3993	187.0965708	18.62	dummy	0.000	C9H16O4	[M-H]-	Hydron;nonanedioate $ Azelaic acid	0.9	0	0.45045045
4337	187.0963796	19.24	dummy	0.000	C9H16O4	[M-H]-	Hydron;nonanedioate $ Azelaic acid	0.9	0	0.45045045
4514	187.0970778	19.63	dummy	0.000	C9H16O4	[M-H]-	Hydron;nonanedioate $ Azelaic acid	0.9	0	0.45045045
4618	143.1066371	19.79	dummy	0.000	C9H16O4	[M-CO2-H]-	Hydron;nonanedioate $ Azelaic acid	0.9	0	0.45045045
4630	187.0965089	19.79	dummy	0.000	C9H16O4	[M-H]-	Hydron;nonanedioate $ Azelaic acid	0.9	0	0.45045045
4790	171.1011341	20.00	dummy	0.000	C9H16O4	[M-O-H]-	Hydron;nonanedioate $ Azelaic acid	0.9	0	0.45045045
4794	187.0962688	19.99	dummy	0.000	C9H16O4	[M-H]-	Hydron;nonanedioate $ Azelaic acid	0.9	0	0.45045045
4843	181.1221409	20.08	Norlabdane diterpenoids	0.270	C11H18O2	[M-H]-	2(3H)-Benzofuranone, hexahydro-4,4,7a-trimethyl-	0.9	1	0.616616617
4845	199.1320386	20.09	dummy	0.000	C11H18O2	[M+H2O-H]-	2(3H)-Benzofuranone, hexahydro-4,4,7a-trimethyl-	0.9	0	0.45045045
5400	136.0760046	21.14	dummy	0.000	C9H11NO3	[M-CO2-H]-	(2S)-2-ammonio-3-(4-hydroxyphenyl)propanoate $ Tyrosine	0.9	0	0.45045045
5404	180.0658179	21.15	dummy	0.000	C9H11NO3	[M-H]-	(2S)-2-ammonio-3-(4-hydroxyphenyl)propanoate $ Tyrosine	0.9	0	0.45045045
5953	289.0699117	22.97	dummy	0.000	C15H14O6	[M-H]-	Cianidanol	0.9	0	0.45045045
6079	577.1304523	23.35	dummy	0.000	C30H26O12	[M-H]-	Proanthocyanidin B2	0.9	0	0.45045045
6079	577.1304523	23.35	dummy	0.000	C30H26O12	[M-H]-	(4R)-2beta,2'beta-Bis(3,4-dihydroxyphenyl)-3,3',4,4'-tetrahydro-4,6'-bi[2H-1-benzopyran]-3beta,3'beta,5,5',7,7'-hexol	0.9	0	0.45045045
6092	181.1220176	23.38	dummy	0.000	C11H18O2	[M-H]-	2(3H)-Benzofuranone, hexahydro-4,4,7a-trimethyl-	0.9	0	0.45045045
6332	179.033569	24.11	dummy	0.000	C9H8O4	[M-H]-	Caffeic Acid	0.9	0	0.45045045
6443	289.0691358	24.38	dummy	0.000	C15H14O6	[M-H]-	Cianidanol	0.9	0	0.45045045
6490	141.1276441	24.46	dummy	0.000	C9H18O	[M-H]-	Nonanal	0.9	0	0.45045045
6491	187.132457	24.46	dummy	0.000	C9H18O	[M+CH2O2-H]-	Nonanal	0.9	0	0.45045045
6567	179.1063886	24.62	notClassified	0.360	C11H16O2	[M-H]-	Actinidiolide, dihydro-	0.9	0.75	0.575075075
6569	197.1168202	24.62	notClassified	0.360	C11H16O2	[M+H2O-H]-	Actinidiolide, dihydro-	0.9	0.75	0.575075075
6828	319.1160726	25.10	dummy	0.000	C12H20N2O8	[M-H]-	Mugineic acid	0.9	0	0.45045045
7826	359.2413242	26.48	dummy	0.000	C18H34O4	[M+CH2O2-H]-	8-[(2S,3S)-3-(8-Hydroxyoctyl)oxirane-2-yl]octanoic acid	0.9	0	0.45045045
7839	367.2251709	26.48	dummy	0.000	C18H34O4	[M+H2O+Cl]-	8-[(2S,3S)-3-(8-Hydroxyoctyl)oxirane-2-yl]octanoic acid	0.9	0	0.45045045
7864	331.2447888	26.51	dummy	0.000	C18H36O5	[M-H]-	Isophloionolic acid	0.9	0	0.45045045
7963	315.1562054	26.66	Gibberellins	0.540	C19H24O4	[M-H]-	Gibberellin A9	0.9	1	0.616616617
7964	333.167235	26.65	dummy	0.000	C19H24O4	[M+H2O-H]-	Gibberellin A9	0.9	0	0.45045045
8596	313.2350241	27.53	dummy	0.000	C18H34O4	[M-H]-	8-[(2S,3S)-3-(8-Hydroxyoctyl)oxirane-2-yl]octanoic acid	0.9	0	0.45045045
8923	313.2354508	28.08	dummy	0.000	C18H34O4	[M-H]-	8-[(2S,3S)-3-(8-Hydroxyoctyl)oxirane-2-yl]octanoic acid	0.9	0	0.45045045
8964	279.2296992	28.13	dummy	0.000	C18H32O2	[M-H]-	Linoleic Acid	0.9	0	0.45045045

9052	313.2360101	28.26	dummy	0.000	C18H34O4	[M-H]-	8-[(2S,3S)-3-(8-Hydroxyoctyl)oxirane-2-yl]octanoic acid	0.9	0	0.45045045
9212	313.2356708	28.64	dummy	0.000	C18H34O4	[M-H]-	8-[(2S,3S)-3-(8-Hydroxyoctyl)oxirane-2-yl]octanoic acid	0.9	0	0.45045045
9286	313.2355578	28.81	dummy	0.000	C18H34O4	[M-H]-	8-[(2S,3S)-3-(8-Hydroxyoctyl)oxirane-2-yl]octanoic acid	0.9	0	0.45045045
9382	313.2358774	29.01	dummy	0.000	C18H34O4	[M-H]-	8-[(2S,3S)-3-(8-Hydroxyoctyl)oxirane-2-yl]octanoic acid	0.9	0	0.45045045
9522	295.2251067	29.32	dummy	0.000	C18H32O3	[M-H]-	Avenoleic acid	0.9	0	0.45045045
9660	295.2255501	29.73	dummy	0.240	C18H32O3	[M-H]-	Avenoleic acid	0.9	0.25	0.491991992
9706	295.2255349	29.86	dummy	0.000	C18H32O3	[M-H]-	Avenoleic acid	0.9	0	0.45045045

Supplementary Table 3.4. *Features statistically significant according to the differential abundance analysis of peak areas. These peaks were shown in the volcano plot in figure 3.7. When present, annotation for the pathway was included and the tool used for the annotation.*

Feature_ID	m/z	RT	FC	log2(FC)	p.ajusted	Annotation tool	NPC Pathway
5614	717.2949	21.75	2818.6	11.461	3.74E-05		
3375	189.0542	16.47	10136	13.307	7.85E-05		
2694	207.0658	14.46	2499.5	11.287	7.85E-05		
7091	741.1964	25.5	522.89	9.0304	0.000129		
1579	369.1165	10.51	19.882	4.3134	0.000284	TimaR_MS2	Shikimates and Phenylpropanoids
6236	555.2437	23.88	24.455	4.6121	0.000608		
8439	703.3152	27.3	20.408	4.3511	0.000608		
7845	725.2025	26.49	19.523	4.2871	0.000608		
5738	719.31	22.14	22.182	4.4713	0.00073		
1743	189.0544	11.22	20.277	4.3417	0.00073		
9485	541.2636	29.26	27.774	4.7957	0.001197		
2695	165.0547	14.46	39.79	5.3143	0.001511	MS1	Shikimates and Phenylpropanoids
5785	245.0437	22.32	23.365	4.5463	0.00152		
4217	403.0638	19.02	25.25	4.6582	0.003096		
7890	344.206	26.55	21.567	4.4308	0.003565	CANOPUS_SIRIUS	Fatty acids
5818	369.222	22.46	0.064398	-3.9568	0.004196	CANOPUS_SIRIUS	Fatty acids
5832	405.2209	22.48	0.011695	-6.418	0.004313		
6286	557.2565	24.02	224.94	7.8134	0.004569		
7547	652.4343	26.13	0.009489	-6.7196	0.004994	CANOPUS_SIRIUS	Fatty acids
4970	565.3288	20.27	0.11227	-3.155	0.00508	FBMN	Shikimates and Phenylpropanoids,
4959	559.3101	20.26	0.10293	-3.2802	0.005167	FBMN	Shikimates and Phenylpropanoids
7004	509.273	25.38	19.911	4.3155	0.006487		
4966	369.2219	20.27	0.2177	-2.1996	0.007064	FBMN	Shikimates and phenylpropanoids
101	249.0604	2.26	91.022	6.5081	0.008139		
6774	391.1735	25.03	21.868	4.4508	0.009126		
9654	399.2501	29.7	35.36	5.144	0.010702	CANOPUS_SIRIUS	Alkaloids
2440	337.1474	13.65	15.717	3.9742	0.013843		
8492	315.1251	27.4	37.75	5.2384	0.016967		
4591	189.0538	19.72	30.244	4.9186	0.016967		
179	333.0917	2.47	0.034489	-4.8577	0.016967		
7175	393.1866	25.62	4.2007	2.0706	0.018537		
1634	351.1173	10.73	31.539	4.9791	0.02787		
1230	468.1686	8.6	1130.6	10.143	0.029987	TimaR_MS2	Polyketides
5188	230.1395	20.7	186.65	7.5442	0.029987	CANOPUS_SIRIUS	Amino acids
7926	395.0411	26.6	29.555	4.8854	0.029987		

8870	315.2506	27.96	0.12971	-2.9467	0.029987		
7537	322.1997	26.12	0.14048	-2.8315	0.029987	FBMN	Fatty acids
5820	173.1166	22.46	0.21257	-2.234	0.029987	TimaR_MS2	Fatty acids
5290	283.0477	20.91	3.8059	1.9282	0.029987		
7466	609.3914	26.04	0.29835	-1.7449	0.029987	FBMN	Fatty acids
7627	215.164	26.24	4.7328	2.2427	0.031907		
6297	459.2667	24.04	0.039601	-4.6583	0.032735		
7496	473.2812	26.15	0.040722	-4.6181	0.032838		
2267	424.0817	13.17	8.4394	3.0771	0.03544		
7861	332.2495	26.52	0.18108	-2.4653	0.03544	FBMN	Fatty acids
5974	197.1166	23.03	0.038187	-4.7108	0.036599		
7448	681.4489	26.01	0.18792	-2.4118	0.036599	FBMN	Fatty acids
7621	635.406	26.21	0.13668	-2.8711	0.039557	GNPS	Polyamines
5815	241.1037	22.46	0.41335	-1.2746	0.039557		
7591	659.4653	26.2	0.12856	-2.9595	0.043753	FBMN	Fatty acids
7589	682.4528	26.2	0.21928	-2.1891	0.048885	FBMN	Fatty acids
2269	356.0957	13.17	7.4143	2.8903	0.057023	GNPS	
8943	316.2547	28.09	0.1592	-2.6511	0.057023	FBMN	Fatty acids
3589	169.0857	17.51	0.1474	-2.7622	0.061837		
7450	659.4678	26.01	0.13056	-2.9372	0.063401		
5293	221.0774	20.91	3.7061	1.8899	0.063401		
8922	381.2216	28.08	0.46978	-1.0899	0.063401		
6830	341.0997	25.09	63.799	5.9955	0.071008		
8023	473.2813	26.74	0.054598	-4.195	0.072563		
7380	259.1889	25.9	11.951	3.579	0.072563		
7533	650.4217	26.12	0.044279	-4.4972	0.07646		
7013	677.4178	25.39	0.04815	-4.3763	0.079046	GNPS	Fatty acids
997	267.0946	7.14	0.16596	-2.5911	0.079046		
3588	237.072	17.51	0.2553	-1.9697	0.079046		
1620	230.0109	10.69	15.703	3.9729	0.080022		
7017	328.2183	25.39	0.18857	-2.4068	0.081027		
7953	379.2063	26.64	3.7909	1.9225	0.084452		
8924	201.1114	28.08	0.3021	-1.7269	0.084452		
8923	313.2355	28.08	0.35872	-1.4791	0.084671	TimaR_MS1 and CANOPUS_SIRIUS	Fatty acids
8484	265.2151	27.38	0.002708	-8.5285	0.088222	TimaR_MS2	Fatty acids
7865	357.2582	26.51	19.462	4.2826	0.088569		
5681	559.2816	22.04	0.26556	-1.9129	0.096842		
1512	265.9964	10.21	6.1484	2.6202	0.097175		
8973	508.2629	28.14	0.11576	-3.1108	0.098393		
7623	283.1891	26.22	0.23379	-2.0967	0.098393		

Chapter 4: Response of bacterial communities at the plant-soil interface in wheat plants under aphid herbivory

Soil microbial communities respond to changes in the chemical signals emitted by plants via root exudates. This chapter addresses the ***third and fourth aims*** *of this project:* ***To investigate the structure and composition of bacterial communities at the root-soil interface in wheat plants under aphid feeding*** *and* ***to investigate changes in culturable bacterial communities exposed to identified key metabolites in root exudates of plants under aphid feeding****. Through a combination of amplicon sequencing and in vitro experiments, this chapter demonstrates that changes in root exudates correlate with those in bacterial communities, with an increase of the* ***Actinobacteria*** *class in plant roots. Furthermore, in vitro assays with herbivory-regulated metabolites (identified in Chapter 3) demonstrate a stress response in Actinobacteria, highlighting the potential of these compounds to influence bacterial metabolism. These findings provide new insights into plant-microbe interactions and the biochemical dialogue shaping root-associated microbiomes in plants under aphid herbivory.*

4.1. Introduction

In Chapter 2, an initial experiment demonstrated that aphid herbivory impacted the bacterial communities in the rhizosphere of wheat plants. *Solstice* is a well-known susceptible cultivar frequently used as a control in studies of aphid resistance in wheat (Borg et al., 2024). The results from this initial experiment revealed that the rhizosphere bacterial communities of aphid-infested plants were less diverse but showed significant changes in the abundance of specific bacterial taxa compared to the rhizobacterial communities from healthy plants. Additionally, microbial

communities from the rhizosphere of plants under herbivory showed faster consumption of carbon sources, including amino acids, carbohydrates, and carboxylic acids, indicating enhanced metabolic activity. Among the differentially abundant taxa, members of the Actinobacteria class were significantly increased in the rhizosphere of plants under herbivory. These findings suggested that plants could be recruiting bacteria from this class as a potential benefit linked to herbivory and raises the question “how wheat plants under herbivory use root exudates to attract bacterial communities".

The Actinobacteriota phylum is known for its remarkable capacity to produce a broad spectrum of bioactive enzymes and metabolites, accounting for over half of the known bioactive compounds derived from microbes (Quiza et al., 2023; Singh & Dubey, 2018). Among the phylum, the genus *Streptomyces,* from the Actinobacteria class, is known as the “supreme antibiotic producers”, with more than 7,600 active compounds currently used in the pharmaceutical industry (Rai & Baiieditors, 2022). These bioactive capabilities give bacteria from this phylum a competitive edge in the rhizosphere, enabling them to modulate surrounding microbial communities and colonise plant roots effectively.

Actinobacteria have been shown to induce plant resistance against various pests and pathogens, including *Fusarium oxysporum*, *Rhizoctonia solani*, and *Ralstonia solanacearum* (Abbasi et al., 2019; Saikia & Bora, 2021; Singh et al., 2017). However, the specific interactions between aphids, plants, and Actinobacteria remain largely unexplored. It is unclear whether Actinobacteria in this context benefit the plant or the herbivore. Given these knowledge gaps, this chapter aims to investigate changes in

bacterial communities, with a particular focus on Actinobacteria, during aphid herbivory.

Building on the initial experiment, which focused solely on the rhizosphere, this study extends the analysis to bacterial communities in plant roots to examine the progression of microbial shifts across compartments. By evaluating the continuum from bulk soil (uninfluenced by plant roots) to the rhizosphere and root-associated microbiomes, this study seeks to determine whether the changes observed in the rhizosphere are mirrored in root-associated bacterial communities.

As introduced in Chapter 3, this chapter presents the microbiome analysis from the experiment described in Section 3.2 (Methods). It is structured around three main objectives:

- Analysis of bacterial communities in the rhizosphere and inside the plant roots.
- Correlation analysis between bacterial taxa and metabolites identified in root exudates of herbivory-treated plants to explore potential plant-microbe interactions.
- *In vitro* testing of isolates belonging to Actinobacteria to assess their ability to utilize herbivory-regulated metabolites as carbon sources.

By addressing these objectives, this chapter aims to deepen our understanding of how bacterial communities, particularly Actinobacteria, respond to aphid herbivory and their potential functional roles in plant-microbe interactions.

4.2. Methods

These materials and methods come from the experimental setup described in Chapter 3, Section 3.2, and in this chapter only details belonging to the microbiome analysis are shown (Figure 4.1).

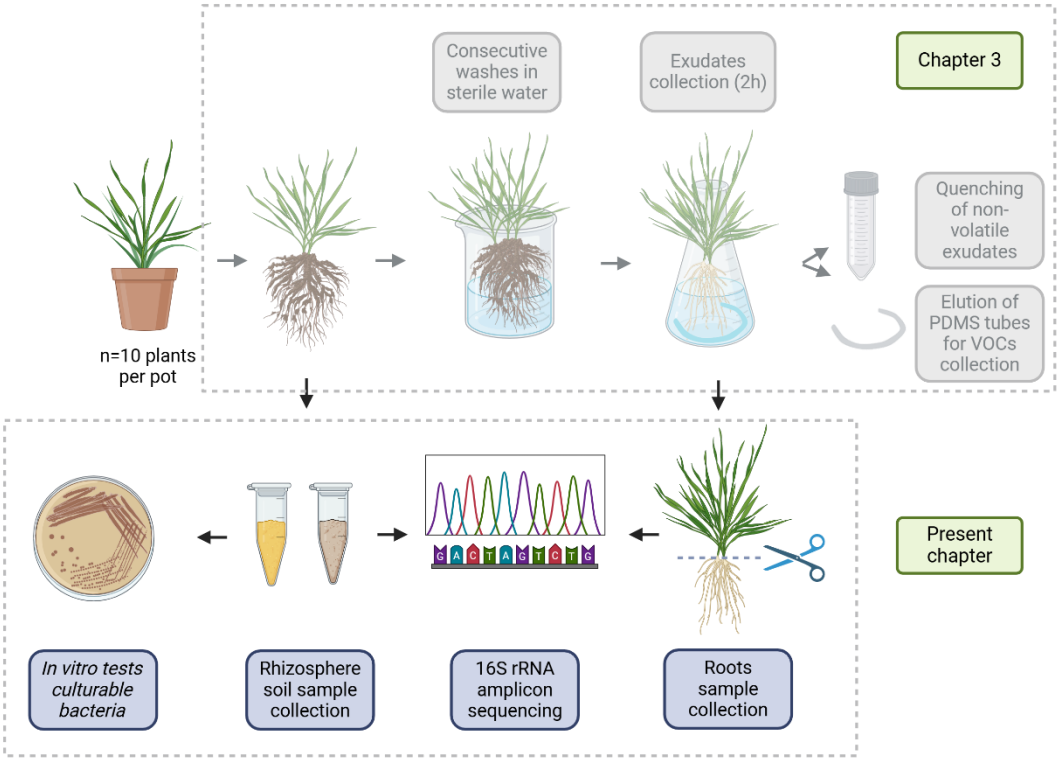

Figure 4.1. *Representation of the sample collection and analysis presented in the previous (Chapter 3) and present chapter. Samples from plant roots and rhizosphere soil samples were collected for amplicon sequencing of the 16S rRNA gene. Glycerol stocks were used for isolation of bacterial strains that were further used for in vitro tests.*

4.2.1. Analysis of bacterial communities

Rhizosphere soil collections were made after carefully removing the wheat plants from the pots, following the protocol described in Chapter 2, Section 2.2.2. After this, root exudates were collected (Chapter 3, Section 3.2.1) and later, the roots from

seven plants per biological replicate were snap frozen in liquid nitrogen for DNA extractions and further ground in liquid nitrogen using sterile mortars. Bulk soil (n=5) samples were collected from pots without plants.

4.2.1.1. DNA extractions and amplicon sequencing

DNA extractions and amplicon sequencing for bulk soil, rhizosphere, and roots was performed as described in Chapter 2, Section 2.2.6. The sequencing depth for soil samples was set to 30k, a standard depth used in the Molecular Microbial Ecology Group (MMEG) to ensure adequate coverage. The sequencing depth for the root samples was increased to 100k to enhance the coverage of bacterial communities, given the likelihood that plant mitochondrial and chloroplast DNA would dominate the sequencing output. This adjustment was made to improve the probability of capturing the microbial communities within the rhizosphere and still be able to compare the results with the soil sequencing data by using the same primer for amplification and sequencing of the 16S rRNA gene.

4.2.1.2. Bioinformatics and statistical analysis

Bioinformatics analyses were performed using the same steps described in Chapter 2, Section 2.2.7.4 (*Bacterial community analysis pipeline*). After processing the amplicon sequencing data in QIIME2 the phylogenetic tree, taxonomic table and ASVs abundance files were imported into RStudio v.4.4.0 (RStudio Team, 2020) where sequence filtering, statistical analyses for alpha and beta diversity, and differential abundance analyses were performed using the same pipeline described in Chapter 2, Section 2.2.7.4. However, as root samples were collected only in the present experiment, adjustments were made for the beta diversity analysis, which

creates a coordinates analysis based on the dissimilarity of the samples. Specifically, a partial dbRDA (constrained analysis) was performed to investigate the impact of aphid herbivory in the composition of the microbial communities using the sample origin (roots, rhizosphere and bulk soil) as a covariate. The model used was the following:

$$\text{Partial\_dbRDA} = \text{assay} \sim \text{Insect} + \text{Condition}(\text{SampleOrigin})$$

The differential abundance analysis of rhizosphere and root bacterial communities was conducted as described in Chapter 2, Section 2.2.7, using the Analysis of Compositions of Microbiomes with Bias Correction (ANCOM-BC) method through the *ANCOM-BC* package v.2.6.0 (Lin & Peddada, 2020). ASVs were not agglomerated for this analysis. Prevalence and library size cutoffs set at 0.10 and 1000, respectively, while the Holm method was used for p-value adjustment (padj < 0.10). This alpha value was used to increase the probability of finding significant differences accounting for the small sample size. Structural zeros—ASVs detected exclusively in either the aphid herbivory or control condition—were not considered in the analysis, as their presence could be due to low read counts rather than true absence. Visualization was performed with *ggplot2* v.3.4.2.

4.2.2. Cross association analysis of herbivory-regulated metabolites and bacterial communities

A cross-association analysis was conducted to evaluate the correlation of bacterial taxa with the metabolites (e.g., features) found to be regulated by aphid herbivory in Chapter 3. To achieve this, the file containing the metabolites dataset was first converted to a *TreeSummarizedExperiment* (TSE) object in the *mia* package v.

1.13.46. The TSE format, commonly used in microbiome and RNA-seq analyses, ensured compatibility between the metabolomics and amplicon sequencing datasets. For ease of interpretation and visualization, microbiome data was agglomerated at the Class level. Both microbiome and metabolomics datasets were log10-transformed prior to analysis. Spearman correlation analysis was performed between metabolite abundances and bacterial taxa, first considering all samples together (root and rhizosphere) and then analysing rhizosphere and root samples separately. Results were visualised using a heatmap generated with the *ComplexHeatmap* package v2.20.0.

4.2.3. Interaction between rhizosphere bacteria and herbivory-regulated metabolites

This section presents the methods used to test the effect of herbivory-regulated metabolites that were previously identified in Chapter 3 on bacterial strains isolated from the rhizosphere of healthy plants and those under aphid herbivory (Figure 4.2).

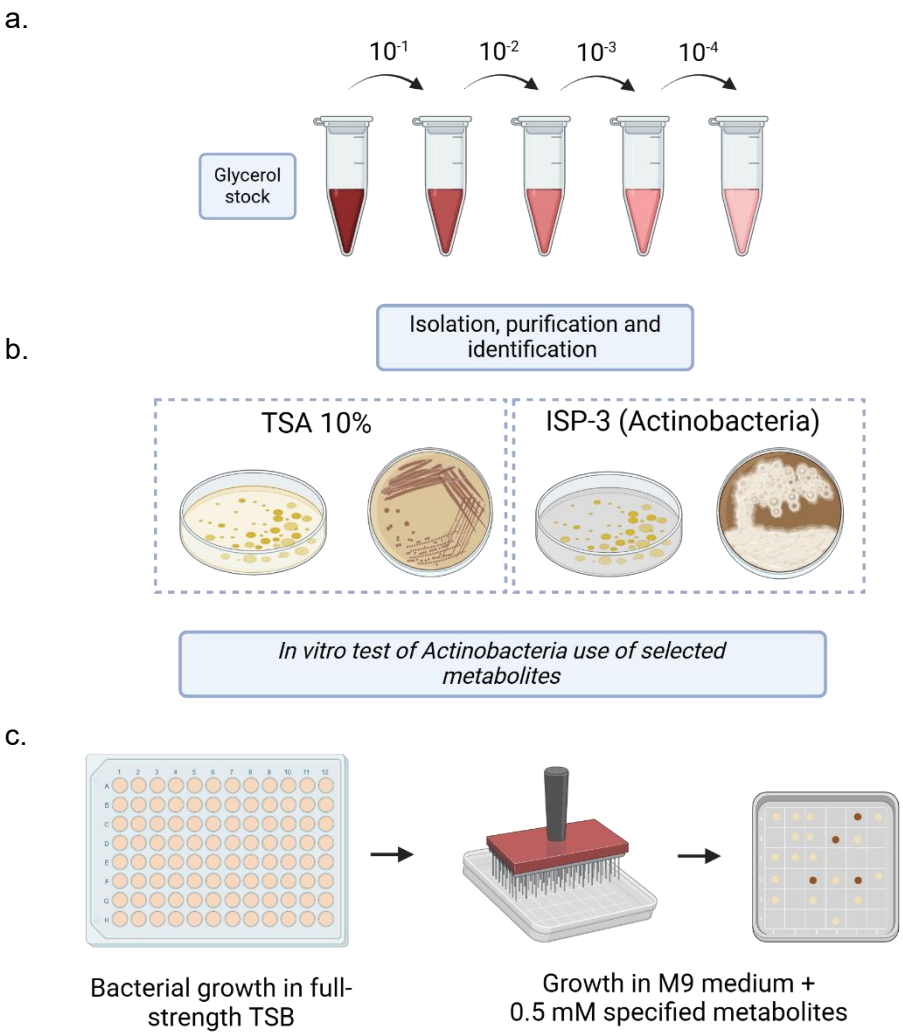

***Figure 4.2**. Diagram of work with culturable bacteria. a) Serial dilutions were made from a 1 mL glycerol stock from rhizosphere soil in 9 mL of NaCl (8.5% w/v), b) Serial dilutions were inoculated in TSA 10% and ISP-3 medium for bacterial isolation, with further purification by picking individual colonies. c) In vitro test with bacteria isolated from ISP-3 medium (Actinobacteria) in media supplemented with salicylic acid, azelaic acid, p-Coumarid acid, and HMBOA-O-Hex at 0.5 mM. Growth presence or absence for each colony was used for further analysis.*

4.2.3.1. Isolation of bacteria from rhizosphere soils

Rhizosphere soil previously preserved in 50% glycerol was used for the isolation of bacteria from both healthy plants and plants under aphid herbivory (Figure 4.2). First, one millilitre of rhizosphere glycerol stock from each sample was suspended in 9 mL

of saline solution (NaCl 0.85% w/v). The solution was incubated in a shaker at room temperature for one hour. After this, dilutions were made from 10^{-1} to 10^{-4} by adding 100 µL in 900 µL of saline solution. Following this, 100 µL of each dilution were plated in TSA 10%, non-specific agar medium, and ISP-3 medium, specific for Actinomyces (per litre: 20 g white oats, 18 g agar, 1 mL trace salts solution: 0.1 g $FeSO_4$ x $7H_2O$, 0.1 g $MnCl_2$ $4H_2O$, 0.1 g $ZnSO_4$ $7H_2O$ in 100 mL dH_2O). The ISP-3 medium was supplemented with nystatin (50 µg/mL) and nalidixic acid (10 µg/mL) according to Zhu et al. (2014) to prevent fungal and non-actinobacterial growth. The TSA plates were left incubating for 72 h at 25°C, while the ISP-3 plates were incubated for 7 days at the same temperature. A purification step was carried out until obtaining 96 bacterial strains per treatment in the TSA 10% agar, and as many isolates in the specialised media for the isolation of Actinobacteria. After purification, glycerol stocks of bacteria were prepared and frozen at -80°C for further use.

4.2.3.2. Identification of bacterial isolates

- *16S rRNA sequencing of bacterial isolates from the rhizosphere*

Colony PCR was used to amplify the 16S rRNA gene to identify bacterial isolates. Isolates from both TSA and ISP-3 agar were first grown on full-strength TSA for 48 hours (TSA isolates) or 72–96 hours (ISP-3 isolates). After incubation, single colonies were picked using sterile tips and transferred into individual wells of a 96-well plate containing 40 µL of sterile lysis buffer (Tris-EDTA, 0.1% Triton X-100). For isolates from ISP-3 agar, a filter-sterilized 50% DMSO solution was used as the lysis buffer to aid in cell wall disruption and to reduce secondary structure formation in the high-GC DNA of Actinobacteria (https://actinobase.org/). Colonies were resuspended by gently mixing with the sterile tips.

The lysis step was performed by heating the plates at 100°C for 5 min (TSA isolates) or 65°C for 20 min (ISP-3 isolates). The lower lysis temperature for ISP-3 isolates was used as DMSO weakens bacterial cell walls, reducing the need for extreme heat. Following lysis, 10 µL of lysate was added to each well of a 96-well PCR plate containing 12.5 µL DreamTaq Green PCR Master Mix (Thermo Fisher Scientific), 0.25 µL each of forward (FD1: 5'-AGAGTTTGATCCTGGCTCAG-3') and reverse (RP2: 5'-ACGGCTACCTTGTTACGACTT-3') primers, and 9.5 µL of nuclease-free water, for a final reaction volume of 22.5 µL. PCR amplification was performed under the following conditions: Initial denaturation: 95°C for 5 min; 35 cycles of: denaturation: 95°C for 30 s, annealing: 56°C for 30 s, extension: 72°C for 1 min; and a final extension: 72°C for 5 min.

PCR products (5 µL) were loaded onto a 2% agarose gel and gel electrophoresis was performed at 100 V for 45 min. The gel was then stained with RedGel for 30 min, de-stained in 1× TAE buffer for 15 min, and visualized under UV light. Finally, PCR products were sent to Eurofins Genomics for purification and Sanger sequencing.

- *Bioinformatics analysis*

The sequencing reads were obtained from Eurofins Genomics and quality was assessed by reviewing the Eurofins sequencing report and inspecting the ".ab1" files in the software *Geneious* v. 10.2.3, where sequences processing was performed. Only sequences with a Contiguous Read Length (CRL) ≥ 500 were retained for further analysis, as this indicates high-quality, uninterrupted reads. These sequences were then trimmed to remove regions with an error probability exceeding 5% per base.

Forward and reverse reads were then aligned using the *De novo* assembly tool with the default parameters, generating the consensus sequences, which were then exported as a single FASTA file.

The FASTA file was uploaded into the SILVA Alignment, Classification and Tree (ACT) service (https://www.arb-silva.de/aligner/) for taxonomic classification. Consensus sequences were aligned against the SILVA database with a minimum sequence identity of 95%. A phylogenetic tree was generated using the GTR model in FastTree in the Silva ACT service. The output of this classification was imported into the online tool iTOL (https://itol.embl.de/) to visualise the phylogenetic tree.

4.2.3.3. Response of bacterial isolates to identified herbivory-regulated metabolites

Based on the findings from Chapter 2 and the current chapter, a growth assay was conducted to evaluate the ability of bacterial strains isolated on ISP-3 medium to use four metabolites whose identities were confirmed in Chapter 3, Section 3.3.2.4 as carbon sources. The metabolites used in this assay were HMBOA-O-Hex (BenchChem, USA; Cat# B095448), Azelaic acid (Merck, Germany; Cat# 46379-2), p-Coumaric acid (Merck, Germany; Cat# 90088), and Salicylic acid (Merck, Germany; Cat# 247588). Another identified metabolite, 9,10-diHOME, was excluded due to an insufficient quantity for testing.

A total of 95 bacterial isolates (53 from plants under aphid herbivory and 42 from healthy plants initially isolated in the ISP-3 medium, selective for Actinobacteria) were tested. Bacteria were initially grown on full-strength TSB medium for 48 hours before

being transferred to M9 minimal medium agar (per litre: 100 mL 5X M9 salt mix, 1 mL 1M $MgSO_4 \cdot 7H_2O$, 50 µL 1M $CaCl_2$, 100 mL 1% Casamino Acids) supplemented with individual metabolites at a final concentration of 0.5 mM as the sole carbon source (Figure 4.2). Metabolites were dissolved in dimethyl sulfoxide (DMSO), selected due to its lower toxicity compared to other solvents. To account for potential solvent effects, control plates with M9 medium containing 20% glucose and corresponding DMSO volumes were included. Additionally, a no-carbon-source control was used to determine whether bacterial growth patterns were influenced by the tested metabolites. Due to limited metabolite availability, the assay was conducted once, restricting the number of plates and replicates.

The ability of bacteria to utilise these metabolites as carbon sources was assessed by recording the presence or absence of bacterial colonies on the plates. Additionally, bacterial colony morphology was examined, distinguishing between sporulation or aerial hyphae formation and vegetative growth. Data analysis was carried out in R Studio v. 4.4.0 and visualization was performed with *ggplot2* v.3.4.2.

4.3. Results

Building on the findings from Chapter 2, this chapter explores the relationship between changes in plant metabolites and bacterial community responses to herbivory. Bacterial responses were assessed through amplicon sequencing to identify differences in root-associated bacterial communities between herbivory-treated and healthy plants (Section 4.3.1). Additionally, a correlation analysis was performed to examine associations between bacterial community composition and metabolites regulated by aphid herbivory (Section 4.3.2). Finally, a growth assay was conducted to evaluate the ability of bacterial isolates from the plant rhizosphere to

utilize specific metabolites identified in the metabolomics analysis from Chapter 3 (Section 4.3.3).

4.3.1. Aphid herbivory impacted root-associated bacterial communities by increasing ASVs from the Actinobacteria class

Aphid herbivory affected the diversity and structure of root-associated bacterial communities

Bacterial community analysis was carried out after processing the amplicon sequencing data to obtain the amplicon sequence variants (ASVs) –high-resolution unique biological sequences identified using the DADA2 denoising algorithm. A total of 1,958,295 reads, corresponding to 3,629 ASVs were obtained after sequencing processing. Details of reads quality after denoising can be found in the Supplementary Table 4.1. The quality-filtering step removed sequences classified as mitochondrial and chloroplast DNA, resulting in a final dataset of 1,036,730 reads and 3,401 ASVs. This filtering step had a minimal impact on soil samples, whereas 72% of ASVs were removed from root-associated samples, reflecting the higher proportion of host-derived sequences in root compartments. Subsequently, all samples were rarefied to the minimum library size (28,680) for alpha diversity analysis. Rarefaction curves (Supplementary Figure 4.1) showed a clear plateau, indicating that sequencing depth was sufficient to capture the bacterial diversity present in each sample.

Bacterial community diversity and richness (i.e., alpha diversity) were assessed using the Observed ASVs and Shannon diversity index. Alpha diversity was significantly different across sample types ($p_{adj} < 0.05$), with bulk soil showing the highest diversity, followed by the rhizosphere and plant roots (Figure 4.3.a, b). In the rhizosphere, bacterial alpha diversity tended to be lower under aphid herbivory compared to healthy plants, but this difference was not statistically significant ($p_{adj} = 0.078$ for Observed ASVs, $p_{adj} = 0.1$ for Shannon index). A similar trend was observed in root samples, though the effect was weaker ($p_{adj} > 0.1$). In terms of community composition, the relative abundance bar plot (Figure 4.3.c) revealed that Actinobacteria was the dominant class in all sample types, with its relative abundance increasing from bulk soil to plant roots. In healthy plant roots, Actinobacteria made up 68% of the community, while in roots of plants under aphid herbivory, it increased to 74%. This likely explains the observed lower alpha diversity in root samples.

To investigate differences in bacterial community structure and composition among groups (i.e., beta diversity), the dataset was filtered to retain only ASVs present in more than 50% of samples within each group. This step reduced the total number of ASVs from 3,401 to 1,178 and ensured that the analysis focused on bacteria consistently detected across samples, minimising the influence of rare taxa. Beta diversity was visualised using a Non-Metric Multidimensional Scaling (NMDS) plot based on Bray-Curtis dissimilarity (Figure 4.3d) that revealed a clear separation between bacterial communities associated with plant roots and those from bulk soil and rhizosphere samples, suggesting distinct microbial assemblages according to the sample origin. PERMANOVA analysis (Supplementary Table 4.2) confirmed that sample origin (bulk soil, rhizosphere or roots) and aphid herbivory significantly influenced bacterial diversity ($p < 0.01$).

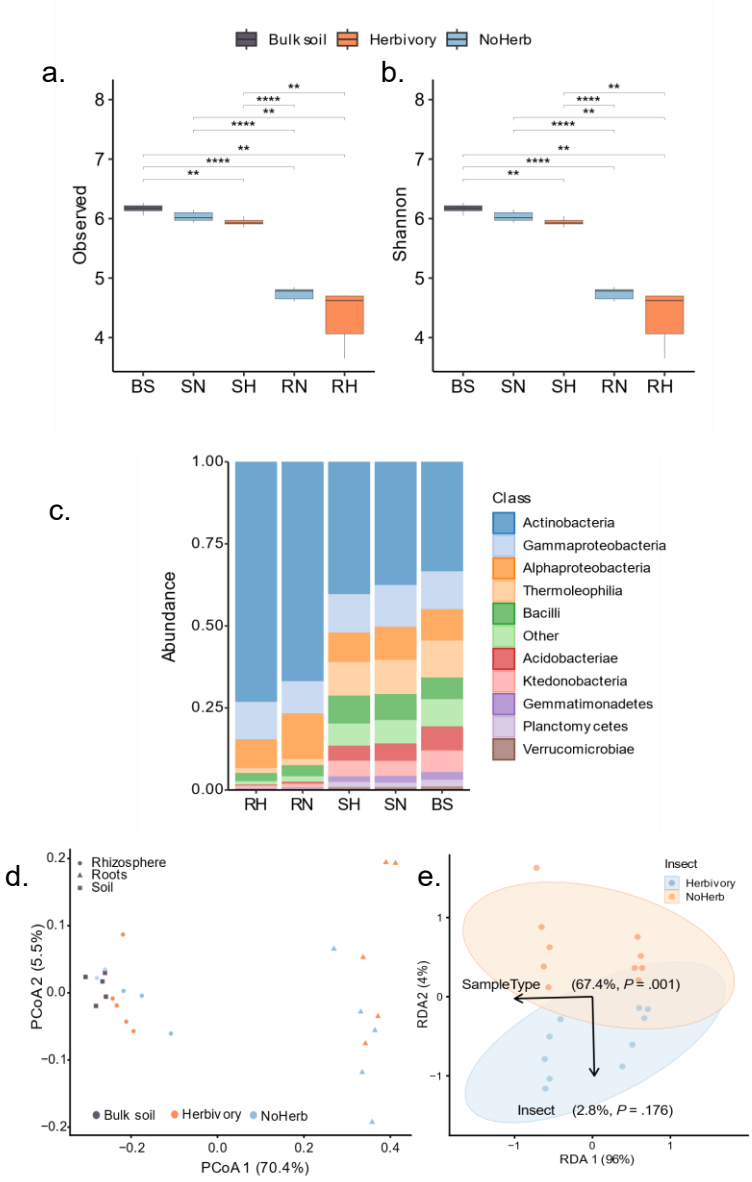

Figure 4.3. *Diversity of microbial communities in the rhizosphere of wheat plants. Alpha diversity analysis using the observed (a) and Shannon index (b). Whiskers show post-hoc Wilcoxon comparison with asterisks showing statistical significance (alpha * < 0.05, ** <0.01, *** < 0.001; c) Rank abundance plot of bacterial communities at the Class taxonomic level; d) non-multidimensional scale analysis (NMDS) of Bray-Curtis dissimilarity distance of bacterial community composition; e) Partial dbRDA of bacterial diversity showing the explained variance of bacterial communities based on compartment and insect herbivory (n=5). RH= Roots of plants under herbivory; RN= Roots of healthy plants; SH= Rhizosphere of plants under herbivory; SN= Rhizosphere of healthy plants; BS= Bulk soil.*

To further evaluate the influence of aphid herbivory, a distance-based redundancy analysis (dbRDA) was performed using only rhizosphere and root samples (Figure 4.3e). Sample origin (root vs. rhizosphere) was the strongest determinant of bacterial community composition, explaining 67.4% of the total variance ($F = 38.53$, $p < 0.01$).

In contrast, aphid herbivory alone accounted for 2.8% of the variance ($F = 1.61$, $p = 0.193$), suggesting a relatively minor direct effect. However, when controlling for sample origin as a covariate in the dbRDA, the effect of aphid herbivory became statistically significant ($F = 1.61$, $p = 0.042$). This indicates that, while the dominant factor shaping bacterial communities was the physical environment (root vs. rhizosphere), aphid herbivory had a measurable impact on microbial composition within these compartments.

Differential abundance analysis reveals an increase in Actinobacteria in roots of plants under aphid herbivory

In the rhizosphere, aphid herbivory was associated with significant increases in bacterial ASVs belonging to the genera *Paenibacillus* and *Frauteria*, as well as several ASVs that could not be assigned to a genus. In contrast, ASVs that decreased in abundance were mostly unclassified at the genus level but were taxonomically assigned to the Alphaproteobacteria and Acidobacteriae classes (Figure 4.4a).

In plant roots, most ASVs that increased in abundance under aphid herbivory belonged to the Actinobacteria class, with the highest enrichment in the genera *Marmoricola, Devosia,* and *Streptacidiphilus* (Figure 4.4b). These shifts suggest that aphid herbivory may selectively influence specific bacterial taxa, particularly Actinobacteria, within the root microbiome. Further details on statistical results and taxonomic classifications are available in Supplementary Table 4.3 and 4.4.

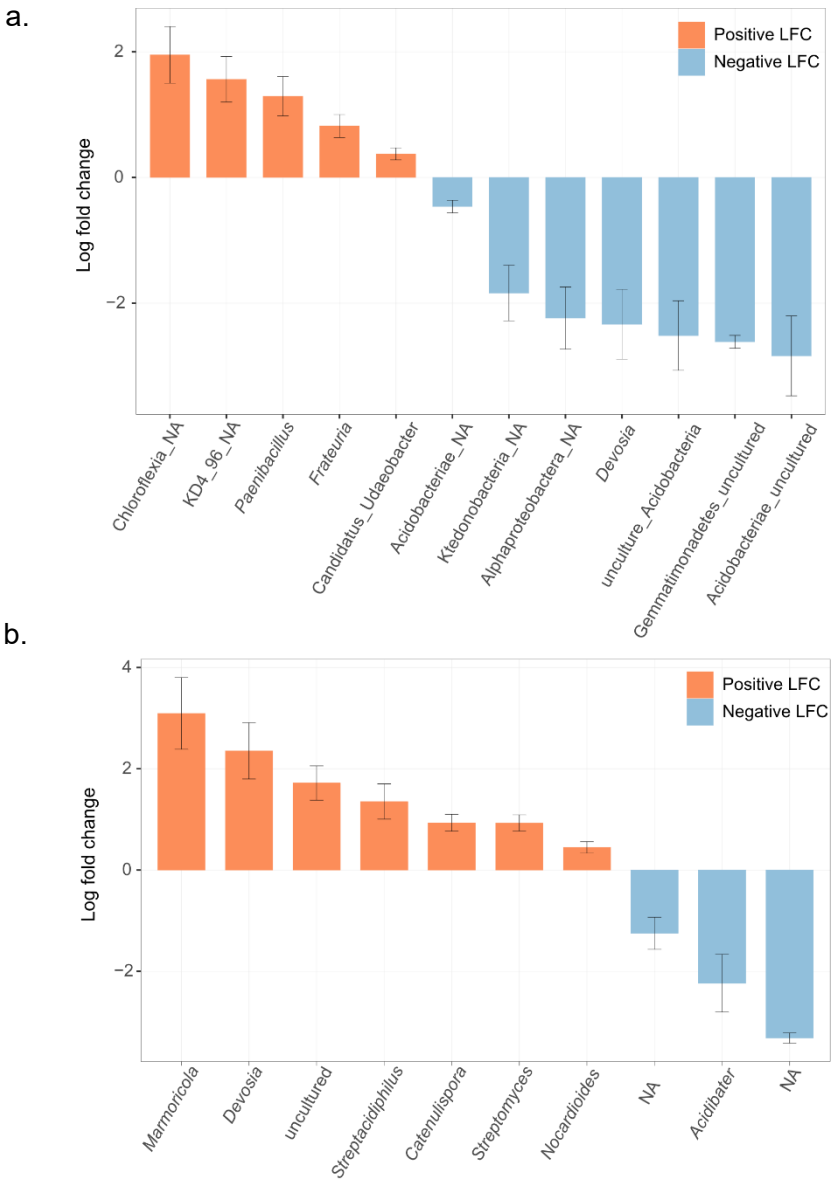

Figure 4.4. *Differential abundance analysis (ANCOM-BC) of amplicon sequence variants (ASVs) in the rhizosphere (a) and plant roots (b). Log-fold change (LFC) indicates enrichment (positive LFC) or reduction (negative LFC) of ASVs in the rhizosphere under herbivory vs. healthy plants. ASVs are labelled by genus (Silva 138 database); unassigned genera are labelled with taxonomy class + NA, or NA if only kingdom was assigned. Bars represent ASVs with a corrected p-value < 0.1 (Holm correction). Error bars indicate standard error (n = 5).*

4.3.2. Cross association of microbial taxa and metabolites showing fold changes in the root exudates of wheat plants under aphid herbivory

The analysis of bacterial communities from the present chapter revealed that most differences were found in the roots of plants under aphid herbivory, with a significant increase in bacteria from the Actinobacteria class. To explore potential correlations between bacterial communities and root exudate metabolites regulated by aphid herbivory (Chapter 3, Section 3.2.5.1), a Spearman correlation analysis was performed. This analysis included metabolites with observed log-fold changes from Chapter 3 and ASVs from rhizosphere and root samples, which were pooled to capture overall trends. The resulting heatmap (Figure 4.5) identified five distinct bacterial clusters (labelled 1 to 5). Clusters 4 and 5 consisted of bacteria positively correlated with metabolites more abundant in control plants (no aphid herbivory), while clusters 1 and 3 contained bacteria positively correlated with metabolites enriched in the exudates of herbivory-treated plants (n = 202). Notably, Cluster 1, dominated by Actinobacteria and Bacilli, exhibited a strong negative correlation with most metabolites abundant in healthy plants.

Statistical analysis identified seven significant correlations ($p_{adj} < 0.05$) between bacterial taxa and specific metabolites (Supplementary Table 4.5). These included a positive correlation between Alphaproteobacteria and two metabolites (Features 7448 and 5818), as well as Gemmatimonadetes with two others (Features 6599 and 7621).

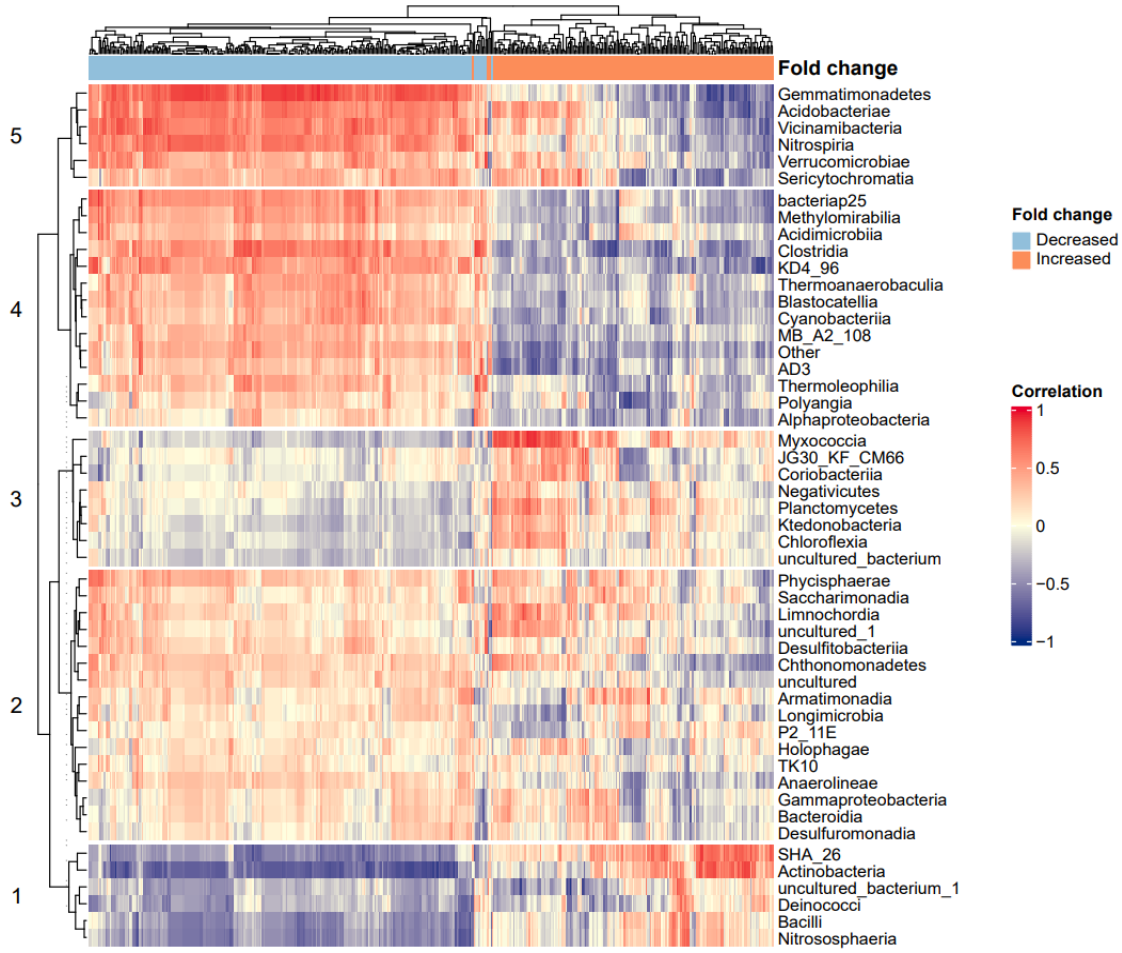

Figure 4.5. *Spearman correlations between log-transformed pooled ASVs (relative abundance) from rhizosphere and root samples and log-transformed metabolite peak areas. The top bar shows metabolite log-fold changes (blue: decreased, orange: increased under aphid herbivory). Clusters 1 and 3 include bacteria positively correlated with metabolites that increased under herbivory, while Clusters 4 and 5 correlate with metabolites that decreased. Cluster 2 contains bacterial classes where associations were less evident.*

The metabolites with observed fold changes were filtered to include only the ones where a chemical class was assigned in the metabolomics analysis in Chapter 3, Section 3.2.3.2. A total of 54 metabolites were selected. In this analysis, the correlations were performed separately for the bacterial communities in the rhizosphere and plant roots. The heatmap (Figure 4.6) shows that most of the metabolites classified as octadecanoids and small peptides were decreased in the root exudates of plants under herbivory, and a positive correlation of these metabolites and bacteria from the Alphaproteobacteria, Gammaproteobacteria and

Gemmatimonadetes classes was found in the rhizosphere of wheat plants. Moreover, most of the metabolites that increased under aphid herbivory were assigned to the flavonoids class and were positively correlated with bacteria from the Myxococcia, Planctomycetes and Bacilli classes, among others. As expected, based on the bacterial community's analysis (Section 4.3.1), the Actinobacteria showed neither strong positive nor negative correlations with metabolites in the rhizosphere; however, in the roots, Actinobacteria were positively correlated with metabolites that increased in response to herbivory.

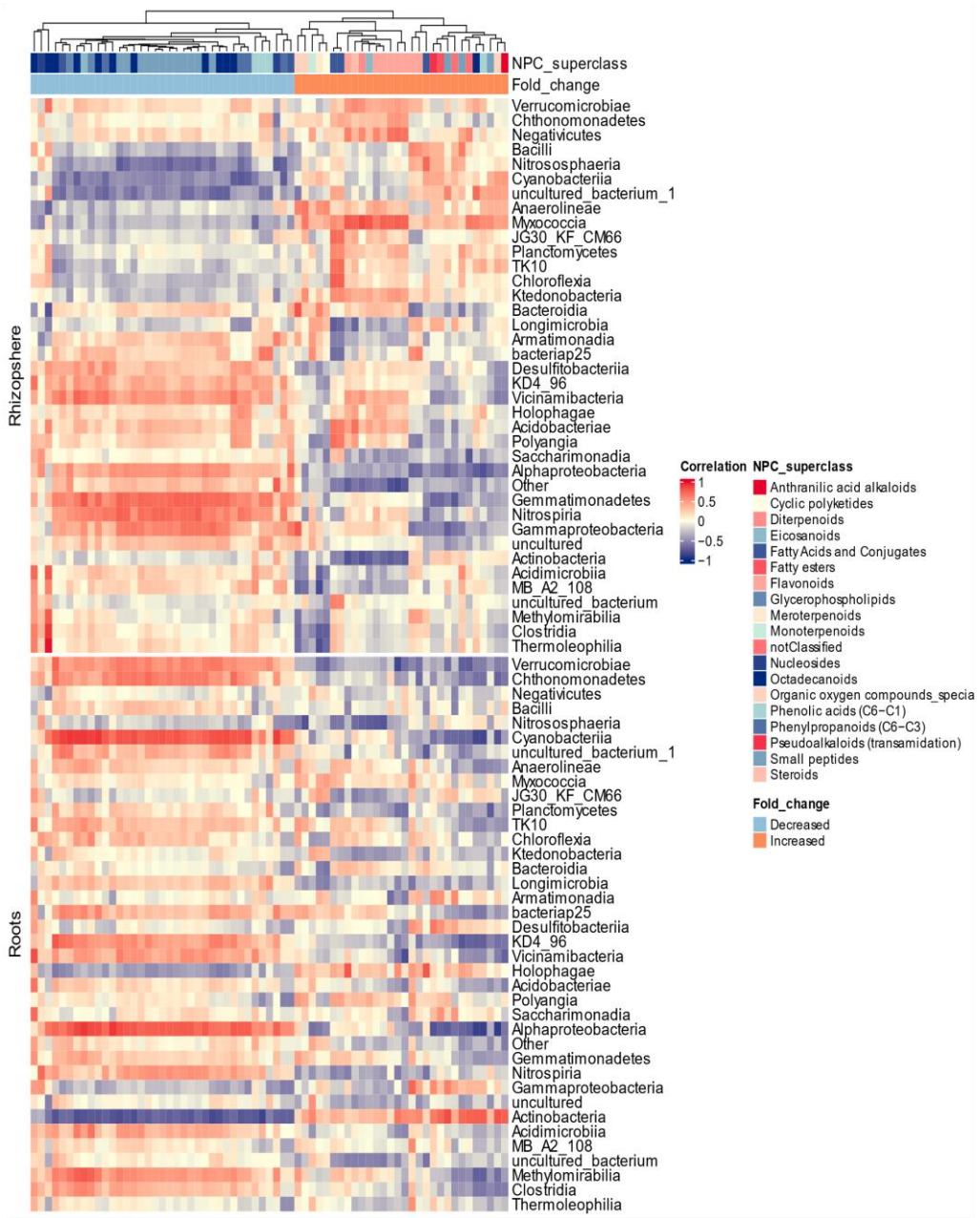

Figure 4.6. *Spearman correlations between log-transformed ASVs (relative abundance) from rhizosphere and root samples and log-transformed metabolite peak areas. The first top bar shows the assigned chemical classification of metabolites. The second top bar shows metabolite log-fold changes (blue: decreased, orange: increased under aphid herbivory).*

4.3.3. Herbivory-regulated metabolites induced sporulation in Actinobacteria

Integration of microbiome and metabolomics data revealed correlations between bacteria and metabolites present in the rhizosphere of plants under herbivory. To

further investigate, bacterial isolation was performed from the rhizosphere using TSA 10% (a non-specific medium) and ISP-3 (for isolating Actinobacteria). A total of 96 isolates were retrieved from the rhizosphere of plants under herbivory on TSA media, compared to 84 from the control plants. On ISP-3, 53 isolates were obtained from the rhizosphere of plants under aphid herbivory, and 46 from control plants.

Due to PCR limitations for some strains, a total of 183 bacterial isolates were sent for 16S rRNA gene amplicon sequencing. Of these, 165 isolates were successfully identified by matching against the Silva database. The phylogenetic tree of these isolates is shown in Figure 4.7. As expected, most isolates were classified as Actinobacteria, belonging to genera such as *Streptomyces*, *Kitasatospora*, *Rhodococcus*, *Leifsonia*, and *Arthrobacter*. Additionally, other isolates from genera like *Burkholderia* and *Paenibacillus*, which were found to be differentially abundant in the first and second experiments, were also identified.

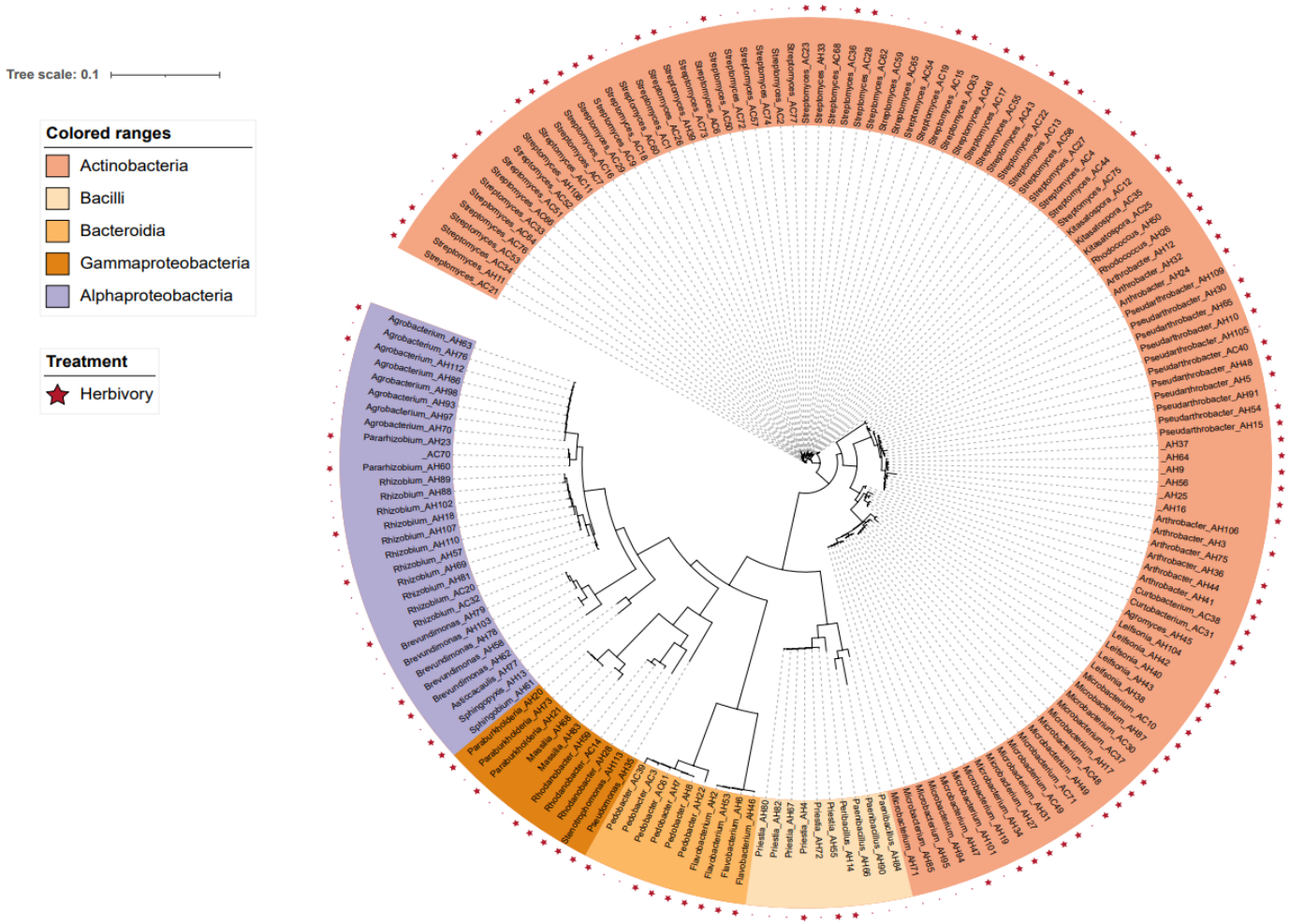

Figure 4.7. *Phylogenetic distance tree of 16S amplicon sequencing of bacterial isolates. The identities were determined using the SILVA Alignment, Classification and Tree (ACT) service at https://www.arb-silva.de/aligner/ after the consensus sequences were obtained using Geneious v. 10.2.3*

4.3.3.1. Herbivory-regulated metabolites induced aerial hyphae formation and sporulation in Actinobacteria

Bacterial isolates from the ISP-3 medium (both from the rhizosphere of plants under aphid herbivory and control plants) were selected for analysis, with a total of 95 bacterial strains selected. Out of the 95, 14 bacterial strains did not grow in the full-strength TSB medium, and consequently did not grow in the plates with M9 minimum medium. After 72 h of incubation, the bacterial isolates grown in minimum medium supplemented with glucose (20% w/v) showed regular, vegetative growth (Figure 4.8), while most bacteria growing in the media without any carbon source, and those grown in plates supplemented with the selected metabolites as a unique carbon source, shown hyphae formation and sporulation, which was observed as early as after 48 h, suggesting that most bacteria starting sporulating as a stress response.

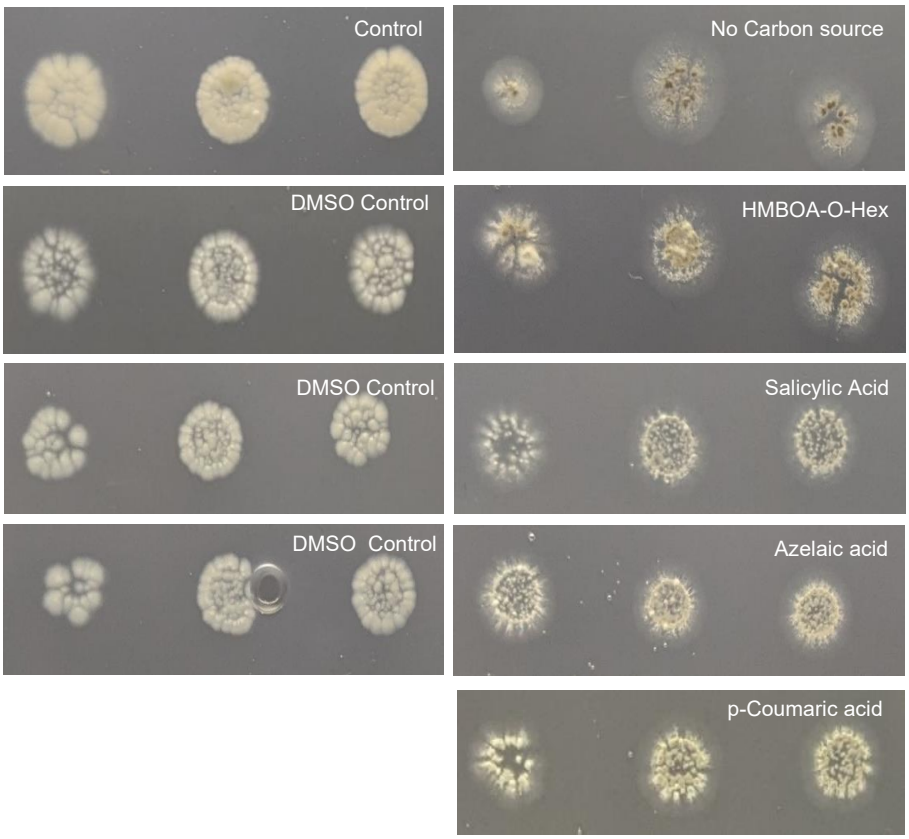

Figure 4.8. *Growth of bacterial strains after 72 hours of incubation in M9 minimal medium supplemented with 0.5 mM of selected compounds as carbon sources. The left panel shows bacterial growth in M9 medium with the corresponding solvent controls (DMSO), while the right panel shows growth in M9 medium supplemented with the metabolites. The bacterial colonies correspond to the same three isolates in different compounds and their solvent controls.*

The total count of bacterial strains in these carbon sources revealed that 81 bacterial strains were able to grow in salicylic acid, either sporulating or in vegetative growth (Figure 4.9). Out of this, 79% (64 isolates) were observed to sporulate in the presence of this compound. In the case of p-coumaric acid, HMBOA-O-Hex and azelaic acid, the percentages were similar, with 81%, 82% and 79% of bacterial isolates showing sporulation, respectively. The most restrictive condition seemed to be the growth on M9 medium without carbon sources. Although this is a qualitative test, it demonstrates that some bacterial isolates were not able to grow in the presence of these compounds, suggesting their inability to use them as carbon sources. Moreover, other bacteria were able to grow, but sporulated quickly showing a stress response, while

others grew without sporulating. Overall, this suggests that the bacterial isolates responded differentially to the application of the compounds in the growth medium.

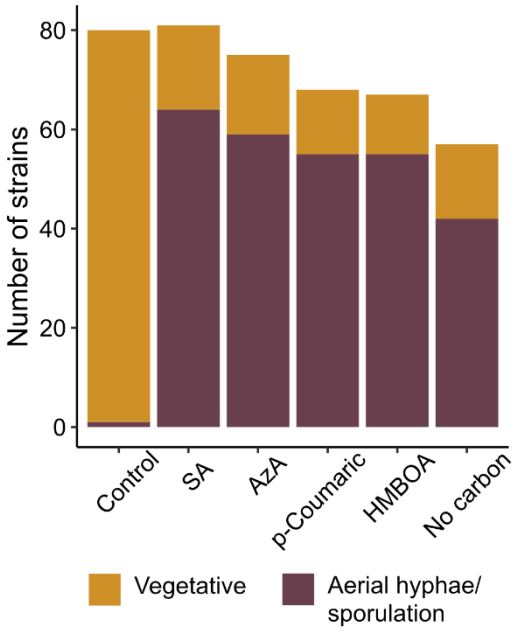

Figure 4.9. *Number of bacterial strains that exhibited growth on M9 medium plates supplemented with 0.5 mM of metabolites identified as regulated by aphid herbivory. SA = Salicylic acid, AzA = Azelaic acid, p-Coumaric = p-Coumaric acid, HMBOA = HMBOA-O-Hex.*

4.4. Discussion

Building on the findings from Chapter 2, where Actinobacteria were identified as one of the most responsive taxa to changes in the rhizosphere of plants under aphid herbivory, this chapter extends the analysis to the plant roots. Aphid herbivory was found to significantly increase the relative abundance of Actinobacteria in the roots, further highlighting their potential role in plant-microbe interactions under herbivory. In addition, a correlation analysis with root exudates (regulated by aphid herbivory, Chapter 3) revealed correlations between the increased Actinobacteria abundance and a diverse array of specialized metabolites, including flavonoids, terpenoids, and

alkaloids. These metabolites, often linked to plant defence responses, may serve as potential drivers of bacterial recruitment, shaping the root microbiome in response to herbivory. An exploratory test suggested that the presence of these metabolites could induce a stress response in bacteria, offering a glimpse into the complex interplay between plants and microbes under stress. Collectively, this chapter demonstrates how aphid herbivory not only alters bacterial composition in plant roots but also points to specific plant-derived metabolites as potential mediators of microbial community dynamics.

Actinobacteria were increased in the roots of plants under aphid herbivory

In the present study, bacterial communities from both the rhizosphere and root compartments were analysed using amplicon sequencing. This approach was taken to identify if the previously observed changes would be limited to the rhizosphere — the zone influenced by roots— or if these changes extended to the communities more closely associated with root tissues. As bacterial communities from the roots analysed in this experiment might not be strictly endophytic (living inside plant tissue) since plant roots were not disinfected, the term *roots* is applied to the combination of both rhizoplane and root endosphere compartments.

Overall analysis of microbial communities from the bulk soil, rhizosphere, and plant roots showed that the most abundant taxa in all samples belong to the Actinobacteria class. Within the top ten of most abundant taxa, other dominant groups included bacteria from the Thermoleophilia (Actinobacteriota phylum) and Ktedonobacteria (Chloroflexi phylum) classes. The dominant presence of these bacterial classes, which have been characterised to thrive in oligotrophic and extreme environments

(Hu et al., 2019; Shivlata & Satyanarayana, 2015; Zheng et al., 2019, 2021) agrees with the history of the soil used for these experiments, which has been maintained as bare fallow for over 50 years and is characterised as a low nutrient soil (Reid et al., 2021).

Microbial metabolic activity is higher in the rhizosphere than in bulk soil as plant roots provide a nutrient-rich environment, which creates a competitive environment for microbes. This selection is further amplified in plant roots, which pose a more selective environment where bacteria need to penetrate the root tissues, evade or suppress plant immune responses, compete for a more limited nutrient supply and adapt to low oxygen levels (Prashar et al., 2014; Simmons et al., 2018; van Dam & Bouwmeester, 2016; Vives-Peris et al., 2020). For this reason, it was not surprising that alpha diversity was higher in the bulk soil and lower in plant roots.

Although some bacteria can transiently enter the plant roots through openings or cracks in roots (e.g., wounds by pathogen attack, lateral root emergence), true endophytes require plant cell-wall degrading enzymes like cellulases, cutinases, pectinases and lignin peroxidases to penetrate root internal tissues (Wippel, 2023). In this experiment, the Actinobacteria class was the most abundant class observed in plant roots. This taxon belongs to the Actinobacteriota phylum, which along with Proteobacteria, are the most common phyla of bacterial endophytes (Mishra et al., 2021; Vandenkoornhuyse et al., 2015). Moreover, bacteria from the Actinobacteria class have been consistently shown to be part of the core microbiome of wheat plants (Gruet et al., 2022; Kavamura et al., 2021; Kuźniar et al., 2020; Viaene et al., 2016) and their presence has been identified as important for soil health in wheat-maize cropping systems (Sun et al., 2024). In the roots of plants under aphid feeding, five

out of the 7 bacterial ASVs that increased belong to the Actinobacteria class, more specifically to the genera: *Marmoricola, Streptacidiphilus*, *Streptomyces*, *Catenulispora, Nocardioides,* and *Mycobacterium*.

Of the bacterial ASVs that increased in roots of plants under herbivory, *Streptomyces* is the most overwhelmingly known as plant growth-promoting genus. The ability of *Streptomyces* to colonise the root endosphere has been documented in plants such as *Arabidopsis thaliana* (van der Meij et al., 2018), lettuce (Bonaldi et al., 2015; X. Chen et al., 2016), and wheat (Gruet et al., 2022; Kavamura et al., 2021; Kuźniar et al., 2020; Viaene et al., 2016), but there are still many questions on the endophytic lifestyle of these bacteria and their role once they colonise plant roots. Their ability to solubilise nutrients or produce siderophores has been observed mainly *in vitro*, as well as their antagonistic function against plant pathogens, both bacterial and fungal, but there is still a need for evidence on how all these abilities can protect plants against pests and pathogens (Viaene et al., 2016). Although evidence of bacteria from the differentially increased genera have not been specifically related with the plant response to aphid herbivory, there is evidence of their role in improving plant resistance to a wide variety of plant pathogens like powdery mildew (Kurth et al., 2014), *Pectobacterium* (Dias et al., 2017) and take-all (*Gaeumannomyces graminis* var. *tritici)* (Worsley et al., 2020). Although currently most information of Actinobacteria comes from *Streptomyces*, recent work has also shown that the genus *Catenulispora* has been positively correlated with wilt resistance in melon plants (Zhu et al., 2024). There is little information about the other Actinobacteria genera and their role as beneficial endophytic bacteria, but it is tempting to suggest that given their metabolic capacity and their ability to produce antibiotics, they could be offering plants more nutrients and helping regulate the rhizosphere and root environment, but more

research is needed to identify if their activity has a direct benefit for plants under aphid feeding.

Moreover, beneficial bacteria can increase plant susceptibility to pests and pathogens by increasing the nutritional value of their hosts (van Dijk et al., 2022), and research suggests that this strategy can be exploited by aphids. Kim et al. (2015) observed that aboveground aphid herbivory modified the root exudates of plants and increased the recruitment of *Paenibacillus polymyxa E681.* Inoculation of plants with this strain resulted in an increase in aphid populations in pepper plants. Furthermore, the aphid *Brevicoryne brassicae,* seemed to increase populations of *Bacillus* spp., and this abundance was negatively correlated with aphid parasitism by wasps (Blubaugh et al., 2018). In the results presented in this chapter, an increase in ASVs from *Paenibacillus* in the rhizosphere of plants under aphid herbivory was observed. It is worth noticing that bacteria from this genus are also well known by their ability to induce systemic resistance (Chen et al., 2022; Figueredo et al., 2023; Samain et al., 2022) so further experiments are needed to investigate the role of these bacteria in plant-aphid interactions.

Correlation of bacterial response and root exudates of plants under aphid herbivory

This study aimed to explore potential metabolites in plant root exudates that may act as signals mediating changes in bacterial communities at the plant-soil interface in response to aphid herbivory. Untargeted metabolomics analysis (Chapter 3) showed significant differences in the composition of exudates from aphid-infested plants compared to healthy plants. Overall, the correlations suggest possible influences of root exudates in the relative abundance of microbial taxa in both the rhizosphere and

roots. Among metabolites assigned to chemical classes, oxylipins and small peptides were found to decrease under aphid feeding, while benzoxazinoids and flavonoids showed a marked increase. Correlation analysis revealed that bacterial classes such as Actinobacteria and Bacilli were more strongly associated with metabolites that increased in plants under aphid herbivory, whereas Alpha proteobacteria, Acidimicrobiia, and Gemmatimonadetes, among many others, were linked to compounds enriched in the exudates of healthy plants.

One of the metabolites included in this study in both the correlation analysis and the test with culturable bacteria was the benzoxazinoid HMBOA-O-Hex, which significantly increased in wheat root exudates from plants under herbivory. The benzoxazinoids family are a class of metabolites that are well known for their allelopathic properties. These indole-derived compounds have multiple functions that include defence against insect pests, bacterial and fungal pathogens, nematodes, and competing plant species. Additionally, they play roles in regulating auxin signalling and can act as iron-binding agents (Cotton et al., 2019; Kudjordjie et al., 2019; Zhou et al., 2018). In response to herbivory, benzoxazinoids inhibit digestive enzymes from insects and stimulate callose formation in plant tissues (Shavit et al., 2018). Recent studies have shown that these compounds have a great role in shaping the rhizosphere microbiome in gramineous plants. Bacterial tolerance to metabolites from this family has been directly correlated with their abundance in plant roots, and evidence suggests that bacterial cell wall structure influences tolerance to different compounds from this family (Thoenen et al., 2023). As mentioned above, benzoxazinoids also have the capacity to act as iron-chelating agents, which is another strategy used by plants and beneficial microbes to make this essential nutrient unavailable for pathogens (Deb & Tatung, 2024). Interestingly, recruitment of *Marmoricola* has been related with the addition of a cereal phytosiderophore (Proline-

2’-deoxymugineic acid) in the rhizosphere of peanut plants, which ultimately resulted in an increase in micronutrients, including iron and nickel (Wang et al., 2023). In this experiment, it is possible that the benzoxazinoids function as antimicrobial and iron-chelating agents, making the rhizoplane and root endosphere a very restrictive environment where Actinobacteria are able to thrive thanks to their tolerance to these compounds, but this needs to be tested in future research.

The role of benzoxazinoids can also be thought of beyond their direct effect on microbial communities. Cotton et al. (2019) proposed that benzoxazinoids biosynthesis regulates the production of flavonoids, another class of secondary metabolites that are key in processes like legume-rhizobia and plant-mycorrhiza symbiosis. Interestingly, some of the metabolites that were increased under herbivory were tentatively annotated as flavonoids, but, as there are many unknown metabolites, and the root exudates are very complex it is not possible to make any assumptions in this dataset. Hopefully, as databases of metabolites spectra grow, it will be possible to characterise and tentatively annotate more compounds, which will help understand these associations between metabolites.

As some metabolites that increased under herbivory are of potential interest in shaping bacterial communities, those that decreased are also significant. An overall decrease was observed in metabolites tentatively annotated as oxidised fatty acids, particularly C18 oxidised unsaturated fatty acids derived from linoleic and oleic acids. Unsaturated fatty acids play a central role in plant membranes, initiating signalling cascades and serving as precursors to oxylipins like the hormone jasmonic acid (Seth et al., 2024). Lipids and fatty acids have been identified as defence markers in plants. For example, maize infection by the pathogen *Fusarium verticillioides* significant

increases oxylipins, suggesting the triggering of defence response (Cavaco et al., 2021). On the contrary, a decrease in fatty acids, was observed after inoculation with bacteria *Candidatus Liberibacter asiaticus*, causal agent of Huanglongbing disease, suggesting manipulation of plant host defence by the pathogen (Suh et al., 2018). Interestingly, bacteria from the *Streptacidiphilus* and *Streptomyces* genera were reported to be susceptible to high concentrations of jasmonic acid, especially *Streptacidiphilus*, which was found to decrease in the root exudates of plants under herbivory. Furthermore, jasmonic acid activated antibiotic production in *Streptomyces (van der Meij et al., 2023)*. The decrease in unsaturated fatty acids in this study suggests that aphids can cause changes in these important defence and signalling molecules belowground, which could have caused the increase in the observed bacterial taxa (mostly Actinobacteria).

Metabolites annotated as “small peptides” were among those that decreased in the exudates of plants under aphid feeding. Small peptides, typically consisting of fewer than 100 amino acids, play a crucial role in plant growth, development, nutrient signalling and response to both abiotic and biotic stresses (Segonzac & Monaghan, 2019; Wu et al., 2022; Zhang et al., 2024). Acting as intercellular signal transducers, some of these peptides also possess antimicrobial activity, contributing directly to plant defence mechanisms (Segonzac & Monaghan, 2019). However, much about this class of compounds remains poorly understood. Their annotation is challenging as most tools have been trained for larger molecules, and many aspects of their synthesis, signalling pathways, and functions remain unknown, earning them the label of “a subset of dark matter in plant proteomes” (Feng et al., 2023). Nevertheless, thanks to the advances in next generation sequencing platforms and bioinformatic analysis, more small peptides have been characterised. Some of these peptides have been linked to induced defence responses in various plants, where they play key roles

in activating immune responses against pathogens and pests (Pastor-Fernández et al., 2023). Observing a decrease in these metabolites in the exudates of plants under aphid herbivory is interesting, as it suggests a possible dysregulation of plant signalling and defence systems.

The decrease in both oxidised fatty acids and small peptides could potentially make the plants more susceptible to secondary infections in plant roots. This could be the result of different processes. One possibility is that aphid herbivory can alter the sink-source transport of nutrients in the plants, and as they take up the phloem sap, they reduce the amount of nutrients going to the plant roots (Hackett et al., 2013). This is supported by the observed decrease in root biomass in this study, as the limited supply of nutrients could directly impair root growth and function. Nevertheless, as discussed above, both unsaturated fatty acids and small peptides are important signalling molecules in plant defence and response to environmental stresses, so their absence in root exudates will most likely affect plant-microbe interactions.

Another possibility is that plants are reallocating resources to prioritise other defence strategies against aphid herbivory. This could include converting the C18-polyunsaturated fatty acids into green leaf volatiles to control aphid herbivory aboveground (Ameye et al., 2018) or producing proteins and enzymes that that enhance their immediate defence against herbivory. While such adjustments might increase aboveground defences, they could leave roots more vulnerable to opportunistic pathogens or other stresses. Interestingly, an increase in colonisation by Actinobacteria could suggest a compensatory strategy by plants. Actinobacteria, well-known for their antimicrobial properties and ability to produce bioactive compounds, might act as plant allies to protect their roots while plants cope with the

herbivory stress. The ability of Actinomycetes to metabolize complex carbon and nitrogen sources, rather than relying on simple compounds typically found in root exudates, allows them to thrive even when plant exudates change under stress. This reliance on microbial allies could represent a form of “outsourcing” defence by the plants while they focus on aboveground stress. Finally, as mentioned above, aphids could be manipulating the plant host to increase the abundance of beneficial bacteria that can help increase nutrient availability in the rhizosphere. As there are different possibilities, future studies using culturable bacteria are needed to unravel the exact mechanisms by which synthesis and release of these compounds are regulated during herbivory and to understand their broader ecological roles in shaping plant-microbe interactions and microbial community dynamics in the rhizosphere.

Although multiple bacterial taxa and metabolites showed correlations in this study, the discussion focuses on Actinobacteria, which results were consistent across both experiments, and on metabolite classes for which sufficient information was available. It is important to mention that in this study, changes in bacterial communities were measured in terms of their structure and composition by using 16S rRNA amplicon sequencing. However, other studies have used isotope labelling of root exudates to increase the understanding of the role of secondary metabolites as signals facilitating Actinobacteria colonization of plant roots. For example, Prudence et al. (2021) found that bacteria from the families *Streptomycetaceae* and *Burkholderiaceae* were consistently found within the wheat root endosphere, but, when using $^{13}CO_2$ stable isotope probing to determine which bacteria are able to use the carbon in root exudates, only the latter was found to utilise the host-derived carbon in root exudates. The authors suggest that as Actinobacteria have the sufficient capacity to metabolise more complex carbon sources found in the rhizosphere, they would prefer these sources instead of the less-complex root exudates. Other authors have observed

similar outcomes in *Streptomyces* colonisation of *Arabidopsis thaliana* (Worsley et al., 2021).

The findings of this study suggest that the root microbiome under herbivory may be shaped by a combination of factors, including the decrease in certain metabolites, such as unsaturated fatty acids, and the tolerance of microbes to a mixture of specialised compounds like benzoxazinoids, flavonoids, and alkaloids. Notably, this shaping effect could occur even if bacteria are not able to metabolise these compounds as carbon sources. This study highlights the significant impact of aphid herbivory on the complete profile of metabolites released by plants via root exudates and the importance of investigating the interactions between these metabolites to better understand how biotic stresses, such as aphid herbivory, influence plant-microbe communication.

4.5. Supplementary information

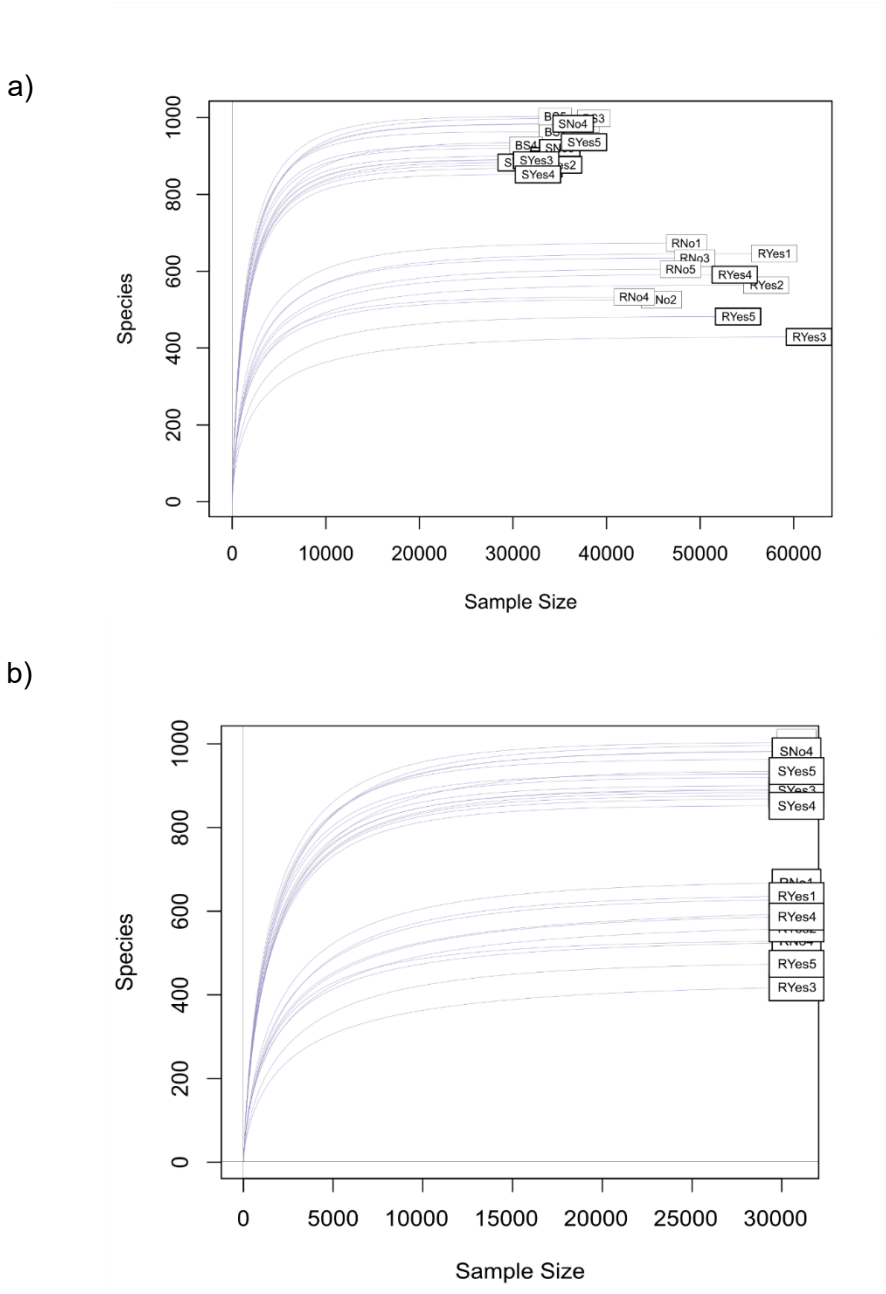

Supplementary Figure 4. 1. *Alpha rarefaction curves a) before and b) after applying rarefaction to the minimum library size*

Supplementary Table 4. 1. *Quality of merged sequences provided by Novogene for analysis*

Sample	RawPE	Combined	Qualified	Nochime	Base(nt)	Avglen(nt)	GC	Q20	Q30
BS1	69906	69512	68989	46939	17536983	373.61	56.72%	99.34%	97.40%
SN1	63708	63269	62754	40247	15044829	373.81	57.19%	99.30%	97.24%
SH1	62193	61593	61164	36824	13766705	373.85	57.33%	99.35%	97.37%
SN2	65191	64465	63942	40267	15045378	373.64	56.89%	99.31%	97.28%
SN3	66647	66063	65473	43051	16089556	373.73	56.61%	99.25%	97.01%
BS2	65962	65720	65190	40711	15221269	373.89	57.61%	99.32%	97.30%
SN4	64241	63974	63465	42158	15757830	373.78	57.43%	99.30%	97.22%
SN5	62193	61652	61161	41644	15556107	373.55	57.35%	99.30%	97.27%
SH2	66745	66208	65635	41806	15613296	373.47	57.05%	99.28%	97.19%
SH3	64686	64227	63731	41236	15408391	373.66	57.20%	99.25%	97.09%
BS3	77354	76748	76138	48075	17965405	373.7	56.80%	99.32%	97.29%
BS4	62848	62408	61946	37492	14009007	373.65	57.95%	99.32%	97.28%
SH4	65608	64791	64291	39275	14676535	373.69	57.27%	99.25%	97.08%
SH5	74240	73722	73213	45694	17079903	373.79	57.31%	99.26%	97.09%
BS5	63657	63355	62833	44239	16530331	373.66	56.53%	99.27%	97.10%

RN1	209207	190436	188399	164219	61132833	372.26	55.74%	99.25%	97.23%
RH1	204990	186122	183877	154166	57421203	372.46	56.00%	99.21%	97.07%
RN2	204272	181115	179073	155188	57772115	372.27	55.68%	99.25%	97.25%
RN3	205160	186939	184747	156551	58265884	372.18	55.60%	99.17%	96.94%
RN4	212367	189367	187061	160573	59720076	371.92	55.74%	99.21%	97.10%
RN5	204628	183503	181374	149069	55477252	372.16	55.87%	99.20%	97.09%
RH2	205883	190270	188072	150898	56184557	372.33	55.99%	99.20%	97.02%
RH3	204670	187884	185650	155694	58028571	372.71	56.43%	99.18%	97.00%
RH4	206479	192630	190665	156508	58357214	372.87	55.50%	99.18%	96.95%
RH5	202028	188009	185580	158442	58986948	372.29	55.62%	99.14%	96.82%

Supplementary Table 4.2. *ANOVA result for alpha diversity analysis of bacterial communities*

	df	sumsq	meansq	statistic	p.value
Insect	2	116420.9	58210.47	33.98874	3.69E-07
SampleOrigin	1	337740.1	337740.1	197.2043	8.07E-12
Insect:SampleType	1	151.25	151.25	0.088314	7.69E-01
Residuals	20	34252.8	1712.64	NA	

Supplementary Table 4. 3. *Differential abundance analysis of bacterial communities in plant roots. Analysis of Compositions of Microbiomes with Bias Correction-ANCOM-BC (q value <0.1)*

Bacterial ASVs differentially abundant in plant roots									
ASV	**LFC**	**W**	**pval**	**qval**	**Phylum**	**Class**	**Order**	**Family**	**Genus**
f218d4f442182d19d57d298ecfecf986	-1.250	-3.940249	0.000	0.078	Proteobacteria	Gammaproteobacteria	Burkholderiales	A21b	NA
771aec4090865e57830b7241a8f4a930	2.354	4.236551	0.000	0.022	Proteobacteria	Alphaproteobacteria	Rhizobiales	Devosiaceae	Devosia
26e47166a0db6185dd602bebd852bd5e	-2.236	-3.918329	0.000	0.085	Proteobacteria	Gammaproteobacteria	Gammaproteobacteria_Incertae_Sedis	Unknown_Family	Acidibacter
df024de18c87921c67886fd28e4b564d	1.719	5.070756	0.000	0.000	Actinobacteriota	Acidimicrobiia	Microtrichales	Ilumatobacteraceae	uncultured
df3f88a334c0e2f68d86ab27186821c3	0.933	5.561848	0.000	0.000	Actinobacteriota	Actinobacteria	Catenulisporales	Catenulisporaceae	Catenulispora
a9c7be654d0b87304df2580974469a6f	0.929	5.792462	0.000	0.000	Actinobacteriota	Actinobacteria	Streptomycetales	Streptomycetaceae	Streptomyces
b83d8bf975727f4d1d2433d406660626	1.353	3.887332	0.000	0.097	Actinobacteriota	Actinobacteria	Streptomycetales	Streptomycetaceae	Streptacidiphilus
1b1919673142a11955491dc5c3186773	3.094	4.363043	0.000	0.012	Actinobacteriota	Actinobacteria	Propionibacteriales	Nocardioidaceae	Marmoricola
5ae3f25fab3e0423d0f14dbe78407e1e	0.445	3.898951	0.000	0.092	Actinobacteriota	Actinobacteria	Propionibacteriales	Nocardioidaceae	Nocardioides
590a14b9cc9dc60f21dfad09a8244666	-3.320	-32.679116	0.000	0.000	Actinobacteriota	Actinobacteria	Kineosporiales	Kineosporiaceae	NA

Supplementary Table 4. 4. *Differential abundance analysis of bacterial communities in the rhizosphere. Analysis of Compositions of Microbiomes with Bias Correction-ANCOM-BC (q value <0.1)*

Bacterial ASVs differentially abundant in rhizosphere									
ASV	**LFC**	**W**	**pval**	**qval**	**Phylum**	**Class**	**Order**	**Family**	**Genus**
cf2e620626c48c69cfb088286ebd5ba5	-2.335	-4.199903	0.000	0.030	Proteobacteria	Alphaproteobacteria	Rhizobiales	Devosiaceae	Devosia
0762e31fb10619117f3c7ae618ec4fd3	-2.237	-4.526374	0.000	0.007	Proteobacteria	Alphaproteobacteria	Rhizobiales	Beijerinckiaceae	NA
081aebbe79ffc2bc9436e4bf929dcf46	0.819	4.477115	0.000	0.009	Proteobacteria	Gammaproteobacteria	Xanthomonadales	Rhodanobacteraceae	Frateuria
b8927f8cbc5e99a8b8e53bef26602e8b	0.376	3.948991	0.000	0.088	Verrucomicrobiota	Verrucomicrobiae	Chthoniobacterales	Chthoniobacteraceae	Candidatus_Udaeobacter
a5ee91896ffdedef01bcbf04b540abeb	-2.516	-4.544209	0.000	0.006	Acidobacteriota	Acidobacteriae	Acidobacteriales	uncultured	uncultured_Acidobacteria_bacterium
5b4ac0d6ad75948e0d742afdaf6ec4d9	-2.839	-4.469427	0.000	0.009	Acidobacteriota	Acidobacteriae	Acidobacteriales	uncultured	uncultured_bacterium
aed27d38a2e553ed17c382db52a2f48d	-0.463	-4.615797	0.000	0.004	Acidobacteriota	Acidobacteriae	Acidobacteriales	Acidobacteriaceae__Subgroup_1	NA
b70c59313b42c51eff8e76d6c2c329e0	1.293	4.129344	0.000	0.041	Firmicutes	Bacilli	Paenibacillales	Paenibacillaceae	Paenibacillus
ed41d63c1a3436f8fead4045efaa0125	-1.839	-4.163805	0.000	0.035	Chloroflexi	Ktedonobacteria	C0119	uncultured_bacterium	NA
9ea33e940485c4937ef2f0c89c98cd2f	1.951	4.320960	0.000	0.017	Chloroflexi	Chloroflexia	Thermomicrobiales	JG30_KF_CM45	NA

ca14f7163c872fb17dd812a5d473e006	1.561	4.310273	0.000	0.018	Chloroflexi	KD4_96	uncultured_bacterium	NA	NA
7c927c86e902b14119423b224327b9fe	-2.615	-25.528458	0.000	0.000	Gemmatimonadota	Gemmatimonadetes	Gemmatimonadales	Gemmatimonadaceae	uncultured

***Supplementary Table 4.5**. Statistically significant correlations from the Spearman correlation analysis*

Bacterial class	Metabolite_ID	padj
bacteriap25	103	0.047695
Gemmatimonadetes	6599	0.00000
Gemmatimonadetes	7621	0.00000
Alphaproteobacteria	7448	0.00000
Alphaproteobacteria	5818	0.00000
uncultured_bacterium_1	4054	0.00000
Myxococcia	2416	0.03025

5. General discussion

This thesis aimed to explore changes in plant-soil microbe interactions under the pressure of aphid herbivory by integrating tools from molecular biology, microbiology, and chemical ecology. In this work, aboveground insect herbivory produced significant changes in both the chemistry and microbial communities belowground, supporting the hypothesis that insect pests can significantly alter plant belowground interactions. Among the key signals altered under herbivory were oxylipins and benzoxazinoids, suggesting their potential roles in mediating plant-microbe interactions under aphid feeding.

The first aim of this study was to identify the impact of aphid herbivory in the rhizosphere chemistry and microbial communities of wheat plants from the Solstice cultivar. To my knowledge, this is the first study to integrate tools from analytical chemistry (volatile and non-volatile metabolic profiling above and belowground), microbial metabolism (Ecoplates) and amplicon sequencing (16S rRNA gene) (Chapter 2) to elucidate belowground changes triggered by aboveground pest pressure. Aboveground, two weeks of herbivory were marked by the release of herbivory-induced plant volatiles; belowground, unique profiles of VOCs and non-VOCs were observed along with a more metabolically active microbial community. This increase in microbial activity indicated higher rates of mineralization in the rhizosphere of plants under aphid herbivory which may result from increased root decay, enhanced root exudation, presence of plant secondary metabolites, and microbial proliferation and dead, promoted by aboveground herbivory (Bardgett & Wardle, 2003; Wardle et al., 2004; Wim et al., 2001).

The increased relative abundance of amplicon sequence variants (ASVs) belonging to bacteria such as *Burkholderia* and *Streptomyces* in the bacterial amplicon sequencing data supports these findings, as these genera are widely recognized for their metabolic plasticity (Barrera-Galicia et al., 2021; Dias et al., 2017; Lessie et al., 1996; Paungfoo-Lonhienne et al., 2016; Viaene et al., 2016; Worsley et al., 2020). Their increased abundance could suggest the presence of more complex metabolites –more complex than plant primary metabolites- in the rhizosphere. The increase of other ASVs belonging to other genera from the Actinobacteria class reinforces this idea, as bacteria from this class are widely recognised not only as metabolically versatile, but as one of the most important microbial sources of antibiotics (van der Meij et al., 2017). This is interesting in the context of a susceptible plant under the attack of aphid feeding where Actinobacteria could potentially protect plants from pests and pathogens belowground. Moreover, endophytic Actinobacteria have consistently been identified as promoting plant protection against stresses like the pathogenic *Rhizoctonia solani* (Singh et al., 2017), *Xanthomonas oryzae* (Saikia & Bora, 2021), and *Sclerotium rolfsii* (Singh & Gaur, 2016).

It is tempting to suggest that the distinct metabolic profiles from the rhizosphere of plants under aphid feeding are due to the presence of secondary metabolites in root exudates and the microbial metabolism of these more complex sources. However, a limitation of the experiment presented in Chapter 2 was that the technique chosen to analyse the metabolites was not sufficient to get identities of these metabolites, or possible classifications. Furthermore, it would have not been possible to separate signals according to their original source (e.g., plants or microorganisms) from rhizosphere soil samples. To help disentangle plant chemical signals from others in the rhizosphere, a second experiment (Chapter 3) was performed which included collection of root exudates instead of rhizosphere metabolites and the use of a wider

set of chemoinformatic tools to improve metabolite annotation. Furthermore, amplicon sequencing of root bacterial communities was performed to assess the structure of bacterial communities in this plant compartment, as roots are a more restrictive environment and bacterial communities there are expected to have a closer relationship with the plant host (Quiza et al., 2023).

The analysis of root exudates (Chapter 3) using a semi-hybrid root exudate collection method, and the data-dependent acquisition analysis allowed to successfully annotate some of the plant signals increased under aphid herbivory. By using untargeted metabolomics approaches, this study demonstrated the significant impact that insect herbivory has on the release of chemicals from plants roots. One of the findings was a significantly distinct profile of root exudates, with some metabolites exhibiting >10-fold increases in the samples from plants under aphid herbivory. Benzoxazinoids, allelopathic and antimicrobial secondary metabolites produced by cereals (Cotton et al., 2019; Neal et al., 2012; Zhou et al., 2018), were increased in root exudates of plants under aphid herbivory, while a cluster of metabolites annotated as oxylipins showed an overall decrease. Other compounds that were impacted by aphid herbivory belong to flavonoids, coumarins and amino acids.

Given the complexity of annotating data from untargeted metabolomics, further research is necessary to identify metabolites that may play key roles in plant-microbe communication. In this thesis, the use of multiple analytical tools enabled the exploration of metabolite responses across diverse metabolic pathways, though a significant number of metabolites remained unidentified. However, their mass spectra and retention times are known, providing a valuable foundation for future studies.

Efforts focused on annotating these metabolites could lead to the discovery of other important compounds in plant root exudates.

In both the rhizosphere and root bacterial communities (Chapter 4), the most notable effect of aphid herbivory was an increased relative abundance of the Actinobacteria class, supporting the findings from Chapter 2. Actinobacteria were predominant in the roots of wheat plants, comprising nearly 74% of the bacterial ASVs in plants under aphid herbivory. This suggests that Actinobacteria function as compatible endophytes in this wheat cultivar. The observed increase in their relative abundance under aphid herbivory indicates a strong association, potentially driven by bacterial responses to plant chemical signals. Correlation analysis further revealed a positive relationship between Actinobacteria and the metabolites that increased under aphid feeding, while also highlighting other bacterial groups of interest, including *Myxococcia*, *Nitrososphaeria*, and *Bacilli*.

Overall, my thesis identified changes in the rhizosphere chemistry and microbial communities of wheat plants under aphid herbivory (Chapter 2), allowing the classification and annotation of differentially abundant metabolites in root exudates under herbivory (Chapter 3) and pointing at the Actinobacteria class as first responders to changes due to insect herbivory in chemical signals from plant roots (Chapters 2 and 4). In the following sections, these main results will be discussed in the context of plant-microbe interactions research.

5.1. Capturing plant signals under natural conditions

The critical role of plant-associated microbes in promoting plant growth, nutrition and health has been extensively demonstrated. For this reason, understanding the factors that shape microbial communities in the rhizosphere has become a top priority in the search for sustainable management practices in agriculture. Root exudates, which mediate interactions between plant roots and microbes, play a central role in microbial recruitment (Huang et al., 2014), and their study is crucial to identify key metabolites involved in the recruitment of beneficial or pathogenic microorganisms.

Capturing the full range of plant root exudates under natural conditions remains challenging, largely due to the heterogeneity of both the soil and the exudation of molecules across the root system (Oburger & Jones, 2018). To improve reproducibility and gain clearer insights into root exudates, many studies have been conducted in controlled systems, such as hydroponics or inert substrates like vermiculite, sand, or glass beads (Oburger & Jones, 2018). However, untargeted metabolic profiling has revealed significant differences in the composition of root exudates between plants grown in hydroponic systems and those grown in unsterile soil, with the latter shown to contain 2.4 to 3.8 times more secondary metabolites than those grown hydroponically (Heuermann et al., 2023). For this reason, to capture the diversity of secondary metabolites involved in plant-microbe interactions, it is preferred to perform experiments in conditions that mimic natural systems.

In this study, I adapted a root exudate collection method that combines the benefits of growing plants under natural conditions while avoiding the complexity of interactions with soil organisms. This approach proved effective in both greenhouse

and field settings. This method seems to be efficient in both greenhouse and field conditions, though it's important to acknowledge that root damage during extraction can impact the exudate composition (Oburger & Jones, 2018). However, consecutive washes of plant roots before collection and acclimation of the roots to the collection solution has been shown to minimize these effects (Williams et al., 2021). A short collection time was sufficient to capture a notable signal from the plant metabolites, as has been shown in other studies, and also reduces the impact of microbial mineralization (Kuijken et al., 2015; McLaughlin et al., 2023). In some studies, addition of antibiotics into the collection water helps prevent microbial degradation of metabolites, but there is evidence that antibiotics can reduce root metabolite secretion, specifically of organic acids and phenylpropanoids by 50% and 70%, respectively (Heuermann et al., 2023; Valentinuzzi et al., 2015). For this reason, antibiotics were avoided in this study, and to prevent microbial degradation samples were quenched in liquid nitrogen immediately after collection and filtered using a 0.22 µm Millipore system.

While no root exudate collection method is entirely free from bias, the approach used in this study proved effective for characterising and comparing the metabolites present in the root exudates of wheat plants under aphid feeding versus control plants. Given the consistency in experimental conditions, I expect these results to reflect processes that occur under natural conditions. Future studies could compare these results with those obtained under field conditions to assess whether the key metabolites identified in this study are also present in the field, or whether other environmental factors influence plant metabolism.

Plant VOCs: Unravelling the Role of Root Volatiles in Plant-Microbe Interactions

Plant root volatile organic compounds (VOCs) are emerging as key mediators of interactions among plants, microbes, and other soil biota (Honeker et al., 2021). Unlike aboveground VOCs, root-derived VOCs remain underexplored due to technical challenges in capturing and analysing them under natural conditions, where their diffusion rates in the soil are poorly understood (Eilers et al., 2015; Gulati et al., 2020). These VOCs can diffuse several centimetres through the soil matrix, potentially extending plant influence beyond the rhizosphere into bulk soil microbial communities (Honeker et al., 2021; Raza et al., 2021).

In Chapter 2, a novel setup using polydimethylsiloxane (PDMS) tubes was employed to passively capture root VOCs released in response to aphid feeding. PDMS tubes are widely used for VOC sampling due to their affordability, robustness, and ease of handling (Eilers et al., 2015). Among the identified VOCs released exclusively under herbivory were aldehydes, toluene, and nonane—compounds commonly associated with plant VOCs (Bouwmeester et al., 2019; Zhou & Jander, 2022). Some of these, however, may originate from microbes. For instance, hexanal, a VOC detected in this study, has been reported as a microbial metabolite in *Fusarium* species, where it exhibits antifungal activity (Katoch et al., 2017). Its presence under herbivory suggests potential antimicrobial roles in shaping microbial communities, though the specific origin—plant or microbial—remains unresolved.

To separate root-derived VOCs from soil-origin VOCs, a complementary method was attempted in Chapter 3, where PDMS tubes were placed in water collecting root exudates. While this approach was limited by low VOC concentrations during the short sampling period (2 hours), β-farnesene—a VOC commonly associated with aphid responses in aboveground tissues (Pu et al., 2019) —was uniquely detected under herbivory. This highlights a potential belowground role for β-farnesene, though its ecological significance needs further investigation.

Root VOCs with known ecological functions, such as diterpenoids in maize, have been shown to modulate microbial communities, influencing *Alphaproteobacteria* and *Sphingomonadales* (Murphy et al., 2021). Similarly, methyl jasmonate can induce biofilm formation in bacterial communities (Kulkarni et al., 2024). Experimental tools such as olfactometer assays have been recently employed to investigate whether bacteria in synthetic communities are differentially attracted to VOCs from healthy or herbivore-infested plants (Schulz-Bohm et al., 2018). This interesting approach allows to separate plants from microbial communities and disentangle the origin of belowground VOCs.

Hexanal Production and the Complexity of Rhizosphere VOCs

The case of hexanal exemplifies the intricate dynamics of rhizosphere VOCs and the challenges in disentangling plant and microbial contributions. Hexanal is synthesized via the lipoxygenase (LOX) pathway through lipid peroxidation of linoleic acid. In the analysis of non-VOCs presented in Chapter 3, a decrease in oxylipins derived from linoleic acid was observed in the root exudates of plants under aphid feeding. This suggests that plants may redirect linoleic acid metabolism towards hexanal and other

green leaf volatiles (GLVs) as a defence mechanism. GLVs, including hexanal, are well-documented for their roles in protecting plants against herbivory and microbial attack (Ameye et al., 2018; Hassan et al., 2015).

Alternatively, the reduction in linoleic acid could result from shifts in plant resource allocation. Aphid feeding likely created a strong sink for phloem sap, reducing the distribution of metabolites to roots and altering metabolic priorities. This may have increased aboveground production of volatile oxylipins at the expense of translocation to the roots. Another plausible explanation is that volatile oxylipins were actively being produced in roots under herbivory, depleting linoleic acid precursors synthesised in the roots. Furthermore, microbial activity in the rhizosphere may also play a role. Soil microbes, competing for plant-derived resources under herbivory, could metabolise linoleic acid derivatives to produce hexanal. For example, *Fusarium* species have been shown to synthesize hexanal with antifungal properties (Katoch et al., 2017). This interplay between plant and microbial metabolism highlights the complexity of rhizosphere interactions and the difficulty of attributing specific metabolite signals to their origins (Chen et al., 2024).

5.2. Untargeted Metabolomics: A Key Tool for Understanding Plant-Soil Microbe Interactions

Untargeted metabolomics is gaining increasing recognition for its unprecedented ability to characterise a vast number of metabolites present in complex samples, including plant metabolites. This approach helps unravel the complexities of plant defence mechanisms, which involve a delicate balance between growth and defence.

These processes are coordinated through the activation and crosstalk of multiple metabolic pathways. As public databases continue to expand and new tools for discovering natural products are developed, the characterization of metabolites and their roles in plant defence is becoming increasingly sophisticated. Initiatives like the LOTUS database (Rutz et al., 2022), which provides access to a curated collection of over 750,000 referenced structure-organism pairs, offer valuable resources for linking chemical structures to their originating organisms. The integration of metabolomics tools enables the streamlined transition from raw data to molecular network analysis, facilitating the discovery of bioactive compounds (Pakkir Shah et al., 2024). Additionally, specialised tools like MicrobeMasst (Zuffa et al., 2024) and PlantMasst (Gomes et al., 2024) are advancing our understanding of plant-microbe interactions by allowing researchers to identify which metabolites have been reported to originate from plants and/or microbes.

However, the success of these tools depends on the accessibility of raw data and analysis pipelines, which are often not as widely shared as they could be in the metabolomics community (Broeckling et al., 2023; Evans et al., 2020). For high-quality results, it is critical to ensure that experimental designs are robust, and that correct quality control measures, as well as appropriate parameters for library matching and metabolite annotation, are employed.

In this thesis, Chapter 3 focused on untargeted metabolomics analysis of wheat root exudates in response to aphid feeding. Significant effort was dedicated to integrating both experimental and in silico tools to improve metabolite annotation. Although the number of annotated metabolites was relatively low—a common limitation of

untargeted metabolomics—chemoinformatic tools enabled the classification of nearly 25% of detected peaks into chemical classes.

A key consideration in using these tools is their tendency to identify potential matches based on available data, which may not always be biologically relevant. While thresholds can help reduce false classifications, it remains the researcher's responsibility to evaluate these annotations in the context of the study. In this work, careful attention was paid to the confidence level of the chemical classifications, with only those exhibiting at least 80% confidence in matching public spectra being accepted. The classifications were consistent with plant systems, and some of the annotated metabolites exhibited significant fold changes across various biochemical pathways, including fatty acids, amino acids, benzoxazinoids, phenolics, and terpenoids. These findings, when integrated with the changes in aboveground plant volatile organic compounds (VOCs) under aphid feeding (Chapter 2), support the observation of a systemic plant response to aphid herbivory, which was coupled with changes in microbial communities.

Untargeted methods complement and improve knowledge in insect-wheat-soil microbe interactions

Conventional methods, or targeted approaches, have been key to understand plants responses to insect herbivory. In the case of cereal crops, benzoxazinoids (BXs) have been long recognised recognized for their role in plant defence against a variety of insect pests, including aphids. These indole-derived compounds have been found to increase in plant leaves and roots in response to different insect pests including mites (Bui et al., 2018), the western corn rootworm (Alouw & Miller, 2015), and the fall

armyworm (Israni et al., 2020), and aphids (Shavit et al., 2018; Zhang et al., 2021). Beyond confirming the importance of BXs, untargeted methods have also identified other metabolites that may be crucial in mediating plant defence. Lavergne et al., (2020) showed that the insect stem sawfly increased the production not only of BXs but also neolignans and phenolics in wheat stems. Similarly, (Wang et al., 2022) observed the induction of phenylpropanoid/flavonoid pathway products in wheat kernels following exposure to the orange wheat blossom midge. With the knowledge generated by this approach, more efficient methods for plant protection can be developed that target not only one compound, but a mixture of protecting compounds that can help improve wheat plant resistance to insect herbivory.

BXs have also been suggested to be responsible for belowground plant-microbe interactions under insect herbivory. Using benzoxazinoid mutant *bx1* maize plants, (Hu et al., 2018), demonstrated that an individual benzoxazinoid –Six-methoxy-benzoxazolin-2-one (MBOA)- was responsible for changes in microbiome that lead to increase in maize resistance against *Spodoptera frugiperda*. More recent untargeted metabolomics studies suggest BXs also regulate root metabolism in maize, with BX-dependent metabolites from other chemical classes contributing to microbial modulation (Cotton et al., 2019). In this thesis, untargeted metabolomics confirmed that certain BX compounds increased under aphid herbivory. Simultaneously, other metabolites, including oxylipins, amino acids, flavonoids, coumarins, and terpenes, were also altered in the wheat rhizosphere, aligning with previous findings (Lavergne et al., 2020; Wang et al., 2022). While increased metabolites likely play a crucial role in recruiting microbial communities, this work emphasizes the need to consider downregulated metabolites and their combined effects with upregulated compounds. For instance, reduced oxylipins might enhance Actinobacteria colonization, as jasmonic acid—a type of oxylipin—has been shown to inhibit the growth of

Actinobacteria (van der Meij et al., 2023). Simultaneously, BXs may stimulate secondary metabolite production by these bacteria, further aiding plants in protecting against rhizosphere threats. Further work using the bacterial collection from this work could help unveil which microbial taxa interact with which (single or mixture) compounds, which would help elucidate the key compounds in recruiting and shaping the rhizosphere microbial communities under aphid herbivory.

5.3. Impact of microbial communities on plant response to aphid herbivory

The reduced diversity of microbial communities in the rhizosphere, compared with the diversity found in the soil, suggests a selection process of microbial communities that are dynamic and change throughout a plant's lifetime, showing that microbes respond to and influence plant growth and response to the environment (de la Fuente Cantó et al., 2020; Finkel et al., 2017). Extensive work has shown that under stress, plants are able to modify the microbial communities in the rhizosphere continuum (rhizosphere, rhizoplane, root endosphere) and point at root exudates as key factors driving these changes (Rolfe et al., 2019). However, the extent to which these changes in composition of microbial communities affect plant response to stresses depends on different factors including the soil physical and chemical properties, the microbial community's composition in the soil, the type of stress, and plant genetics (Dastogeer et al., 2020).

Most of the current literature evidence the ability of plants to modify the microbial communities under stress, recruiting microbes that enhance plant response to the

stress. Under insect herbivory, such shifts in microbial communities have been shown to support plant defence responses (Hu et al., 2018; Hubbard et al., 2019; Pineda et al., 2010; Sobhy et al., 2022). Moreover, studies have reported the ability of bacterial inoculants to increase resistance of plants to aphid herbivory. Inoculation of wheat seeds with a combination of bacterial strains belonging to *Azotobacter, Azospirillum* and *Pseudomonas* reduced the reproductive rate of the aphid *Sitobion avenae*, correlated with an increase in content of flavonoids, total phenols, and anthocyanin on plant leaves (Pourya et al., 2020). Other studies have found that inoculation with *Bacillus velenzis* induces systemic resistance by triggering reactive oxygen species (ROS) generation and callose deposition, without relying on classical hormonal pathways like salicylic acid (SA), jasmonic acid (JA), or abscisic acid (ABA) (Harun-Or-Rashid et al., 2017). Conversely, some studies have reported that changes in microbial communities –single strains or entire communities- resulted in increased susceptibility to the insect pest. For instance, Kim et al. (2015) showed that aphid herbivory increased the colonization of plants by bacteria from the genus *Paenibacillus* which, in turn, increased aphids' population on inoculated plants. (Katayama et al., 2014) showed that aphid herbivory reduced the contribution of fixed nitrogen by rhizobia and propose that aphid herbivory weakens plant-rhizobia symbiosis via carbon stress (legumes need to dedicate around 6 to 14% of their carbon to nodulation). Furthermore, Blubaugh et al. (2018) reported that an increase in bacteria from the *Bacillus* and *Pseudomonas* genera can alter both the plant ability to attract natural enemies of the aphids and increased plant susceptibility. These examples show that plant-soil bacteria interactions are species-specific, and *in vitro,* greenhouse and field studies are necessary for individual insect-plant-soil microbe interactions.

In this thesis, a top-to-bottom effect of insect herbivory was observed, where aphid feeding stress aboveground affected bacterial communities in the rhizosphere and plant roots. These results align with other studies of insect herbivory reducing bacterial diversity in tomato (French et al., 2021) and European beech plants (Potthast et al., 2022). However, other studies have failed to find differences in bacterial communities and point at the soil fertilization and plant growth stage as the defining factors that shape microbial communities (O'Brien et al., 2018; Vestergård et al., 2004). The lack of significant differences after four weeks of aphid herbivory in the first experiment (Chapter 2) might be attributed to plant growth stage, which potentially had a more substantial impact on microbial communities than aphid herbivory itself.

A consistent result in the analysis of bacterial communities' composition was the increase in ASVs corresponding to the Actinobacteria class in the rhizosphere (Chapter 2) and roots (Chapter 4) of wheat plants under aphid feeding. While other studies have found increases in *Bacillus, Paenibacillus, Pseudomonas* and *Stenotrophomonas* (Blubaugh et al., 2018; Ourry et al., 2018) in the rhizosphere in response to aphid herbivory, Actinobacteria have been not previously reported in this context. This observation may be specific to wheat cultivar interactions with soil microbial communities. Further research testing different soil types and wheat cultivars with varying aphid resistance could help clarify whether these bacteria also increase in other wheat cultivars under different conditions. Interestingly, extracts of the metabolites produced by Actinobacteria from the *Streptomyces* genera have been observed to have insecticidal activity against vetch aphid (*Medoura viciae* Buckt.), cotton aphid *(Aphis gossypii* Glov.), green peach aphid (*Myzus persicae* Sulz.), pea aphid *(Acyrthosiphon pisum* Harr.) and crescent-marked lily aphid *(Neomyzus circumflexus* Buckt.) (Boykova et al., 2023), pointing at the ability of these bacteria to directly impact aphid herbivory via production of antibiotic compounds.

Although not measured here, given the diverse traits of these bacteria, it is plausible to suggest different scenarios in which Actinobacteria could potentially impact wheat plant response to aphid feeding. These include 1) enhancing the mineralization of complex carbon and nitrogen sources in the soil, helping plants balance growth and defence, 2) potentially inducing systemic resistance via root colonisation or VOCs release, which could enhance plant's ability to produce defence compounds, or 3) producing antimicrobial metabolites to regulate microbial communities and prevent pest and pathogen attacks. However, there are other scenarios in which Actinobacteria could increase plant susceptibility, such as promoting nutrient availability that benefit aphids, and competing with plant roots for resources in the soil, adding another layer of stress for the plants. To test these scenarios, further work using approaches like the use of synthetic microbial communities, transcriptomics and metabolomics could help elucidate the role of these bacteria in their interaction with plant roots by analysing which metabolic pathways are activated in the bacteria in response to the root exudates of plants under aphid feeding.

5.4. Impact of timing of aphid herbivory on soil microbial communities

The timing of aphid herbivory plays a crucial role in plant defence mechanisms and may also influence soil microbial communities. In this study, no differences in volatile organic compounds (VOCs) were observed in wheat plants after four weeks of aphid herbivory (Chapter 2). A plausible explanation emerges from the work of Xu et al. (2021), who demonstrated that the dynamics of plant resistance and enzymatic activity vary over time in susceptible and resistant wheat cultivars. Their study highlighted that in susceptible wheat cultivars enzymatic markers such as

peroxidases, PAL (phenylalanine ammonia-lyase), and TAL (tyrosine ammonia-lyase) peak at specific times, particularly around 30 days after aphid herbivory, but decline afterward. This suggests that susceptible plants may prioritize tolerance mechanisms over-active defence as time progresses, contrasting with resistant cultivars that maintained consistently higher levels of enzymatic activity and defence metabolites.

The work of Xu et al. (2021), also emphasized that phenolic content in susceptible wheat plants increased significantly at 15 days post-herbivory but dropped to a minimum by 45 days. These temporal changes in plant defence align with the hypothesis that sampling at a single time point, as is common in many greenhouse studies, risks missing critical phases of plant defence and tolerance strategies. For example, early time points, typically within 96 hours post-infection (e.g., Stewart et al. (2016), often capture the immediate plant response but may overlook the transition to longer-term tolerance mechanisms.

Future studies could investigate the interplay between plant enzymatic activity, metabolite production, and microbial community dynamics in response to aphid herbivory. Correlating these enzymatic markers with shifts in root-associated microbial communities over time could increase our understanding of how changes in benzoxazinoids, phenolic content and other defence metabolites influence microbial recruitment in the rhizosphere and root compartments and help elucidate whether specific microbes contribute to sustaining plant tolerance or enhancing resistance over prolonged periods of insect herbivory.

5.5. Insect endosymbionts add another layer of complexity to insect-plant-soil microbe interactions

Aphids rely on their endosymbionts to synthesize essential amino acids. Beyond their nutritional role, aphid endosymbionts are increasingly recognized as key players in modulating plant defence responses. Some aphid endosymbionts suppress plant defence by manipulating the salicylic acid signalling pathway, which is typically involved in responses to microbial pathogens, while also downregulating the jasmonic acid pathway, reducing herbivory-induced plant volatiles and other secondary metabolites (Lee et al., 2012). These changes leave plants more vulnerable to aphid herbivory while potentially altering their interaction with soil microbes.

Aphid endosymbionts can also alter aphid resistance to plant specialised metabolites. For example, the endosymbiont *Regiella insecticola* alters aphid performance on wheat plants with varying levels of the benzoxazinoid DIMBOA, increasing aphid population rate in cultivars with medium DIMBOA levels, while significantly decreasing it in cultivars with high DIMBOA levels (Gonzalez-Gonzalez et al., 2024). It has also been suggested that the aphid endosymbionts can counteract plant-induced resistance by the beneficial strain *Bacillus amyloliquefaciens* FZB42 (Serteyn et al., 2020). Furthermore, Hackett et al. (2013) also demonstrated that aphid endosymbionts reduce carbon allocation to plant roots, potentially influencing microbial community composition by altering the availability of carbon exudates.

While endosymbionts are well-documented to confer resistance against parasitoids, their broader ecological roles, particularly in modulating plant-soil microbe

interactions, remain largely unexplored. Understanding how aphid endosymbionts influence microbial communities and plant defence pathways could provide novel insights into insect-plant-microbe dynamics. Future research should investigate how these endosymbionts affect microbial recruitment and function within the rhizosphere and explore the potential for targeted application of beneficial bacteria. For example, screening for microbes capable of enhancing jasmonic acid signalling could strengthen plant resistance to aphid herbivory and offset the negative effects of salicylic acid pathway manipulation by aphid endosymbionts. Such approaches could form the basis of sustainable pest management strategies that leverage plant-microbe interactions to reduce aphid damage.

5.6. Connecting above and belowground: The need for multidisciplinary studies

As demonstrated throughout this discussion, the intricate interactions between insects, plants, and soil microbes cannot be fully understood when studied in isolation. Addressing these complex relationships requires a multidisciplinary approach that integrates ecological, physiological, biochemical, and molecular perspectives. Combining these disciplines will provide a more comprehensive understanding of how these organisms influence one another, leading to practical applications in sustainable agriculture and pest management.

The following points summarise key areas where a multidisciplinary perspective is essential:

- **Active Rhizobacterial Communities:** While amplicon sequencing has provided valuable insights into bacterial diversity, further investigation into the active bacterial communities in the rhizosphere is needed. Techniques such

as metatranscriptomics and stable isotope probing (SIP) could help elucidate which bacterial taxa are directly interacting with plant root exudates and which are benefiting from microbial cross-feeding. Integrating microbial ecology, biochemistry, and plant physiology will enhance the design of synthetic bacterial communities, improving our understanding of the role of microbial communities on plant defence against aphid herbivory.

- **Microbial Metabolome in Response to Plant Stress:** This thesis work demonstrated that aphid herbivory alters the rhizosphere metabolome and plant root exudates. Employing untargeted and targeted metabolomics can help identify volatile and non-volatile microbial metabolites that could influence plant response to herbivory. Collaborations between the fields of chemistry, microbiology and plant physiology will uncover how these metabolites shape plant-microbe interactions and contribute to plant defence mechanisms.

- **Beyond Bacteria:** The soil is a complex system where microbes are part of a trophic chain that includes nematodes, protozoa, and arthropods. Beyond bacterial and fungal interactions, other soil biota are known to affect plant response to biotic and abiotic stresses. Multidisciplinary research that incorporates soil ecology, entomology, and plant sciences can provide a broader perspective on how diverse soil organisms influence plant resilience under aphid herbivory.

- **Aphids as Complex Ecosystems:** Aphids are not merely herbivores; they host diverse microbial communities, including bacteria, fungi, and viruses that impact plant defences. Understanding the ecological role of aphid-associated microbes requires a combination of entomological studies, microbial ecology, and molecular biology. Investigating how these microbial communities' mediate aphid-plant interactions could uncover novel strategies for pest management.

- **Comparing Ancestral and Modern Wheat Cultivars:** The differences in root exudate profiles between ancestral and modern wheat cultivars influence the composition of rhizosphere bacterial communities. Combining metabolomics, microbiome analysis, and plant breeding research can clarify whether microbial communities recruited by resistant ancestral cultivars contribute to plant defence. Such insights could guide the development of more resilient crop varieties.
- **Climate Change and Multifactorial Stress Responses:** With the uncertainty of climatic events and the increase of drought and floods, plants in agricultural fields will almost certainly be subjected to both biotic and abiotic stresses. Investigating how these combined stresses affect insect-plant-soil microbe interactions demands an integrated research approach. Combining expertise in climate science, plant physiology, microbial ecology, and entomology will be critical for predicting and mitigating the effects of climate change on crop health.

5.7. Conclusions

This work presents the first step and the foundation to the question*: Herbivore-Plant-Soil microbe interaction: Who is helping whom?* Through a multidisciplinary approach, I explored the chemical and microbial responses of wheat plants under aphid herbivory, providing new insights into the complexity of belowground interactions.

The initial challenge was to detect measurable changes in plant-soil microbe interactions under aboveground herbivory. Given the limited knowledge on the

chemical signalling involved in these interactions, I applied a broad profiling strategy to evaluate both soil chemistry and microbial community dynamics. In Chapter 2, I observed that plant aboveground response –measured in unique volatile organic compounds (VOCs) released under herbivory- correlated with changes in the profile of root VOCs and non-volatile metabolites present in the rhizosphere. Furthermore, a significant increase in microbial metabolic activity, especially in the presence of carbohydrates and carboxylic acids, suggested changes in the rate of mineralisation of nutrients by microbial communities, further indicating an involvement of microbial communities in plant-aphid interaction. Analysis of bacterial community's structure using amplicon sequencing revealed an increase in the relative abundance of amplicon sequence variants (ASVs) classified as *Burkholderia, Streptomyces, Streptacidiphilus,* among others. Of all the ASVs that were enriched under aphid herbivory, 53% belong to the Actinobacteria class, suggesting that these bacteria might be able to respond to the changes occurring in the root chemical signalling under aphid herbivory.

To further investigate the chemical signals involved in plant-soil microbe interactions, I conducted an untargeted metabolomics analysis to capture root exudate profiles (Chapter 3). While previous research mainly focused on targeted metabolites (e.g., benzoxazinoids), the untargeted approach revealed the complexity of the chemical signalling in root exudates, with a diverse set of metabolites (flavonoids, alkaloids, benzoxazinoids, terpenoids), which increased in root exudates of plants under herbivory. On the other hand, some primary metabolites (fatty acids, small peptides) were reduced. These results underscore the complexity of root exudate chemistry and highlight the limitations of targeted approaches. The untargeted strategy used here offers a baseline for future investigations into the specific roles of these metabolites in shaping microbial communities.

In Chapter 4, I further analysed bacterial communities more closely associated with plant roots. The Actinobacteria class was consistently shown to be closely associated with wheat plant roots. However, under herbivory, this association seemed to be even stronger for some of the genera first observed in Chapter 2. For example, ASVs from the *Streptomyces* and *Streptacidiphilus* genera were increased. An interesting result was that, in the roots, other Actinobacteria genus that are less well-known and explored, like *Marmoricola* genus, were also increased, suggesting novel directions for further research in the impact of these bacteria on plant-aphid interactions.

While the complexity of the interactions occurring between aphids, plants and soil microbes prevented to fully unravel the role of soil microbes on plant-aphid interactions, this thesis work presents clear evidence of aboveground herbivory influencing belowground chemical and microbial processes, measured by chemical profile in the rhizosphere, changes in microbial metabolic activity and changes in bacterial communities' composition. Furthermore, candidate metabolites and responsive bacterial taxa identified in this work offer unexplored areas for further research.

In conclusion, this thesis improves our understanding of the effect of aboveground herbivory on plant-soil microbe interactions. Future studies can use this knowledge to experimentally test the functional roles of the identified metabolites and microbial taxa. By helping disentangle the complexity of belowground interactions occurring in plants under aphid herbivory, this research could help elucidate how to use plant root exudates and microbial communities to improve plant responses to aphid herbivory, further developing sustainable strategies of pest management.

Key contributions for further research:

- A complete protocol was developed for the analysis of plant root exudates. The pipeline and analysis allowed to annotate 2.8% of the detected metabolites, while using other chemoinformatic tools allowed to chemically classify almost 25% of the metabolites. These analyses allowed to successfully identify key metabolites that changed in exudates of plants under herbivory, and pointed at key chemical classes, like Benzoxazinoids and oxylipins as key compounds responsive to aphid herbivory. This protocol, and the knowledge generated will be fundamental to following projects aiming to understand the role of these compounds on microbial recruitment in the rhizosphere.

- A bacterial culture collection was created by isolating bacterial strains in an Actinobacteria-specific media and a nutrient-rich media. The bacterial identification made by 16S rRNA sequencing allowed to identify isolates belonging to different genera in the Actinobacteria class including *Streptomyces, Kitasatospora,* and *Pseudoarthrobacter,* as well as *Paenibacillus* and *Burkholderia.* This bacterial collection will be useful for further research testing their individual and combined interactions with identified metabolites in root exudates, and their effects on plant-aphid interactions.

References

Abbasi, S., Safaie, N., Sadeghi, A., & Shamsbakhsh, M. (2019). Streptomyces Strains Induce Resistance to Fusarium oxysporum f. Sp. Lycopersici Race 3 in Tomato through Different Molecular Mechanisms. *Frontiers in Microbiology*, *10*(JUL). https://doi.org/10.3389/fmicb.2019.01505

Abd-Allah, E. F., Alqarawi, A. A., Hashem, A., Radhakrishnan, R., Al-Huqail, A. A., Al-Otibi, F. O. N., Malik, J. A., Alharbi, R. I., & Egamberdieva, D. (2018). Endophytic bacterium Bacillus subtilis (BERA 71) improves salt tolerance in chickpea plants by regulating the plant defense mechanisms. *Journal of Plant Interactions*, *13*(1), 37–44. https://doi.org/10.1080/17429145.2017.1414321

Abdullaeva, Y., Ratering, S., Ambika Manirajan, B., Rosado-Porto, D., Schnell, S., & Cardinale, M. (2022). Domestication Impacts the Wheat-Associated Microbiota and the Rhizosphere Colonization by Seed- and Soil-Originated Microbiomes, Across Different Fields. *Frontiers in Plant Science*, *12*. https://doi.org/10.3389/fpls.2021.806915

Affeldt, K. J., Brodhagen, M., & Keller, N. P. (2012). Aspergillus oxylipin signaling and quorum sensing pathways depend on G protein-coupled receptors. *Toxins*, *4*(9), 695–717. https://doi.org/10.3390/toxins4090695

Al-Khayri, J. M., Rashmi, R., Toppo, V., Chole, P. B., Banadka, A., Sudheer, W. N., Nagella, P., Shehata, W. F., Al-Mssallem, M. Q., Alessa, F. M., Almaghasla, M. I., & Rezk, A. A. S. (2023). Plant Secondary Metabolites: The Weapons for Biotic Stress Management. In *Metabolites* (Vol. 13, Issue 6). MDPI. https://doi.org/10.3390/metabo13060716

Alouw, J. C., & Miller, N. J. (2015). Effects of benzoxazinoids on specialist and generalist Diabrotica species. *Journal of Applied Entomology*, *139*(6), 424–431. https://doi.org/10.1111/jen.12194

Álvarez-Lagazzi, A. P., Cabrera, N., Francis, F., & Ramírez, C. C. (2021). Bacillus subtilis (Bacillales, Bacillaceae) Spores Affect Survival and Population Growth in the Grain Aphid Sitobion avenae (Hemiptera, Aphididae) in Relation to the Presence of the Facultative Bacterial Endosymbiont Regiella insecticola (Enterobacteriales, Enterobacteriaceae). *Journal of Economic Entomology*, *114*(5), 2043–2050. https://doi.org/10.1093/jee/toab164

Ameye, M., Allmann, S., Verwaeren, J., Smagghe, G., Haesaert, G., Schuurink, R. C., & Audenaert, K. (2018). Green leaf volatile production by plants: a meta-analysis. In *New Phytologist* (Vol. 220, Issue 3, pp. 666–683). Blackwell Publishing Ltd. https://doi.org/10.1111/nph.14671

Anwar, S., Ali, B., & Sajid, I. (2016). Screening of rhizospheric actinomycetes for various in-vitro and in-vivo plant growth promoting (PGP) traits and for agroactive compounds. *Frontiers in Microbiology*, *7*(AUG). https://doi.org/10.3389/fmicb.2016.01334

Aradottir, G. I., & Crespo-Herrera, L. (2021). Host plant resistance in wheat to barley yellow dwarf viruses and their aphid vectors: a review. In *Current Opinion in Insect Science* (Vol. 45, pp. 59–68). Elsevier Inc. https://doi.org/10.1016/j.cois.2021.01.002

Arimura, G. ichiro. (2021). Making Sense of the Way Plants Sense Herbivores. In *Trends in Plant Science* (Vol. 26, Issue 3, pp. 288–298). Elsevier Ltd. https://doi.org/10.1016/j.tplants.2020.11.001

Armanda, D. T., Guinée, J. B., & Tukker, A. (2019). The second green revolution: Innovative urban agriculture's contribution to food security and sustainability – A review. In *Global Food Security* (Vol. 22, pp. 13–24). Elsevier B.V. https://doi.org/10.1016/j.gfs.2019.08.002

Aron, A. T., Gentry, E. C., McPhail, K. L., Nothias, L. F., Nothias-Esposito, M., Bouslimani, A., Petras, D., Gauglitz, J. M., Sikora, N., Vargas, F., van der Hooft, J. J. J., Ernst, M., Kang, K. Bin, Aceves, C. M., Caraballo-Rodríguez, A. M., Koester, I., Weldon, K. C., Bertrand, S., Roullier, C., … Dorrestein, P. C. (2020). Reproducible molecular networking of untargeted mass spectrometry data using GNPS. *Nature Protocols*, *15*(6), 1954–1991. https://doi.org/10.1038/s41596-020-0317-5

Auguie B (2017). _gridExtra: Miscellaneous Functions for "Grid" Graphics_. R package version 2.3, <https://CRAN.R-project.org/package=gridExtra>.

Ayoubi, A., Talebi, A. A., Fathipour, Y., & Mehrabadi, M. (2020). Coinfection of the secondary symbionts, Hamiltonella defensa and Arsenophonus sp. contribute to the performance of the major aphid pest, Aphis gossypii (Hemiptera: Aphididae). Insect Science, 27(1), 86–98. https://doi.org/10.1111/1744-7917.12603

Bakker, P. A. H. M., Pieterse, C. M. J., de Jonge, R., & Berendsen, R. L. (2018). The Soil-Borne Legacy. In *Cell* (Vol. 172, Issue 6, pp. 1178–1180). Cell Press. https://doi.org/10.1016/j.cell.2018.02.024

Balcerowicz, M. (2024). Lost in domestication: Has modern wheat left its microbial allies behind? *The Plant Journal: For Cell and Molecular Biology*, *120*(4), 1261–1262. https://doi.org/10.1111/tpj.17137

Baldwin, I. T., & Preston, C. A. (1999). *The eco-physiological complexity of plant responses to insect herbivores* (Vol. 208, Issue 2). https://www.jstor.org/stable/23385542?seq=1&cid=pdf-

Bardgett, R. D., & Wardle, D. A. (2003). Herbivore-mediated linkages between aboveground and belowground communities. In *Ecology* (Vol. 84, Issue 9, pp. 2258–2268). Ecological Society of America. https://doi.org/10.1890/02-0274

Barrera-Galicia, G. C., Peniche-Pavía, H. A., Peña-Cabriales, J. J., Covarrubias, S. A., Vera-Núñez, J. A., & Délano-Frier, J. P. (2021). Metabolic footprints of burkholderia sensu lato rhizosphere bacteria active against maize fusarium pathogens†. *Microorganisms*, *9*(10). https://doi.org/10.3390/microorganisms9102061

Batyrshina, Z. S., Yaakov, B., Shavit, R., Singh, A., & Tzin, V. (2020). Comparative transcriptomic and metabolic analysis of wild and domesticated wheat genotypes reveals differences in chemical and physical defense responses against aphids. *BMC Plant Biology*, *20*(1). https://doi.org/10.1186/s12870-019-2214-z

Bending, G. D., Newman, A., Picot, E., Mushinski, R. M., Jones, D. L., & Carré, I. A. (2024). Diurnal Rhythmicity in the Rhizosphere Microbiome—Mechanistic Insights

and Significance for Rhizosphere Function. In *Plant Cell and Environment*. John Wiley and Sons Inc. https://doi.org/10.1111/pce.15283

Benjamin, G., Pandharikar, G., & Frendo, P. (2022). Salicylic Acid in Plant Symbioses: Beyond Plant Pathogen Interactions. In *Biology* (Vol. 11, Issue 6). MDPI. https://doi.org/10.3390/biology11060861

Berenbaum, M. R., & Zanger, A. R. (2008). Facing the future of plant-insect interaction research: Le retour à la “raison d’être.” In *Plant Physiology* (Vol. 146, Issue 3, pp. 804–811). American Society of Plant Biologists. https://doi.org/10.1104/pp.107.113472

Berg, G., Rybakova, D., Fischer, D., Cernava, T., Vergès, M. C. C., Charles, T., Chen, X., Cocolin, L., Eversole, K., Corral, G. H., Kazou, M., Kinkel, L., Lange, L., Lima, N., Loy, A., Macklin, J. A., Maguin, E., Mauchline, T., McClure, R., … Schloter, M. (2020). Microbiome definition re-visited: old concepts and new challenges. In *Microbiome* (Vol. 8, Issue 1). BioMed Central Ltd. https://doi.org/10.1186/s40168-020-00875-0

Bittremieux, W., Schmid, R., Huber, F., Van Der Hooft, J. J. J., Wang, M., & Dorrestein, P. C. (2022). Comparison of Cosine, Modified Cosine, and Neutral Loss Based Spectrum Alignment For Discovery of Structurally Related Molecules. *Journal of the American Society for Mass Spectrometry*, *33*(9), 1733–1744. https://doi.org/10.1021/jasms.2c00153

Blubaugh, C. K., Carpenter-Boggs, L., Reganold, J. P., Schaeffer, R. N., & Snyder, W. E. (2018). Bacteria and competing herbivores weaken top–down and bottom–up aphid suppression. *Frontiers in Plant Science*, *9*. https://doi.org/10.3389/fpls.2018.01239

Bokulich, N. A., Kaehler, B. D., Rideout, J. R., Dillon, M., Bolyen, E., Knight, R., Huttley, G. A., & Gregory Caporaso, J. (2018). Optimizing taxonomic classification of marker-gene amplicon sequences with QIIME 2’s q2-feature-classifier plugin. *Microbiome*, *6*(1). https://doi.org/10.1186/s40168-018-0470-z

Bolyen, E., Rideout, J. R., Dillon, M. R., Bokulich, N. A., Abnet, C. C., Al-Ghalith, G. A., Alexander, H., Alm, E. J., Arumugam, M., Asnicar, F., Bai, Y., Bisanz, J. E., Bittinger, K., Brejnrod, A., Brislawn, C. J., Brown, C. T., Callahan, B. J., Caraballo-Rodríguez, A. M., Chase, J., … Caporaso, J. G. (2019). Reproducible, interactive, scalable and extensible microbiome data science using QIIME 2. In *Nature Biotechnology* (Vol. 37, Issue 8, pp. 852–857). Nature Publishing Group. https://doi.org/10.1038/s41587-019-0209-9

Bonaldi, M., Chen, X., Kunova, A., Pizzatti, C., Saracchi, M., & Cortesi, P. (2015). Colonization of lettuce rhizosphere and roots by tagged Streptomyces. *Frontiers in Microbiology*, *6*(FEB). https://doi.org/10.3389/fmicb.2015.00025

Borg, A. N., Vuts, J., Caulfield, J. C., Withall, D. M., Foulkes, M. J., & Birkett, M. A. (2024). Characterisation of aphid antixenosis in aphid-resistant ancestor wheat, Triticum monococcum. *Pest Management Science*. https://doi.org/10.1002/ps.8380

Borman T, Ernst F, Lahti L (2024). _miaViz: Microbiome Analysis Plotting and Visualization_. R package version 1.13.14, commit 69ef62c96d11ec4ce5d4a658228725366d68f59c, <https://github.com/microbiome/miaViz>.

Bouwmeester, H., Schuurink, R. C., Bleeker, P. M., & Schiestl, F. (2019). The role of volatiles in plant communication. In *Plant Journal* (Vol. 100, Issue 5, pp. 892–907). Blackwell Publishing Ltd. https://doi.org/10.1111/tpj.14496

Boykova, I., Yuzikhin, O., Novikova, I., Ulianich, P., Eliseev, I., Shaposhnikov, A., Yakimov, A., & Belimov, A. (2023). Strain Streptomyces sp. P-56 Produces Nonactin and Possesses Insecticidal, Acaricidal, Antimicrobial and Plant Growth-Promoting Traits. *Microorganisms*, *11*(3). https://doi.org/10.3390/microorganisms11030764

Broeckling, C. D., Beger, R. D., Cheng, L. L., Cumeras, R., Cuthbertson, D. J., Dasari, S., Davis, W. C., Dunn, W. B., Evans, A. M., Fernández-Ochoa, A., Gika, H., Goodacre, R., Goodman, K. D., Gouveia, G. J., Hsu, P. C., Kirwan, J. A., Kodra, D., Kuligowski, J., Lan, R. S. L., … Mosley, J. D. (2023). Current Practices in LC-MS Untargeted Metabolomics: A Scoping Review on the Use of Pooled Quality Control Samples. In *Analytical Chemistry* (Vol. 95, Issue 51, pp. 18645–18654). American Chemical Society. https://doi.org/10.1021/acs.analchem.3c02924

Broeckling, C. D., Broz, A. K., Bergelson, J., Manter, D. K., & Vivanco, J. M. (2008). Root exudates regulate soil fungal community composition and diversity. *Applied and Environmental Microbiology*, *74*(3), 738–744. https://doi.org/10.1128/AEM.02188-07

Bruce, T. J. A. (2015). Interplay between insects and plants: Dynamic and complex interactions that have coevolved over millions of years but act in milliseconds. In *Journal of Experimental Botany* (Vol. 66, Issue 2, pp. 455–465). Oxford University Press. https://doi.org/10.1093/jxb/eru391

Bui, H., Greenhalgh, R., Ruckert, A., Gill, G. S., Lee, S., Ramirez, R. A., & Clark, R. M. (2018). Generalist and specialist mite herbivores induce similar defense responses in maize and barley but differ in susceptibility to benzoxazinoids. *Frontiers in Plant Science*, *9*. https://doi.org/10.3389/fpls.2018.01222

Caesar, L. K., Kellogg, J. J., Kvalheim, O. M., & Cech, N. B. (2019). Opportunities and Limitations for Untargeted Mass Spectrometry Metabolomics to Identify Biologically Active Constituents in Complex Natural Product Mixtures. *Journal of Natural Products*, *82*(3), 469–484. https://doi.org/10.1021/acs.jnatprod.9b00176

Callahan, B. J., McMurdie, P. J., & Holmes, S. P. (2017). Exact sequence variants should replace operational taxonomic units in marker-gene data analysis. *ISME Journal*, *11*(12), 2639–2643. https://doi.org/10.1038/ismej.2017.119

Callahan, B. J., McMurdie, P. J., Rosen, M. J., Han, A. W., Johnson, A. J. A., & Holmes, S. P. (2016). DADA2: High-resolution sample inference from Illumina amplicon data. *Nature Methods*, *13*(7), 581–583. https://doi.org/10.1038/nmeth.3869

Callahan, B. J., Wong, J., Heiner, C., Oh, S., Theriot, C. M., Gulati, A. S., McGill, S. K., & Dougherty, M. K. (2019). High-throughput amplicon sequencing of the full-length 16S rRNA gene with single-nucleotide resolution. *Nucleic Acids Research*, *47*(18), E103. https://doi.org/10.1093/NAR/GKZ569

Canarini, A., Kaiser, C., Merchant, A., Richter, A., & Wanek, W. (2019). Root exudation of primary metabolites: Mechanisms and their roles in plant responses to environmental stimuli. In *Frontiers in Plant Science* (Vol. 10). Frontiers Media S.A. https://doi.org/10.3389/fpls.2019.00157

Caporaso, J. G., Lauber, C. L., Walters, W. A., Berg-Lyons, D., Lozupone, C. A., Turnbaugh, P. J., Fierer, N., & Knight, R. (2011). Global patterns of 16S rRNA diversity at a depth of millions of sequences per sample. *Proceedings of the National Academy of Sciences of the United States of America*, *108*(SUPPL. 1), 4516–4522. https://doi.org/10.1073/pnas.1000080107

Cavaco, A. R., Matos, A. R., & Figueiredo, A. (2021). Speaking the language of lipids: the cross-talk between plants and pathogens in defence and disease. In *Cellular and Molecular Life Sciences* (Vol. 78, Issue 9, pp. 4399–4415). Springer Science and Business Media Deutschland GmbH. https://doi.org/10.1007/s00018-021-03791-0

Charters, M. D., Sait, S. M., & Field, K. J. (2020). Aphid Herbivory Drives Asymmetry in Carbon for Nutrient Exchange between Plants and an Arbuscular Mycorrhizal Fungus. *Current Biology*, *30*(10), 1801-1808.e5. https://doi.org/10.1016/j.cub.2020.02.087

Chaturvedi, H., & Singh, V. (2016). Potential of Bacterial Endophytes as Plant Growth Promoting Factors. *Journal of Plant Pathology & Microbiology*, *7*(9). https://doi.org/10.4172/2157-7471.1000376

Chen, B., Han, H., Hou, J., Bao, F., Tan, H., Lou, X., Wang, G., & Zhao, F. (2022). Control of Maize Sheath Blight and Elicit Induced Systemic Resistance Using Paenibacillus polymyxa Strain SF05. *Microorganisms*, *10*(7). https://doi.org/10.3390/microorganisms10071318

Chen H (2022). _VennDiagram: Generate High-Resolution Venn and Euler Plots_. R package version 1.7.3, <https://CRAN.R-project.org/package=VennDiagram>.

Chen, P., Dai, C., Liu, H., & Hou, M. (2022). Identification of Key Headspace Volatile Compounds Signaling Preference for Rice over Corn in Adult Females of the Rice Leaf Folder Cnaphalocrocis medinalis. *Journal of Agricultural and Food Chemistry*, *70*(32), 9826–9833. https://doi.org/10.1021/acs.jafc.2c01948

Chen, W., He, P., Zhang, H., & Lü, F. (2024). Effects of volatile fatty acids on soil properties, microbial communities, and volatile metabolites in wheat rhizosphere of loess. *Journal of Cleaner Production*, *476*. https://doi.org/10.1016/j.jclepro.2024.143798

Chen, X., Pizzatti, C., Bonaldi, M., Saracchi, M., Erlacher, A., Kunova, A., Berg, G., & Cortesi, P. (2016). Biological control of lettuce drop and host plant colonization by rhizospheric and endophytic streptomycetes. *Frontiers in Microbiology*, *7*(MAY). https://doi.org/10.3389/fmicb.2016.00714

Chong, R. A., & Moran, N. A. (2018). Evolutionary loss and replacement of Buchnera, the obligate endosymbiont of aphids. *The ISME journal*, *12*(3), 898–908. https://doi.org/10.1038/s41396-017-0024-6

Chukwuneme, C. F., Babalola, O. O., Kutu, F. R., & Ojuederie, O. B. (2020). Characterization of actinomycetes isolates for plant growth promoting traits and their effects on drought tolerance in maize. *Journal of Plant Interactions*, *15*(1), 93–105. https://doi.org/10.1080/17429145.2020.1752833

Chung Kim, K. (1993). Biodiversity, conservation and inventory: why insects matter. In *Biodiversity and Conservation* (Vol. 2).

Cotton, T. E. A., Pétriacq, P., Cameron, D. D., Meselmani, M. Al, Schwarzenbacher, R., Rolfe, S. A., & Ton, J. (2019a). Metabolic regulation of the maize rhizobiome by benzoxazinoids. *ISME Journal*, *13*(7), 1647–1658. https://doi.org/10.1038/s41396-019-0375-2

Dastogeer, K. M. G., Tumpa, F. H., Sultana, A., Akter, M. A., & Chakraborty, A. (2020). Plant microbiome–an account of the factors that shape community composition and diversity. In *Current Plant Biology* (Vol. 23). Elsevier B.V. https://doi.org/10.1016/j.cpb.2020.100161

de la Fuente Cantó, C., Simonin, M., King, E., Moulin, L., Bennett, M. J., Castrillo, G., & Laplaze, L. (2020). An extended root phenotype: the rhizosphere, its formation and impacts on plant fitness. In *Plant Journal* (Vol. 103, Issue 3, pp. 951–964). Blackwell Publishing Ltd. https://doi.org/10.1111/tpj.14781

Deb, C. R., & Tatung, M. (2024). Siderophore producing bacteria as biocontrol agent against phytopathogens for a better environment: A review. In *South African Journal of Botany* (Vol. 165, pp. 153–162). Elsevier B.V. https://doi.org/10.1016/j.sajb.2023.12.031

Deboever, E., Deleu, M., Mongrand, S., Lins, L., & Fauconnier, M. L. (2020). Plant–Pathogen Interactions: Underestimated Roles of Phyto-oxylipins. In *Trends in Plant Science* (Vol. 25, Issue 1, pp. 22–34). Elsevier Ltd. https://doi.org/10.1016/j.tplants.2019.09.009

Defossez, E., Bourquin, J., von Reuss, S., Rasmann, S., & Glauser, G. (2023). Eight key rules for successful data-dependent acquisition in mass spectrometry-based metabolomics. In *Mass Spectrometry Reviews* (Vol. 42, Issue 1, pp. 131–143). John Wiley and Sons Inc. https://doi.org/10.1002/mas.21715

Delory, B. M., Delaplace, P., Fauconnier, M. L., & du Jardin, P. (2016). Root-emitted volatile organic compounds: Can they mediate belowground plant-plant interactions? In *Plant and Soil* (Vol. 402, Issues 1–2, pp. 1–26). Springer International Publishing. https://doi.org/10.1007/s11104-016-2823-3

DeWolf, E., Brock, M. T., Calder, W. J., Kliebenstein, D. J., Katz, E., Li, B., Morrison, H. G., Maïgnien, L., & Weinig, C. (2023). The rhizosphere microbiome and host plant glucosinolates exhibit feedback cycles in Brassica rapa. *Molecular Ecology*, *32*(3), 741–751. https://doi.org/10.1111/mec.16782

Di, T., Zhao, L., Chen, H., Qian, W., Wang, P., Zhang, X., & Xia, T. (2019). Transcriptomic and Metabolic Insights into the Distinctive Effects of Exogenous Melatonin and Gibberellin on Terpenoid Synthesis and Plant Hormone Signal Transduction Pathway in Camellia sinensis. *Journal of Agricultural and Food Chemistry*, *67*(16), 4689–4699. https://doi.org/10.1021/acs.jafc.9b00503

Dias, M. P., Bastos, M. S., Xavier, V. B., Cassel, E., Astarita, L. V., & Santarém, E. R. (2017). Plant growth and resistance promoted by Streptomyces spp. in tomato. *Plant Physiology and Biochemistry*, *118*, 479–493. https://doi.org/10.1016/j.plaphy.2017.07.017

Dimkić, I., Janakiev, T., Petrović, M., Degrassi, G., & Fira, D. (2022). Plant-associated Bacillus and Pseudomonas antimicrobial activities in plant disease suppression via biological control mechanisms - A review. In *Physiological and Molecular Plant Pathology* (Vol. 117). Academic Press. https://doi.org/10.1016/j.pmpp.2021.101754

Disi, J. O., Kloepper, J. W., & Fadamiro, H. Y. (2018). Seed treatment of maize with Bacillus pumilus strain INR-7 affects host location and feeding by Western corn rootworm, Diabrotica virgifera virgifera. *Journal of Pest Science*, *91*(2), 515–522. https://doi.org/10.1007/s10340-017-0927-z

Douglas, A. E., & Werren, J. H. (2016). Holes in the hologenome: Why host-microbe symbioses are not holobionts. In *mBio* (Vol. 7, Issue 2). American Society for Microbiology. https://doi.org/10.1128/mBio.02099-15

Dudareva, N., Pichersky, E., & Gershenzon, J. (2004). Biochemistry of plant volatiles. In *Plant Physiology* (Vol. 135, Issue 4, pp. 1893–1902). American Society of Plant Biologists. https://doi.org/10.1104/pp.104.049981

Dudzik, D., Barbas-Bernardos, C., García, A., & Barbas, C. (2018). Quality assurance procedures for mass spectrometry untargeted metabolomics. a review. In *Journal of Pharmaceutical and Biomedical Analysis* (Vol. 147, pp. 149–173). Elsevier B.V. https://doi.org/10.1016/j.jpba.2017.07.044

Dührkop, K., Fleischauer, M., Ludwig, M., Aksenov, A. A., Melnik, A. V., Meusel, M., Dorrestein, P. C., Rousu, J., & Böcker, S. (2019). SIRIUS 4: a rapid tool for turning tandem mass spectra into metabolite structure information. *Nature Methods*, *16*(4), 299–302. https://doi.org/10.1038/s41592-019-0344-8

Ehrlich, P. R., & Raven, P. H. (1964). BUTTERFLIES AND PLANTS: A STUDY IN COEVOLUTION. *Evolution*, *18*(4), 586–608. https://doi.org/10.1111/j.1558-5646.1964.tb01674.x

Eichmann, R., Richards, L., & Schäfer, P. (2021). Hormones as go-betweens in plant microbiome assembly. *Plant Journal*, *105*(2), 518–541. https://doi.org/10.1111/tpj.15135

Eilers, E. J., Pauls, G., Rillig, M. C., Hansson, B. S., Hilker, M., & Reinecke, A. (2015). Novel Set-Up for Low-Disturbance Sampling of Volatile and Non-volatile Compounds from Plant Roots. *Journal of Chemical Ecology*, *41*(3), 253–266. https://doi.org/10.1007/s10886-015-0559-9

El Abiead, Y., Rutz, A., Zuffa, S., Amer, B., Xing, S., Brungs, C., Schmid, R., Correia, M. S. P., Caraballo-Rodriguez, A. M., Zarrinpar, A., Mannochio-Russo, H., Witting, M., Mohanty, I., Pluskal, T., Bittremieux, W., Knight, R., Patterson, A. D., van der Hooft, J. J. J., Böcker, S., … Dorrestein, P. C. (2025). Discovery of metabolites prevails amid in-source fragmentation. In *Nature Metabolism*. Nature Research. https://doi.org/10.1038/s42255-025-01239-4

Elston, K. M., Leonard, S. P., Geng, P., Bialik, S. B., Robinson, E., & Barrick, J. E. (2022). Engineering insects from the endosymbiont out. Trends in Microbiology, 30(1), 79–96. https://doi.org/10.1016/j.tim.2021.05.004

Erb, M., & Kliebenstein, D. J. (2020). Plant Secondary Metabolites as Defenses, Regulators, and Primary Metabolites: The Blurred Functional Trichotomy1[OPEN]. In *Plant Physiology* (Vol. 184, Issue 1, pp. 39–52). American Society of Plant Biologists. https://doi.org/10.1104/PP.20.00433

Erb, M., Meldau, S., & Howe, G. A. (2012). Role of phytohormones in insect-specific plant reactions. In *Trends in Plant Science* (Vol. 17, Issue 5, pp. 250–259). https://doi.org/10.1016/j.tplants.2012.01.003

Ernst F, Shetty S, Borman T, Lahti L (2024). _mia: Microbiome analysis_. R package version 1.13.46, commit c76bc909b1dc8f30886ada7cdbc94138c592a14c, <https://github.com/microbiome/mia>.

Evans, A. M., O'Donovan, C., Playdon, M., Beecher, C., Beger, R. D., Bowden, J. A., Broadhurst, D., Clish, C. B., Dasari, S., Dunn, W. B., Griffin, J. L., Hartung, T., Hsu, P. C., Huan, T., Jans, J., Jones, C. M., Kachman, M., Kleensang, A., Lewis, M. R., … Vuckovic, D. (2020). Dissemination and analysis of the quality assurance (QA) and quality control (QC) practices of LC–MS based untargeted metabolomics practitioners. *Metabolomics*, *16*(10). https://doi.org/10.1007/s11306-020-01728-5

Fan, K., Holland-Moritz, H., Walsh, C., Guo, X., Wang, D., Bai, Y., Zhu, Y. guan, Fierer, N., & Chu, H. (2022). Identification of the rhizosphere microbes that actively consume plant-derived carbon. *Soil Biology and Biochemistry*, *166*. https://doi.org/10.1016/j.soilbio.2022.108577

Fatima, S., & Anjum, T. (2017). Identification of a potential ISR determinant from pseudomonas aeruginosa PM12 against fusarium wilt in tomato. *Frontiers in Plant Science*, *8*. https://doi.org/10.3389/fpls.2017.00848

Felton, G. W., Chung, S. H., Estrada, M. G., Louis, J., Peiffer, M., & Tian, D. (2014). Herbivore Oral Secretions are the First Line of Protection AgainstPlant-Induced Defences. In C. Voelckel & G. Jander (Eds.), *Insect-Plant interactions* (First, Vol. 47, pp. 37–76). Wiley Blackwell.

Feng, J. L., Zhang, J., Yang, J., Zou, L. P., Fang, T. T., Xu, H. L., & Cai, Q. N. (2021). Exogenous salicylic acid improves resistance of aphid-susceptible wheat to the grain aphid, Sitobion avenae (F.) (Hemiptera: Aphididae). *Bulletin of Entomological Research*, *111*(5), 544–552. https://doi.org/10.1017/S0007485321000237

Feng, Y. Z., Zhu, Q. F., Xue, J., Chen, P., & Yu, Y. (2023). Shining in the dark: the big world of small peptides in plants. In *aBIOTECH* (Vol. 4, Issue 3, pp. 238–256). Springer. https://doi.org/10.1007/s42994-023-00100-0

Feng, Z., Liang, Q., Yao, Q., Bai, Y., & Zhu, H. (2024). The role of the rhizobiome recruited by root exudates in plant disease resistance: current status and future directions. In *Environmental Microbiome* (Vol. 19, Issue 1). BioMed Central Ltd. https://doi.org/10.1186/s40793-024-00638-6

Fernie, A. R., Trethewey, R. N., Krotzky, A. J., & Willmitzer I N N Ovat I O N, L. (2004). *Metabolite profiling: from diagnostics to systems biology*. www.nature.com/reviews/molcellbio

Figueredo, M. S., Álamo, T., Tonelli, M. L., & Fabra, A. (2023). The native strain Paenibacillus sp. A224 induces systemic tolerance and mitigates stresses caused in peanut plants by high temperatures and the pathogen Sclerotium rolfsii. *Plant and Soil*, *486*(1–2), 375–390. https://doi.org/10.1007/s11104-023-05876-0

Finkel, O. M., Castrillo, G., Herrera Paredes, S., Salas González, I., & Dangl, J. L. (2017). Understanding and exploiting plant beneficial microbes. In *Current Opinion in Plant Biology* (Vol. 38, pp. 155–163). Elsevier Ltd. https://doi.org/10.1016/j.pbi.2017.04.018

Florean, M., Luck, K., Hong, B., Nakamura, Y., O'Connor, S. E., & Köllner, T. G. (2023). Reinventing metabolic pathways: Independent evolution of benzoxazinoids in

flowering plants. *Proceedings of the National Academy of Sciences of the United States of America*, *120*(42). https://doi.org/10.1073/pnas.2307981120

Flors, V., Kyndt, T., Mauch-Mani, B., Pozo, M. J., Ryu, C.-M., & Ton, J. (2024). Enabling sustainable crop protection with induced resistance in plants. *Frontiers in Science*, *2*. https://doi.org/10.3389/fsci.2024.1407410

Food and Agriculture Organization of the United Nations (FAO). (2024). *Wheat market summary*. FAO. https://www.fao.org/worldfoodsituation/csdb/en

Fraenkel, G. S. (1959). The Raison d'Etre of Secondary Plant Substances. *Science*, *129*(3361), 1466–1470. https://www.science.org

Frago, E., Mala, M., Weldegergis, B. T., Yang, C., McLean, A., Godfray, H. C. J., Gols, R., & Dicke, M. (2017). Symbionts protect aphids from parasitic wasps by attenuating herbivore-induced plant volatiles. Nature Communications, 8(1), 1860. https://doi.org/10.1038/s41467-017-01935-0

French, E., Kaplan, I., & Enders, L. (2021). Foliar Aphid Herbivory Alters the Tomato Rhizosphere Microbiome, but Initial Soil Community Determines the Legacy Effects. *Frontiers in Sustainable Food Systems*, *5*. https://doi.org/10.3389/fsufs.2021.629684

Friman, J., Karssemeijer, P. N., Haller, J., de Kreek, K., van Loon, J. J. A., & Dicke, M. (2021a). Shoot and root insect herbivory change the plant rhizosphere microbiome and affects cabbage–insect interactions through plant–soil feedback. *New Phytologist*, *232*(6), 2475–2490. https://doi.org/10.1111/nph.17746

Friman, J., Pineda, A., van Loon, J. J. A., & Dicke, M. (2021b). Bidirectional plant-mediated interactions between rhizobacteria and shoot-feeding herbivorous insects: a community ecology perspective. In *Ecological Entomology* (Vol. 46, Issue 1, pp. 1–10). Blackwell Publishing Ltd. https://doi.org/10.1111/een.12966

Fuloria, N. K., Raheja, R. K., Shah, K. H., Oza, M. J., Kulkarni, Y. A., Subramaniyan, V., Sekar, M., & Fuloria, S. (2022). Biological activities of meroterpenoids isolated from different sources. In *Frontiers in Pharmacology* (Vol. 13). Frontiers Media S.A. https://doi.org/10.3389/fphar.2022.830103

Gaiero, J. R., McCall, C. A., Thompson, K. A., Day, N. J., Best, A. S., & Dunfield, K. E. (2013). Inside the root microbiome: Bacterial root endophytes and plant growth promotion. *American Journal of Botany*, *100*(9), 1738–1750. https://doi.org/10.3732/ajb.1200572

Giordanengo, P., Brunissen, L., Rusterucci, C., Vincent, C., Van Bel, A., Dinant, S., Girousse, C., Faucher, M., & Bonnemain, J. L. (2010). Compatible plant-aphid interactions: How aphids manipulate plant responses. *Comptes Rendus - Biologies*, *333*(6–7), 516–523. https://doi.org/10.1016/j.crvi.2010.03.007

Goggin, F. L. (2007). Plant-aphid interactions: molecular and ecological perspectives. In *Current Opinion in Plant Biology* (Vol. 10, Issue 4, pp. 399–408). https://doi.org/10.1016/j.pbi.2007.06.004

Gomes, P. W. P., Mannochio-Russo, H., Schmid, R., Zuffa, S., Damiani, T., Quiros-Guerrero, L.-M., Caraballo-Rodríguez, A. M., Zhao, H. N., Yang, H., Xing, S., Charron-Lamoureux, V., Chigumba, D. N., Sedio, B. E., Myers, J. A., Allard, P.-M., Harwood, T. V., Tamayo-Castillo, G., Kang, K. Bin, Defossez, E., … Dorrestein, P. C.

(2024). *plantMASST - Community-driven chemotaxonomic digitization of plants*. https://doi.org/10.1101/2024.05.13.593988

Gonzalez-Gonzalez, A., Cabrera, N., Rubio-Meléndez, M. E., Sepúlveda, D. A., Ceballos, R., Fernández, N., Francis, F., Figueroa, C. C., & Ramirez, C. C. (2024). Facultative endosymbionts modulate the aphid reproductive performance on wheat cultivars differing in contents of benzoxazinoids. *Pest Management Science*, *80*(4), 1949–1956. https://doi.org/10.1002/ps.7932

Granér, G., Hamberg, M., & Meijer, J. (2003). Screening of oxylipins for control of oilseed rape (Brassica napus) fungal pathogens. *Phytochemistry*, *63*(1), 89–95. https://doi.org/10.1016/S0031-9422(02)00724-0

Greenslade, A. F. C., Ward, J. L., Martin, J. L., Corol, D. I., Clark, S. J., Smart, L. E., & Aradottir, G. I. (2016). Triticum monococcum lines with distinct metabolic phenotypes and phloem-based partial resistance to the bird cherry-oat aphid Rhopalosiphum padi. *Annals of Applied Biology*, *168*(3), 435–449. https://doi.org/10.1111/aab.12274

Grigorescu, A. S., Renoz, F., Sabri, A., Foray, V., Hance, T., & Thonart, P. (2018). Accessing the Hidden Microbial Diversity of Aphids: An Illustration of How Culture-Dependent Methods Can Be Used to Decipher the Insect Microbiota. Microbial Ecology, 75(4), 1035–1048. https://doi.org/10.1007/s00248-017-1092-x

Gruet, C., Muller, D., & Moënne-Loccoz, Y. (2022). Significance of the Diversification of Wheat Species for the Assembly and Functioning of the Root-Associated Microbiome. In *Frontiers in Microbiology* (Vol. 12). Frontiers Media S.A. https://doi.org/10.3389/fmicb.2021.782135

Gu, Y., Wei, Z., Wang, X., Friman, V. P., Huang, J., Wang, X., Mei, X., Xu, Y., Shen, Q., & Jousset, A. (2016). Pathogen invasion indirectly changes the composition of soil microbiome via shifts in root exudation profile. *Biology and Fertility of Soils*, *52*(7), 997–1005. https://doi.org/10.1007/s00374-016-1136-2

Gu, Z., Eils, R., & Schlesner, M. (2016). Complex heatmaps reveal patterns and correlations in multidimensional genomic data. *Bioinformatics*, *32*(18), 2847–2849. https://doi.org/10.1093/bioinformatics/btw313

Gulati, S., Ballhausen, M. B., Kulkarni, P., Grosch, R., & Garbeva, P. (2020). A non-invasive soil-based setup to study tomato root volatiles released by healthy and infected roots. *Scientific Reports*, *10*(1). https://doi.org/10.1038/s41598-020-69468-z

Guo, J., & Huan, T. (2020). Comparison of Full-Scan, Data-Dependent, and Data-Independent Acquisition Modes in Liquid Chromatography-Mass Spectrometry Based Untargeted Metabolomics. *Analytical Chemistry*, *92*(12), 8072–8080. https://doi.org/10.1021/acs.analchem.9b05135

Guo, J., Hatt, S., He, K., Chen, J., Francis, F., & Wang, Z. (2017). Nine facultative endosymbionts in aphids. A review. Journal of Asia-Pacific Entomology, 20(3), 794–801. https://doi.org/10.1016/j.aspen.2017.03.025

Guo K, McGregor B (2024). _VennDetail: A package for visualization and extract details_. R package version 1.20.0, <https://github.com/guokai8/VennDetail>.

Gurung, K., Wertheim, B., & Falcao Salles, J. (2019). The microbiome of pest insects: It is not just bacteria. Entomologia Experimentalis et Applicata, 167(3), 156–170. https://doi.org/10.1111/eea.12768

Hackett, S. C., Karley, A. J., & Bennett, A. E. (2013). Unpredicted impacts of insect endosymbionts on interactions between soil organisms, plants and aphids. *Proceedings of the Royal Society B: Biological Sciences*, *280*(1768). https://doi.org/10.1098/rspb.2013.1275

Hall, R., Beale, M., Fiehn, O., Hardy, N., Sumner, L., & Bino, R. (2002). *Plant Metabolomics: The Missing Link in Functional Genomics Strategies*. https://academic.oup.com/plcell/article/14/7/1437/6009774

Hammer, T. J., Sanders, J. G., & Fierer, N. (2019). Not all animals need a microbiome. In *FEMS Microbiology Letters* (Vol. 366, Issue 10). Oxford University Press. https://doi.org/10.1093/femsle/fnz117

Hao, P., Liu, C., Wang, Y., Chen, R., Tang, M., Du, B., Zhu, L., & He, G. (2008). Herbivore-induced callose deposition on the sieve plates of rice: An important mechanism for host resistance. *Plant Physiology*, *146*(4), 1810–1820. https://doi.org/10.1104/pp.107.111484

Hardoim, P. R., van Overbeek, L. S., & Elsas, J. D. van. (2008). Properties of bacterial endophytes and their proposed role in plant growth. *Trends in Microbiology*, *16*(10), 463–471. https://doi.org/10.1016/j.tim.2008.07.008

Haribal, M., & Jander, G. (2015). Stable isotope studies reveal pathways for the incorporation of non-essential amino acids in Acyrthosiphon pisum (pea aphids). *Journal of Experimental Biology*, *218*(23), 3797–3806. https://doi.org/10.1242/jeb.129189

Harun-Or-Rashid, M., Khan, A., Hossain, M. T., & Chung, Y. R. (2017). Induction of systemic resistance against aphids by endophytic bacillus velezensis YC7010 via expressing PHYTOALEXIN DEFICIENT4 in arabidopsis. *Frontiers in Plant Science*, *8*. https://doi.org/10.3389/fpls.2017.00211

Hassan, M. N., Zainal, Z., & Ismail, I. (2015). Green leaf volatiles: Biosynthesis, biological functions and their applications in biotechnology. In *Plant Biotechnology Journal* (Vol. 13, Issue 6, pp. 727–739). Blackwell Publishing Ltd. https://doi.org/10.1111/pbi.12368

Hawes, M., Allen, C., Turgeon, B. G., Curlango-Rivera, G., Tran, T. M., Huskey, D. A., & Xiong, Z. (2016). Root Border Cells and Their Role in Plant Defense. *Annual Review of Phytopathology*, *54*, 143–161. https://doi.org/10.1146/annurev-phyto-080615-100140

Hawes, M. C., Brigham, L. A., Wen, F., Woo, H. H., & Zhu, Y. (1998). FUNCTION OF ROOT BORDER CELLS IN PLANT HEALTH: Pioneers 1 in the Rhizosphere. In *Annu. Rev. Phytopathol* (Vol. 36). www.annualreviews.org.

He, B., Chen, X., Yang, H., & Cernava, T. (2021). Microbiome Structure of the Aphid Myzus persicae (Sulzer) Is Shaped by Different Solanaceae Plant Diets. Frontiers in Microbiology, 12, 667257. https://doi.org/10.3389/fmicb.2021.667257

He, M., & Ding, N. Z. (2020). Plant Unsaturated Fatty Acids: Multiple Roles in Stress Response. In *Frontiers in Plant Science* (Vol. 11). Frontiers Media S.A. https://doi.org/10.3389/fpls.2020.562785

Hedden, P. (2003). The genes of the Green Revolution. *TRENDS in Genetics*, *19*(1), 5–9.

Heuermann, D., Döll, S., Schweneker, D., Feuerstein, U., Gentsch, N., & von Wirén, N. (2023). Distinct metabolite classes in root exudates are indicative for field- or hydroponically-grown cover crops. *Frontiers in Plant Science*, *14*. https://doi.org/10.3389/fpls.2023.1122285

Heyworth, E. R., Smee, M. R., & Ferrari, J. (2020). Aphid Facultative Symbionts Aid Recovery of Their Obligate Symbiont and Their Host After Heat Stress. Frontiers in Ecology and Evolution, 8, 56. https://doi.org/10.3389/fevo.2020.00056

Hickman, D. T., Rasmussen, A., Ritz, K., Birkett, M. A., & Neve, P. (2021). Review: Allelochemicals as multi-kingdom plant defence compounds: towards an integrated approach. In *Pest Management Science* (Vol. 77, Issue 3, pp. 1121–1131). John Wiley and Sons Ltd. https://doi.org/10.1002/ps.6076

Honeker, L. K., Graves, K. R., Tfaily, M. M., Krechmer, J. E., & Meredith, L. K. (2021). The Volatilome: A Vital Piece of the Complete Soil Metabolome. *Frontiers in Environmental Science*, *9*. https://doi.org/10.3389/fenvs.2021.649905

Hou, K., Wu, Z. X., Chen, X. Y., Wang, J. Q., Zhang, D., Xiao, C., Zhu, D., Koya, J. B., Wei, L., Li, J., & Chen, Z. S. (2022). Microbiota in health and diseases. In *Signal Transduction and Targeted Therapy* (Vol. 7, Issue 1). Springer Nature. https://doi.org/10.1038/s41392-022-00974-4

Howe, G. A., & Jander, G. (2008). Plant immunity to insect herbivores. In *Annual Review of Plant Biology* (Vol. 59, pp. 41–66). https://doi.org/10.1146/annurev.arplant.59.032607.092825

Hoysted, G. A., Bell, C. A., Lilley, C. J., & Urwin, P. E. (2018). Aphid colonization affects potato root exudate composition and the hatching of a soil borne pathogen. *Frontiers in Plant Science*, *9*. https://doi.org/10.3389/fpls.2018.01278

Hu, D., Zang, Y., Mao, Y., & Gao, B. (2019). Identification of molecular markers that are specific to the class thermoleophilia. *Frontiers in Microbiology*, *10*(MAY). https://doi.org/10.3389/fmicb.2019.01185

Hu, L., Mateo, P., Ye, M., Zhang, X., Berset, J. D., Handrick, V., Radisch, D., Grabe, V., Köllner, T. G., Gershenzon, J., Robert, C. A. M., & Erb, M. (2018). Plant iron acquisition strategy exploited by an insect herbivore. In *Science* (Vol. 361, Issue 6403, pp. 694–697). https://doi.org/10.1093/pcp/pcy064

Hu, L., Robert, C. A. M., Cadot, S., Zhang, X., Ye, M., Li, B., Manzo, D., Chervet, N., Steinger, T., Van Der Heijden, M. G. A., Schlaeppi, K., & Erb, M. (2018). Root exudate metabolites drive plant-soil feedbacks on growth and defense by shaping the rhizosphere microbiota. *Nature Communications*, *9*(1). https://doi.org/10.1038/s41467-018-05122-7

Huang, J., Shrestha, K., & Huang, Y. (2022). Revealing Differential Expression of Phytohormones in Sorghum in Response to Aphid Attack Using the Metabolomics Approach. *International Journal of Molecular Sciences*, *23*(22). https://doi.org/10.3390/ijms232213782

Huang, X. F., Chaparro, J. M., Reardon, K. F., Zhang, R., Shen, Q., & Vivanco, J. M. (2014). Rhizosphere interactions: Root exudates, microbes, and microbial communities1. In *Botany* (Vol. 92, Issue 4, pp. 267–275). National Research Council of Canada. https://doi.org/10.1139/cjb-2013-0225

Huang, X., Liu, S., Liu, X., Zhang, S., Li, L., Zhao, H., Zhao, J., Zhang, J., & Cai, Z. (2020). Plant pathological condition is associated with fungal community succession triggered by root exudates in the plant-soil system. *Soil Biology and Biochemistry*, *151*. https://doi.org/10.1016/j.soilbio.2020.108046

Hubbard, C. J., Li, B., McMinn, R., Brock, M. T., Maignien, L., Ewers, B. E., Kliebenstein, D., & Weinig, C. (2019). The effect of rhizosphere microbes outweighs host plant genetics in reducing insect herbivory. *Molecular Ecology*, *28*(7), 1801–1811. https://doi.org/10.1111/mec.14989

Hugerth, L. W., & Andersson, A. F. (2017). Analysing microbial community composition through amplicon sequencing: From sampling to hypothesis testing. In *Frontiers in Microbiology* (Vol. 8, Issue SEP). Frontiers Media S.A. https://doi.org/10.3389/fmicb.2017.01561

Israni, B., Wouters, F. C., Luck, K., Seibel, E., Ahn, S. J., Paetz, C., Reinert, M., Vogel, H., Erb, M., Heckel, D. G., Gershenzon, J., & Vassão, D. G. (2020). The Fall Armyworm Spodoptera frugiperda Utilizes Specific UDP-Glycosyltransferases to Inactivate Maize Defensive Benzoxazinoids. *Frontiers in Physiology*, *11*. https://doi.org/10.3389/fphys.2020.604754

Jankielsohn, A. (2018). The Importance of Insects in Agricultural Ecosystems. *Advances in Entomology*, *06*(02), 62–73. https://doi.org/10.4236/ae.2018.62006

Jaouannet, M., Rodriguez, P. A., Thorpe, P., Lenoir, C. J. G., Macleod, R., Escudero-Martinez, C., & Bos, J. I. B. (2014). Plant immunity in plant-aphid interactions. In *Frontiers in Plant Science* (Vol. 5, Issue DEC). Frontiers Media S.A. https://doi.org/10.3389/fpls.2014.00663

John, D. A., & Babu, G. R. (2021). Lessons From the Aftermaths of Green Revolution on Food System and Health. In *Frontiers in Sustainable Food Systems* (Vol. 5). Frontiers Media S.A. https://doi.org/10.3389/fsufs.2021.644559

Kaloshian, I., & Walling, L. (2016). Plant Immunity: Connecting the Dots Between Microbial and Hemipteran Immune Responses. In H. Czosnek, R. H. , Smith, & M. Ghanim (Eds.), *Management of Insect Pests to Agriculture* (pp. 217–244). Springer.

Kameoka, S., Motooka, D., Watanabe, S., Kubo, R., Jung, N., Midorikawa, Y., Shinozaki, N. O., Sawai, Y., Takeda, A. K., & Nakamura, S. (2021). Benchmark of 16S rRNA gene amplicon sequencing using Japanese gut microbiome data from the V1–V2 and V3–V4 primer sets. *BMC Genomics*, *22*(1). https://doi.org/10.1186/s12864-021-07746-4

Kassambara A (2023). _rstatix: Pipe-Friendly Framework for Basic Statistical Tests_. R package version 0.7.2, <https://CRAN.R-project.org/package=rstatix>.

Kassambara A (2023). _ggpubr: 'ggplot2' Based Publication Ready Plots_. R package version 0.6.0, <https://CRAN.R-project.org/package=ggpubr>.

Kassambara A, & Mundt F (2020). _factoextra: Extract and Visualize the Results of Multivariate Data Analyses_. R package version 1.0.7, <https://CRAN.R-project.org/package=factoextra>.

Karssemeijer, P. N., Reichelt, M., Gershenzon, J., van Loon, J., & Dicke, M. (2020). Foliar herbivory by caterpillars and aphids differentially affects phytohormonal signalling in roots and plant defence to a root herbivore. *Plant Cell and Environment*, *43*(3), 775–786. https://doi.org/10.1111/pce.13707

Katayama, N., Silva, A. O., Kishida, O., Ushio, M., Kita, S., & Ohgushi, T. (2014). Herbivorous insect decreases plant nutrient uptake: The role of soil nutrient availability and association of below-ground symbionts. *Ecological Entomology*, *39*(4), 511–518. https://doi.org/10.1111/een.12125

Katoch, M., Bindu, K., Phull, S., & Verma, M. K. (2017). An endophytic Fusarium sp. isolated from Monarda citriodora produces the industrially important plant-like volatile organic compound hexanal. *Microbiology (United Kingdom)*, *163*(6), 840–847. https://doi.org/10.1099/mic.0.000479

Katoh, K., Misawa, K., Kuma, K.-I., & Miyata, T. (2002). MAFFT: a novel method for rapid multiple sequence alignment based on fast Fourier transform. *Nucleic Acids Research*, *30*(14), 3059–3066.

Kavamura, V. N., Mendes, R., Bargaz, A., & Mauchline, T. H. (2021). Defining the wheat microbiome: Towards microbiome-facilitated crop production. In *Computational and Structural Biotechnology Journal* (Vol. 19, pp. 1200–1213). Elsevier B.V. https://doi.org/10.1016/j.csbj.2021.01.045

Kavamura, V. N., Robinson, R. J., Hughes, D., Clark, I., Rossmann, M., Melo, I. S. de, Hirsch, P. R., Mendes, R., & Mauchline, T. H. (2020). Wheat dwarfing influences selection of the rhizosphere microbiome. *Scientific Reports*, *10*(1). https://doi.org/10.1038/s41598-020-58402-y

Kawahara, A. Y., Reeves, L. E., Barber, J. R., & Black, S. H. (2021). Eight simple actions that individuals can take to save insects from global declines. *PNAS*, *118*(2). https://doi.org/10.1073/pnas.2002547117/-/DCSupplemental

Kim, B., Song, G. C., & Ryu, C. M. (2015). Root exudation by aphid leaf infestation recruits root-associated Paenibacillus spp. To lead plant insect susceptibility. *Journal of Microbiology and Biotechnology*, *26*(3), 549–557. https://doi.org/10.4014/jmb.1511.11058

Kim, H. W., Wang, M., Leber, C. A., Nothias, L. F., Reher, R., Kang, K. Bin, Van Der Hooft, J. J. J., Dorrestein, P. C., Gerwick, W. H., & Cottrell, G. W. (2021). NPClassifier: A Deep Neural Network-Based Structural Classification Tool for Natural Products. In *Journal of Natural Products* (Vol. 84, Issue 11, pp. 2795–2807). American Chemical Society. https://doi.org/10.1021/acs.jnatprod.1c00399

Kim, J. H., Lee, B. W., Schroeder, F. C., & Jander, G. (2008). Identification of indole glucosinolate breakdown products with antifeedant effects on Myzus persicae (green peach aphid). *Plant Journal*, *54*(6), 1015–1026. https://doi.org/10.1111/j.1365-313X.2008.03476.x

Kloth, K. J., & Dicke, M. (2022). Rapid systemic responses to herbivory. In *Current Opinion in Plant Biology* (Vol. 68). Elsevier Ltd. https://doi.org/10.1016/j.pbi.2022.102242

Knight, R., Vrbanac, A., Taylor, B. C., Aksenov, A., Callewaert, C., Debelius, J., Gonzalez, A., Kosciolek, T., McCall, L. I., McDonald, D., Melnik, A. V., Morton, J. T., Navas, J., Quinn, R. A., Sanders, J. G., Swafford, A. D., Thompson, L. R., Tripathi, A., Xu, Z. Z., … Dorrestein, P. C. (2018). Best practices for analysing microbiomes. In *Nature Reviews Microbiology* (Vol. 16, Issue 7, pp. 410–422). Nature Publishing Group. https://doi.org/10.1038/s41579-018-0029-9

Kong, H. G., Kim, B. K., Song, G. C., Lee, S., & Ryu, C. M. (2016). Aboveground whitefly infestation-mediated reshaping of the root microbiota. *Frontiers in Microbiology*, *7*(SEP). https://doi.org/10.3389/fmicb.2016.01314

Koprivova, A., & Kopriva, S. (2022). Plant secondary metabolites altering root microbiome composition and function. In *Current Opinion in Plant Biology* (Vol. 67). Elsevier Ltd. https://doi.org/10.1016/j.pbi.2022.102227

Kranawetter, C., & Sumner, L. W. (2025). Differential root zone secretions and the role of root border cells in rhizosphere manipulation. *Phytochemistry Reviews*. https://doi.org/10.1007/s11101-025-10084-y

Kudjordjie, E. N., Sapkota, R., Steffensen, S. K., Fomsgaard, I. S., & Nicolaisen, M. (2019). Maize synthesized benzoxazinoids affect the host associated microbiome. *Microbiome*, *7*(1). https://doi.org/10.1186/s40168-019-0677-7

Kuhlisch, C., & Pohnert, G. (2015). Metabolomics in chemical ecology. *Natural Product Reports*, *32*(7), 937–955. https://doi.org/10.1039/c5np00003c

Kuijken, R. C. P., Snel, J. F. H., Heddes, M. M., Bouwmeester, H. J., & Marcelis, L. F. M. (2015). The importance of a sterile rhizosphere when phenotyping for root exudation. *Plant and Soil*, *387*(1–2), 131–142. https://doi.org/10.1007/s11104-014-2283-6

Kulkarni, O. S., Mazumder, M., Kini, S., Hill, E. D., Aow, J. S. B., Phua, S. M. L., Elejalde, U., Kjelleberg, S., & Swarup, S. (2024). Volatile methyl jasmonate from roots triggers host-beneficial soil microbiome biofilms. *Nature Chemical Biology*, *20*(4), 473–483. https://doi.org/10.1038/s41589-023-01462-8

Kurth, F., Mailänder, S., Bönn, M., Feldhahn, L., Herrmann, S., Groe, I., Buscot, F., Schrey, S. D., & Tarkka, M. T. (2014). Streptomyces-induced resistance against oak powdery mildew involves host plant responses in defense, photosynthesis, and secondary metabolism pathways. *Molecular Plant-Microbe Interactions*, *27*(9), 891–900. https://doi.org/10.1094/MPMI-10-13-0296-R

Kuźniar, A., Włodarczyk, K., Grządziel, J., Goraj, W., Gałązka, A., & Wolińska, A. (2020). Culture-independent analysis of an endophytic core microbiome in two species of wheat: Triticum aestivum L. (cv. ‘Hondia’) and the first report of microbiota in Triticum spelta L. (cv. ‘Rokosz’). *Systematic and Applied Microbiology*, *43*(1). https://doi.org/10.1016/j.syapm.2019.126025

Lavergne, F. D., Broeckling, C. D., Brown, K. J., Cockrell, D. M., Haley, S. D., Peairs, F. B., Pearce, S., Wolfe, L. M., Jahn, C. E., & Heuberger, A. L. (2020a). Differential Stem Proteomics and Metabolomics Profiles for Four Wheat Cultivars in Response

to the Insect Pest Wheat Stem Sawfly. *Journal of Proteome Research*, *19*(3), 1037–1051. https://doi.org/10.1021/acs.jproteome.9b00561

Lê, S., Josse, J., Rennes, A., & Husson, F. (2008). FactoMineR: An R Package for Multivariate Analysis. In *JSS Journal of Statistical Software* (Vol. 25). http://www.jstatsoft.org/

Lebeis, S., Paredes, S. H., Lundberg, D. S., Breakfield, N., Gehring, J., McDonald, M., Malfatti, S., Glavina del Rio, T., Jones, C. D., Tringe, S. G., & Dangl, J. L. (2015). Salicylic acid modulates colonization of the root microbiome by specific bacterial taxa. *Science*, *349*(6250), 860–864.

Lee, B., Lee, S., & Ryu, C. M. (2012). Foliar aphid feeding recruits rhizosphere bacteria and primes plant immunity against pathogenic and non-pathogenic bacteria in pepper. *Annals of Botany*, *110*(2), 281–290. https://doi.org/10.1093/aob/mcs055

Lessie, T. G., Hendrickson, W., Manning, B. D., & Devereux, R. (1996). Genomic complexity and plasticity of Burkholderia cepacia . *FEMS Microbiology Letters*, *144*(2–3), 117–128. https://doi.org/10.1111/j.1574-6968.1996.tb08517.x

Li, Q., Sun, J., Qin, Y., Fan, J., Zhang, Y., Tan, X., Hou, M., & Chen, J. (2021). Reduced insecticide susceptibility of the wheat aphid SITOBION MISCANTHI after infection by the secondary bacterial symbiont *Hamiltonella defensa*. Pest Management Science, 77(4), 1936–1944. https://doi.org/10.1002/ps.6221

Li, Y., Zhao, Q., Duan, X., Song, C., & Chen, M. (2017). Transcription of four Rhopalosiphum padi (L.) heat shock protein genes and their responses to heat stress and insecticide exposure. *Comparative Biochemistry and Physiology -Part A : Molecular and Integrative Physiology*, *205*, 48–57. https://doi.org/10.1016/j.cbpa.2016.12.021

Li, Z., Jing, S., Wang, D., Song, Z., An, B., Wang, S., Liu, F., Di, N., Aradottir, G. I., Sun, J., Tan, X., Qu, C., & Kang, Z. (2025). Plant Volatile Methyl Salicylate Primes Wheat Defense Against the Grain Aphid by Altering the Synthesis of Defense Metabolites. *Plant, Cell and Environment*. https://doi.org/10.1111/pce.15351

Lieutier, F., Torres, K. B., Cook, J. M., & Harris, M. O. (2017). *From Plant Exploitation to Mutualism* (N. Sauvion, D. Thiery, & P.-A. Calatayud, Eds.; Vol. 81, pp. 55–110). Elsevier. https://www.researchgate.net/publication/341985342

Lin, H., & Peddada, S. Das. (2020). Analysis of compositions of microbiomes with bias correction. *Nature Communications*, *11*(1). https://doi.org/10.1038/s41467-020-17041-7

Liu, Y. X., Qin, Y., Chen, T., Lu, M., Qian, X., Guo, X., & Bai, Y. (2021). A practical guide to amplicon and metagenomic analysis of microbiome data. In *Protein and Cell* (Vol. 12, Issue 5, pp. 315–330). Higher Education Press Limited Company. https://doi.org/10.1007/s13238-020-00724-8

Lohse, M., Santangeli, M., Steininger-Mairinger, T., Oburger, E., Reemtsma, T., Lechtenfeld, O. J., & Hann, S. (2023). The effect of root hairs on exudate composition: a comparative non-targeted metabolomics approach. *Analytical and Bioanalytical Chemistry*, *415*(5), 823–840. https://doi.org/10.1007/s00216-022-04475-9

Lombardi, N., Vitale, S., Turr À, D., Reverberi, M., Fanelli, C., Vinale, F., Marra, R., Ruocco, M., Pascale, A., D'Errico, G., Woo, S. L., & Lorito, M. (2018). Root exudates of stressed plants stimulate and attract trichoderma soil fungi. *Molecular Plant-Microbe Interactions*, *31*(10), 982–994. https://doi.org/10.1094/MPMI-12-17-0310-R

Lopes, L. D., Wang, P., Futrell, S. L., & Schachtman, D. P. (2022). Sugars and Jasmonic Acid Concentration in Root Exudates Affect Maize Rhizosphere Bacterial Communities. *Applied and Environmental Microbiology*, *88*(18). https://doi.org/10.1128/aem.00971-22

López-Isasmendi, G., Alvarez, A. E., Petroselli, G., Erra-Balsells, R., & Audisio, M. C. (2019). Aphicidal activity of Bacillus amyloliquefaciens strains in the peach-potato aphid (Myzus persicae). *Microbiological Research*, *226*, 41–47. https://doi.org/10.1016/j.micres.2019.05.006

Loreto, F., & D'Auria, S. (2022). How do plants sense volatiles sent by other plants? In *Trends in Plant Science* (Vol. 27, Issue 1, pp. 29–38). Elsevier Ltd. https://doi.org/10.1016/j.tplants.2021.08.009

Luna, E., van Eck, L., Campillo, T., Weinroth, M., Metcalf, J., Perez-Quintero, A. L., Botha, A.-M., Thannhauser, T. W., Pappin, D., Tisserat, N. A., Lapitan, N. L. V., Argueso, C. T., Ode, P. J., Heck, M. L., & Leach, J. E. (2018). Bacteria Associated with Russian Wheat Aphid (Diuraphis noxia) Enhance Aphid Virulence to Wheat. Phytobiomes Journal, 2(3), 151–164. https://doi.org/10.1094/PBIOMES-06-18-0027-R

Luque de Castro, M. D., & Priego-Capote, F. (2018). The analytical process to search for metabolomics biomarkers. In *Journal of Pharmaceutical and Biomedical Analysis* (Vol. 147, pp. 341–349). Elsevier B.V. https://doi.org/10.1016/j.jpba.2017.06.073

Lyu, M., Bian, X., & He, C. (2024). The Deconvolution Method for Obtaining Correspondence in Data-Independent Acquisition Mass Spectrometry Data. *Journal of Computer and Communications*, *12*(02), 11–25. https://doi.org/10.4236/jcc.2024.122002

Ma, W., Tang, S., Dengzeng, Z., Zhang, D., Zhang, T., & Ma, X. (2022). Root exudates contribute to belowground ecosystem hotspots: A review. In *Frontiers in Microbiology* (Vol. 13). Frontiers Media S.A. https://doi.org/10.3389/fmicb.2022.937940

Ma, X., Zarebanadkouki, M., Kuzyakov, Y., Blagodatskaya, E., Pausch, J., & Razavi, B. S. (2018). Spatial patterns of enzyme activities in the rhizosphere: Effects of root hairs and root radius. *Soil Biology and Biochemistry*, *118*, 69–78. https://doi.org/10.1016/j.soilbio.2017.12.009

Maksimov, I. V., Blagova, D. K., Veselova, S. V., Sorokan, A. V., Burkhanova, G. F., Cherepanova, E. A., Sarvarova, E. R., Rumyantsev, S. D., Alekseev, V. Y., & Khayrullin, R. M. (2020). Recombinant Bacillus subtilis 26DCryChS line with gene Btcry1Ia encoding Cry1Ia toxin from Bacillus thuringiensis promotes integrated wheat defense against pathogen Stagonospora nodorum Berk. and greenbug Schizaphis graminum Rond. *Biological Control*, *144*. https://doi.org/10.1016/j.biocontrol.2020.104242

Malacrinò, A., Wang, M., Caul, S., Karley, A. J., & Bennett, A. E. (2021). Herbivory shapes the rhizosphere bacterial microbiota in potato plants. *Environmental Microbiology Reports*, *13*(6), 805–811. https://doi.org/10.1111/1758-2229.12998

Malik, A. A., Martiny, J. B. H., Brodie, E. L., Martiny, A. C., Treseder, K. K., & Allison, S. D. (2020). Defining trait-based microbial strategies with consequences for soil carbon cycling under climate change. *ISME Journal*, *14*(1), 1–9. https://doi.org/10.1038/s41396-019-0510-0

Marti, G., Erb, M., Boccard, J., Glauser, G., Doyen, G. R., Villard, N., Robert, C. A. M., Turlings, T. C. J., Rudaz, S., & Wolfender, J. L. (2013). Metabolomics reveals herbivore-induced metabolites of resistance and susceptibility in maize leaves and roots. *Plant, Cell and Environment*, *36*(3), 621–639. https://doi.org/10.1111/pce.12002

Matsui, K., & Engelberth, J. (2022). Green Leaf Volatiles - The Forefront of Plant Responses Against Biotic Attack. *Plant and Cell Physiology*, *63*(10), 1378–1390. https://doi.org/10.1093/pcp/pcac117

Matsumoto, A., & Takahashi, Y. (2017). Endophytic actinomycetes: Promising source of novel bioactive compounds. In *Journal of Antibiotics* (Vol. 70, Issue 5, pp. 514–519). Nature Publishing Group. https://doi.org/10.1038/ja.2017.20

Mbaluto, C. M., & Zytynska, S. E. (2024). *Rhizobacteria prime the activation of defence and nutritional responses to suppress aphid populations on barley*. https://doi.org/10.1101/2024.09.04.611222

Mbiza, N. I. T., Hu, Z., Zhang, H., Zhang, Y., Luo, X., Wang, Y., Wang, Y., Liu, T., Li, J., Wang, X., Zhang, J., & Yu, Y. (2022). GhCalS5 is involved in cotton response to aphid attack through mediating callose formation. *Frontiers in Plant Science*, *13*. https://doi.org/10.3389/fpls.2022.892630

McLaughlin, S., Zhalnina, K., Kosina, S., Northen, T. R., & Sasse, J. (2023). The core metabolome and root exudation dynamics of three phylogenetically distinct plant species. *Nature Communications*, *14*(1). https://doi.org/10.1038/s41467-023-37164-x

McLean, A. H. C., Godfray, H. C. J., Ellers, J., & Henry, L. M. (2019). Host relatedness influences the composition of aphid microbiomes. Environmental Microbiology Reports, 11(6), 808–816. https://doi.org/10.1111/1758-2229.12795

McMurdie, P. J., & Holmes, S. (2013). Phyloseq: An R Package for Reproducible Interactive Analysis and Graphics of Microbiome Census Data. *PLoS ONE*, *8*(4). https://doi.org/10.1371/journal.pone.0061217

Meihls, L. N., Handrick, V., Glauser, G., Barbier, H., Kaur, H., Haribal, M. M., Lipka, A. E., Gershenzon, J., Buckler, E. S., Erb, M., Köllner, T. G., & Jander, G. (2013). Natural variation in maize aphid resistance is associated with 2,4-dihydroxy-7-methoxy-1,4-benzoxazin-3-one glucoside methyltransferase activity. *Plant Cell*, *25*(6), 2341–2355. https://doi.org/10.1105/tpc.113.112409

Mendes, L. W., de Chaves, M. G., Fonseca, M. de C., Mendes, R., Raaijmakers, J. M., & Tsai, S. M. (2019). Resistance Breeding of Common Bean Shapes the Physiology of the Rhizosphere Microbiome. *Frontiers in Microbiology*, *10*. https://doi.org/10.3389/fmicb.2019.02252

Mercado-Blanco, J., & Lugtenberg, B. (2014). Biotechnological Applications of Bacterial Endophytes. *Current Biotechnology*, *3*, 60–75. https://doi.org/10.2174/2211550111302666003 8

Mishra, S., Bhattacharjee, A., & Sharma, S. (2021). An Ecological Insight into the Multifaceted World of Plant-Endophyte Association. *Critical Reviews in Plant Sciences*, *40*(2), 127–146. https://doi.org/10.1080/07352689.2021.1901044

Mitter, B., Trognitz, F., Ma, L., & Sessitsch, A. (2017). Ecology and Genomic Insights on Plant-Pathogenic and -Nonpathogenic Endophytes. *Annual Review of Phytopathology*, *55*(May), 1–23. https://doi.org/10.1146/annurev-phyto-080516-035641

Moran, N. A., & Sloan, D. B. (2015). The Hologenome Concept: Helpful or Hollow? *PLoS Biology*, *13*(12). https://doi.org/10.1371/journal.pbio.1002311

Morkunas, I., Mai, V. C., & Gabryś, B. (2011). Phytohormonal signaling in plant responses to aphid feeding. In *Acta Physiologiae Plantarum* (Vol. 33, Issue 6, pp. 2057–2073). https://doi.org/10.1007/s11738-011-0751-7

Mosblech, A., Feussner, I., & Heilmann, I. (2009). Oxylipins: Structurally diverse metabolites from fatty acid oxidation. In *Plant Physiology and Biochemistry* (Vol. 47, Issue 6, pp. 511–517). https://doi.org/10.1016/j.plaphy.2008.12.011

Mostafa, S., Wang, Y., Zeng, W., & Jin, B. (2022). Plant Responses to Herbivory, Wounding, and Infection. In *International Journal of Molecular Sciences* (Vol. 23, Issue 13). MDPI. https://doi.org/10.3390/ijms23137031

Mou, D. F., Kundu, P., Pingault, L., Puri, H., Shinde, S., & Louis, J. (2023). Monocot crop–aphid interactions: plant resilience and aphid adaptation. In *Current Opinion in Insect Science* (Vol. 57). Elsevier Inc. https://doi.org/10.1016/j.cois.2023.101038

Murphy, K. M., Edwards, J., Louie, K. B., Bowen, B. P., Sundaresan, V., Northen, T. R., & Zerbe, P. (2021). Bioactive diterpenoids impact the composition of the root-associated microbiome in maize (Zea mays). *Scientific Reports*, *11*(1). https://doi.org/10.1038/s41598-020-79320-z

Naeem, M., Aslam, Z., Khaliq, A., Ahmed, J. N., Nawaz, A., & Hussain, M. (2018). Plant growth promoting rhizobacteria reduce aphid population and enhance the productivity of bread wheat. *Brazilian Journal of Microbiology*, *49*, 9–14. https://doi.org/10.1016/j.bjm.2017.10.005

Nagrale, D. T., Chaurasia, A., Kumar, S., Gawande, S. P., Hiremani, N. S., Shankar, R., Gokte-Narkhedkar, N., Renu, & Prasad, Y. G. (2023). PGPR: the treasure of multifarious beneficial microorganisms for nutrient mobilization, pest biocontrol and plant growth promotion in field crops. In *World Journal of Microbiology and Biotechnology* (Vol. 39, Issue 4). Springer Science and Business Media B.V. https://doi.org/10.1007/s11274-023-03536-0

Nalam, V., Louis, J., & Shah, J. (2019). Plant defense against aphids, the pest extraordinaire. In *Plant Science* (Vol. 279, pp. 96–107). Elsevier Ireland Ltd. https://doi.org/10.1016/j.plantsci.2018.04.027

Narsing Rao, M. P., Lohmaneeratana, K., Bunyoo, C., & Thamchaipenet, A. (2022). Actinobacteria–Plant Interactions in Alleviating Abiotic Stress. In *Plants* (Vol. 11, Issue 21). MDPI. https://doi.org/10.3390/plants11212976

Nazir, M., Saleem, M., Tousif, M. I., Anwar, M. A., Surup, F., Ali, I., Wang, D., Mamadalieva, N. Z., Alshammari, E., Ashour, M. L., Ashour, A. M., Ahmed, I., Elizbit, Green, I. R., & Hussain, H. (2021). Meroterpenoids: A comprehensive update insight on structural diversity and biology. In *Biomolecules* (Vol. 11, Issue 7). MDPI AG. https://doi.org/10.3390/biom11070957

Neal, A. L., Ahmad, S., Gordon-Weeks, R., & Ton, J. (2012). Benzoxazinoids in root exudates of maize attract pseudomonas putida to the rhizosphere. *PLoS ONE*, *7*(4). https://doi.org/10.1371/journal.pone.0035498

Nearing, J. T., Douglas, G. M., Hayes, M. G., MacDonald, J., Desai, D. K., Allward, N., Jones, C. M. A., Wright, R. J., Dhanani, A. S., Comeau, A. M., & Langille, M. G. I. (2022). Microbiome differential abundance methods produce different results across 38 datasets. *Nature Communications*, *13*(1). https://doi.org/10.1038/s41467-022-28034-z

Nguyen, P.L. & Van Baalen, M. (2020) 'On the difficult evolutionary transition from the free-living lifestyle to obligate symbiosis', PLOS ONE. Edited by S.R. Proulx, 15(7), p. e0235811. Available at: https://doi.org/10.1371/journal.pone.0235811.

Nie, P., Li, X., Wang, S., Guo, J., Zhao, H., & Niu, D. (2017). Induced systemic resistance against botrytis cinerea by Bacillus cereus AR156 through a JA/ET- and NPR1-dependent signaling pathway and activates PAMP-triggered immunity in arabidopsis. *Frontiers in Plant Science*, *8*. https://doi.org/10.3389/fpls.2017.00238

Ninkovic, V., Markovic, D., & Rensing, M. (2021). Plant volatiles as cues and signals in plant communication. In *Plant Cell and Environment* (Vol. 44, Issue 4, pp. 1030–1043). Blackwell Publishing Ltd. https://doi.org/10.1111/pce.13910

Nobeli, I., Ponstingl, H., Krissinel, E. B., & Thornton, J. M. (2003). A structure-based anatomy of the E. coli metabolome. *Journal of Molecular Biology*, *334*(4), 697–719. https://doi.org/10.1016/j.jmb.2003.10.008

Nothias, L. F., Petras, D., Schmid, R., Dührkop, K., Rainer, J., Sarvepalli, A., Protsyuk, I., Ernst, M., Tsugawa, H., Fleischauer, M., Aicheler, F., Aksenov, A. A., Alka, O., Allard, P. M., Barsch, A., Cachet, X., Caraballo-Rodriguez, A. M., Da Silva, R. R., Dang, T., … Dorrestein, P. C. (2020). Feature-based molecular networking in the GNPS analysis environment. *Nature Methods*, *17*(9), 905–908. https://doi.org/10.1038/s41592-020-0933-6

Nothias, L.-F., Schmid, R., Garlet, A., Cameron, H., Leoty-Okombi, S., André-Frei, V., Fuchs, R., Dorrestein, P. C., & Ternes, P. (2024). Functional metabolomics of the human scalp: a metabolic niche for Staphylococcus epidermidis. In *mSystems* (Vol. 9, Issue 2, pp. 828–837). American Society For Microbiology. https://doi.org/10.1128/msystems.00356-23

O'Brien, F. J. M., Dumont, M. G., Webb, J. S., & Poppy, G. M. (2018). Rhizosphere bacterial communities differ according to fertilizer regimes and cabbage (Brassica oleracea var. capitata l.) harvest time, but not aphid herbivory. *Frontiers in Microbiology*, *9*(JUL). https://doi.org/10.3389/fmicb.2018.01620

Oburger, E., & Jones, D. L. (2018). Sampling root exudates – Mission impossible? *Rhizosphere*, *6*, 116–133. https://doi.org/10.1016/j.rhisph.2018.06.004

Oksanen J, Simpson G, Blanchet F, Kindt R, Legendre P, Minchin P, O'Hara R, Solymos P, Stevens M, Szoecs E, Wagner H, Barbour M, Bedward M, Bolker B, Borcard D, Carvalho G, Chirico M, De Caceres M, Durand S, Evangelista H, FitzJohn R, Friendly M, Furneaux B, Hannigan G, Hill M, Lahti L, McGlinn D, Ouellette M, Ribeiro Cunha E, Smith T, Stier A, Ter Braak C, Weedon J (2024). _vegan: Community Ecology Package_. R package version 2.6-8, <https://CRAN.R-project.org/package=vegan>.

Oleńska, E., Małek, W., Wójcik, M., Swiecicka, I., Thijs, S., & Vangronsveld, J. (2020). Beneficial features of plant growth-promoting rhizobacteria for improving plant growth and health in challenging conditions: A methodical review. In *Science of the Total Environment* (Vol. 743). Elsevier B.V. https://doi.org/10.1016/j.scitotenv.2020.140682

Omoboye, O. O., Oni, F. E., Batool, H., Yimer, H. Z., de Mot, R., & Höfte, M. (2019). Pseudomonas cyclic lipopeptides suppress the rice blast fungus Magnaporthe oryzae by induced resistance and direct antagonism. *Frontiers in Plant Science*, *10*. https://doi.org/10.3389/fpls.2019.00901

Ottensmann, M., Stoffel, M. A., Nichols, H. J., & Hoffman, J. I. (2018). GCalignR: An R package for aligning gas-chromatography data for ecological and evolutionary studies. *PLoS ONE*, *13*(6). https://doi.org/10.1371/journal.pone.0198311

Ourry, M., Lebreton, L., Chaminade, V., Guillerm-Erckelboudt, A. Y., Hervé, M., Linglin, J., Marnet, N., Ourry, A., Paty, C., Poinsot, D., Cortesero, A. M., & Mougel, C. (2018). Influence of belowground herbivory on the dynamics of root and rhizosphere microbial communities. *Frontiers in Ecology and Evolution*, *6*(JUN). https://doi.org/10.3389/fevo.2018.00091

Pachú, J. K. S., Macedo, F. C. O., Malaquias, J. B., Ramalho, F. S., Oliveira, R. F., Godoy, W. A. C., & Salustino, A. S. (2023). Electrical signalling and plant response to herbivory: A short review. *Plant Signaling and Behavior*, *18*(1). https://doi.org/10.1080/15592324.2023.2277578

Pakkir Shah, A. K., Walter, A., Ottosson, F., Russo, F., Navarro-Diaz, M., Boldt, J., Kalinski, J. C. J., Kontou, E. E., Elofson, J., Polyzois, A., González-Marín, C., Farrell, S., Aggerbeck, M. R., Pruksatrakul, T., Chan, N., Wang, Y., Pöchhacker, M., Brungs, C., Cámara, B., … Petras, D. (2024). Statistical analysis of feature-based molecular networking results from non-targeted metabolomics data. *Nature Protocols*. https://doi.org/10.1038/s41596-024-01046-3

Paliwal, D., Hamilton, A. J., Barrett, G. A., Alberti, F., van Emden, H., Monteil, C. L., Mauchline, T. H., Nauen, R., Wagstaff, C., Bass, C., & Jackson, R. W. (2022). Identification of novel aphid-killing bacteria to protect plants. *Microbial Biotechnology*, *15*(4), 1203–1220. https://doi.org/10.1111/1751-7915.13902

Pan, L., Huang, R., Lu, Z., Duan, W., Sun, S., Yan, L., Cui, G., Niu, L., Wang, Z., & Zeng, W. (2024). Combined transcriptome and metabolome analysis identifies triterpenoid-induced defense responses in Myzus persicae Sülzer-infested peach . *Journal of Experimental Botany*. https://doi.org/10.1093/jxb/erae339

Pang, Z., Lu, Y., Zhou, G., Hui, F., Xu, L., Viau, C., Spigelman, A. F., Macdonald, P. E., Wishart, D. S., Li, S., & Xia, J. (2024). MetaboAnalyst 6.0: towards a unified platform for metabolomics data processing, analysis and interpretation. *Nucleic Acids Research*, *52*(W1), W398–W406. https://doi.org/10.1093/nar/gkae253

Parry, H. R. (2013). *Cereal aphid movement: general principles and simulation modelling*. http://www.movementecologyjournal.com/content/1/1/14

Pastor-Fernández, J., Sánchez-Bel, P., Flors, V., Cerezo, M., & Pastor, V. (2023). Small Signals Lead to Big Changes: The Potential of Peptide-Induced Resistance in Plants. In *Journal of Fungi* (Vol. 9, Issue 2). MDPI. https://doi.org/10.3390/jof9020265

Paungfoo-Lonhienne, C., Lonhienne, T. G. A., Yeoh, Y. K., Donose, B. C., Webb, R. I., Parsons, J., Liao, W., Sagulenko, E., Lakshmanan, P., Hugenholtz, P., Schmidt, S., & Ragan, M. A. (2016). Crosstalk between sugarcane and a plant-growth promoting Burkholderia species. *Scientific Reports*, *6*. https://doi.org/10.1038/srep37389

Peccoud, J., Simon, J. C., Von Dohlen, C., Coeur d'acier, A., Plantegenest, M., Vanlerberghe-Masutti, F., & Jousselin, E. (2010). Evolutionary history of aphid-plant associations and their role in aphid diversification. *Comptes Rendus - Biologies*, *333*(6–7), 474–487. https://doi.org/10.1016/j.crvi.2010.03.004

Pellegrini, P., & Fernández, R. J. (2018). Crop intensification, land use, and on-farm energy-use efficiency during the worldwide spread of the green revolution. *Proceedings of the National Academy of Sciences of the United States of America*, *115*(10), 2335–2340. https://doi.org/10.1073/pnas.1717072115

Peng, X., Liu, L., Guo, X., Wang, P., Song, C., Su, S., Fang, G., & Chen, M. (2020). The survival and reproduction of rhopalosiphum padi (Hemiptera: Aphididae) on different plants: Exploring the possible host range for a serious wheat pest. *Journal of Economic Entomology*, *113*(1), 185–193. https://doi.org/10.1093/jee/toz263

Perez de Souza, L., Alseekh, S., Scossa, F., & Fernie, A. R. (2021). Ultra-high-performance liquid chromatography high-resolution mass spectrometry variants for metabolomics research. In *Nature Methods* (Vol. 18, Issue 7, pp. 733–746). Nature Research. https://doi.org/10.1038/s41592-021-01116-4

Pétriacq, P., Williams, A., Cotton, A., McFarlane, A. E., Rolfe, S. A., & Ton, J. (2017). Metabolite profiling of non-sterile rhizosphere soil. *Plant Journal*, *92*(1), 147–162. https://doi.org/10.1111/tpj.13639

Pieterse, C. M. J., Berendsen, R. L., de Jonge, R., Stringlis, I. A., van Dijken, A. J. H., van Pelt, J. A., van Wees, S. C. M., Yu, K., Zamioudis, C., & Bakker, P. A. H. M. (2021). Pseudomonas simiae WCS417: star track of a model beneficial rhizobacterium. In *Plant and Soil* (Vol. 461, Issues 1–2, pp. 245–263). Springer Science and Business Media Deutschland GmbH. https://doi.org/10.1007/s11104-020-04786-9

Pieterse, C. M. J., Zamioudis, C., Berendsen, R. L., Weller, D. M., van Wees, S. C. M., & Bakker, P. A. H. M. (2014). Induced systemic resistance by beneficial microbes. *Annual Review of Phytopathology*, *52*, 347–375. https://doi.org/10.1146/annurev-phyto-082712-102340

Pineda, A., Soler, R., Weldegergis, B. T., Shimwela, M. M., Van Loon, J. J. A., & Dicke, M. (2013). Non-pathogenic rhizobacteria interfere with the attraction of parasitoids to aphid-induced plant volatiles via jasmonic acid signalling. *Plant, Cell and Environment*, *36*(2), 393–404. https://doi.org/10.1111/j.1365-3040.2012.02581.x

Pineda, A., Zheng, S. J., van Loon, J. J. A., & Dicke, M. (2012). Rhizobacteria modify plant-aphid interactions: A case of induced systemic susceptibility. *Plant Biology*, *14*(SUPPL. 1), 83–90. https://doi.org/10.1111/j.1438-8677.2011.00549.x

Pineda, A., Zheng, S. J., van Loon, J. J. A., Pieterse, C. M. J., & Dicke, M. (2010). Helping plants to deal with insects: The role of beneficial soil-borne microbes. In *Trends in Plant Science* (Vol. 15, Issue 9, pp. 507–514). https://doi.org/10.1016/j.tplants.2010.05.007

Pohl, C. H., & Kock, J. L. F. (2014). Oxidized fatty acids as inter-kingdom signaling molecules. In *Molecules* (Vol. 19, Issue 1, pp. 1273–1285). https://doi.org/10.3390/molecules19011273

Potthast, K., Tischer, A., Herrmann, M., Weinhold, A., Küsel, K., van Dam, N. M., & Michalzik, B. (2022). Woolly beech aphid infestation reduces soil organic carbon availability and alters phyllosphere and rhizosphere bacterial microbiomes. *Plant and Soil*, *473*(1–2), 639–657. https://doi.org/10.1007/s11104-022-05317-4

Pourya, M., Shakarami, J., Mardani-Talaee, M., Sadeghi, A., & Serrão, J. E. (2020). Induced resistance in wheat Triticum aestivum L. by chemical- and bio- fertilizers against English aphid Sitobion avenae (Fabricius) (Hemiptera: Aphididae) in greenhouse. *International Journal of Tropical Insect Science*, *40*, 1043–1052. https://doi.org/10.1007/s42690-020-00164-1/Published

Powell, G., Tosh, C. R., & Hardie, J. (2006). Host plant selection by aphids: Behavioral, evolutionary, and applied perspectives. In *Annual Review of Entomology* (Vol. 51, pp. 309–330). https://doi.org/10.1146/annurev.ento.51.110104.151107

Prashar, P., Kapoor, N., & Sachdeva, S. (2014). Rhizosphere: Its structure, bacterial diversity and significance. In *Reviews in Environmental Science and Biotechnology* (Vol. 13, Issue 1, pp. 63–77). https://doi.org/10.1007/s11157-013-9317-z

Prudence, S. M. M., Newitt†, J. T., Worsley, S. F., Macey, M. C., Murrell, J. C., Lehtovirta-Morley, L. E., & Hutchings, M. I. (2021). Soil, senescence and exudate utilisation: characterisation of the Paragon var. spring bread wheat root microbiome. *Environmental Microbiomes*, *16*(1). https://doi.org/10.1186/s40793-021-00381-2

Pu, Q., Liang, J., Shen, Q., Fu, J., Pu, Z., Liu, J., Wang, X., & Wang, Q. (2019). A wheat β-patchoulene synthase confers resistance against herbivory in transgenic arabidopsis. *Genes*, *10*(6). https://doi.org/10.3390/genes10060441

Qiu, C. L., Li, W., Wang, L. N., Wang, S. C., Falert, S., Wang, C., Yu, S. Y., Abdelkhalek, S. T., Lu, J., Lin, Y. J., & Wang, M. Q. (2024). Limonene enhances rice plant resistance to a piercing-sucking herbivore and rice pathogens. *Plant Biotechnology Journal*. https://doi.org/10.1111/pbi.14481

Quast, C., Pruesse, E., Yilmaz, P., Gerken, J., Schweer, T., Yarza, P., Peplies, J., & Glöckner, F. O. (2013). The SILVA ribosomal RNA gene database project: Improved data processing and web-based tools. *Nucleic Acids Research*, *41*(D1). https://doi.org/10.1093/nar/gks1219

Quiros-Guerrero, L. M., Allard, P. M., Nothias, L. F., David, B., Grondin, A., & Wolfender, J. L. (2024). Comprehensive mass spectrometric metabolomic profiling of a chemically diverse collection of plants of the Celastraceae family. *Scientific Data*, *11*(1). https://doi.org/10.1038/s41597-024-03094-6

Quiza, L., Tremblay, J., Pagé, A. P., Greer, C. W., Pozniak, C. J., Li, R., Haug, B., Hemmingsen, S. M., St-Arnaud, M., & Yergeau, E. (2023). The effect of wheat genotype on the microbiome is more evident in roots and varies through time. *ISME Communications*, *3*(1). https://doi.org/10.1038/s43705-023-00238-4

RStudio Team (2020). RStudio: Integrated Development for R. RStudio, PBC, Boston, MA URL http://www.rstudio.com/ .

Rai, R., & Baiieditors, J. A. (2022). *Natural Products from Actinomycetes Diversity, Ecology and Drug Discovery*.

Rani, L., Thapa, K., Kanojia, N., Sharma, N., Singh, S., Grewal, A. S., Srivastav, A. L., & Kaushal, J. (2021). An extensive review on the consequences of chemical pesticides on human health and environment. In *Journal of Cleaner Production* (Vol. 283). Elsevier Ltd. https://doi.org/10.1016/j.jclepro.2020.124657

Rashid, S., Charles, T. C., & Glick, B. R. (2012). Isolation and characterization of new plant growth-promoting bacterial endophytes. *Applied Soil Ecology*, *61*, 217–224. https://doi.org/10.1016/j.apsoil.2011.09.011

Rasool, S., Vidkjær, N. H., Hooshmand, K., Jensen, B., Fomsgaard, I. S., & Meyling, N. V. (2021). Seed inoculations with entomopathogenic fungi affect aphid populations coinciding with modulation of plant secondary metabolite profiles across plant families. *New Phytologist*, *229*(3), 1715–1727. https://doi.org/10.1111/nph.16979

Rattray, N. J. W., Deziel, N. C., Wallach, J. D., Khan, S. A., Vasiliou, V., Ioannidis, J. P. A., & Johnson, C. H. (2018). Beyond genomics: Understanding exposotypes through metabolomics. In *Human Genomics* (Vol. 12, Issue 1). BioMed Central Ltd. https://doi.org/10.1186/s40246-018-0134-x

Raza, W., Wei, Z., Jousset, A., Shen, Q., & Friman, V.-P. (2021). *Extended Plant Metarhizobiome: Understanding Volatile Organic Compound Signaling in Plant-Microbe Metapopulation Networks*. https://doi.org/10.1128/mSystems

Razak, N. A., & Gange, A. C. (2023). Multitrophic Interactions Between Arbuscular Mycorrhizal Fungi, Foliar Endophytic Fungi and Aphids. Microbial Ecology, 85(1), 146–156. https://doi.org/10.1007/s00248-021-01937-y

Reid, T. E., Kavamura, V. N., Abadie, M., Torres-Ballesteros, A., Pawlett, M., Clark, I. M., Harris, J., & Mauchline, T. H. (2021). Inorganic Chemical Fertilizer Application to Wheat Reduces the Abundance of Putative Plant Growth-Promoting Rhizobacteria. *Frontiers in Microbiology*, *12*. https://doi.org/10.3389/fmicb.2021.642587

Reinhold-Hurek, B., & Hurek, T. (2011). Living inside plants: Bacterial endophytes. *Current Opinion in Plant Biology*, *14*(4), 435–443. https://doi.org/10.1016/j.pbi.2011.04.004

Renoz, F., Lopes, M. R., Gaget, K., Duport, G., Eloy, M.-C., Geelhand de Merxem, B., Hance, T., & Calevro, F. (2022). Compartmentalized into Bacteriocytes but Highly Invasive: The Puzzling Case of the Co-Obligate Symbiont Serratia symbiotica in the Aphid Periphyllus lyropictus. Microbiology Spectrum, 10(3), e00457-22. https://doi.org/10.1128/spectrum.00457-22

Rivero, J., Lidoy, J., Llopis-Giménez, Á., Herrero, S., Flors, V., & Pozo, M. J. (2021). Mycorrhizal symbiosis primes the accumulation of antiherbivore compounds and

enhances herbivore mortality in tomato. *Journal of Experimental Botany*, *72*(13), 5038–5050. https://doi.org/10.1093/jxb/erab171

Rizaludin, M. S., Stopnisek, N., Raaijmakers, J. M., & Garbeva, P. (2021). The chemistry of stress: Understanding the 'cry for help' of plant roots. In *Metabolites* (Vol. 11, Issue 6). MDPI AG. https://doi.org/10.3390/metabo11060357

Rolfe, S. A., Griffiths, J., & Ton, J. (2019). Crying out for help with root exudates: adaptive mechanisms by which stressed plants assemble health-promoting soil microbiomes. In *Current Opinion in Microbiology* (Vol. 49, pp. 73–82). Elsevier Ltd. https://doi.org/10.1016/j.mib.2019.10.003

Ropitaux, M., Bernard, S., Schapman, D., Follet-Gueye, M. L., Vicré, M., Boulogne, I., & Driouich, A. (2020). Root Border Cells and Mucilage Secretions of Soybean, Glycine Max (Merr) L.: Characterization and Role in Interactions with the Oomycete Phytophthora Parasitica. *Cells*, *9*(10). https://doi.org/10.3390/cells9102215

Rosenkranz, M., Chen, Y., Zhu, P., & Vlot, A. C. (2021). Volatile terpenes – mediators of plant-to-plant communication. In *Plant Journal* (Vol. 108, Issue 3, pp. 617–631). John Wiley and Sons Inc. https://doi.org/10.1111/tpj.15453

Rutz, A., Dounoue-Kubo, M., Ollivier, S., Bisson, J., Bagheri, M., Saesong, T., Ebrahimi, S. N., Ingkaninan, K., Wolfender, J. L., & Allard, P. M. (2019). Taxonomically Informed Scoring Enhances Confidence in Natural Products Annotation. *Frontiers in Plant Science*, *10*. https://doi.org/10.3389/fpls.2019.01329

Rutz, A., Sorokina, M., Galgonek, J., Mietchen, D., Willighagen, E., Gaudry, A., Graham, J. G., Stephan, R., Page, R., Vondrášek, J., Steinbeck, C., Pauli, G. F., Wolfender, J. L., Bisson, J., & Allard, P. M. (2022). The LOTUS initiative for open knowledge management in natural products research. *ELife*, *11*. https://doi.org/10.7554/eLife.70780

Saikia, K., & Bora, L. C. (2021). Exploring actinomycetes and endophytes of rice ecosystem for induction of disease resistance against bacterial blight of rice. *European Journal of Plant Pathology*, *159*(1), 67–79. https://doi.org/10.1007/s10658-020-02141-3

Samain, E., Ernenwein, C., Aussenac, T., & Selim, S. (2022). Effective and durable systemic wheat-induced resistance by a plant-growth-promoting rhizobacteria consortium of Paenibacillus sp. strain B2 and Arthrobacter spp. strain AA against Zymoseptoria tritici and drought stress. *Physiological and Molecular Plant Pathology*, *119*. https://doi.org/10.1016/j.pmpp.2022.101830

Sanchez-Arcos, C., Kai, M., Svatoš, A., Gershenzon, J., & Kunert, G. (2019). Untargeted metabolomics approach reveals differences in host plant chemistry before and after infestation with different pea aphid host races. *Frontiers in Plant Science*, *10*. https://doi.org/10.3389/fpls.2019.00188

Santos, F., Peñaflor, M. F. G. V., Pulido, H., Bampi, D., Bento, J. M. S., Mescher, M. C., & De Moraes, C. M. (2025). The plant growth-promoting rhizobacterium *Azospirillum brasilense* reduces symptoms and aphid population growth on wheat plants infected with barley yellow dwarf virus. *Proceedings of the Royal Society B: Biological Sciences*, *292*(2041). https://doi.org/10.1098/rspb.2024.2857

Sasse, J., Martinoia, E., & Northen, T. (2018). Feed Your Friends: Do Plant Exudates Shape the Root Microbiome? In *Trends in Plant Science* (Vol. 23, Issue 1, pp. 25–41). Elsevier Ltd. https://doi.org/10.1016/j.tplants.2017.09.003

Schmid, R., Heuckeroth, S., Korf, A., Smirnov, A., Myers, O., Dyrlund, T. S., Bushuiev, R., Murray, K. J., Hoffmann, N., Lu, M., Sarvepalli, A., Zhang, Z., Fleischauer, M., Dührkop, K., Wesner, M., Hoogstra, S. J., Rudt, E., Mokshyna, O., Brungs, C., … Pluskal, T. (2023). Integrative analysis of multimodal mass spectrometry data in MZmine 3. In *Nature Biotechnology* (Vol. 41, Issue 4, pp. 447–449). Nature Research. https://doi.org/10.1038/s41587-023-01690-2

Schulz-Bohm, K., Gerards, S., Hundscheid, M., Melenhorst, J., De Boer, W., & Garbeva, P. (2018). Calling from distance: Attraction of soil bacteria by plant root volatiles. *ISME Journal*, *12*(5), 1252–1262. https://doi.org/10.1038/s41396-017-0035-3

Scott, A. C., Stephenson, J., & Chaloner, W. (1992). Interaction and coevolution of plants and arthropods during the Palaeozoic and Mesozoic. *Phil. Trans. R. Soc. Lond.*, *335*, 129–165. https://royalsocietypublishing.org/

Segonzac, C., & Monaghan, J. (2019). Modulation of plant innate immune signaling by small peptides. In *Current Opinion in Plant Biology* (Vol. 51, pp. 22–28). Elsevier Ltd. https://doi.org/10.1016/j.pbi.2019.03.007

Seitz, V. A., McGivern, B. B., Daly, R. A., Chaparro, J. M., Borton, M. A., Sheflin, A. M., Kresovich, S., Shields, L., Schipanski, M. E., Wrighton, K. C., & Prenni, J. E. (2022). Variation in Root Exudate Composition Influences Soil Microbiome Membership and Function. *Applied and Environmental Microbiology*, *88*(11). https://doi.org/10.1128/aem.00226-22

Serteyn, L., Quaghebeur, C., Ongena, M., Cabrera, N., Barrera, A., Molina-Montenegro, M. A., Francis, F., & Ramírez, C. C. (2020). Induced systemic resistance by a plant growth-promoting rhizobacterium impacts development and feeding behavior of aphids. *Insects*, *11*(4). https://doi.org/10.3390/insects11040234

Seth, T., Asija, S., Umar, S., & Gupta, R. (2024). The intricate role of lipids in orchestrating plant defense responses. In *Plant Science* (Vol. 338). Elsevier Ireland Ltd. https://doi.org/10.1016/j.plantsci.2023.111904

Shan, Y., & Osborne, C. P. (2024). Diversification of quantitative morphological traits in wheat. *Annals of Botany*, *133*(3), 413–426. https://doi.org/10.1093/aob/mcad202

Shavit, R., Batyrshina, Z. S., Dotan, N., & Tzin, V. (2018). Cereal aphids differently affect benzoxazinoid levels in durum wheat. *PLoS ONE*, *13*(12). https://doi.org/10.1371/journal.pone.0208103

Shen, S., Zhan, C., Yang, C., Fernie, A. R., & Luo, J. (2023). Metabolomics-centered mining of plant metabolic diversity and function: Past decade and future perspectives. In *Molecular Plant* (Vol. 16, Issue 1, pp. 43–63). Cell Press. https://doi.org/10.1016/j.molp.2022.09.007

Shigenobu, S., & Yorimoto, S. (2022). Aphid hologenomics: Current status and future challenges. Current Opinion in Insect Science, 50, 100882. https://doi.org/10.1016/j.cois.2022.100882

Shih, P.-Y., Sugio, A., & Simon, J.-C. (2022). *Molecular Mechanisms Underlying Host Plant Specificity in Aphids Zig-zag model: a model to explain the plant immune*

system by induction and suppression of plant immunity by biotrophic pathogens. https://doi.org/10.1146/annurev-ento-120220

Shivlata, L., & Satyanarayana, T. (2015). Thermophilic and alkaliphilic Actinobacteria: Biology and potential applications. In *Frontiers in Microbiology* (Vol. 6, Issue SEP). Frontiers Media S.A. https://doi.org/10.3389/fmicb.2015.01014

Silva-Sanzana, C., Gangas, M. V., Zavala, D., & Blanco-Herrera, F. (2023). A Recipe for Success: Three Key Strategies Used by Aphids and Pseudomonas syringae to Colonize the Phyllosphere. In *Microbial Ecology* (Vol. 85, Issue 1, pp. 1–8). Springer. https://doi.org/10.1007/s00248-022-01965-2

Simmons, T., Caddell, D. F., Deng, S., & Coleman-Derr, D. (2018). Exploring the root microbiome: Extracting bacterial community data from the soil, rhizosphere, and root endosphere. *Journal of Visualized Experiments*, *2018*(135). https://doi.org/10.3791/57561

Simon, A. L., Caulfield, J. C., Hammond-Kosack, K. E., Field, L. M., & Aradottir, G. I. (2021). Identifying aphid resistance in the ancestral wheat Triticum monococcum under field conditions. *Scientific Reports*, *11*(1). https://doi.org/10.1038/s41598-021-92883-9

Simonin, M., Dasilva, C., Terzi, V., Ngonkeu, E. L. M., DIouf, Di., Kane, A., Béna, G., & Moulin, L. (2020). Influence of plant genotype and soil on the wheat rhizosphere microbiome: Evidences for a core microbiome across eight African and European soils. *FEMS Microbiology Ecology*, *96*(6). https://doi.org/10.1093/femsec/fiaa067

Singh, B., Simon, A., Halsey, K., Kurup, S., Clark, S., & Aradottir, G. I. (2020). Characterisation of bird cherry-oat aphid (Rhopalosiphum padi L.) behaviour and aphid host preference in relation to partially resistant and susceptible wheat landraces. *Annals of Applied Biology*, *177*(2), 184–194. https://doi.org/10.1111/aab.12616

Singh, R., & Dubey, A. K. (2018). Diversity and applications of endophytic actinobacteria of plants in special and other ecological niches. In *Frontiers in Microbiology* (Vol. 9, Issue AUG). Frontiers Media S.A. https://doi.org/10.3389/fmicb.2018.01767

Singh, S. P., & Gaur, R. (2016). Evaluation of antagonistic and plant growth promoting activities of chitinolytic endophytic actinomycetes associated with medicinal plants against Sclerotium rolfsii in chickpea. *Journal of Applied Microbiology*, *121*(2), 506–518. https://doi.org/10.1111/jam.13176

Singh, S. P., Gupta, R., Gaur, R., & Srivastava, A. K. (2017). Antagonistic Actinomycetes Mediated Resistance in Solanum lycopersicon Mill. Against Rhizoctonia solani Kühn. *Proceedings of the National Academy of Sciences India Section B - Biological Sciences*, *87*(3), 789–798. https://doi.org/10.1007/s40011-015-0651-5

Smee, M. R., & Hendry, T. A. (2022). Context-Dependent Benefits of Aphids for Bacteria in the Phyllosphere. *The American Naturalist*, *199*(3). https://doi.org/10.5061/dryad.c2fqz616n

Sobhy, I. S., Lou, Y., & Bruce, T. J. A. (2022). Editorial: Inducing Plant Resistance Against Insects Using Exogenous Bioactive Chemicals: Key Advances and Future Perspectives. In *Frontiers in Plant Science* (Vol. 13). Frontiers Media S.A. https://doi.org/10.3389/fpls.2022.890884

Sochard, C., Bellec, L., Simon, J.-C., & Outreman, Y. (2021). Influence of “protective” symbionts throughout the different steps of an aphid–parasitoid interaction. Current Zoology, 67(4), 441–453. https://doi.org/10.1093/cz/zoaa053

Stassen, M.J.J. et al. (2021) ‘Coumarin Communication Along the Microbiome–Root–Shoot Axis’, Trends in Plant Science, 26(2), pp. 169–183. Available at: https://doi.org/10.1016/j.tplants.2020.09.008.

Stewart, S. A., Hodge, S., Bennett, M., Mansfield, J. W., & Powell, G. (2016). Aphid induction of phytohormones in Medicago truncatula is dependent upon time post-infestation, aphid density and the genotypes of both plant and insect. *Arthropod-Plant Interactions*, *10*(1), 41–53. https://doi.org/10.1007/s11829-015-9406-8

Stringlis, I. A., De Jonge, R., & Pieterse, C. M. J. (2019). The Age of Coumarins in Plant-Microbe Interactions. In *Plant and Cell Physiology* (Vol. 60, Issue 7, pp. 1405–1419). Oxford University Press. https://doi.org/10.1093/pcp/pcz076

Sugimoto, K., Allmann, S., & Kolomiets, M. V. (2022). Editorial: Oxylipins: The Front Line of Plant Interactions. In *Frontiers in Plant Science* (Vol. 13). Frontiers Media S.A. https://doi.org/10.3389/fpls.2022.878765

Suh, J. H., Niu, Y. S., Wang, Z., Gmitter, F. G., & Wang, Y. (2018). Metabolic Analysis Reveals Altered Long-Chain Fatty Acid Metabolism in the Host by Huanglongbing Disease. *Journal of Agricultural and Food Chemistry*, *66*(5), 1296–1304. https://doi.org/10.1021/acs.jafc.7b05273

Sun, C., Liu, L., Wang, L., Li, B., Jin, C., & Lin, X. (2021). Melatonin: A master regulator of plant development and stress responses. In *Journal of Integrative Plant Biology* (Vol. 63, Issue 1, pp. 126–145). Blackwell Publishing Ltd. https://doi.org/10.1111/jipb.12993

Sun, H., Wang, L., Zhang, B., Ma, J., Hettenhausen, C., Cao, G., Sun, G., Wu, J., & Wu, J. (2014). Scopoletin is a phytoalexin against Alternaria alternata in wild tobacco dependent on jasmonate signalling. *Journal of Experimental Botany*, *65*(15), 4305–4315. https://doi.org/10.1093/jxb/eru203

Sun, X., Li, T., & Zhang, J. (2024). Soil health and microbial network analysis in a wheat-maize cropping system under different wheat yields. *Frontiers of Agricultural Science and Engineering*, *11*(4), 615–625. https://doi.org/10.15302/J-FASE-2024570

Tahir, H. A. S., Gu, Q., Wu, H., Niu, Y., Huo, R., & Gao, X. (2017). Bacillus volatiles adversely affect the physiology and ultra-structure of Ralstonia solanacearum and induce systemic resistance in tobacco against bacterial wilt. *Scientific Reports*, *7*. https://doi.org/10.1038/srep40481

Takishita, Y., Charron, J. B., & Smith, D. L. (2018). Biocontrol rhizobacterium Pseudomonas sp. 23S induces systemic resistance in Tomato (Solanum lycopersicum L.) against bacterial Canker Clavibacter michiganensis subsp. michiganensis. *Frontiers in Microbiology*, *9*(SEP). https://doi.org/10.3389/fmicb.2018.02119

Thaler, J. S., Humphrey, P. T., & Whiteman, N. K. (2012). Evolution of jasmonate and salicylate signal crosstalk. In *Trends in Plant Science* (Vol. 17, Issue 5, pp. 260–270). https://doi.org/10.1016/j.tplants.2012.02.010

Thangaraj, K., Liu, S., Li, J., Zhao, Z., Han, R., Mei, H., Jeyaraj, A., Chen, X., & Li, X. (2022). Exogenous melatonin alleviates sooty mould on tea plants (Camellia sinensis L.). *Scientia Horticulturae*, *299*. https://doi.org/10.1016/j.scienta.2022.111056

Thoenen, L., Giroud, C., Kreuzer, M., Waelchli, J., Gfeller, V., Deslandes-Hérold, G., Mateo, P., Robert, C. A. M., Ahrens, C. H., Rubio-Somoza, I., Bruggmann, R., Erb, M., & Schlaeppi, K. (2023). Bacterial tolerance to host-exuded specialized metabolites structures the maize root microbiome. *Proceedings of the National Academy of Sciences of the United States of America*, *120*(44). https://doi.org/10.1073/pnas.2310134120

Tholl, D., Hossain, O., Weinhold, A., Röse, U. S. R., & Wei, Q. (2021). Trends and applications in plant volatile sampling and analysis. In *Plant Journal* (Vol. 106, Issue 2, pp. 314–325). Blackwell Publishing Ltd. https://doi.org/10.1111/tpj.15176

Thomas, S. N., French, D., Jannetto, P. J., Rappold, B. A., & Clarke, W. A. (2022). Liquid chromatography–tandem mass spectrometry for clinical diagnostics. *Nature Reviews Methods Primers*, *2*(1). https://doi.org/10.1038/s43586-022-00175-x

Tian, B., Pei, Y., Huang, W., Ding, J., & Siemann, E. (2021). Increasing flavonoid concentrations in root exudates enhance associations between arbuscular mycorrhizal fungi and an invasive plant. *ISME Journal*, *15*(7), 1919–1930. https://doi.org/10.1038/s41396-021-00894-1

Tian, T., Reverdy, A., She, Q., Sun, B., & Chai, Y. (2020). The role of rhizodeposits in shaping rhizomicrobiome. In *Environmental Microbiology Reports* (Vol. 12, Issue 2, pp. 160–172). Wiley-Blackwell. https://doi.org/10.1111/1758-2229.12816

Tong, Y., Zheng, X., Hu, Y., Wu, J., Liu, H., Deng, Y., Lv, W., Yao, H., Chen, J., & Ge, T. (2024). Root exudate-mediated plant–microbiome interactions determine plant health during disease infection. *Agriculture, Ecosystems and Environment*, *370*. https://doi.org/10.1016/j.agee.2024.109056

Trivedi, P., Leach, J. E., Tringe, S. G., Sa, T., & Singh, B. K. (2020). Plant–microbiome interactions: from community assembly to plant health. In *Nature Reviews Microbiology* (Vol. 18, Issue 11, pp. 607–621). Nature Research. https://doi.org/10.1038/s41579-020-0412-1

Turlings, T. C. J., & Erb, M. (2017). *Tritrophic Interactions Mediated by Herbivore-Induced Plant Volatiles: Mechanisms, Ecological Relevance, and Application Potential*. https://doi.org/10.1146/annurev-ento-020117

Tzin, V., Fernandez-Pozo, N., Richter, A., Schmelz, E. A., Schoettner, M., Schäfer, M., Ahern, K. R., Meihls, L. N., Kaur, H., Huffaker, A., Mori, N., Degenhardt, J., Mueller, L. A., & Jander, G. (2015). Dynamic maize responses to aphid feeding are revealed by a time series of transcriptomic and metabolomic assays. *Plant Physiology*, *169*(3), 1727–1743. https://doi.org/10.1104/pp.15.01039

Valentinuzzi, F., Cesco, S., Tomasi, N., & Mimmo, T. (2015). Influence of different trap solutions on the determination of root exudates in Lupinus albus L. *Biology and Fertility of Soils*, *51*(6), 757–765. https://doi.org/10.1007/s00374-015-1015-2

van Dam, N. M., & Bouwmeester, H. J. (2016). Metabolomics in the Rhizosphere: Tapping into Belowground Chemical Communication. In *Trends in Plant Science*

(Vol. 21, Issue 3, pp. 256–265). Elsevier Ltd. https://doi.org/10.1016/j.tplants.2016.01.008

van der Meij, A., Elsayed, S. S., Du, C., Willemse, J., Wood, T. M., Martin, N. I., Raaijmakers, J. M., & van Wezel, G. P. (2023). The plant stress hormone jasmonic acid evokes defensive responses in streptomycetes. *Applied and Environmental Microbiology*, *89*(11). https://doi.org/10.1128/aem.01239-23

van der Meij, A., Willemse, J., Schneijderberg, M. A., Geurts, R., Raaijmakers, J. M., & van Wezel, G. P. (2018). Inter- and intracellular colonization of Arabidopsis roots by endophytic actinobacteria and the impact of plant hormones on their antimicrobial activity. *Antonie van Leeuwenhoek, International Journal of General and Molecular Microbiology*, *111*(5), 679–690. https://doi.org/10.1007/s10482-018-1014-z

van der Meij, A., Worsley, S. F., Hutchings, M. I., & van Wezel, G. P. (2017). Chemical ecology of antibiotic production by actinomycetes. In *FEMS Microbiology Reviews* (Vol. 41, Issue 3, pp. 392–416). Oxford University Press. https://doi.org/10.1093/femsre/fux005

van Dijk, L. J. A., Abdelfattah, A., Ehrlén, J., & Tack, A. J. M. (2022). Soil microbiomes drive aboveground plant–pathogen–insect interactions. *Oikos*, *2022*(12). https://doi.org/10.1111/oik.09366

Vandenkoornhuyse, P., Quaiser, A., Duhamel, M., Le Van, A., & Dufresne, A. (2015). The importance of the microbiome of the plant holobiont. In *New Phytologist* (Vol. 206, Issue 4, pp. 1196–1206). https://doi.org/10.1111/nph.13312

Vegan: Community Ecology Package. (2024). https://github.com/vegandevs/vegan

Vestergård, M., Bjørnlund, L., & Christensen, S. (2004). Aphid effects on rhizosphere microorganisms and microfauna depend more on barley growth phase than on soil fertilization. *Oecologia*, *141*(1), 84–93. https://doi.org/10.1007/s00442-004-1651-y

Viaene, T., Langendries, S., Beirinckx, S., Maes, M., & Goormachtig, S. (2016). Streptomyces as a plant's best friend? *FEMS Microbiology Ecology*, *92*(8). https://doi.org/10.1093/femsec/fiw119

Vismans, G., van Bentum, S., Spooren, J., Song, Y., Goossens, P., Valls, J., Snoek, B. L., Thiombiano, B., Schilder, M., Dong, L., Bouwmeester, H. J., Pétriacq, P., Pieterse, C. M. J., Bakker, P. A. H. M., & Berendsen, R. L. (2022). Coumarin biosynthesis genes are required after foliar pathogen infection for the creation of a microbial soil-borne legacy that primes plants for SA-dependent defenses. *Scientific Reports*, *12*(1). https://doi.org/10.1038/s41598-022-26551-x

Vives-Peris, V., de Ollas, C., Gómez-Cadenas, A., & Pérez-Clemente, R. M. (2020). Root exudates: from plant to rhizosphere and beyond. In *Plant Cell Reports* (Vol. 39, Issue 1, pp. 3–17). Springer. https://doi.org/10.1007/s00299-019-02447-5

Waines, J. G., & Ehdaie, B. (2007). Domestication and crop physiology: Roots of green-revolution wheat. In *Annals of Botany* (Vol. 100, Issue 5, pp. 991–998). https://doi.org/10.1093/aob/mcm180

Walker, T. W. N., Alexander, J. M., Allard, P. M., Baines, O., Baldy, V., Bardgett, R. D., Capdevila, P., Coley, P. D., David, B., Defossez, E., Endara, M. J., Ernst, M., Fernandez, C., Forrister, D., Gargallo-Garriga, A., Jassey, V. E. J., Marr, S., Neumann, S., Pellissier, L., … Salguero-Gómez, R. (2022). Functional Traits 2.0:

The power of the metabolome for ecology. In *Journal of Ecology* (Vol. 110, Issue 1, pp. 4–20). John Wiley and Sons Inc. https://doi.org/10.1111/1365-2745.13826

Wang, P., Lopes, L. D., Lopez-Guerrero, M. G., Van Dijk, K., Alvarez, S., Riethoven, J. J., & Schachtman, D. P. (2022). Natural variation in root exudation of GABA and DIMBOA impacts the maize root endosphere and rhizosphere microbiomes. *Journal of Experimental Botany*, *73*(14), 5052–5066. https://doi.org/10.1093/jxb/erac202

Wang, Q., Liu, X., Liu, H., Fu, Y., Cheng, Y., Zhang, L., Shi, W., Zhang, Y., & Chen, J. (2022). Transcriptomic and Metabolomic Analysis of Wheat Kernels in Response to the Feeding of Orange Wheat Blossom Midges (Sitodiplosis mosellana) in the Field. *Journal of Agricultural and Food Chemistry*, *70*(5), 1477–1493. https://doi.org/10.1021/acs.jafc.1c06239

Wang, S., Alseekh, S., Fernie, A. R., & Luo, J. (2019). The Structure and Function of Major Plant Metabolite Modifications. In *Molecular Plant* (Vol. 12, Issue 7, pp. 899–919). Cell Press. https://doi.org/10.1016/j.molp.2019.06.001

Wang, T., Wang, N., Wang, K., Lu, Q., Dou, Z., Chi, Z., Cui Dongming, Suzuki, M., & Zuo, Y. (2023). Proline-2′-deoxymugineic acid, a phytosiderophore analog, drives beneficial rhizobacterial community formation to promote peanut micronutrition. *Frontiers of Agricultural Science and Engineering*, *0*(0), 0. https://doi.org/10.15302/j-fase-2023531

Wang, Y., Di, B., Sun, Z., Sonali, Donovan-Mak, M., Chen, Z. H., & Wang, M. Q. (2024). Multi-Omics and Physiological Analysis Reveal Crosstalk Between Aphid Resistance and Nitrogen Fertilization in Wheat. *Plant Cell and Environment*. https://doi.org/10.1111/pce.15282

Wang, Y., Li, X., Fan, B., Zhu, C., & Chen, Z. (2021). Regulation and function of defense-related callose deposition in plants. In *International Journal of Molecular Sciences* (Vol. 22, Issue 5, pp. 1–15). MDPI AG. https://doi.org/10.3390/ijms22052393

Wang, Z., & Song, Y. (2022). Toward understanding the genetic bases underlying plant-mediated “cry for help” to the microbiota. In *iMeta* (Vol. 1, Issue 1). John Wiley and Sons Inc. https://doi.org/10.1002/imt2.8

War, A. R., Taggar, G. K., Hussain, B., Taggar, M. S., Nair, R. M., & Sharma, H. C. (2018). Special Issue: Using non-model systems to explore plant-pollinator and plant-herbivore interactions: Plant defence against herbivory and insect adaptations. In *AoB PLANTS* (Vol. 10, Issue 4). Oxford University Press. https://doi.org/10.1093/aobpla/ply037

Wardle, D. A., Yeates, G. W., Williamson, W. M., Bonner, K. I., & Barker, G. M. (2004). Linking aboveground and belowground communities: The indirect influence of aphid species identity and diversity on a three trophic level soil food web. *Oikos*, *107*(2), 283–294. https://doi.org/10.1111/j.0030-1299.2004.13523.x

Warren, C. R. (2016). Simultaneous efflux and uptake of metabolites by roots of wheat. *Plant and Soil*, *406*(1–2), 359–374. https://doi.org/10.1007/s11104-016-2892-3

Webster, B. (2012). The role of olfaction in aphid host location. In *Physiological Entomology* (Vol. 37, Issue 1, pp. 10–18). https://doi.org/10.1111/j.1365-3032.2011.00791.x

Weibull, J. (1990). Host Plant Discrimination in the Polyphagous Aphid Rhopalosiphum padi: The Role of Leaf Anatomy and Storage Carbohydrate. In *Source: Oikos* (Vol. 57, Issue 2). https://about.jstor.org/terms

Wen, T., Zhao, M., Yuan, J., Kowalchuk, G. A., & Shen, Q. (2021). Root exudates mediate plant defense against foliar pathogens by recruiting beneficial microbes. *Soil Ecology Letters*, *3*(1), 42–51. https://doi.org/10.1007/s42832-020-0057-z

Wickham H, François R, Henry L, Müller K, Vaughan D (2023). _dplyr: A Grammar of Data Manipulation_. R package version 1.1.4, https://CRAN.R-project.org/package=dplyr

Wickham H. ggplot2: Elegant Graphics for Data Analysis. Springer-Verlag New York, 2016.

Wickham H, Averick M, Bryan J, Chang W, McGowan LD, François R, Grolemund G, Hayes A, Henry L, Hester J, Kuhn M, Pedersen TL, Miller E, Bache SM, Müller K, Ooms J, Robinson D, Seidel DP, Spinu V, Takahashi K, Vaughan D, Wilke C, Woo K, Yutani H (2019). “Welcome to the tidyverse.” _Journal of Open Source Software_, *4*(43), 1686. doi:10.21105/joss.01686 <https://doi.org/10.21105/joss.01686>.

Williams, A., Langridge, H., Straathof, A. L., Fox, G., Muhammadali, H., Hollywood, K. A., Xu, Y., Goodacre, R., & de Vries, F. T. (2021). Comparing root exudate collection techniques: An improved hybrid method. *Soil Biology and Biochemistry*, *161*. https://doi.org/10.1016/j.soilbio.2021.108391

Wim H.Van der Putten, Louise E.M. Vet, Jeffrey A. Harvey, & Felix L.Wäckers. (2001). Linking above- and belowground multitrophic interactions of plants, herbivores, pathogens, and their antagonists. *TRENDS in Ecology & Evolution*, *16*(10), 547–554.

Wippel, K. (2023). Plant and microbial features governing an endophytic lifestyle. In *Current Opinion in Plant Biology* (Vol. 76). Elsevier Ltd. https://doi.org/10.1016/j.pbi.2023.102483

Wolfgang, A., Tack, A. J. M., Berg, G., & Abdelfattah, A. (2023). Reciprocal influence of soil, phyllosphere, and aphid microbiomes. *Environmental Microbiome*, *18*(1). https://doi.org/10.1186/s40793-023-00515-8

Worsley, S. F., Macey, M. C., Prudence, S. M. M., Wilkinson, B., Murrell, J. C., & Hutchings, M. I. (2021). Investigating the Role of Root Exudates in Recruiting Streptomyces Bacteria to the Arabidopsis thaliana Microbiome. *Frontiers in Molecular Biosciences*, *8*. https://doi.org/10.3389/fmolb.2021.686110

Worsley, S. F., Newitt, J., Rassbach, J., Batey, S. F. D., Holmes, N. A., Murrell, J. C., Wilkinson, B., & Hutchings, M. I. (2020). *Streptomyces Endophytes Promote Host Health and Enhance Growth across Plant Species*. https://doi.org/10.1128/AEM

Wu, Q., Schmidt, W., Aalen, R. B., Xu, C., & Takahashi, F. (2022). Editorial: Peptide Signaling in Plants. In *Frontiers in Plant Science* (Vol. 13). Frontiers Media S.A. https://doi.org/10.3389/fpls.2022.843918

Xiao, D., Liu, J., Liu, Y., Wang, Y., Zhan, Y., & Liu, Y. (2022). Exogenous Application of a Plant Elicitor Induces Volatile Emission in Wheat and Enhances the Attraction of an Aphid Parasitoid Aphidius gifuensis. *Plants*, *11*(24). https://doi.org/10.3390/plants11243496

Xing, Z., Ma, T., Wu, L., Zhang, Z., Ding, J., & Siemann, E. (2024). Foliar herbivory modifies arbuscular mycorrhizal fungal colonization likely through altering root flavonoids. *Functional Ecology*, *38*(1), 259–271. https://doi.org/10.1111/1365-2435.14461

Xu, Y., Guo, H., Geng, G., Zhang, Q., & Zhang, S. (2021). Changes in defense-related enzymes and phenolics in resistant and susceptible common wheat cultivars under aphid stress. *Acta Physiologiae Plantarum*, *43*(2). https://doi.org/10.1007/s11738-021-03207-3

Yang, L., Ding, W., Xu, Y., Wu, D., Li, S., Chen, J., & Guo, B. (2016). New insights into the antibacterial activity of hydroxycoumarins against ralstonia solanacearum. *Molecules*, *21*(4). https://doi.org/10.3390/molecules21040468

Yue, H., Yue, W., Jiao, S., Kim, H., Lee, Y. H., Wei, G., Song, W., & Shu, D. (2023). Plant domestication shapes rhizosphere microbiome assembly and metabolic functions. *Microbiome*, *11*(1). https://doi.org/10.1186/s40168-023-01513-1

Zeier, J. (2021). Metabolic regulation of systemic acquired resistance. In *Current Opinion in Plant Biology* (Vol. 62). Elsevier Ltd. https://doi.org/10.1016/j.pbi.2021.102050

Zhang, K. X., Li, H. Y., Quandahor, P., Gou, Y. P., Li, C. C., Zhang, Q. Y., Haq, I. U., Ma, Y., & Liu, C. Z. (2022). Responses of Six Wheat Cultivars (Triticum aestivum) to Wheat Aphid (Sitobion avenae) Infestation. *Insects*, *13*(6). https://doi.org/10.3390/insects13060508

Zhang, L., Chen, C., Li, Y., Suo, C., Zhou, W., Liu, X., Deng, Y., Sohail, H., Li, Z., Liu, F., Chen, X., & Yang, X. (2024). Enhancing aphid resistance in horticultural crops: a breeding prospective. In *Horticulture Research* (Vol. 11, Issue 12). Oxford University Press. https://doi.org/10.1093/hr/uhae275

Zhang, Y., Duan, X., Xie, Y., & Xuan, W. (2024). Uncovering the function of peptides: Bridging hormone signaling, microbial interactions, and root development in plants. *New Crops*, *1*, 100011. https://doi.org/10.1016/j.ncrops.2024.100011

Zhang, Y., Fan, J., Fu, Y., Francis, F., & Chen, J. (2019). Plant-Mediated Interactions between Two Cereal Aphid Species: Promotion of Aphid Performance and Attraction of More Parasitoids by Infestation of Wheat with Phytotoxic Aphid Schizaphis graminum. *Journal of Agricultural and Food Chemistry*, *67*(10), 2763–2773. https://doi.org/10.1021/acs.jafc.8b06150

Zhang, Z., Lan, H., Cao, H., Hu, X., Fan, Y., Song, Y., Wu, L., & Liu, T. X. (2021). Impacts of constitutive and induced benzoxazinoids levels on wheat resistance to the grain aphid (Sitobion avenae). *Metabolites*, *11*(11). https://doi.org/10.3390/metabo11110783

Zheng, Y., Maruoka, M., Nanatani, K., Hidaka, M., Abe, N., Kaneko, J., Sakai, Y., Abe, K., Yokota, A., & Yabe, S. (2021). High cellulolytic potential of the Ktedonobacteria lineage revealed by genome-wide analysis of CAZymes. *Journal of Bioscience and Bioengineering*, *131*(6), 622–630. https://doi.org/10.1016/j.jbiosc.2021.01.008

Zheng, Y., Saitou, A., Wang, C. M., Toyoda, A., Minakuchi, Y., Sekiguchi, Y., Ueda, K., Takano, H., Sakai, Y., Abe, K., Yokota, A., & Yabe, S. (2019). Genome features and secondary metabolites biosynthetic potential of the class Ktedonobacteria. *Frontiers in Microbiology*, *10*(APR). https://doi.org/10.3389/fmicb.2019.00893

Zheng, Y., Wang, J., Zhang, X., Lei, L., Yu, R., Yao, M., Han, D., Zeng, Q., & Li, X. (2023). Core root-associated prokaryotic community and its relationship to host traits across wheat varieties. *Journal of Experimental Botany*, *74*(8), 2740–2753. https://doi.org/10.1093/jxb/erad066

Zhou, C., Cheng, H., Wu, Y., Zhang, J., Li, D., & Pan, C. (2022). Bensulfuron-Methyl, Terbutylazine, and 2,4-D Butylate Disturb Plant Growth and Resistance by Deteriorating Rhizosphere Environment and Plant Secondary Metabolism in Wheat Seedlings. *Journal of Agricultural and Food Chemistry*, *70*(40), 12796–12806. https://doi.org/10.1021/acs.jafc.2c03126

Zhou, C., Li, D., Shi, X., Zhang, J., An, Q., Wu, Y., Kang, L., Li, J. Q., & Pan, C. (2021). Nanoselenium Enhanced Wheat Resistance to Aphids by Regulating Biosynthesis of DIMBOA and Volatile Components. *Journal of Agricultural and Food Chemistry*, *69*(47), 14103–14114. https://doi.org/10.1021/acs.jafc.1c05617

Zhou, S., & Jander, G. (2022). Molecular ecology of plant volatiles in interactions with insect herbivores. In *Journal of Experimental Botany* (Vol. 73, Issue 2, pp. 449–462). Oxford University Press. https://doi.org/10.1093/jxb/erab413

Zhou, S., Richter, A., & Jander, G. (2018). Beyond defense: Multiple functions of benzoxazinoids in maize metabolism. In *Plant and Cell Physiology* (Vol. 59, Issue 8, pp. 1528–1533). Oxford University Press. https://doi.org/10.1093/pcp/pcy064

Zhou, W., Li, M., & Achal, V. (2025). A comprehensive review on environmental and human health impacts of chemical pesticide usage. In *Emerging Contaminants* (Vol. 11, Issue 1). KeAi Communications Co. https://doi.org/10.1016/j.emcon.2024.100410

Zhu, H., Swierstra, J., Wu, C., Girard, G., Choi, Y. H., Van Wamel, W., Sandiford, S. K., & van Wezel, G. P. (2014). Eliciting antibiotics active against the ESKAPE pathogens in a collection of actinomycetes isolated from mountain soils. *Microbiology (United Kingdom)*, *160*(PART 8), 1714–1726. https://doi.org/10.1099/mic.0.078295-0

Zhu, Y., Yin, Y., Wei, Y., Li, J. M., Wei, X., Li, G., Ye, Y., Huang, J., & Yang, S. (2024). Differences of endophytic microbial compositions and metabolites in roots between fusarium wilt resistant and susceptible melon varieties. *Chemical and Biological Technologies in Agriculture*, *11*(1). https://doi.org/10.1186/s40538-024-00623-8

Zilber-Rosenberg, I., & Rosenberg, E. (2008). Role of microorganisms in the evolution of animals and plants: the hologenome theory of evolution. *FEMS microbiology reviews*, *32*(5), 723-735.

Zuffa, S., Schmid, R., Bauermeister, A., Paulo, P. W., Caraballo-Rodriguez, A. M., El Abiead, Y., Aron, A. T., Gentry, E. C., Zemlin, J., Meehan, M. J., Avalon, N. E., Cichewicz, R. H., Buzun, E., Terrazas, M. C., Hsu, C. Y., Oles, R., Ayala, A. V., Zhao, J., Chu, H., … Dorrestein, P. C. (2024). microbeMASST: a taxonomically informed mass spectrometry search tool for microbial metabolomics data. *Nature Microbiology*, *9*(2), 336–345. https://doi.org/10.1038/s41564-023-01575-9

Züst, T., & Agrawal, A. A. (2016). Mechanisms and evolution of plant resistance to aphids. In *Nature Plants* (Vol. 2). Palgrave Macmillan. https://doi.org/10.1038/nplants.2015.206

Zytynska, S. E., & Meyer, S. T. (2019). Effects of biodiversity in agricultural landscapes on the protective microbiome of insects–a review. *Entomologia Experimentalis et Applicata*, *167*(1), 2-13.